Investigating the role of Neuronatin in neural development

Lin, Hsuan-Hwai

Awarding institution:
King's College London

Title: Investigating the role of Neuronatin in neural development

Author: Hsuan-Hwai Lin

Investigating the role of Neuronatin in neural development

Hsuan-Hwai Lin

Institute of Psychiatry, King's College London

Thesis submitted for the degree of Ph.D

2012

Abstract

Neural induction is the process that occurs during embryogenesis whereby ectoderm is converted into neural tissue. However, the cellular and molecular mechanisms that govern this process are still not completely understood. For instance, in *Xenopus,* calcium signalling is known to play a pivotal role in neural induction but whether a similar mechanism occurs in mammals is unknown. As part of a wider study on genes regulating neural stem cell (NSC) development, we have discovered a novel role for Neuronatin (*Nnat*), a regulator of intracellular Ca^{2+} concentration. In my thesis, I describe the use of a mouse embryonic stem cell (ESC)-derived neural differentiation model to dissect the function of Nnat in neural development.

Using gain- and loss-of function experiments I show that ESCs in which Nnat expression had been knocked-down have a dramatically decreased ability to generate NSCs, and subsequently neurons, while ESCs that over-expressed Nnat generate an excess of NSCs and neurons. I reveal that Nnat interacts directly with the sarcoendoplasmic reticulum Ca^{2+}-ATPase 2 (Apt2a2/SERCA2), and that Apt2a/SERCA inhibitors cause an increase in cytosolic calcium levels rescuing the ability of Nnat knockdown cells to generate neural cell-types. From these experiments I conclude that Apt2a/SERCA inhibition mimics the function of Nnat and, via the increase of cytosolic calcium, causes neural induction in Nnat knocked-down ESCs. I go on to show that this increase in cytosolic Ca^{2+}, caused by inhibiting Apt2a/SERCA, activates Erk signalling and that inhibition of Erk signalling dramatically reduces the ability of ESCs to generate NSC.

Together these results suggest that Nnat functions by increasing cytosolic Ca^{2+} levels, which in turn causes activation of Erk signalling leading to neural induction. In line with this, the expression of *BMP4,* which is an inhibitor of neural induction, was found to be up-regulated by Nnat knocked-down. Overall my thesis research indicates that Nnat plays a pivotal role in enabling ESCs to differentiate along a neural lineage.

Publication arising from this thesis

Lin, H. H., Bell, E., Uwanogho, D., Perfect, L. W., Noristani, H., Bates, T. J., Snetkov, V., Price, J. and Sun, Y. M. (2010). Neuronatin promotes neural lineage in ESCs via Ca^{2+} signaling. *Stem Cells* **28**, 1950-60.

Acknowledgements

I would like to express my sincere gratitude to my supervisors, Dr. Yuh-Man Sun and Dr. Brenda Williams, throughout this project. Without their inspiration and guidance, this work would not have been finished. I am also extremely grateful to Dr. Dafe Uwanogho for his help in the lab and the proof reading of this thesis. I would like to express my appreciation to Professor Jack Price for his support in difficult situations.

I would wish to thank all the other members of the CCBB for their kind cooperation and advice. I would also like to thank the Taiwanese government for funding my PhD. I particularly acknowledge my friend Dr. Tsung-Neng Tsai for his patience and encouragement. Finally, I would like to thank all my family for their unquestioning love and support over the past few years.

Table of Contents

List of Figures

List of Tables

Abbreviations

-/-	Null mutant
2-APB	2-aminoethoxydiphenyl borate
ANOVA	Analysis of variance
Apt2a/SERCA	Sarcoendoplasmic reticulum Ca^{2+}-ATPase
BAPTA-AM	1,2-Bis (2-aminophenoxy) ethane-N,N,N',N'-tetraacetic acid tetrakis (acetoxymethyl ester)
BHQ	2,5-Di-t-butyl-1,4-benzohydroquinone
BMP	Bone morphogenetic protein
BMPR	Bone morphogenetic protein receptor
BSA	Bovine serum albumin
Ca^{2+}	Calcium ion
$[Ca^{2+}]_i$	Concentration of cytosolic calcium ion
cAMP	Cyclic adenosine monophosphate
cDNA	Complementary deoxyribonucleic acid
cGMP	Cyclic guanosine monophosphate
Co-IP	Co-immunoprecipitation
C-ter-p-Smad1	C-terminal phosphorylated Samd1
DAG	Diacylglycerol
DAPI	4',6-diamidino-2-phenylindole
dpc	Days post coitum
EBs	Embryoid bodies
EGTA	Ethylene glycol tetraacetic acid
ER	Endoplasmic reticulum

Erk	Extracellular signal-regulated kinase
ERNI	Early response to neural induction
ESCs	Embryonic stem cells
FGF	Fibroblast growth factor
FGFR	Fibroblast growth factor receptor
FRS2	Fibroblast growth factor receptor substrate 2
GDF3	Growth differentiation factor 3
GFP	Green fluorescent protein
Grb2	Growth factor receptor bound protein 2
GSK3	Glycogen synthase kinase 3
Hnf4	Hepatocyte nuclear factor 4
ICM	Inner cell mass
IgG	Immunoglobulin G
IP_3	Inositol 1,4,5-triphosphate
IP_3R	Inositol 1,4,5-triphosphate receptor
kD	kiloDalton
LB	Luria Bertani
LIF	Leukaemia inhibitory factor
MAP2	Microtubule-associated protein 2
MEK	Mitogen-activated Protein/Extracellular Signal-regulated Kinase Kinase
Mesp1	Mesoderm posterior 1
MH1	N-terminal Mad Homology 1
MH2	C-terminal Mad Homology 2
mRNA	Messenger ribonucleic acid

NCAM	Neural cell adhesion molecule
NCKX	Na^+/Ca^{2+}-K^+ exchangers
NCX	Na^+/Ca^{2+} exchangers
NeuN	Neuronal nuclear antigen
Nnat	Neuronatin
Nnat-KD	Nnat-knockdown
Nnat-OE	Nnat-overexpression
NPCs	Neural progenitor cells
Nrp1	Neuropilin-1
NSCs	Neural stem cells
PARP-1	poly (ADP-ribose) polymerase 1
PBS	Phosphate-Buffered Saline
PCR	Polymerase chain reaction
PDK1	3-phosphoinositide dependent protein kinase-1
p-Erk1/2	Phosphorylated Erk1/2
PI3K	Phosphoinositide 3-kinase
PIP_2	Phosphatidylinositol 4,5-bisphosphate
PKC	Protein kinase C
PLCγ	Phospholipase C gamma
PMCA	Plasma membrane Ca^{2+}-ATPase
RC2	Radial glial cell marker-2
RNAi	Ribonucleic acid interference
RT-PCR	Reverse transcriptase polymerase chain reaction
RyR	Ryanodine receptors
SE	Standard error

shRNA	short hairpin ribonucleic acid
Sfrp2	Secreted frizzled-related protein 2
Sos	Son of sevenless
Sox1	Sex determining region Y-box 1
Sox2	Sex determining region Y-box 2
Sox3	Sex determining region Y-box 3
SVZ	Subventricular zones
TBS	Tris buffered saline
TBST	Tris buffered saline with Tween 20
TEMED	Tetramethylethylenediamine
Tg	Thapsigargin
TGFβ	Transforming growth factor β
xPRMT1b	Xenopus protein arginine methyltransferase type I b

Chapter 1. General Introduction

1.0 Introduction

Neural induction is the earliest step of vertebrate neural development (Munoz-Sanjuan and Brivanlou, 2002). During embryogenesis, neural induction is the process by which part of ectoderm is specified as neuroectoderm that ultimately gives rise to the central nervous system (Stern, 2006). The remaining ectoderm gives rise to epidermis and becomes skin (Wilson and Hemmati-Brivanlou, 1995). The process of neural induction is complex and, as will be discussed in greater details below, involves the interaction of both instructive and inhibitory cues; however, the precise molecular mechanisms that govern this process have yet to be fully understood (Gaulden and Reiter, 2008). Within this introduction, I will discuss what is known about neural induction in vertebrates, focusing on similarities and differences between mammals and amphibians.

1.1 Neural induction occurs during gastrulation

During mammalian embryonic development, a fertilized egg goes through several cycles of cell division to form a solid ball-like structure called a morula (Tam and Loebel, 2007). The morula further develops into the blastocyst which consists of the inner cell mass (ICM) and the trophoblast, which is the outer layer of the blastocyst and will develop into the placenta (Adamson et al., 2002). The ICM differentiates into primitive ectoderm that goes on to generate the three primary germ layers (ectoderm, mesoderm and endoderm); a process called gastrulation (Tam and Loebel, 2007). Ultimately, the ectoderm (the external layer) forms skin, and nervous system, the mesoderm (the middle layer) forms the cardiovascular system, skeletal muscles, and hematopoietic cells, while the endoderm (the internal layer) forms the lungs, liver, and pancreas.

The process by which the ectoderm is specified along a neural pathway (neuroectoderm) is called neural induction and requires signals from the underlying mesoderm (Fig. 1.1A; Hemmati-Brivanlou and Melton, 1997b; Munoz-Sanjuan and Brivanlou, 2002; Stern, 2005). The neuroectoderm develops into the neural plate whose boarders become elevated forming neural folds, leaving a deep neural groove at the midline (Fig. 1.1B-C). Next the neural folds move towards each other and fuse at the midline (Fig. 1.1D)

transforming the neural groove into a tubular structure called neural tube (Clarke et al., 1991; Downs and Davies, 1993; Gammill and Bronner-Fraser, 2003). The caudal region of this neural tube develops into the spinal cord while the rostral region gives rise to the brain (Downs and Davies, 1993; Greene and Copp, 2009).

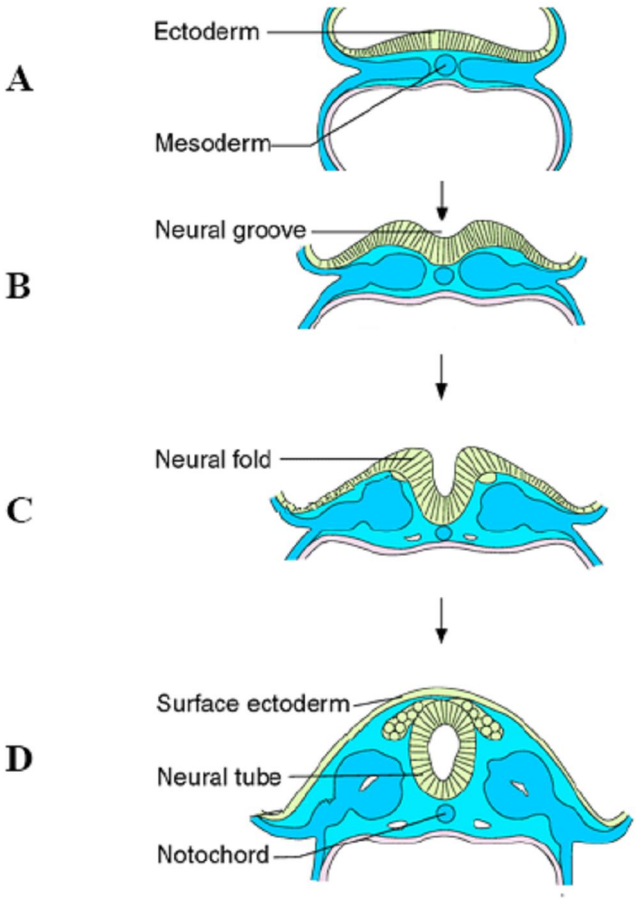

Fig. 1.1. The formation of neural tube in vertebrates.
(A) During gastrulation, primitive ectoderm gives rise to three primary germ layers known as ectoderm, mesoderm, and endoderm. The medial ectoderm overlying the notochord (derived from mesoderm) receives signals from the mesoderm and takes on a neural fate. This process is called neural induction. The peripheral ectoderm becomes the prospective epidermis. (B, C) After neural induction, the cells at the border of the neural plate become elevated neural folds, leaving a deep neural groove at the midline. (D) Both sides of neural folds move towards each other and fuse at the midline, forming the neural tube and surface ectoderm. The neural tube and surface ectoderm further give rise to central nervous system and epidermis respectively.
(Adapted from
http//www.elu.sgul.ac.uk/rehash/guest/scorm/138/package/content/neurulation.htm)

Amphibian embryos have been widely used to study embryonic development (Harland and Grainger, 2011), mainly because they are large,

making it relatively easy to perform surgical procedures. In addition, gene-expression in these embryos can be manipulated easily, through injections of mRNA or antisense RNA into embryos to evaluate their role in embryogenesis (Hulstrand et al., 2010). During *Xenopus* embryogenesis, after fertilization the egg goes through several rounds of cell division to form a hollow ball of cells called a blastula. At this stage the embryo consists of three portions, the animal cap, marginal zone, and the vegetal mass (Fig. 1.2; Heasman, 2006). The animal cap is located around the animal pole and the vegetal mass, consisting of yolky cells, is located opposite the animal cap. As its name suggests, the marginal zone is located between the animal cap and vegetal mass (Daniels et al., 2004). During gastrulation, the animal cap, marginal zone, and vegetal mass differentiate into embryonic ectoderm, mesoderm, and endoderm respectively (Gaulden and Reiter, 2008; Schneider and Mercola, 2001; Wylie et al., 1987). Further, the dorsal and ventral embryonic ectoderm gives rise to the neural plate and epidermis respectively (De Robertis and Kuroda, 2004; Suzuki et al., 1997). Like the mammalian neural plate, described above, the amphibian neural plate further differentiates into the neural tube and eventually into the central nervous system.

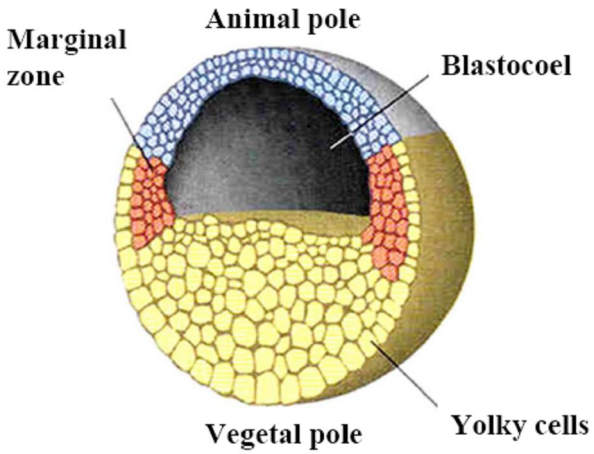

Fig. 1.2. Schematic amphibian embryo at the blastula stage.
After several cell divisions the amphibian embryo forms a blastula with a fluid-filled blastocoel. The blastula consists of three portions, the animal cap, marginal zone, and the vegetal mass. The marginal zone is located between the animal cap and vegetal mass. The animal cap is located around the animal pole and the vegetal mass contains yolky cells and is located opposite the animal cap.
(Adapted from http://www.proprofs.com/flashcards/upload/a4183539.jpg)

Because of their size and ease of manipulating gene-expression, amphibian embryos have often been used as a neural developmental model to study the mechanisms of neural induction (Munoz-Sanjuan and Brivanlou, 2002; Wilson and Edlund, 2001).

1.2 Neural induction through BMP inhibition

How neural induction is controlled is a long-standing question in vertebrate development. Over the past decades, many studies carried out in amphibian embryos have tried to answer this question (Munoz-Sanjuan and Brivanlou, 2002; Wilson and Edlund, 2001). In the 1920s, Spemann and Mangold conducted transplantation studies in amphibian embryos and these studies provided the first insight into the regulation of neural induction (Spemann and Mangold, 2001). They found a group of mesodermal cells located at the dorsal lip (dorsal margin of the blastopore) of the amphibian embryo that could induce the development of an ectopic neural axis when transplanted into another amphibian embryo. They called this group of cells the 'organiser' (Fig. 1.3A; Kuroda et al., 2004; Spemann and Mangold, 2001; Wilson and Edlund, 2001). When the organiser region was removed from the blastula, the *Xenopus* embryo no longer generated a brain (Kuroda et al., 2004). This result suggested that the organiser plays a pivotal role in neural induction of *Xenopus* embryos. An equivalent organiser region, called Hensen's node, was identified in chick embryos at the cranial end of the primitive streak, which consists of mesenchymal cells along the prospective midline (Selleck and Stern, 1991). The transplantation of Hensen's node into a host chick embryo induced the generation of ectopic neural tissue (Fig. 1.3B; Storey et al., 1992; Streit et al., 2000). Similarly in mouse embryos, 'the node' is located at the anterior end of the primitive streak and has the ability to induce the formation of a second neural axis when transplanted into host mouse embryos (Fig. 1.1C; Beddington, 1994; Kinder et al., 2001). These results lead to an assumption that the organiser (or equivalents in chick and mouse) is the origin of the inductive signals that induce the generation of neural tissue from ectoderm.

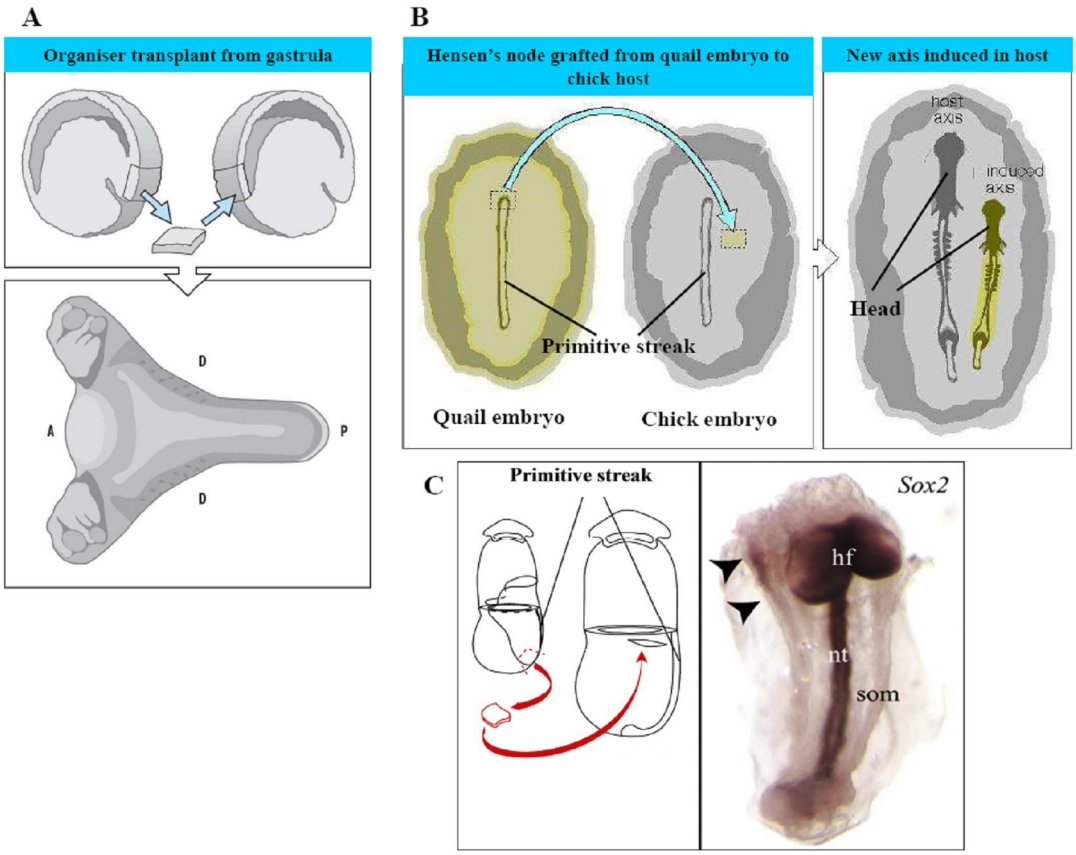

Fig. 1.3. Transplantation of the organiser induces a second neural axis in a host embryo.
(A) In *Xenopus* embryos, the organiser is the region at the dorsal lip of the blastopore and when this region was grafted to the ventral marginal zone of a host embryo during gastrulation, it induced the generation of a second head structure. (B) Hensen's node is the organiser equivalent in birds and is located at the cranial end of the primitive streak. When the Hensen's node of a quail embryo was transplanted to a chick embryo, a second neural axis developed in the host embryo. (C) 'The node' is the organiser equivalent in mouse and is located at the anterior end of the primitive streak. When tissue cut from this organiser region was transplanted to a host mouse embryo, ectopic *Sox2*-expressing neural tissue (black arrowheads) was induced from the host embryo.
Abbreviations: A, anterior; D, dorsal; hf, head folds; nt, neural tube; P, posterior; som, somites; *Sox2*, SRY (sex determining region Y)-box 2.
(Adapted from http://www.mun.ca/biology/desmid/brian/BIOL3530/DEVO_05/ch05f03.jpg, http://www.mun.ca/biology/desmid/brian/BIOL3530/DB_04/fig4_20.jpg, and Kinder et al., 2001)

To verify the assumption that the organiser was the source of neural inductive signals, researchers tried to identity these signals. In 1992, Smith and Harland found that a BMP (Bone morphogenetic protein) antagonist, Noggin, was expressed in the organiser region (Fig. 1.4), and the injection of *Noggin* mRNA into *Xenopus* embryos enlarged the head structures and induced a second neural axis (Molenaar et al., 1996; Smith and Harland,

1992). This observation was consistent with the idea that Noggin acts as a neural inducer. In addition to Noggin, *in situ* hybridization studies revealed that two other BMP antagonists, *Chordin* and *Follistatin,* were also expressed in the organiser region (Hemmati-Brivanlou et al., 1994; Sasai et al., 1994). The injection of *Chordin* or *Follistatin* mRNA into *Xenopus* embryos induced the generation of a second neural axis and expanded the neural tissue (Iemura et al., 1998; Pera et al., 2003; Piccolo et al., 1996; Sasai et al., 1994). These results suggest that BMP antagonists, Noggin, Chordin, and Follistatin, are secreted from the organiser region and convert the surrounding ectodermal cells into neural cells during gastrulation.

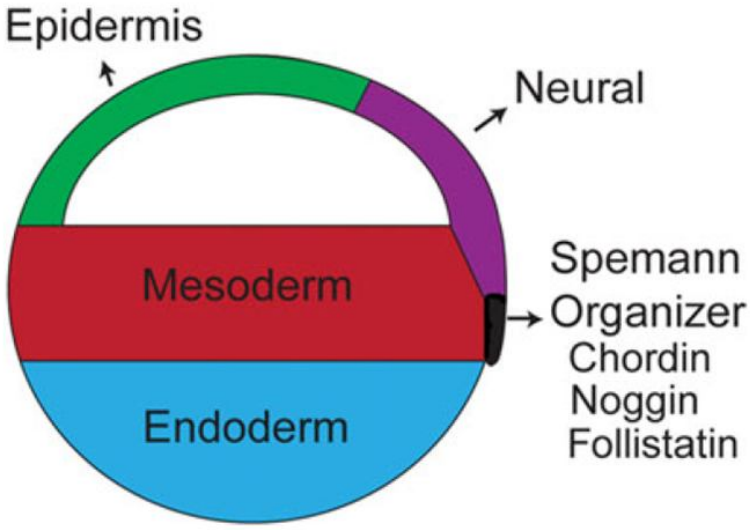

Fig. 1.4. The organiser of *Xenopus* embryo expresses BMP antagonists.
During gastrulation, the three germ layers are formed; ectoderm (green and purple), mesoderm (red), and endoderm (blue). Spemann's organiser (black) is a group of mesodermal cells located at the dorsal lip of blastopore. It has been demonstrated that BMP antagonists Chordin, Noggin, and Follistatin are expressed in the organiser region, and these secreted BMP antagonists can induce neural specificity of the dorsal ectoderm (purple, close to the organiser) and let the ventral ectoderm (green, away from the organiser) give rise to epidermis.
Abbreviations: BMP, Bone morphogenetic protein.
(Adapted from Gaulden and Reiter, 2008)

The neural markers *NCAM* (Neural cell adhesion molecule), *Nrp1* (Neuropilin-1), *Sox2* (SRY (sex determining region Y)-box 2), and *Sox3* (SRY-box 3) are expressed in the neural plate of *Xenopus* embryos, but not in the non-neural ectoderm, so these genes are considered to be the markers

of neural induction (Kintner and Melton, 1987; Knecht et al., 1995; Stern, 2005). If BMP antagonists are required for neural induction in *Xenopus*, then inhibiting their function should suppress the expression of these neural markers. However, knocking down the expression of Noggin by injection of antisense oligos into *Xenopus* embryos did not inhibit the generation of *Sox2*-expressing neural plate (Khokha et al., 2005). This was most probably due to the compensatory role played by the other antagonists present; Chordin, and Follistatin. Indeed, when antisense oligos for *Noggin*, *Chordin*, and *Follistatin* were injected together into *Xenopus* embryos, the expression of the neural plate markers *Sox2* and *Sox3* was abolished and the domain of *Cytokeratin*-expressing epidermal tissue was expanded (Khokha et al., 2005). These results suggest that BMP antagonists are needed for neural induction in *Xenopus* embryos.

As well as the BMP antagonists discussed above, BMP signalling can also be suppressed by Smad6 and Smad7, the inhibitory effectors of the BMP signalling pathway (for details see section 1.4.1; Hata et al., 1998; Imamura et al., 1997; Nakao et al., 1997). The injection of *Smad6* mRNA into *Xenopus* embryos induced the formation of a second neural axis (Linker and Stern, 2004). Similarly the over-expression of *Smad7* in *Xenopus* embryos expanded the domain of *Sox2*-expressing neural plate cells and induced the generation of ectopic neural tissue (Wawersik et al., 2005). Therefore, like BMP antagonists, the inhibition of intracellular pathway of BMP signalling also induces neural induction in *Xenopus* embryos.

In mouse embryos, if the inhibition of BMP signalling is needed for neural induction, like *Xenopus* embryos, then in the absence of BMP antagonists should cause abnormal neural plate development, yet *Noggin* or *Follistatin* null mice show normal gastrulation and neural induction (Bachiller et al., 2000; Matzuk et al., 1995). This suggests that another BMP antagonist Chordin, whose expression overlaps with that of Noggin and Follistatin at 'the node' (an equivalent organiser in mouse), can compensate for the lack of this antagonist (Bachiller et al., 2000; Feijen et al., 1994). This was confirmed by experiments where *Noggin* and *Chordin* have both been

knocked out since these double-homozygous mutants show defects in neural plate generation (Bachiller et al., 2000). Thus BMP antagonists play an important role in neural induction in mouse embryos. Further to this, in *BMPR1a* (BMP receptor 1a) null mouse embryos, not only are the domains of *Six3* and *Sox1*-expressing neuroectoderm expanded, but the generation of neuroectoderm occurs prematurely compared with wild type embryos (Di-Gregorio et al., 2007). This finding suggested that, like *Xenopus* embryo, the inhibition of BMP signalling induces neural induction in mouse embryos.

1.3 Default model of neural induction in *Xenopus* embryos

Based on the data obtained from experiments in *Xenopus* embryos, the 'default model' of neural induction was hypothesised by Hemmati-Brivanlou and Melton, which proposed that ectodermal cells will adopt a 'default' neural fate in the absence of BMP signalling (Fig. 1.5; Hemmati-Brivanlou and Melton, 1997a). However, the embryonic ectoderm expresses BMP4 that directs the embryonic ectoderm to take up an epithelium fate, preventing a neural fate; its natural tendency according to the default model (Hemmati-Brivanlou and Melton, 1997b; Wilson et al., 1997). During gastrulation, the organiser secrets the BMP antagonists Noggin, Chordin, and Follistatin, to inhibit the action of BMP and enable the surrounding ectodermal cells to take up their 'default' neural fate (Wilson et al., 1997; Zimmerman et al., 1996). This finding suggests that after BMP antagonists counteract the instructive effects of BMP signalling, the embryonic ectoderm cells receive no further instructive signal and are committed to a neural fate by the 'default' mechanism.

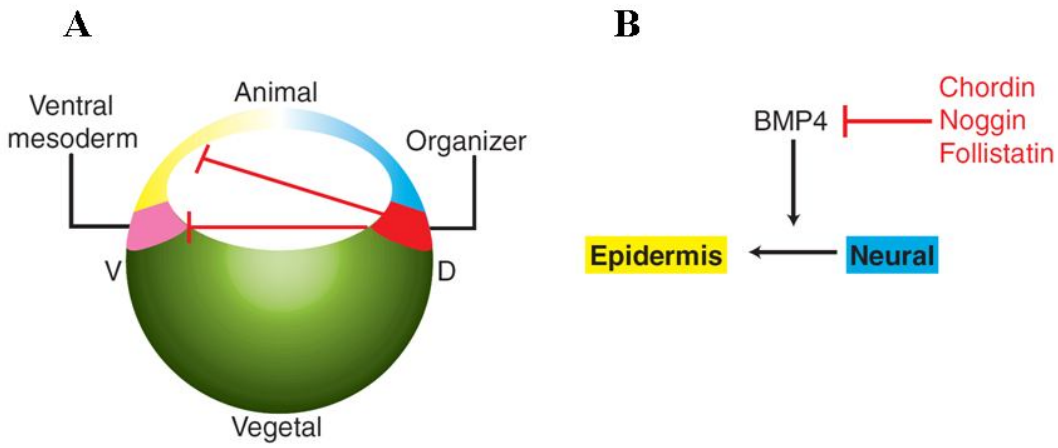

Fig. 1.5. Default model of neural induction in *Xenopus* embryos.
(A) In *Xenopus* embryos, the organiser region is located at the dorsal mesoderm (red). During gastrulation, the dorsal ectoderm (blue) in the animal cap gives rise to neuroectoderm and the ventral ectoderm (yellow) gives rise to epidermis. (B) The ectodermal cells have a default fate to become neural cells (blue). Although ectodermal cells generate BMP4 that leads the ectoderm to differentiate into epidermis (yellow), the ectodermal cells will adopt their default fate autonomously when the endogenous BMP signalling is antagonised by Chordin, Noggin, or Follistatin (red) that emanate from the organiser.
Abbreviations: BMP, Bone morphogenetic protein; D, dorsal; V, ventral.
(Adapted from Stern, 2005)

Experiments on *Xenopus* animal cap cells also supported this default model (Grunz and Tacke, 1989; Munoz-Sanjuan and Brivanlou, 2002). The animal cap of the blastula consists of the embryonic ectoderm that will differentiate into neuroectoderm (neural plate) or non-neural ectoderm (epidermis) during gastrulation (Lamb and Harland, 1995; Munoz-Sanjuan and Brivanlou, 2002). Isolated intact animal cap explants cultured in the absence of growth factors give rise to epidermal tissue, due to the expression of BMP by these animal cap cells, which leads explants to acquire an epidermal fate (Hemmati-Brivanlou and Melton, 1997b; Sasai et al., 1995; Wilson and Hemmati-Brivanlou, 1995). When animal cap explants were cultured with the BMP antagonist Noggin, cells within the explants began to express the neural plate markers *NCAM* or *Nrp1*. Such expression was not observed in Noggin untreated explants (Knecht et al., 1995; Lamb and Harland, 1995). This finding implies that the exposure of animal caps to the BMP antagonist Noggin suppressed the effect of endogenous BMP4, resulting in the generation of neural tissue by default. Similarly, expression of the neural

plate marker *NCAM* was observed to be up-regulated in animal caps isolated from *Xenopus* embryos into which *Chordin* or *Follistatin* mRNA has been injected at 2 to 8-cell stage (Hemmati-Brivanlou et al., 1994; Pera et al., 2003; Sasai et al., 1995). Again, these results fit with the default model which states that ectodermal cells in animal caps give rise to neural tissue autonomously when the action of BMP is suppressed by its antagonists Noggin, Chordin, or Follistatin.

Further to this, the generation of *NCAM*, *Sox2*, and *Sox3*-expressing neural tissue was induced in animal cap explants that were isolated from *Smad6* or *Smad7* (intracellular inhibitors of BMP signalling, for details see section 1.4.1) injected *Xenopus* embryos (Casellas and Brivanlou, 1998; Delaune et al., 2005; Linker and Stern, 2004; Wawersik et al., 2005). This suggested that the inhibition of the downstream effectors of BMP signalling also enabled neural development to occur. Similarly, when a dominant-negative BMP receptor RNA (acted antagonistically to the wild-type BMP receptor) was injected into *Xenopus* embryos at the 2-cell stage, to suppress BMP signalling, and the animal cap explants were subsequently removed at the late blastula stage, the expression of the neural plate marker *NCAM* was up-regulated in the intact explants (Wilson et al., 1997). In contrast, in control non-injection embryos, the expression of the epidermal marker *Epidermal keratin* was up-regulated in the animal cap explants and the neural plate marker *NCAM* was not expressed. Thus, the inhibition of BMP signalling causes neuralisation of intact animal caps.

Similarly, if animals cap cells were dissociated and grown as dispersed cells in the absence of any growth factors or inhibitors, neural tissue was generated from these dispersed cells and the expression of the neural cell marker *NCAM* was up-regulated (Grunz and Tacke, 1989; Munoz-Sanjuan and Brivanlou, 2002; Wilson et al., 1997). This is due to the fact that dispersed cells are unable to signal to each other via BMP signalling to prevent neural induction. In line with this, if the dispersed cells are allowed to reassociate, then the expression of neural markers is inhibited with the concomitant up-regulation of epidermal markers (Kuroda et al., 2005;

Munoz-Sanjuan and Brivanlou, 2002). Thus, overall, the results obtained from experiments using animal cap explants suggested that in the absence of BMP signalling, embryonic ectoderm generates neural tissue by default.

1.4 BMP signalling represses neural induction

In contrast to what happens upon inhibition of BMP signalling, when dispersed animal cap cells were cultured with BMP4 to activate BMP signalling, epidermis was induced, as detected by the expression of the epidermal markers *Epi1* and *Epidermal keratin*, and the expression of the neural plate marker *NCAM* was abolished (Wilson and Hemmati-Brivanlou, 1995; Wilson et al., 1997). Similarly the injection of *BMP2*, *BMP4*, or *BMP7* mRNA into *Xenopus* embryos was shown to activate *Msx1* (target gene of BMP signalling), which in turn induced expression of the epidermal marker *Epidermal keratin* and inhibition of neural induction (Fainsod et al., 1997; Suzuki et al., 1997). These findings suggest that activation of BMP signalling induces the generation of epidermis and suppresses neural induction in *Xenopus* embryos.

Similarly, in chick embryos, the activation of BMP signalling also inhibits neural induction (Wilson et al., 2000). When prospective epidermal and prospective neural plate explants were isolated from the embryonic ectoderm of chick embryos and cultured for 40 hours, the expression of *BMP4* was down-regulated in prospective neural plate explants but up-regulated in prospective epidermal explants. At the same time, the prospective epidermal explants expressed Msx1 and Msx2 proteins (target genes of BMP signalling, for details see section 1.4.1) but not the neural plate markers Sox2 and Sox3; in contrast, the prospective neural plate explants expressed neural markers Sox2 and Sox3 proteins but not Msx1 and Msx2 (Wilson et al., 2000). These results suggested that BMP signalling was active in prospective epidermal explants of chick embryos and inactive in the prospective neural plate explants. If the prospective neural plate explants were cultured with BMP4, then the generation of Sox2 and Sox3-expressing neural tissue was significantly reduced and epidermal differentiation was increased compared with BMP4 untreated explants (Wilson et al., 2000). Experiments in whole

chick embryos also showed that BMP signalling inhibited neural induction *in vivo*. Before gastrulation, *BMP4* is expressed throughout the epiblast (has the ability to differentiate into the three germ layers) of chick embryos, but during the period of neural induction, *BMP4* is only expressed in the non-neural tissue of chick embryos (Streit et al., 1998). Thus, BMP4 is not expressed in the neuroectoderm of chick embryos. However, when *BMP4* was electroporated into the prospective neural plate of chick embryos *in vivo*, expression of the neural plate markers *Sox2* and *Sox3* was inhibited (Linker and Stern, 2004). Thus, BMP signalling can repress neural induction in chick embryos.

1.4.1 BMP signalling through Smad proteins

As well as their role in neural development, as described above, BMPs play other diverse roles in development, including in bone and cartilage formation (Wang et al., 1990), epidermal induction (Munoz-Sanjuan and Brivanlou, 2002), limbs development (Yi et al., 2000), hematopoietic differentiation (Chadwick et al., 2003), and heart formation (Shi et al., 2000). BMPs are members of the TGFβ (Transforming growth factor β) superfamily and the binding of BMP to type II and type I BMP receptors (BMPR) results in their phosphorylation (Heldin et al., 1997; Miyazono et al., 2005; Shi and Massague, 2003). The active type I BMPR phosphorylates Smad1, Smad5, and Smad8 (Fig. 1.6; Kretzschmar et al., 1997; Shi and Massague, 2003) and once phosphorylated these proteins form a complex with Smad4 and this complex enters the nucleus to activate target genes, such as *Msx1*, *Msx2*, and *Vent2* (Hardwick et al., 2008; Marazzi et al., 1997; Phippard et al., 1996; Postigo, 2003; Tucker et al., 1998). As described above (see section 1.4), Msx1 and Msx2 play an important role in epidermal induction and the over-expression of *Msx1* induces the expression of the epidermal marker *Epidermal keratin* and inhibits neural induction in *Xenopus* embryos (Suzuki et al., 1997), while knocking down *Msx1* and *Msx2* induced ectopic *Sox2*-expressing neural tissue and suppressed the generation of epidermis in *Xenopus* embryos (Khadka et al., 2006). Similarly, it has been demonstrated that the

promoter region of *Vent2* contains a Smad1 binding site, and the injection of *Xenopus* embryos with *BMP4* mRNA up-regulated the expression of *Vent2* (Karaulanov et al., 2004). Further, the over-expression of *Vent2* in *Xenopus* embryos resulted in suppression of expression of the neural plate marker Sox3 (Rogers et al., 2008). Thus, BMP signalling activates Smad1 and in turn up-regulates the expression of *Msx1*, *Msx2*, and *Vent2* to repress neural induction.

BMP signalling can be suppressed by a number of inhibitors including Noggin, Chordin, Follistatin, Smad6, and Smad7. Noggin and Chordin act by binding to BMP ligands thus preventing BMP binding to its receptors (Munoz-Sanjuan and Brivanlou, 2002; Piccolo et al., 1996; Zimmerman et al., 1996), while Follistatin forms a trimeric complex with BMP ligands, and BMPR to inhibit the phosphorylation of Smad1 and block BMP signalling (Fig. 1.7, Fainsod et al., 1997; Glister et al., 2004; Iemura et al., 1998). Thus, the treatment of Noggin, Chordin, or Follistatin could reduce the expression of BMP target genes, *Msx1*, *Msx2*, and *Vent2* (Iemura et al., 1998; Ishimura et al., 2000; Pera et al., 2003; Streit and Stern, 1999a). Smad7 interacts with BMPR to inhibit the phosphorylation of Smad1 (Nakao et al., 1997) and Smad6 competes with Smad4 for binding to Smad1/5/8, so Smad7 and Smad6 prevent BMP signalling from activation (Hata et al., 1998).

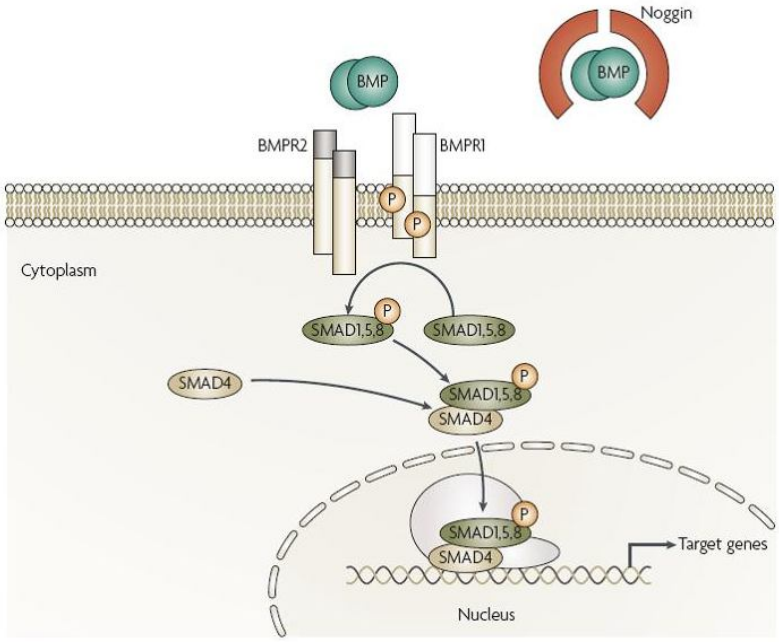

Fig. 1.6. The BMP signalling pathway.
The binding of BMP to its receptors (BMPR1 and BMPR2) phosphorylates Smad1/5/8. The phosphorylated Smad1/5/8 forms a complex with Smad4 and this complex enters the nucleus to bind to the promoter region of target genes, such as *Msx1*, *Msx2*, and *Vent2*, and then activates these genes. BMP antagonists including Noggin and Chordin, can prevent the binding of BMP ligands with BMPR thus inhibiting BMP signalling.
Abbreviations: BMP, bone morphogenetic protein; BMPR, BMP receptor; P, phosphorylation.
(Adapted from Hardwick et al., 2008)

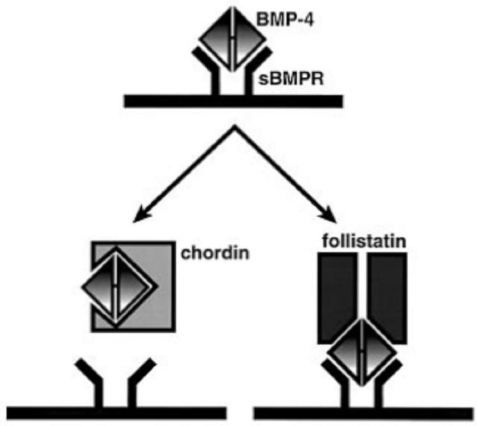

Fig. 1.7. The different inhibitory mechanisms of Chordin and Follistatin.
Chordin binds with BMP ligands to prevent the binding of these ligands to receptors, thus preventing BMP signalling. In contrast, Follistatin forms a trimeric complex with BMP ligands, and BMPR to block BMP signalling.
Abbreviations: BMP, bone morphogenetic protein; BMPR, BMP receptor.
(Adapted from Iemura et al., 1998)

Thus, studies in *Xenopus*, Chick and mouse show that BMP signalling needs to be suppressed in order for neural induction to occur.

1.5 The insufficiency of default model

The default model of neural induction proposes that the ectodermal cells give rise to neural tissue autonomously in the absence of BMP activation (for details see sections 1.3 and 1.4). Although the default model gives a simple and attractive way to understand the mechanism of neural induction, it cannot completely explain neural induction. For example, administration of BMP antagonists Noggin or Chordin to the non-neural embryonic ectoderm of chick embryos did not induce ectopic neural tissue (Streit et al., 1998; Streit and Stern, 1999b). Therefore, in contrast to what was observed in *Xenopus* embryos, inhibition of BMP signalling is not sufficient to induce neural induction in chick embryos (Stern, 2005). Furthermore, it has been demonstrated that as well as BMP signalling discussed above, other signals have been shown to be involved in this process, such as FGF (Fibroblast growth factor), Wnt, Activin/Nodal, and calcium (Batut et al., 2005; Camus et al., 2006; del Barco Barrantes et al., 2003; Kuroda et al., 2005; Stern, 2005; Wessely et al., 2001; Wilson et al., 2001). In the following sections, I will discuss what is known about the role these signals in neural induction of vertebrates.

1.5.1 The role of FGF signalling in neural induction

FGFs are a family of growth factors and are highly conserved between mouse and human (Bottcher and Niehrs, 2005; Itoh and Ornitz, 2004; Ornitz and Itoh, 2001). FGFs can be divided into 7 subfamilies: FGF1/2, FGF4/5/6, FGF3/7/10/22, FGF8/17/18, FGF9/16/20, FGF11/12/13/14 and FGF15/19/21/23 (Itoh and Ornitz, 2011), with the members of each having similar biological properties. Most FGFs are secreted from cells to interact with receptors on the cell surface (Itoh and Ornitz, 2004; Ratzka et al., 2011), but the FGF11/12/13/14 subfamily are non-secreted proteins and bind to the intracellular C-terminal region of voltage-gated sodium channels to modulate action potentials in hippocampal neurons (Goetz et al., 2009; Munoz-Sanjuan et al., 2000; Smallwood et al., 1996).

FGF receptors (FGFRs) belong to the receptor tyrosine kinase family of receptors, which have an extracellular ligand-binding domain, a transmembrane domain and an intracellular tyrosine kinase domain (Schlessinger, 2004; Turner and Grose, 2010). The extracellular ligand-binding domain of FGFR contains a heparin binding site (Schlessinger et al., 2000). Heparin or heparan sulfate proteoglycans promote the binding of FGF ligands to FGFRs (Pellegrini, 2001; Schlessinger et al., 2000), and the binding of heparin is required for FGF signal transduction (Lanner et al., 2010). There are four highly conserved *Fgfr* genes (*Fgfr1,2,3,4*) in vertebrates and each gene, except *Fgfr4,* encodes two isoforms, b and c. The ligand-specificities of FGFRs are shown in Table 1.1 (Itoh and Ornitz, 2004; Turner and Grose, 2010; Zhang et al., 2006). Because the FGF15/19/21/23 subfamily have a lower affinity for FGFRs compared with other secreted FGFs (Itoh and Ornitz, 2011), this subfamily was not listed in Table 1.1.

Table 1.1. Ligand-specificities of FGFRs

Gene	Receptor	Ligand-specificity
Fgfr1	**FGFR1b**	**FGF1, 2, 3, 10 and 22**
	FGFR1c	**FGF1, 2, 4, 5, 6 and 8**
Fgfr2	**FGFR2b**	**FGF1, 3, 7, 10, and 22**
	FGFR2c	**FGF1, 2, 4, 6, 8, 9, 17, 18, and 20**
Fgfr3	**FGFR3b**	**FGF1 and 9**
	FGFR3c	**FGF1, 2, 4, 8, 9, 16, 17, 18, and 20**
Fgfr4	**FGFR4**	**FGF1, 2, 4, 6, 8, 9, 17 and 18**

FGF has a range of functions; in angiogenesis (Cross and Claesson-Welsh, 2001), wound repair (Doukas et al., 2002), tumorigenesis (Grose and Dickson, 2005), and endocrine homeostasis (Shimada et al., 2004). FGF signalling also plays an important role in many aspects of development.

For instance, during embryonic development, FGF signalling is involved in cell migration (Sun et al., 1999), patterning of the cortex (Cholfin and Rubenstein, 2007), mesoderm induction (Schulte-Merker and Smith, 1995), limb development (Martin, 1998), and bone formation (Coumoul and Deng, 2003). Furthermore, a body of evidence shows that FGF signalling is required for neural induction in chick, mouse, and even *Xenopus* (Dang and Tropepe, 2010; Harland, 1994; Kengaku and Okamoto, 1993; Lamb and Harland, 1995; Stavridis et al., 2007; Streit et al., 2000; Wilson et al., 2000), suggesting that FGFs are involved in the neural specification of ectodermal cells.

1.5.1.1 FGFs induce neural induction

Extracellular signal-regulated kinase (Erk) is the effector of FGF signalling and is phosphorylated while FGF signalling is active (for details see section 1.5.1.3). Before gastrulation, the immunostaining for phosphorylated Erk in wild type *Xenopus* embryos showed that Erk was active in the dorsal margin of the blastopore (organiser region) at the blastula stage (Christen and Slack, 1999). Further, during gastrulation, activated Erk was found in the developing neural plate and this activation could be blocked by the injection of a dominant-negative FGFR RNA into *Xenopus* embryos (Christen and Slack, 1999). This finding suggested that FGF signalling is active in the forming neural plate and that FGFs play a role in neural induction. Furthermore, reports have also shown that when *Xenopus* embryos were cultured with the FGFR inhibitor (SU5402), the generation of *NCAM*-expressing neural tissue was reduced, and this effect was dose dependent (Delaune et al., 2005). This result implies that the activation of FGF signalling is required for neural induction in *Xenopus*.

According to the default model, the injection of BMP antagonist *Noggin* mRNA into *Xenopus* embryos induced ectopic neural tissue (Molenaar et al., 1996; Smith and Harland, 1992). However, when the *Noggin* injected embryos were cultured with SU5402, no ectopic neural tissue was observed (Delaune et al., 2005). This study showed that the inhibition of

BMP signalling alone is not enough to induce neural induction. Similarly, ectopic *Sox2*-expressing neural tissue was induced and the generation of *Keratin 81*-expressing epidermal tissue was suppressed in *Xenopus* embryos when BMP signalling was blocked by knocking down *Smad5* (Marchal et al., 2009). Yet, when these *Smad5* knock-down embryos were treated with SU5402 to inhibit FGF signalling, the knocking down *Smad5* no longer induced ectopic *Sox2*-expressing neural tissue, but the epidermal marker *Keratin 81* was still suppressed because of inhibition of BMP signalling (Marchal et al., 2009). These results suggested that the default model of neural induction is not the whole story, and activation of FGF signalling plays a pivotal role in neural induction of *Xenopus*.

During *Xenopus* gastrulation, *Fgf1*, *Fgf2*, *Fgf4*, *Fgf8* and *Fgf20* are expressed in the mesoderm (Lea et al., 2009). If FGF signalling is required for neural induction in *Xenopus* embryos, then at least one of these five FGFs may be involved. The injection of *Fgf8* mRNA into *Xenopus* embryos at the 4 to 8-cell stage to activate FGF signalling induced the ectopic expression of the neural plate marker *Sox2* (Pera et al., 2003). This finding suggested that FGF8 mediated signalling can induce neural induction in *Xenopus* embryos. Similarly, culturing animal cap explants (details see section 1.3) with FGF2 up-regulated the expression of the neural marker Sox2 and this inductive effect of FGF2 was dose dependent, while the expression of the epidermal marker *Epidermal keratin* was reduced (Hongo et al., 1999; Kengaku and Okamoto, 1993). Another report also confirmed these observations showing that exposure of animal caps to FGF2 induced the generation of the neural plate marker *Nrp1* (Lamb and Harland, 1995). These results imply that activation of FGF signalling induces the generation of neural cells from ectodermal cells of *Xenopus* embryos or animal caps.

Similar experiments have been carried out in chick providing evidence that FGF signalling is also instructive for neural induction in avian embryos. For example, the implantation of FGF4 soaked beads into the

embryonic ectoderm of chick embryo induces the formation of ectopic neural tissue (Rodriguez-Gallardo et al., 1997). Another two reports also showed that implanting FGF2 or FGF4 soaked beads into the embryonic ectoderm of chick embryos induced the expression of *EphA7* (which is usually expressed in the forebrain and hindbrain of embryos (Araujo and Nieto, 1997)), *Krox-20* (which is usually expressed in the hindbrain of embryos (Graham and Lumsden, 1996)), *Cash4, Hoxb9* and *Sax1* (which are expressed in the caudal neural plate of embryos (Grapin-Botton et al., 1997; Henrique et al., 1997; Spann et al., 1994)) in non-neural ectoderm (Alvarez et al., 1998; Storey et al., 1998). Futher, the implantation of FGF8-coated beads into the embryonic ectoderm of chick embryos induced strong expression of *ERNI* an early marker of neural induction (Streit et al., 2000). Together, these results suggested that FGF signalling caused neural induction in chick embryos.

Since the findings observed in *Xenopus* and chick embryos showed that FGF signalling induces neural induction in ectodermal cells, the role of FGF signalling in neural induction was also investigated in mouse embryos. In mammals, *Fgf2, Fgf3, Fgf4, Fgf5, Fgf8,* and *Fgf17* are expressed prior to or at gastrulation, when neural induction occurs, so these FGFs may be involved in this process (Hannon et al., 1992; Haub and Goldfarb, 1991; Hebert et al., 1990; Maruoka et al., 1998; Penkov et al., 2001; Sun et al., 1999; Wilkinson et al., 1988). *Fgf4* is the first member of the FGF family to be expressed in mouse embryos, with the ICM of the blastocyst already expressing *Fgf4* (Niswander and Martin, 1992; Rappolee et al., 1994). During gastrulation, the expression of *Fgf4* is restricted to the primitive streak (Niswander and Martin, 1992; Rappolee et al., 1994). Unfortunately, *Fgf4* null mouse embryos die before gastrulation (Feldman et al., 1995), so it is not certain whether *Fgf4* is required in neural induction *in vivo*. However, the data obtained from experiments using *Fgf4*$^{-/-}$ mouse embryonic stem cells (ESCs) reveals that *Fgf4* is required for neural induction of these cells (details see section 1.6.2; Kunath et al., 2007).

The expression of *Fgf2* is not detected until 10.5 dpc (days post coitum), which is later than the formation of neural plate at 7.5 dpc (Hannon et al., 1992; Hebert et al., 1990). It has been shown that FGF2 regulates the proliferation of neural stem cells (NSCs) (Vaccarino et al., 1999; Zheng et al., 2004) rather than being involved in neural induction of mouse embryos. The expression of *Fgf3* is not detected until 7.5 dpc (Wilkinson et al., 1988). Although *Fgf3* null mouse embryos have defects in the caudal vertebrae and inner ear (Mansour et al., 1993), the neural tube is still formed, suggesting that FGF3 is not involved in neural induction (Wilkinson et al., 1988). Like *Fgf2*, the expression of *Fgf5* is not detected until 10.5 dpc (Hebert et al., 1990), and the number of motor neurons generated within the spinal cord and the morphology of the hippocampus are normal in *Fgf5* null mutants (Hebert et al., 1994). These finding indicated that neural induction can proceed normally in the absence of FGF5. Thus, *Fgf2*, *Fgf3*, and *Fgf5* may not be necessary for neural induction in mouse.

The expression of *Fgf8* is first detected at 5.5 dpc before the generation of neural plate in mouse embryos (Mahmood et al., 1995). Although, *Fgf8* null mutants die at 9.5 dpc, by this stage it was possible to determine that, in these mutants, the anterior neuroectoderm was generated, but not the posterior neuroectoderm (Sun et al., 1999). This suggested that FGF8 plays a role in the generation of the posterior neuroectoderm. The expression of *Fgf17* is detected at 8.0 dpc (Maruoka et al., 1998). The *Fgf17* knockout is not embryonic lethal but no obvious morphological defects were observed in the central nervous system of these *Fgf17* null animals (Cholfin and Rubenstein, 2007; Xu et al., 2000), suggesting FGF17 is not involved in neural induction.

Taken together, the *in vivo* expression pattern of FGFs described above suggests that compared with other FGFs, FGF4 and FGF8 are more likely to be the neural inducers in mouse embryogenesis.

1.5.1.2 Inhibition of FGF signalling suppresses neural induction

As discussed in the above section, the activation of FGF signalling promotes neural induction in *Xenopus*, chick, and mouse embryos, thus, the inhibition of FGF signalling should suppress this action. It has been shown that knocking down *Fgf4* by injecting antisense oligonucleotides into *Xenopus* embryos inhibited the generation of *Sox2*-expressing cells of the neural plate (Marchal et al., 2009). Similarly, the exposure of *Xenopus* embryos to the FGFR inhibitor (SU5402) inhibited the generation of *NCAM*-expressing neural tissue (Delaune et al., 2005). During gastrulation, *Fgfr1*, *Fgfr2*, and *Fgfr4* are expressed in the three primary germ layers of *Xenopus* embryos, with expression of *Fgfr4* being higher than that of the others (Hongo et al., 1999; Lea et al., 2009). Further to this, the expression of *Fgfr4* is relatively abundant in the ectoderm compared with the mesoderm (Hongo et al., 1999). The injection of a dominant-negative FGFR4 mRNA into *Xenopus* embryos at the 4-cell stage inhibited the generation of *NCAM*-expressing neural plate cells (Delaune et al., 2005), suggesting that *Fgfr4* is important for neural induction in *Xenopus* embryos.

As mentioned in section 1.5.1.1, *Fgf8* injected *Xenopus* embryos or FGF2 treated animal caps can generate neural tissue without the inhibition of BMP signalling (Hongo et al., 1999; Kengaku and Okamoto, 1993; Pera et al., 2003). These observations suggested that, in *Xenopus,* FGF could induce neural induction in the presence of BMP signalling. This finding dose not fit with the 'default' model (details see section 1.3). Further, injecting a BMP antagonist (*Noggin* mRNA) into *Xenopus* embryos could neuralise isolated animal cap explants, but the expression of the neural plate marker *NCAM* was suppressed when a truncated *FGFR* mRNA was injected at the same time (Launay et al., 1996). These observations do not fit with the default model hypothesis, revealing that the activation of FGF signalling is pivotal for neural induction to occur in *Xenopus* even in the absence of BMP signalling. In line with this, although injecting inhibitors of BMP signalling into *Xenopus* embryos caused the generation of ectopic neural tissue, this effect was inhibited

when embryos were treated with the FGF receptor inhibitor SU5402 (Delaune et al., 2005; Marchal et al., 2009; Wawersik et al., 2005). Thus, in *Xenopus*, an inhibition of BMP signalling together with an instructive signal, FGF, is required for neural induction. However, dissociated animal cap explants give rise to neural tissue in the absence of FGFs or other growth factor being added to the culture medium (Grunz and Tacke, 1989), and this finding is considered as a great support of default model (details see section 1.3). This observation can be explained by the fact that dissociation of animal caps causes activation of the Erk signalling pathway which is one of the intracellular pathways activated by FGF (details see section 1.5.1.3), and this in turn neuralises the dissociated explants (Kuroda et al., 2005). When the dissociated explants were treated with a MEK (Mitogen-activated Protein/Extracellular Signal-regulated Kinase Kinase) specific inhibitor U0126 to inhibit the Erk signalling, the dissociated cells no longer generated neural tissue, as indicated by a significant reduction in expression of the neural plate markers *NCAM* and *Sox2* and an up-regulation of the epidermal marker *Cytokeratin* (Kuroda et al., 2005). Therefore, signalling via the FGF/Erk pathway provides the instructive signal needed for neural induction of dissociated animal caps.

Similarly to what occurs in *Xenopus* embryos, the inhibition of FGF signalling also represses neural induction in chick embryos. When prospective neural plate explants were isolated from the embryonic ectoderm of chick embryos and cultured *in vitro* for 40 hours, explants expressed neural markers Sox2 and Sox3. If the isolated explants were cultured with the FGFR inhibitor SU5402, then the generation of Sox2 and Sox3-expressing neural tissue was lost (Wilson et al., 2000). This finding suggested that the prospective neural ectoderm of chick embryos fails to give rise to neural tissue if FGF signalling is inhibited. Experiments in whole chick embryos also showed similar results. When SU5402 soaked beads were implanted into the prospective neural plate of chick embryos, the expression of the neural plate makers *ERNI* and *Sox3* were suppressed (Streit et al., 2000). This implies that inhibition of

endogenous FGF signalling in the prospective neural plate represses neural induction in chick embryos. Further, as descried above (section 1.2) the transplantation of Hensen's node (equivalent to the organiser in chick) into the epiblast of host chick embryos induced the generation of ectopic neural tissue. However, this neural induction was inhibited when SU5402 soaked beads were implanted at the same time (Streit et al., 2000).

Since the findings observed in *Xenopus* and chick embryos show that inhibition of FGF signalling inhibits the neural differentiation of ectodermal cells, the presence of the same mechanism was also tested in mouse embryos. During mouse embryogenesis, the neural plate is detected at 7.5 dpc (Downs and Davies, 1993; Rowitch and McMahon, 1995; Yang et al., 1998). The activation of FGF signalling by injection of FGF8b into the proamniotic cavity (centre of the epiblast) at 7 dpc increased the number of NSCs derived form the anterior neural plate at 8.5 dpc, while, inhibiting FGF signalling by injection of the FGFR inhibitor SU5402 reduced the number of NSCs (Dang and Tropepe, 2010). This finding suggests that FGF also promotes neural induction in mouse embryos. Although the treatment of mouse embryos with SU5402 reduced the generation of NSCs, it did not completely inhibit neural induction. This may be due to insufficient SU5402 being given, the time of treatment not being long enough, or FGF not being the only instructive neural induction signal in mouse embryos (Gaulden and Reiter, 2008).

1.5.1.3 Erk signalling is responsible for FGF-directed neural induction

FGFs exert their actions via binding to heparin or heparan sulfate proteoglycans, which helps FGFs bind to FGFRs and cause their dimerisation (Pellegrini, 2001; Schlessinger et al., 2000). Autophosphorylation of the receptors occurs upon dimerisation (Furdui et al., 2006), and this leads to the activation of three intracellular signal transduction pathways, Erk1/2, PLCγ (phospholipase C gamma), and

PI3K (phosphoinositide 3-kinase) (Fig. 1.8; Carballada et al., 2001; Kim et al., 2003; Kouhara et al., 1997; Tsang and Dawid, 2004). FGF signalling via Erk signalling is the pathway that is most important for neural induction (Kuroda et al., 2005; Stavridis et al., 2007; Yoo et al., 2011). Evidence for this statement arises from the observation that when FGF/PLC or FGF/PI3K signalling is inhibited during the period of neural induction, neural progenitors are still generated (Nutt et al., 2001; Stavridis et al., 2007).

In FGF/PLC signalling, the activation of PLCγ converts phosphatidylinositol 4,5-bisphosphate (PIP_2) to inositol 1,4,5-triphosphate (IP_3) and diacylglycerol (DAG) (Peters et al., 1992). IP_3 activates the IP_3 receptor (IP_3R) in the membrane of endoplasmic reticulum (ER) causing the release of Ca^{2+} into the cytosol and thus an increase in cytosolic Ca^{2+} ($[Ca^{2+}]_i$, for further detail on this process see section 1.5.4.4). DAG activates protein kinase C (PKC) and then PKC interacts with Raf and activates the MEK/Erk cascade (Ueda et al., 1996). If FGF/PLC signalling is required in neural induction, then the inactivation of the PLC pathway should suppress neural specificity of ectodermal cells. Sprouty is an intracellular antagonist of FGF/PLC signalling and its expression is not down-regulated in *Xenopus* embryos until the late gastrula stage by which time neural induction is complete (Nutt et al., 2001; Sivak et al., 2005). Therefore during gastrulation, FGF/PLC signalling is repressed by Sprouty, suggesting that the activation of FGF/PLC signalling is not crucial for neural induction in *Xenopus*. This is further supported by the observation that PLCγ1 null mouse embryos die at 9.0 dpc, but the neural tube is already formed at this stage (Ji et al., 1997).

In FGF/PI3K signalling, the activation of PI3K phosphorylates phosphatidylinositol-4,5-bisphosphate and turns it into phosphatidylinositol-3,4,5-trisphosphate, which activates 3-phosphoinositide dependent protein kinase-1 (PDK1) (Stitt et al., 2004).

In turn, PDK1 activates Akt (also known as protein kinase B) and Akt interacts with downstream targets, including glycogen synthase kinase 3, forkhead box O transcription factors, mammalian target of rapamycin (mTOR), $p70^{S6K}$, and BCL2-associated agonist of cell death, to regulate apoptosis and cell cycle entry (Cross et al., 1995; Engelman, 2009; Nave et al., 1999; Scott and Lawrence, 1997; Stitt et al., 2004). If FGF/PI3K signalling is required in neural induction, then the inactivation of PI3K pathway should suppress neural specificity of ectodermal cells; however, this is not the case. In chick embryos, the implantation of LY294002 (a specific inhibitor of PI3K) soaked beads into the embryonic ectoderm did not inhibit expression of the neural plate marker *Sox3* (Stavridis et al., 2007). Furthermore, PDK1-deficient ESCs (where PI3K/PDK1/Akt signalling will not be activated) still express the neuroectodermal marker Sox1 and generate Nestin-expressing NSCs (Stavridis et al., 2007). In addition, PDK1 null mouse embryos die at 9.5 dpc with a normal neural tube having been formed (Lawlor et al., 2002). These findings suggest that PI3K signalling like PLC signalling is not necessary for neural induction.

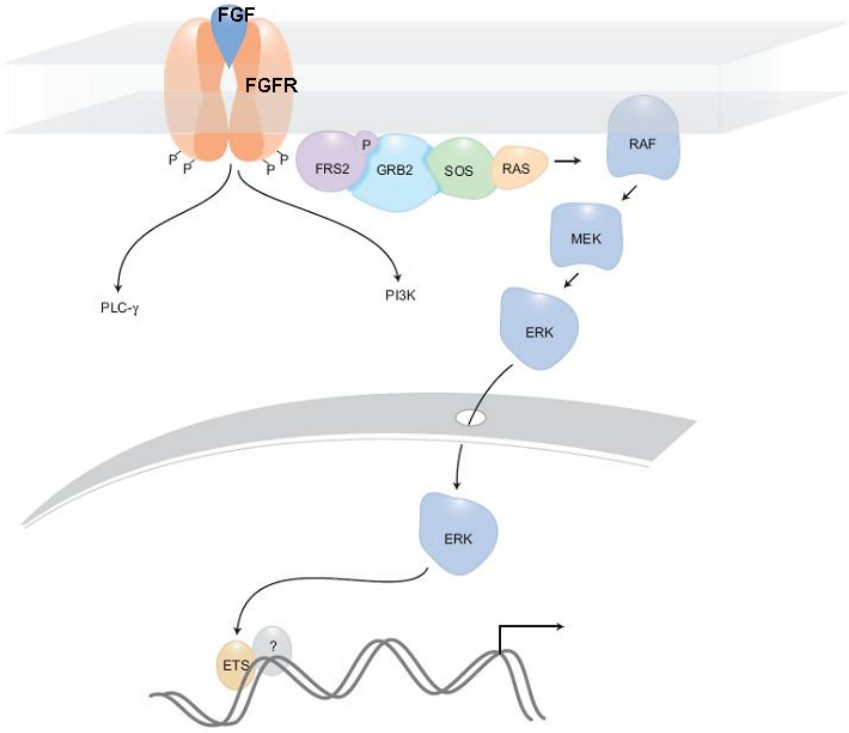

Fig. 1.8. The FGF/Erk signalling pathway.
The binding of FGF to FGFR induces the dimerisation and autophosphorylation of FGFR leading to the activation of three intracellular signal transduction pathways, Erk1/2, PLCγ, and PI3K. In FGF/Erk signalling, the activated FGFR phosphorylates FRS2, and then recruits GRB2 and SOS to activate Ras through the exchange of bound GDP for GTP. Ras-GTP binds with Raf and then phosphorylates MEK. In turn MEK phosphorylates Erk1/2. p-Erk1/2 can phosphorylate the C-terminal domain of the transcription factor Elk1 (a member of the ternary complex factor family of Ets domain proteins), and then changes its ternary complex formation to facilitate the binding to the promoter region of *c-fos*, *Mcl1*, *Zif268* or *Bcl10*, resulting in the up-regulating of genes that control the cell cycle. In addition, tp-Erk1/2 phosphorylates PARP-1 and induces the generation of neural progenitors in human ESCs.
Abbreviations: Erk1/2, Extracellular Signal-regulated Kinase 1/2; ESC, embryonic stem cell; FGF, Fibroblast growth factor; FGFR, FGF receptor; FRS2, Fibroblast growth factor receptor substrate 2; GDP, Guanosine diphosphate; GTP, Guanosine triphosphate; GRB2, Growth factor receptor bound protein 2; MEK, Mitogen-activated Protein/Extracellular Signal-regulated Kinase Kinase; PARP-1, poly (ADP-ribose) polymerase 1 ; PI3K, phosphoinositide 3-kinase; PLCγ, phospholipase C gamma; p-Erk1/2, phosphorylated Erk1/2; SOS, Son of sevenless.
(Adapted from Tsang and Dawid, 2004)

In FGF/Erk signalling, the activated FGFR phosphorylates FRS2 (Fibroblast growth factor receptor substrate 2), and then recruits Grb2 (Growth factor receptor bound protein 2) and Sos (Son of sevenless) to activate Ras through the exchange of bound GDP for GTP (Fig. 1.8). Ras-GTP binds with Raf and then phosphorylates MEK. In turn MEK

phosphorylates Erk1/2 (Thisse and Thisse, 2005; Tsang and Dawid, 2004). The phosphorylated Erk1/2 (p-Erk1/2) can then phosphorylate specific transcription factors that regulate expression of target genes (Chang et al., 2003). For example, p-Erk1/2 phosphorylates the C-terminal domain of the transcription factor Elk1, and this changes its ternary complex formation to facilitate the binding to the promoter region of *c-fos, Mcl1, Zif268* or *Bcl10*, resulting in up-regulating genes expression to control the cell cycle (Boros et al., 2009; Davis et al., 2000; Gille et al., 1995; Huang et al., 2000; Janknecht et al., 1993). In addition, it has been shown that the p-Erk1/2 phosphorylates PARP-1 (poly (ADP-ribose) polymerase 1) activating it (Kauppinen et al., 2006). Indeed, the activity of PARP-1 was increased during neural differentiation of human ESCs and was reduced by treatment with the FGFR inhibitor SU5402 or the MEK inhibitor U0126 (Yoo et al., 2011). Further, PARP-1 can bind to the promotor region of the NSC markers SOX2 and PAX6, and the treatment of human ESCs with a specific inhibitor of PARP-1 significantly reduced the generation of SOX2 or PAX6-epxressing neural progenitors (Yoo et al., 2011), suggesting that the activation of PARP-1 promotes neural induction in human ESCs and FGF/Erk signalling may induce neural induction by activation of PARP-1.

If FGF/Erk signalling is required for neural induction, then the inactivation of Erk1/2 should suppress the expression of neural specific genes in ectodermal cells. This assumption was tested using animal cap cells that upon dispersion give rise to neural tissue (for details see section 1.3, Munoz-Sanjuan and Brivanlou, 2002). When these dispersed ectodermal cells were cultured with the MEK specific inhibitor U0126 to inhibit the phosphorylation of Erk1/2, *Cytokeratin*-expressing epidermal tissue was generated instead of neural tissue (Kuroda et al., 2005). This suggests that the activation of Erk1/2 is pivotal in neural induction of *Xenopus*. In chicken embryos, the implantation of PD184352 (a specific inhibitor of MEK) soaked beads into the prospective neural ectoderm inhibited the expression of the neural plate markers *Sox2* and *Sox3* (Stavridis et al., 2007). Further to this, the generation of Sox1-expressing

neuroectodermal cells form mouse ESCs or PAX6-expressing NSCs form human ESCs was significantly reduced when the phosphorylation of Erk1/2 was inhibited by PD184352 or U0126 (details see section 1.6.2; Stavridis et al., 2007; Yoo et al., 2011).

In conclusion, form the experiments described above, it appears that FGF signalling via Erk is important for neural induction in vertebrates.

1.5.1.4 The crosstalk between FGF/Erk and BMP signalling in neural induction

As described above both FGF/Erk (for details see section 1.5.1.1 and 1.5.1.3) and BMP signalling pathways (for details see section 1.2 and 1.3) are involved in neural induction in vertebrates, and data reveals that there is crosstalk between these two pathways (Fig. 1.9; Kuroda et al., 2005; Pera et al., 2003). In the BMP signalling pathway, BMPs bind and activate their receptors, that in turn phosphorylate Smad1 at the C-terminus (Massague and Chen, 2000). The C-ter-p-Smad1 (C-terminal phosphorylated Samd1) goes on to activate target genes, such as *Msx1*, *Msx2*, and *Vent2* that inhibit neural induction (for details see section 1.1.4; Pera et al., 2003; Phippard et al., 1996; Suzuki et al., 1997). Smad1 consists of MH1 (N-terminal Mad Homology 1) and MH2 (C-terminal Mad Homology 2) domains, which are separated by a linker region (Pera et al., 2003; Shi and Massague, 2003). The activated BMPR interacts with the MH2 domain of Smad1 and this interaction results in the Smad1 C-terminal region being phosphorylated. C-ter-p-Smad1 translocates to the nucleus and once there the MH1 domain binds the promoter region of its target genes, activating them. The linker region of Smad1 contains Erk1/2 phosphorylation sites (Pera et al., 2003; Sapkota et al., 2007). In *Xenopus,* mouse, and human cell lines, it has been demonstrated that the linker region is phosphorylated by p-Erk1/2 and this phosphorylation results in the inhibition of BMP signalling through C-ter-p-Smad1 polyubiquitination (Aubin et al., 2004; Fuentealba et al., 2007; Kretzschmar et al., 1997a; Kuroda et al., 2005; Pera et al., 2003; Sapkota et al., 2007).

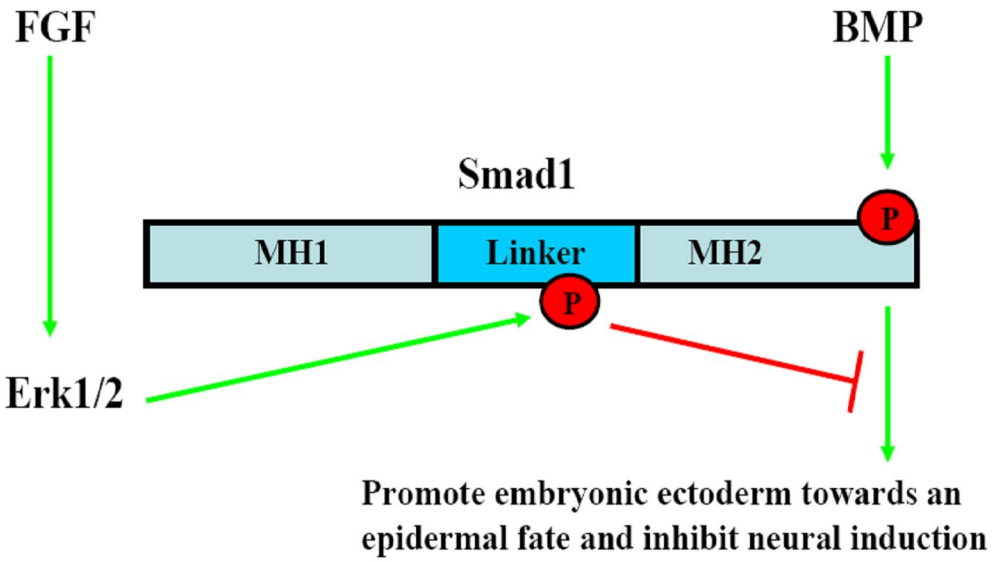

Fig. 1.9. The BMP signalling pathway is inhibited by FGF/Erk signalling during *Xenopus* neural induction.
Smad1 is the intracellular protein that mediates BMP signalling. It consists of MH1 and MH2 domains that are separated by a linker region. The activation of the BMP signalling pathway causes the phosphorylation of Smad1 at its C-terminus. The C-ter-p-Smad1 goes on to activate target genes, such as *Msx1*, *Msx2*, and *Vent2*, and this pushes embryonic ectoderm towards an epidermal fate and inhibits a neural fate in *Xenopus*. The linker region of Smad1 contains Erk1/2 phosphorylation sites. When FGF/Erk signalling is activated, the linker region is phosphorylated by p-Erk1/2, and this causes polyubiquitination and degradation of Smad1, and inhibition of BMP signalling.
Abbreviations: BMP, Bone morphogenetic protein; C-ter-p-Smad1, C-terminus phosphorylated Smad1; Erk1/2, Extracellular Signal-regulated Kinase 1/2; FGF, Fibroblast growth factor; MH1, N-terminal Mad Homology 1; MH2, C-terminal Mad Homology 2; p-Erk1/2, phosphorylated Erk1/2.
(Modified from Pera et al., 2003)

When the Erk1/2 phosphorylation sites of the linker region are mutated preventing phosphorylation by p-Erk1/2, the Smad1 C-terminal region can still be phosphorylated by the activation of BMP signalling (Kretzschmar et al., 1997a). As described in section 1.5.1.1, the injection of *Fgf8* mRNA into *Xenopus* embryos induced the formation of ectopic *Sox2*-expressing neural tissue. It had been shown that this neural induction was blocked when a linker mutant Smad1 mRNA was co-injected with *Fgf8* (Pera et al., 2003). This occurs because the linker mutant Smad1 cannot be phosphorylated and therefore marked for degradation by p-Erk1/2, thus the inhibitory effect of BMP signalling on neural induction remains. Similarly, the injection of *Fgf8* mRNA into

animal cap explants caused the up-regulation of expression of the neural plate marker *NCAM* and the down-regulated of expression of the epidermal markers *Cytokeratin*, *Msx1*, and *Vent2*. When *Fgf8* and the linker mutant Smad1 mRNA were injected at the same time, the expression of the epidermal markers *Cytokeratin*, *Msx1*, and *Vent2* were up-regulated, and the neural marker *NCAM* was down-regulated (Pera et al., 2003). These results suggest that the inhibitory effect of BMP signalling on neural induction in *Xenopus* is repressed when the linker region of Smad1 is phosphorylated by the activation of FGF/Erk signalling (Fig. 1.9). However, these experiments did not exclude the possibility that as well as antagonising BMP signalling, FGF/Erk signalling also provides an instructive cue to induce neural induction.

If FGF/Erk signalling was only required for blockage of BMP signalling to allow neural induction to occur, then one might expect that inhibition of BMP signalling would induce neural induction in *Xenopus* regardless of FGF/Erk signalling. However, this is not the case, since in the absence of FGF signalling, inhibition of BMP signalling does not induce neural induction (Delaune et al., 2005; Marchal et al., 2009). Delaune et al. found that although the injection of *Smad6* mRNA into *Xenopus* embryos induced the expression of neural plate markers *Sox2* and *NCAM* in animal cap explants, which may be due to the repressive effect of Smad6 on BMP signalling (see section 1.4.1), this generation of *Sox2* and *NCAM*-expressing neural tissue was abolished when the explants were co-treated with *Smad6* and FGFR inhibitor SU5402. This study showed that the inhibition of BMP signalling alone is not enough to induce neural induction. Similarly, ectopic *Sox2*-expressing neural tissue was induced and the generation of *Keratin 81*-expressing epidermal tissue was suppressed in *Xenopus* embryos when BMP signalling was blocked by knocking down *Smad5* (Marchal et al., 2009). Further, when these *Smad5* knock-down embryos were treated with SU5402 or injected with antisense oligos to *Fgf4* to inhibit FGF signalling, the knocking down *Smad5* no longer induced ectopic *Sox2*-expressing neural tissue, but the epidermal marker *Keratin 81* was still suppressed because of

inhibition of BMP signalling (Marchal et al., 2009). In addition, inhibiting BMP signalling by injection of *Smad7* mRNA into *Xenopus* embryos induced ectopic neural tissue and this ectopic neural induction was enhanced by FGF activation (Wawersik et al., 2005). These findings imply that FGF signalling not only acts by inhibiting BMP signalling, but also provides an instructive signal to the ectoderm of *Xenopus* to develop along a neural pathway (Aruga and Mikoshiba, 2011).

Evidence has shown that Wnt signalling also plays a role in neural induction (del Barco Barrantes et al., 2003), but unlike FGF/Erk signalling that promotes neural induction, Wnt signalling suppresses the neural differentiation of embryonic ectodermal cells (Glinka et al., 1998; Wilson et al., 2001).

1.5.2 The role of Wnt signalling in neural induction

During early embryogenesis in *Xenopus*, Wnt signalling has complex roles in neural induction (Gaulden and Reiter, 2008). At the blastula stage, the organiser region expresses the BMP antagonist *Chordin*. The activation of Wnt signalling by injection of *Xenopus* embryos with *Wnt8* or *β-catenin* mRNA increased the expression of *Chordin* in the organiser region, and conversely the inactivation of Wnt signalling by injection of *Xenopus* embryos with a dominant-negative Wnt8 mRNA inhibited the expression of *Chordin* (Glinka et al., 1998; Wessely et al., 2001). These observations suggest that prior to the gastrulation, Wnt signalling promotes the formation of the organiser, which in turn enhances neural induction during gastrulation. However, the organiser also expresses the Wnt antagonist, *Dickkopf-1* (Glinka et al., 1998; Kazanskaya et al., 2000). At the late blastula stage when the orgainser is formed, an antibody against Dickkopf-1 was injected into the blastocoel of *Xenopus* embryos, and this resulted in the generation of embryos with severe microcephaly and even (in 5% of embryos) complete deletion of brain structures, suggesting that the Wnt antagonist Dickkopf-1 is required for neural differentiation of the ectoderm after the formation of the organiser (Glinka et al., 1998).

The animal cap of *Xenopus* embryos consists of embryonic ectodermal cells, and dissociated animal cap cells cultured in the absence of any growth factors give rise to neural tissue and express the neural plate marker *NCAM* (for details see section 1.2 and 1.3; Grunz and Tacke, 1989; Munoz-Sanjuan and Brivanlou, 2002). When the dissociated animal cap cells were cultured with lithium chloride to activate Wnt signalling, the expression of *NCAM* was decreased while the expression of epidermal marker *Cytokeratin was increased* (Fuentealba et al., 2007). This result implies that the activation of Wnt signalling in embryonic ectodermal cells reduces the generation of neuroectoderm. In conclusion, the above experiments suggest that Wnt signalling is needed at the blastula stage for specification of the organiser, but this signalling then needs to be suppressed to allow neural induction to occur.

Similarly in chick and mouse, Wnt signalling also plays a role in neural induction (del Barco Barrantes et al., 2003; Wilson et al., 2001). Prospective neural ectodermal explants isolated from chick embryos do not express *Wnt3a*, *Wnt8*, or *BMP4* (Wilson et al., 2001). When such explants were cultured with Wnt3a, the expression of *BMP4* was induced, which promoted the generation of Msx1 and Msx2-expressing epidermal tissue, and neural tissue was no longer generated from the prospective neural ectodermal explants (Patthey et al., 2009; Wilson et al., 2001), suggesting that the activation of Wnt signalling suppresses neural induction in chick. Conversely, the prospective non-neural ectodermal explants isolated from chick embryos express *Wnt3a*, *Wnt8*, and *BMP4* (Wilson et al., 2001). When these explants were cultured with a soluble fragment of Frizzled protein to suppress Wnt signalling, not only was the expression of Msx1, Msx2, and BMP4 inhibited, but the generation of Sox2 and Sox3-expressing neural tissue was induced (Patthey et al., 2009; Wilson et al., 2001). This result suggests that inhibiting Wnt signalling induces neural induction in chick. Further to this, *Wnt3a* is expressed in the ectoderm of wild type mouse embryos and *Wnt3a* knockout mouse embryos develop an additional neural tube at 8 dpc (Yoshikawa et al.,

1997). This finding implies that inhibiting Wnt signalling induces ectodermal cells to take on a neural phenotype. In line with this, *Dickkopf-1* null mouse embryos did not express the anterior neuroectodermal markers *Hesx1* and *Six3* (Mukhopadhyay et al., 2001). *Hesx1* and *Six3* are expressed in the anterior neural plate of wild type mouse embryos and are required for the development of forebrain (Dattani et al., 1998; Lagutin et al., 2003; Martinez-Barbera et al., 2000; Mukhopadhyay et al., 2001; Oliver et al., 1995).

It has been shown that Activin/Nodal signalling also plays a role in neural induction (Wessely et al., 2001). Like Wnt and BMP signals, the activation of Activin/Nodal signalling suppresses the neural differentiation of embryonic ectodermal cells (Chang and Harland, 2007).

1.5.3 The role of Activin/Nodal signalling in neural induction

In vertebrates, Activin/Nodal signalling plays important roles in embryogenesis and the activation of this pathway promotes mesodermal and endodermal development (Agius et al., 2000; Aoki et al., 2002; Camus et al., 2006; Johansson and Wiles, 1995; Kispert et al., 1995; Osada and Wright, 1999; Poulain et al., 2006; Tremblay et al., 2000). Smad2 and Smad3 are the intracellular effectors of Activin/Nodal signalling (in contrast to BMP signalling where the effectors are Smad1/5/8, see section 1.4.1). The activation of Activin/Nodal signalling causes the phosphorylation of Smad2 and Smad3, and in turn phosphorylated Smad2/3 forms a protein complex with Smad4 (Nakao et al., 1997). This complex enters the nucleus to activate target genes, such as *Foxa2*, *Goosecoid*, and *Pitx2* (Arnold and Robertson, 2009; Faucourt et al., 2001; Heldin et al., 1997; Vincent et al., 2003). Foxa2 is expressed in the anterior primitive streak of mouse embryos, and *Foxa2* null mouse embryos failed to develop foregut and midgut endoderm, suggesting that Foxa2 is required for endodermal development (Dufort et al., 1998). Goosecoid is expressed in anterior mesoderm during gastrulation and controls the migration of mesodermal cells, suggesting that Goosecoid plays an important role in mesodermal patterning (Blum et al., 1992; Niehrs et al.,

1993; Niehrs et al., 1994). Pitx2 is expressed in the prospective mesoderm and endoderm of *Xenopus* embryos, and the injection of *Pitx2* mRNA into *Xenopus* embryos at the 4-cell stage induced the ectopic expression of the mesodermal marker *Goosecoid* and endodermal marker *Sox17*, suggesting that Pitx2 is involved in mesodermal and endodermal induction (Faucourt et al., 2001).

When *Smad2* mRNA was injected into *Xenopus* embryos at the 32 to 64-cell stage to activate Activin/Nodal signalling, ectopic MyoD-expressing mesodermal tissue was observed together with an inhibition of expression of the neural markers *Sox2* and *Sox3* in the neural plate (Chang and Harland, 2007). This result suggested that Activin/Nodal signalling inhibited the development of embryonic ectoderm along a neural pathway in *Xenopus*. Conversely the injection of a truncated Activin receptor IB or mRNA of the Nodal antagonist *Lefty* into *Xenopus* embryos to suppress Activin/Nodal signalling induced the generation of ectopic neural tissue, as assessed by the expression of the neural plate marker *NCAM*, and decreased the expression of the mesoderm markers *Actin* and *Globin* (Wessely et al., 2001). This result suggests that inhibition of Activin/Nodal signalling helps specify ectoderm along a neural pathway. Similarly *Nodal* null mouse embryos generate Sox1-expressing neuroectodermal cells precociously; at 6.25 dpc rather than at 7.75 dpc as observed in wild type embryos. Further, when the neural plate of *Nodal* null embryos was dissected and cultured for 48 hours *in vitro*, it generated more neuronal cells than did wild type embryos (Camus et al., 2006). These results suggest that inhibition of Activin/Nodal signalling promotes neural induction in mouse.

Evidence has shown that calcium also plays a role in neural induction in *Xenopus* embryos (Leclerc et al., 2003; Leclerc et al., 2000), but unlike BMP, Wnt, and Activin/Nodal pathways that act to repress neural induction, an increase in $[Ca^{2+}]_i$ helps specify ectoderm along a neural pathway in *Xenopus* embryos (Batut et al., 2005).

1.5.4 Calcium plays a pivotal role in neural induction of *Xenopus*

In addition to FGF, an increase in cytosolic Ca^{2+} has also been demonstrated to be required for neural induction in Zebrafish and *Xenopus*. So far, most of reports regarding the role of calcium in neural induction have been obtained from non-mammalian models (Leclerc et al., 2011). In Zebrafish embryos, levels of Ca^{2+} have been imaged throughout early embryogenesis by injecting the Ca^{2+} indicator aequorin into eggs. Using this methodology it has been shown that during early gastrulation when neural induction occurs, $[Ca^{2+}]_i$ is increased in the prospective neural ectoderm (Creton et al., 1998; Gilland et al., 1999), suggesting that an increase in $[Ca^{2+}]_i$ may play a role in neural induction of Zebrafish.

Furthermore, some studies have revealed that calcium also plays a role in neural induction in amphibians (Batut et al., 2005; Leclerc et al., 1997; Leclerc et al., 2003; Moreau et al., 2008). Again the Ca^{2+} indicator aequorin was used. In aequorin injected *Xenopus* embryos, an increase in $[Ca^{2+}]_i$ was observed during gastrulation in the dorsal ectoderm, which contains the prospective neural ectoderm. In contrast, no increase in $[Ca^{2+}]_i$ was observed in the ventral ectoderm, which will differentiate into epidermis (Leclerc et al., 2003; Leclerc et al., 2000). Thus an increase in $[Ca^{2+}]_i$ is seen in the prospective neural ectoderm during neural induction in *Xenopus* embryos, suggesting that Ca^{2+} may play a role in this process, as reported for Zebrafish.

1.5.4.1 An increase in $[Ca^{2+}]_i$ induces neural induction in *Xenopus*

Animal cap assays (see section 1.3 for details) reveal that an increase in $[Ca^{2+}]_i$ induces ectodermal cells to take on a neural identity (Batut et al., 2005). The treatment of animal cap explants with caffeine to increase $[Ca^{2+}]_i$, by activation of the RyRs (ryanodine receptors) in the membrane of ER (details see section 1.5.4.4; McPherson et al., 1991), up-regulated the expression of *xPRMT1b* (*Xenopus* protein arginine methyltransferase type I b) (Batut et al., 2005). xPRMT1b is a member of the protein arginine N-methyltransferase family that catalyses the methylation of arginine residues to regulate transcriptional activation (Pawlak et al.,

2000; Wang et al., 2001). This increased expression of *xPRMT1b* activates the expression of neural genes (*Zic3*, *Neurogenin*, *NCAM*, and *N-tubulin*) to drive animal cap explants towards to a neural fate (Batut et al., 2005; Moreau et al., 2008). Further to this, injecting *xPRMT1b* into one side of a *Xenopus* embryo expanded the domain of *Zic3* and *N-tubulin*-expressing neural plate cells when compared with the uninjected side (Batut et al., 2005). Thus, the exposure of animal caps to caffeine caused an increase in $[Ca^{2+}]_i$ that in turn increased the expression of *xPRMT1b* promoting neural induction in *Xenopus*. Therefore the increase in $[Ca^{2+}]_i$ is an instructive signal for neural induction in *Xenopus*.

1.5.4.2 Preventing the elevation of $[Ca^{2+}]_i$ suppresses neural induction in *Xenopus*

If an increase in $[Ca^{2+}]_i$ induces neural induction in *Xenopus*, then preventing the increase in $[Ca^{2+}]_i$ should suppress this process. This is supported by studies where *Xenopus* embryos were cultured with an L-type calcium channel blocker, R(+)BayK, from the blastula stage to the gastrula stage. Here the Ca^{2+} influx from extracellular fluids into the cytosol through L-type calcium channels was blocked and the elevation of $[Ca^{2+}]_i$ was abolished in the dorsal ectoderm (Leclerc et al., 2000). In this culture condition, the expression of the early neural genes *Zic3* and *Geminin* was down-regulated (Leclerc et al., 2000) at the gastrula stage, while both genes were normally expressed in neuroectoderm of untreated embryos (Fujimi et al., 2006; Kroll et al., 1998; Rogers et al., 2009). The finding suggests that preventing the elevation of $[Ca^{2+}]_i$ suppresses neural induction of *Xenopus* embryos. In Zebrafish embryos, the number of motor neurons was reduced within the spinal cord when embryos were treated with a Ca^{2+} chelator, BAPTA, to reduce the free cytosolic Ca^{2+} (Ashworth et al., 2001). This result suggested that an increase in $[Ca^{2+}]_i$ is required for neurogenesis, but it is unknown whether the reduction in neurogenesis is due to the suppression of neural induction in Zebrafish embryos or the inhibition of neuronal differentiation of neural progenitors to generate neurons. So far, there is no published data to

distinguish if or not the increase in $[Ca^{2+}]_i$ is required for neural induction in Zebrafish embryos.

Similarly, as describe above, culturing animal cap explants with a BMP antagonist Noggin induced the generation of neural tissue and the expression of the neural plate marker *NCAM* (see section 1.3). This expression of *NCAM* was shown to be diminished significantly by adding R(+)BayK or BAPTA into the culture medium to prevent an increased in $[Ca^{2+}]_i$ (Batut et al., 2005; Leclerc et al., 2000). Thus preventing an increase in $[Ca^{2+}]_i$ suppressed neural induction, which was induced by the treatment of animal cap explants with the BMP antagonist Noggin. When *Xenopus* animals cap cells were dissociated and grown as dispersed cells in culture in the absence of any growth factors or inhibitors, these dissociated cells gave rise to neural tissue, as detected by the expression of *NCAM* (see section 1.3; Grunz and Tacke, 1989; Wilson et al., 1997). This *NCAM* expression could again be reduced by addition of the calcium chelator BAPTA into the culture medium (Leclerc et al., 2000). These results suggested that the increase in $[Ca^{2+}]_i$ was required for neural induction, and that preventing this increase repressed neural induction in *Xenopus* embryos or animal cap explants.

1.5.4.3 An increase in $[Ca^{2+}]_i$ activates Erk signalling

As discussed in section 1.5.1, the activation of FGF/Erk signalling induces neural induction. It has also been demonstrated that an increase in $[Ca^{2+}]_i$ activates Erk signalling (Kupzig et al., 2005; Riddle et al., 2006). RasGRP (Ras guanyl-releasing protein) is a nucleotide exchange factor with calcium and DAG binding motifs. An increase in $[Ca^{2+}]_i$ activates RasGRP, which in turn activates Ras through the exchange of bound GDP for GTP, and then Ras-GTP activates the Raf/MEK/Erk protein kinase cascade (Fig.1.10; Agell et al., 2002; Ebinu et al., 1998; Kupzig et al., 2005). This leads to a reasonable assumption that an increase in $[Ca^{2+}]_i$ induces ectodermal cells in *Xenopus* to take on a neural fate via the activation of Erk signalling. Within my thesis, I

investigate this assumption and ask whether an increase in $[Ca^{2+}]_i$ induces the activation of Erk signalling in mouse ESCs and promotes the generation of NSCs (see Chapter 5).

Tg (thapsigargin) is a specific inhibitor of Apt2a/SERCA (sarcoendoplasmic reticulum Ca^{2+}-ATPase) (Lytton et al., 1991). It prevents cytosolic Ca^{2+} being pumped into the ER by Apt2a/SERCA thus causing an increase in $[Ca^{2+}]_i$ (details see section 1.5.4.4). In Hela cells, treatment with Tg increases the $[Ca^{2+}]_i$, Ras-GTP (the active form of Ras), and p-Erk1/2. Erk1/2 is no longer phosphorylated when Hela cells are treated with a MEK inhibitor, U0126 (Kupzig et al., 2005). These results suggest that Tg induces an increase in $[Ca^{2+}]_i$ and activates Erk signalling via the Ras/Raf/MEK/Erk protein kinase cascade (Fig. 1.10). In line with this, when human mesenchymal stem cells or Jurkat T-cells were treated with Tg, p-Erk1/2 was increased. The phosphorylation of Erk1/2 can be inhibited by the membrane permeable calcium chelator BAPTA-AM and the MEK inhibitor U0126, but not by the PLC inhibitor U73343 or the PKC inhibitor GF109203X (Denys et al., 2004; Riddle et al., 2006). The results imply that an interaction between Ca^{2+} and Erk signalling happens in different cell-types. If this interaction exists in ectodermal cells of *Xenopus*, then an increase in $[Ca^{2+}]_i$ may induce neural induction by the activation of Erk signalling.

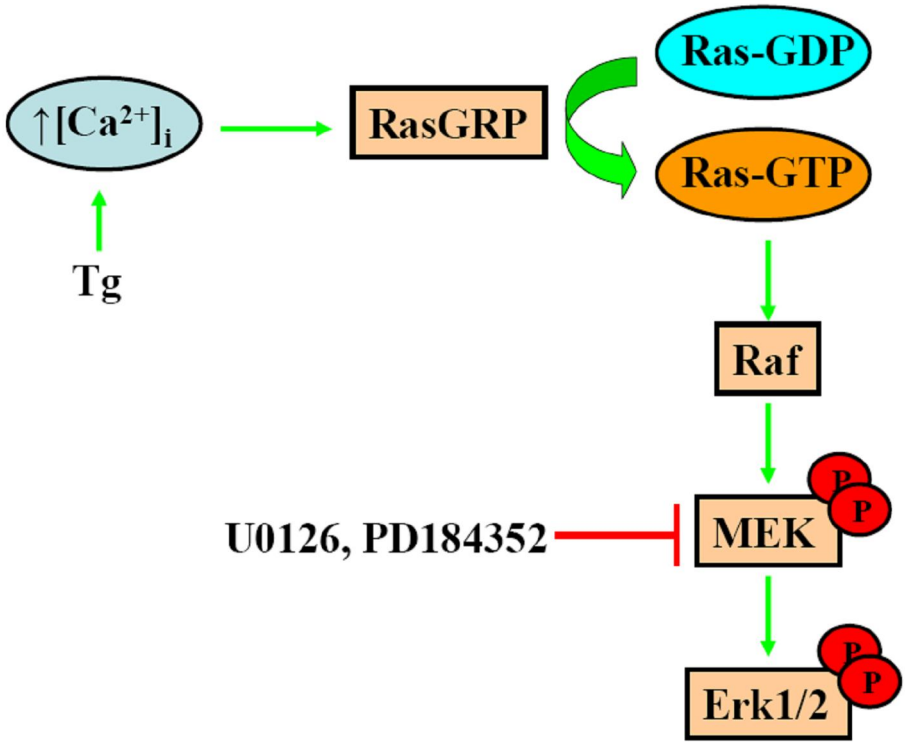

Fig. 1.10. An increase in $[Ca^{2+}]_i$ activates Erk signalling pathway.
Tg causes an increase in $[Ca^{2+}]_i$ and in turn activates RasGRP. The active RasGRP activates Ras through the exchange of bound GDP for GTP. Ras-GTP activates the Raf/MEK/Erk protein kinase cascade. Therefore an increase in $[Ca^{2+}]_i$ activates Erk1/2 through this pathway. U0126 and PD184352 are inhibitors of MEK and can block the phosphorylation of Erk1/2 to inhibit Erk signalling.
Abbreviations: Erk1/2, Extracellular Signal-regulated Kinase 1/2; GDP, Guanosine diphosphate; GTP, Guanosine triphosphate; MEK, Mitogen-activated Protein/Extracellular Signal-regulated Kinase Kinase; RasGRP, Ras guanyl-releasing protein; Tg, Thapsigargin.
(Adapted from Cullen and Lockyer, 2002; Thomas and Huganir, 2004)

1.5.4.4 The movement of Ca^{2+} in cells

Since an increase in $[Ca^{2+}]_i$ induces ectodermal cells to take on a neural fate in *Xenopus*, the movement of Ca^{2+} in cells should be discussed. Ca^{2+} is an important second messenger that is involved in regulating cell proliferation, differentiation, and apoptosis (Berridge et al., 2000; Boehning et al., 2003; Boyce and Ham, 1983; Rodriguez-Mora et al., 2005). When cells are in a resting state, the $[Ca^{2+}]_i$ is approximately 100 nM and the extracellular Ca^{2+} concentration is kept at approximately 2 mM (Fig. 1.11; Clapham, 2007). In eukaryotic cells, Ca^{2+} is stored in the ER, an intracellular network of folded membranes and flattened sacs. The ER is also the site of synthesis of proteins, lipids, and sterols, and

post-translational modification and folding of proteins (Kaufman, 1999). In the membrane of the ER, there are two Ca^{2+} channels, IP_3R (inositol 1,4,5-triphosphate receptor) and RyR, which can release Ca^{2+} from the ER into the cytosol (Clapham, 2007). When non-excitable cells are exposed to growth factors (such as epidermal growth factor and platelet-derived growth factor) or neurotransmitters (dopamine, glutamate, and serotonin), RTKs, and G protein-coupled receptors respectively are activated. In turn, PLCγ is activated by the receptors, and this converts PIP_2 to IP_3 and DAG (Meisenhelder et al., 1989; Peters et al., 1992). The IP_3 binds to the IP_3R in the ER resulting in Ca^{2+} being released into the cytosol (Clapham, 2007). This increase in cytosolic Ca^{2+} also activates RyR and IP_3R, in a feed back loop, further increasing Ca^{2+} releases from the ER. This feedback stimulation is called the Ca^{2+}–induced Ca^{2+} release (Slusarski and Pelegri, 2007). Therefore IP_3R and RyR play important roles in regulating cytosolic Ca^{2+}. Further to this, Ca^{2+} can also be released from the ER through IP_3R or RyR spontaneously by a process known as spontaneous calcium oscillation (Carroll and Swann, 1992; Missiaen et al., 1991; Stern et al., 1988; Yu et al., 2008b).

In addition to Ca^{2+} being released from the ER, Ca^{2+} also enters the cytosol from the extracellular fluid through Ca^{2+} channels in the plasma membrane of excitable cells, such as neuronal and muscle cells (Clapham, 2007; Gilmore et al., 2009). When these channels are activated by a change of membrane potential (action potential) or ligands (such as acetylcholine, glutamate, serotonin, and ATP) binding to their cell-surface receptors, then the extracellular Ca^{2+} flows rapidly into the cytosol along a large electrochemical potential gradient (Cornell-Bell et al., 1990; Cotrina et al., 1998; Ferezou et al., 2002; Helmchen et al., 1996; Sharma and Vijayaraghavan, 2001). This influx of extracellular Ca^{2+} triggers the release of Ca^{2+} from the ER (Ca^{2+}–induced Ca^{2+} release) by activation of the IP_3R and RyR, as discussed above, resulting in an increase in $[Ca^{2+}]_i$.

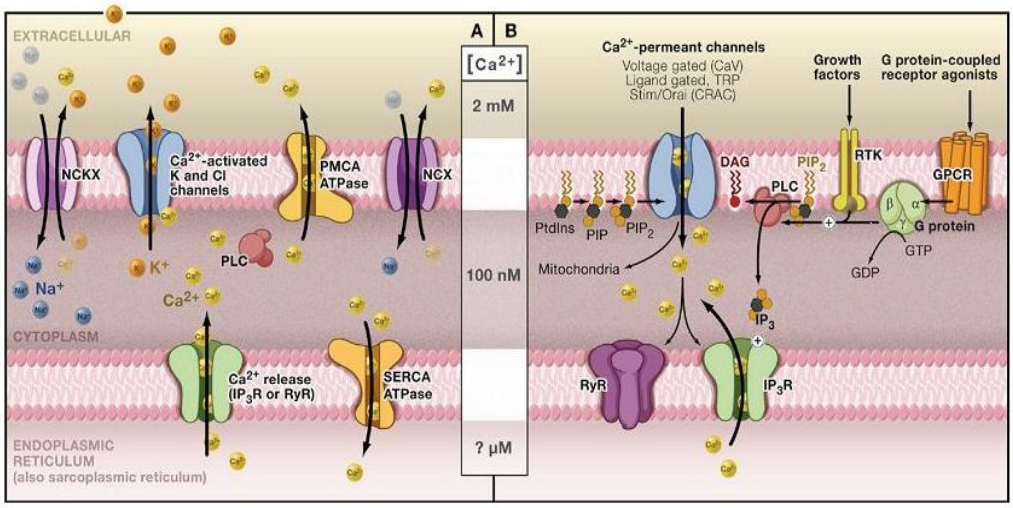

Fig. 1.11. Schematic diagram of the movement of Ca^{2+} in cells.
At rest the Ca^{2+} concentration in the cytosol is low (~100nM), compared with that of the extracellular fluid (~2mM). (A) To maintain this low $[Ca^{2+}]_i$, the Ca^{2+} is extruded by PMCA, NCX, and NCKX. The cytosolic Ca^{2+} is also pumped into the ER via the Atp2a/SERCA. Although some Ca^{2+} is released from the ER into the cytosol through IP_3R or RyR automatically (the so called spontaneous calcium oscillation), $[Ca^{2+}]_i$ is kept at a low level. (B) In non-excitable cells, growth factors (for example, EGF and PDGF) and neurotransmitters (dopamine, glutamate, and serotonin) activate RTKs and GPCRs respectively. The activated RTK or GPCR activates PLC and this results in the conversion of PIP_2 to IP_3 and DAG. IP_3 activates IP_3R and releases Ca^{2+} from the ER into the cytosol. The cytosolic Ca^{2+} also activates the RyR and causes more Ca^{2+} release. In excitable cells, there are voltage- or ligand-gated calcium channels in the plasma membrane. Activation of these channels by an action potential or neurotransmitters leads to rapid Ca^{2+} influx. The influx of extracellular Ca^{2+} also triggers the release of Ca^{2+} from the ER (Ca^{2+}–induced Ca^{2+} release) by activation of the IP_3R and RyR, resulting in an increase in $[Ca^{2+}]_i$.
Abbreviations: Atp2a/SERCA, sarcoendoplasmic reticulum Ca^{2+}-ATPase; $[Ca^{2+}]_i$, concentration of cytosolic Ca^{2+}; DAG, diacylglycerol; EGF, epidermal growth factor; ER, endoplasmic reticulum; GPCR, G protein-coupled receptor; IP_3 ,inositol 1,4,5-triphosphate; IP_3R, IP_3 receptor; NCKX, Na^+/Ca^{2+}-K^+ exchanger; NCX, Na^+/Ca^{2+} exchanger; PDGF, platelet-derived growth factor; PIP_2, phosphatidylinositol 4,5-bisphosphate; PLC, phospholipases C; PMCA, plasma membrane Ca^{2+}-ATPase; RTK, receptor tyrosine kinase; RyR, ryanodine receptor. (Adapted from Clapham, 2007)

The increase in $[Ca^{2+}]_i$ furthers the binding of cytosolic Ca^{2+} to intracellular Ca^{2+}-binding proteins, and then triggers Ca^{2+}-dependent events (Klipp and Liebermeister, 2006). For example, calmodulin is a well-known intracellular Ca^{2+}-binding protein (Chin and Means, 2000; Goldbeter et al., 1990). Ca^{2+}/calmodulin has been reported to interact with many proteins including neuromodulin, CaM kinase II, and phosphodiesterase (Alexander et al., 1988; Borisy et al., 1992; De

Koninck and Schulman, 1998; Heinzel et al., 1992; Klee et al., 1979; Sobue et al., 1981). Neuromodulin is a neural-specific calmodulin binding protein and its expression is up-regulated during axon growth (He et al., 1997). The interaction between Ca^{2+}, calmodulin, and neuromodulin is involved in the modulation of synaptic plasticity (Husson et al., 2004; Xia and Storm, 2005). CaM kinase II is activated by Ca^{2+}/calmodulin (De Koninck and Schulman, 1998), and it has been demonstrated that CaM kinase II plays an important role in learning and memory (Lisman, 1994; Wei et al., 2002). Ca^{2+}/calmodulin also activates phosphodiesterases that degrade the phosphodiester bond in cAMP (cyclic AMP) and cGMP (cyclic GMP) converting them to AMP and GMP respectively and inhbiting their function (Borisy et al., 1992; Rybalkin et al., 2003). The calmodulin-dependent phosphodiesterases are highly expressed in olfactory sensory neurons where Ca^{2+}/calmodulin terminates the odorant-induced cAMP signalling by phosphodiesterase activation (Borisy et al., 1992; Yan et al., 1995). Therefore, through the interaction of cytosolic Ca^{2+} and Ca^{2+}-binding proteins, the regulation of $[Ca^{2+}]_i$ affects many aspects of biological function. In addition to calmodulin, intracellular Ca^{2+} also binds and activates another protein RasGRP, resulting in the activation of Erk signalling (see section 1.5.4.3). Because the activation of Erk signalling is important for neural induction (for details see section 1.5.1.3), within Chapter 5, I will investigate the interaction between an increase in $[Ca^{2+}]_i$ and Erk signalling during neural induction.

To return $[Ca^{2+}]_i$ to the basal state, cytosolic Ca^{2+} is pushed into the ER or out of the cell by Ca^{2+}-ATPase pumps (Fig. 1.11). In the plasma membrane, the plasma membrane Ca^{2+}-ATPase (PMCA) pump removes Ca^{2+} from the cytosol (Di Leva et al., 2008; Yamoah et al., 1998). Na^+/Ca^{2+} exchangers (NCX) and Na^+/Ca^{2+}-K^+ exchangers (NCKX) also transport cytosolic Ca^{2+} out of the cell (Bers and Bridge, 1989; Clapham, 2007; Kang et al., 2005). Thus PMCA pumps, NCX, and NCKX play roles in maintaining the $[Ca^{2+}]_i$ basal state of these cells (Yanagida et al., 2004). In the ER, the Atp2a/SERCA transports cytosolic Ca^{2+} into the

internal ER store (Slusarski and Pelegri, 2007; Zhong and Inesi, 1998). There are three Atp2a/SERCA genes in vertebrates: ATPase, Ca^{2+} transporting, cardiac muscle, fast twitch 1 (Atp2a1) encoding Atp2a1/SERCA1; ATPase, Ca^{2+} transporting, cardiac muscle, slow twitch 2 (Atp2a2) encoding Atp2a2/SERCA2; and ATPase, Ca^{2+} transporting, ubiquitous (Atp2a3) encoding Atp2a3/SERCA3. In mammals, three Atp2a/SERCA genes encode 12 isoforms through alternative splicing (Pegoraro et al., 2011; Periasamy and Kalyanasundaram, 2007). Atp2a1a/SERCA1a is expressed in adult fast-twitch sketetal muscles, Atp2a1b/SERCA1b is expressed in fetal fast-twitch sketetal muscles, Atp2a2a/SERCA2a and Atp2a2c/SERCA2c are expressed in cardiomyocytes, Atp2a2b/SERCA2b is expressed ubiquitously, and Atp2a3/SERCA3 encodes 6 isoforms and are expressed in non-muscle cells, such as endothelial cells, lymphocytes, fibroblasts, platelets, and epithelial cells (Periasamy and Kalyanasundaram, 2007). Apt2a1/SERCA1 null mutant mice can survive and appear normal at birth, and Apt2a3/SERCA3 null mutant mice develop normally (Prasad et al., 2004). In contrast, Apt2a2/SERCA2 has been shown to be essential for embryonic development as Apt2a2/SERCA2 null mice are embryonic lethal (Periasamy et al., 1999). During *Xenopus* embryonic development, Apt2a2/SERCA2 (but not Apt2a1/SERCA1 and Apt2a3/SERCA3) is expressed in the neural plate and neural tube indicating a role for this gene in aspects of neurogenesis (Pegoraro et al., 2011).

In summary (Fig. 1.12), BMP, Wnt, and Activin/Nodal signals act as negative cues for neural induction in vertebrates, preventing ectodermal cells giving rise to neuroectoderm. The activation of BMP signalling activates Smad1 and its target gene *Msx1,* which pushes ectoderm to an epidermal fate and suppresses neural induction (for details see section 1.4). The BMP antagonists (Noggin, Chordin, and Follistatin) prevent BMP ligands binding to their receptors, resulting in inhibition of BMP signalling and promotion of neural development (for details see sections 1.2 and 1.3). As well as the BMP signal, the activation of Wnt or Activin/Nodal pathways keeps ectodermal cells from taking on a neural fate (for details see sections 1.5.2 and 1.5.3). Conversely, antagonising Wnt or Activin/Nodal signallings by Dickkopf1 or Lefty respectively helps the ectoderm become specified to give rise to neuroectoderm.

In contrast, FGF/Erk and calcium signals function as positive cues for neural induction, with the activation of FGF/Erk signalling or an increase in $[Ca^{2+}]_i$ specifying ectoderm along a neural pathway (Fig. 1.12). Erk1/2 is the effector of FGF signalling and the activated Erk1/2 not only inhibits Smad1 to suppress BMP signalling, but also has an instructive effect on neural induction (for details see sections 1.5.1.3 and 1.5.1.4). Therefore the activation of FGF/Erk signalling helps convert ectodermal cells into neuroectodermal cells. Further, an increase in $[Ca^{2+}]_i$ is required for neural induction in *Xenopus* embryos (for details see sections 1.5.4.1 and 1.5.4.2), and this increase in $[Ca^{2+}]_i$ also activates Erk signalling (for details see section 1.5.4.3). Thus, the increase in $[Ca^{2+}]_i$ may promote neural specification of the ectoderm by activation of Erk signalling.

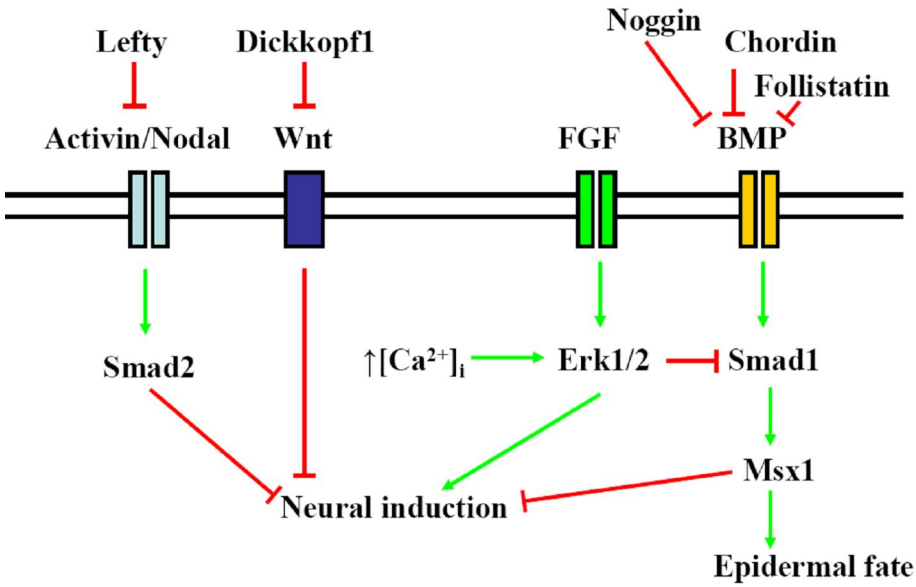

Fig. 1.12. Schematic representation of the mechanisms of neural induction in vertebrates.
The binding of BMP ligands with their receptors activates Smad1, resulting in expression of its target gene *Msx1* which pushes the ectoderm along an epidermal fate and inhibits neural induction. Conversely, the BMP antagonists (Noggin, Chordin, and Follistatin) prevent the binding of BMP ligands to their receptors, resulting in suppression of BMP signalling and promotion of neural induction. The Wnt antagonist Dickkopf1 suppresses Wnt signalling to help the neural specification of ectodermal cells. Activin/Nodal signalling activates Smad2 to prevent the ectoderm taking up a neural fate. Conversely, the Nodal antagonist Lefty suppresses Activin/Nodal signalling resulting in promotion of neural induction. The activation of FGF signalling promotes neural induction via activation of Erk1/2 and suppression of BMP signalling by inhibition of Smad1. In *Xenopus* embryos, an increase in $[Ca^{2+}]_i$ may activate the Erk1/2, and in turn promotes neural induction.
Abbreviations: BMP, Bone morphogenetic protein; $[Ca^{2+}]_i$, concentration of cytosolic Ca^{2+}; Erk1/2, Extracellular Signal-regulated Kinase 1/2; FGF, Fibroblast growth factor.

As discussed above, many studies on neural induction are carried out in amphibian and chick embryos, but only a few experiments are carried out in mouse embryos, because compared with amphibian and chick embryos, mammalian embryos are difficult to access and it is not easy to obtain them in large numbers or to make transgenic embryos. In order to solve this issue, mouse and human ESCs have been used to set up *in vitro* neural differentiation models, which provide platforms to study the mechanism of neural induction in mouse and humans (Abranches et al., 2009; Chambers et al., 2009; Ying et al., 2003).

1.6 Neural induction in ESCs

ESCs are derived from the ICM of the blastocyst and ESCs are pluripotent, being able to differentiate into all cell-types in the body (Evans and Kaufman, 1981; Murry and Keller, 2008). Thus, ESCs have the ability to differentiate into neuroectodermal cells, NSCs, NPCs, and neurons (Ying et al., 2003). Neural induction in ESCs is the process by which neuroectodermal cells or NSCs are generated (Gerrard et al., 2005; Munoz-Sanjuan and Brivanlou, 2002). NSCs have two primary characteristics the ability to self-renewal and the potential to give rise to all the different cell types on the adult central nervous system - neurons, astrocytes and oligodendrocytes (Gage, 2000; Kornblum, 2007; Raff et al., 1983; Reynolds and Rietze, 2005).

1.6.1 ESCs: a tool for studying neural induction in mammals

In vitro ESC-based neural differentiation models use two different culturing techniques to drive ESCs down the neural lineage (Abranches et al., 2009). In the first method, ESCs are grown as aggregates, while in the second method ESCs are grown as a monolayer. In the aggregate culture system, ESCs are suspended in serum containing culture medium to form embryoid bodies (EBs). These EB are then differentiated by the addition of growth factors, such as retinoic acid and FGF2, to induce neural differentiation and expand the resulting neural stem and progenitor cell populations (Bain et al., 1995; Carpenter et al., 2001; Lee et al., 2000b). Ying et al. (2003) created a system where ESCs are grown as a monolayer, and cultured in a chemically defined, serum free, medium. By not using serum this system removes any experimental variability caused from using different serum batches (Peck and Bach, 1973), and also any problems associated with unspecified serum components that may affect the proliferation and differentiation of ESCs (Glassy et al., 1988). Thus, compared with the aggregate culture system, the monolayer culture system produces more consistent and reproducible results (Argentin et al., 1993). In addition, most of cells grown in a two-dimensional culture (monolayer culture system) are exposed to similar concentrations of signals present in the culture medium, but in a three-dimensional culture (aggregate culture

system) the inner and outer cells of the aggregate will be exposed to different signal concentrations due to these signals being required to penetrate the outer cell layers in order to reach those on the inside (Derda et al., 2009). Therefore, the monolayer culture model is widely used and provides an ideal system to study neural development of ESCs (Abranches et al., 2009; Stavridis et al., 2007; Sun et al., 2008). Moreover, when grown as a monolayer, ESCs generate neural cell in a reproducible and sequential manner: NSCs, neural progenitor cells (NPCs), and neurons after 2, 6, and 12 days of differentiation respectively (Sun et al., 2008; Ying et al., 2003; also see section 3.2.1). It is for the above reasons that I have chosen this system for my studies on neural cell development.

1.6.2 Signals involved in neural induction of ESCs

Studies on ESCs differentiation have shown that, as described above from studies using *Xenopus*, chick and mouse embryos, BMP, Activin/Nodal, FGF, and Wnt signalling pathways are all involved in neural induction (Aubert et al., 2002; Chambers et al., 2009; Gerrard et al., 2005; LaVaute et al., 2009). Culturing mouse or human ESCs with medium containing BMP4 reduced the generation of neural progenitors and neurons compared with cultures that received no BMP4 treatment, and this reduction of neural generation could be reversed by exposure to the BMP antagonist Noggin (Finley et al., 1999; LaVaute et al., 2009; Stavridis et al., 2007; Tropepe et al., 2001), suggesting that activation of BMP signalling suppresses the neural development of mouse and human ESCs. Similarly flow cytometry profiling of differentiated mouse ESCs showed that treatment of mouse ESCs with BMP4 not only reduced the generation of Sox1 or Nestin-expressing neural progenitors, but also increased the number of Cytokeratin 18-expressing epithelium cells (Gambaro et al., 2006). Another report also revealed that the generation of Sox1-expressing neuroectodermal cells was reduced by over 90% when mouse ESCs were cultured with BMP4 and differentiated for three days (Stavridis et al., 2007). These results imply that BMP signalling is a repressive signal for neural induction in ESCs, as observed from studies in *Xenopus*, chick, and mouse embryos (see section 1.4; Bachiller et al., 2000; Wilson et al., 1997;

Wilson et al., 2000).

Conversely when the BMP antagonists *Noggin* or *Chordin* were over-expressed in mouse ESCs, they promoted their neural differentiation (Gratsch and O'Shea, 2002). In line with this, adding the BMP antagonist Noggin to the culture medium of human ESCs increased the production of neural progenitors and reduced the generation of Cytokeratin 8-expressing epithelium cells when compared with Noggin untreated human ESCs (Gerrard et al., 2005; Itsykson et al., 2005). The results suggest that inhibition of BMP signalling promotes neural induction in mouse and human ESCs.

When mouse or human ESCs are cultured with Activin A to activate Activin/Nodal signalling, it drives mouse and human ESCs to differentiate into Enolase-expressing mesodermal or Sox17 and FoxA2-expressing endodermal cells, and away from a neural pathway (Borowiak et al., 2009; Schuldiner et al., 2000). This finding implies that Activin/Nodal signalling is a repressive signal for neural induction in mouse and human ESCs, as observed in *Xenopus* and mouse embryos. Cripto is a co-receptor of Activin/Nodal signalling, so the binding of Cripto with Activin/Nodal ligand and receptor activates Activin/Nodal signalling in mouse ESCs (Minchiotti, 2005; Yan et al., 2002). Conversely when mouse ESCs were treated with a blocker of Cripto (Cripto BP), the generation of Nestin-expressing NSCs was increased compared with Cripto BP untreated mouse ESCs (Lonardo et al., 2010). Likewise in *Cripto* null ESCs, the generation of neurons was increased compared with wild type ESCs, and adding Cripto to the culture medium of *Cripto* null ESCs reduced their ability to generate neurons (Parisi et al., 2003). Similarly, treatment of human ESCs with a specific Activin receptor inhibitor (SB431542) promotes the generation of MUSASHI and SOX1-expressing neural progenitors (Patani et al., 2009). Inhibiting Activin/Nodal and BMP signalling pathways at the same time by the treatment of human ESCs with SB431542 and Noggin robustly converts human ESCs into PAX6-expressing neural progenitors (Chambers et al., 2009). These results suggest that the inactivation of

Activin/Nodal signalling promotes neural induction in mouse and human ESCs.

The over-expression of Wnt1 or knocking down Dickkopf-1 (Wnt antagonist) in mouse ESCs to activate Wnt signalling reduces the expression of Sox1 and decreases the generation of neurons (Aubert et al., 2002; Verani et al., 2007). Another study also demonstrated that the activation of the canonical Wnt signalling pathway by introducing a dominant active form of β-catenin not only reduced the generation of Sox1-expressing neural progenitors, but also increased the expression of non-neural markers, such as Brachyury, Cytokeratin, and Smooth muscle actin (Haegele et al., 2003). These findings imply that Wnt signalling is a suppressive signal of neural induction in mouse ESCs, just like in *Xenopus*, chick, and mouse embryos. Conversely, mouse ESCs transfected with the Wnt antagonist Sfrp2 (secreted frizzled-related protein 2) have been shown to generate more Sox1-expressing neural precursors than their wild type ES counterparts (Aubert et al., 2002). In line with this, when mouse ESCs were exposed to the Wnt antagonist Dickkopf-1, the generation of Nestin-expressing neural progenitors was increased (Verani et al., 2007). These results imply that the inhibition of Wnt signalling promotes neural specificity of mouse ESCs.

Unlike Activin/Nodal, BMP, and Wnt signalling that act to inhibit neural differentiation, the activation of FGF signalling promotes neural induction of mouse and human ESCs. The treatment of mouse ESCs with the FGF receptor inhibitor PD173074 reduces the generation of Sox1-expressing neuroectoderm (Stavridis et al., 2007). Similarly the generation of Nestin-expressing NSCs has been shown to be significantly decreased in *Fgf4*$^{-/-}$ mouse ESCs compared with their wild type ESC counterparts, and the generation of neural progenitors and neurons form the *Fgf4*$^{-/-}$ mouse ESCs was regained when *Fgf4*$^{-/-}$ mouse ESCs were exposed to FGF4 (Kunath et al., 2007). Further to this, when human ESCs were treated with the FGF receptor inhibitor SU5402, the generation of PAX6-expressing neural

progenitors was reduced and the expression of *NCAM* (a marker of early neural progenitors) was down-regulated with the concomitant up-regulation of expression of the epithelial marker *Cytokeratin 8* (LaVaute et al., 2009; Yoo et al., 2011). Conversely when human ESCs were exposed to FGF2, the expression of *NCAM* was up-regulated and the expression of *Cytokeratin 8* was down-regulated (Cohen et al., 2010). These results suggest that the activation of FGF signalling promotes neural induction while the inhibition of this signalling pathway suppresses neural induction in both human and mouse ESCs; similar effects for FGF signalling on neural induction are found in *Xenopus*, chick, and mouse embryos (see section 1.5.1).

Thus, signalling pathways shown to be important for neural induction in mouse embryos are also important for the neural differentiation of ESCs, indicating that these cells provide a valid model to study the mechanisms of neural induction in mouse.

1.7 Transcription factors and neural induction in vertebrates

As discussed in above sections, different signalling pathways have been identified that induce or suppress the neural fate of embryonic ectoderm. However, how these pathways interact with transcription factors to regulate genes that control neural induction is still poorly understood (Kamiya et al., 2011; Stern, 2006).

Transcription factors have been demonstrated to play an important role during embryogenesis (Arnold and Robertson, 2009; Guillemot, 2007; Nichols et al., 1998). For example, *octamere-binding transcription factor 4* (*Oct4*; also known as *POU5F1*) and *Nanog* are expressed in the pluripotent cells of the pre-gastrulation embryo during early embryogenesis in mammals (Hart et al., 2004; Palmieri et al., 1994; Rosner et al., 1990). In *Oct4* null embryos the pluripotent ICM failed to develop, instead differentiated along the extraembryonic trophoblast lineage (Nichols et al., 1998). Although the *Nanog* null embryo could generate ICM, these embryos failed to generate the pluripotent epiblast, instead generating extraembryonic endoderm

(Mitsui et al., 2003). Similarly, when *Oct4* and *Nanog* were temporarily suppressed in mouse ESCs using RNA interference (RNAi), the generation of extraembryonic lineages were induced (Hough et al., 2006). Therefore, *Oct4* and *Nanog* are crucial for the development and maintenance of pluripotent ESCs (Loh et al., 2006). When ESCs differentiated into the three primary germ layers, the expression of *Oct4* and *Nanog* was down-regulated (Hart et al., 2004; Rosner et al., 1990). This down-regulation of both transcription factors is considered as the beginning of mammalian development (Chambers et al., 2007; Pesce and Scholer, 2001).

Similar to *Oct4* and *Nanog*, *Sox2* is also expressed in pluripotent cells of the pre-gastrulation embryo and *Sox2* null mouse embryos failed to generate ICM (Avilion et al., 2003). In mouse ESCs, the expression of *Oct4* and *Nanog* were down-regulated when *Sox2* was knocked down, suggesting that *Sox2* is an important transcription factor to regulate the pluripotency of ESCs (Fong et al., 2008; Masui et al., 2007). However, unlike *Oct4* and *Nanog*, that are down-regulated upon epiblast differentiation, *Sox2* is still expressed in extraembryonic ectoderm and neural progenitors from neural plate stages to adulthood (Ellis et al., 2004; Ferri et al., 2004; Rex et al., 1997; Wood and Episkopou, 1999), suggesting a role of *Sox2* in neural development.

In *Xenopus* embryo, *Sox2* is expressed in the prospective neural ectoderm at the time of neural induction (Pevny and Placzek, 2005). The injection of *Sox2* mRNA into *Xenopus* embryos induced the generation of ectopic *NCAM*-expression neural tissue. In contrast, the injection of dominant-negative forms of *Sox2* mRNA into *Xenopus* embryos inhibited the generation of *NCAM*-expression neural tissue and up-regulated the expression of the epidermal marker *Keratin* (Kishi et al., 2000). Therefore, *Sox2* is crucial for neural induction in *Xenopus*, so the understanding how *Sox2* expression is regulated is important.

In the chick embryo, 25 conserved enhancers of *Sox2* have been identified and two enhancers (N1 and N2) were found to be relevant for neural

induction (Papanayotou et al., 2008; Uchikawa et al., 2003) with N2 being expressed earlier than N1 (Uchikawa et al., 2003).The enhancer N2 was found to be responsible for *Sox2* expression in the neural plate, and in *N2* null mouse embryos, the generation of *Sox2*-expression neuroectoderm was abolished (Iwafuchi-Doi et al., 2011). The enhancer N1 was found to be responsible for *Sox2* expression in the future caudal hindbrain and spinal cord, and over-expressing *N1* in the epiblast of chick embryo during early embryogenesis induced ectopic expression of *Sox2* (Uchikawa et al., 2003; Uchikawa et al., 2004). These results suggested that the enhancers N1 and N2 activated the expression of *Sox2* during neural induction of vertebrates.

During the generation of ectoderm, these pluripotent factors (such as *Oct4* and *Nanog*) are down-regulated. When ectodermal cells further differentiate into neuroectodermal cells, some transcription factors (such as *Zic1*, *Zic3*, *Churchill*, *Sip1*, and *Zfp521*) are up-regulated (Dang et al., 2012; Kamiya et al., 2011; Nakata et al., 1997; Nakata et al., 1998; Nitta et al., 2004; Sheng et al., 2003). *Zic1* and *Zic3* encode zinc-finger proteins that are first expressed in the prospective neural plate during gastrulation of *Xenopus* embryos (Nakata et al., 1997; Nakata et al., 1998). The injection of *Zic1* or *Zic3* mRNA into these embryos at the two-cell stage induced the ectopic expression of the neural plate marker *NCAM* in both the embryos or in isolated animal caps (Nakata et al., 1997; Nakata et al., 1998). However, knocking down the expression of either *Zic1* or *Zic3* by injection of antisense oligos into *Xenopus* embryos did not inhibit the generation of *Sox2*-expressing neural plate (Marchal et al., 2009). Because amino acid sequences of Zic1 and Zic3 are highly conserved (Furushima et al., 2000), their may compensate for each other during neural induction when only one of the genes was knocked down. Indeed, when both of these transcription factors were knocked down at the same time the generation of *Sox2*-expressing neural tissue was suppressed (Marchal et al., 2009). These results suggested that *Zic1* and *Zic3* are involved in the neural induction of *Xenopus* embryo. As discussed in sections 1.2, 1.3, and 1.4, the suppression of BMP signalling is needed for neural induction. The promoter region of *Zic1* was shown to contain a BMP inhibitor-responsive promoter module that was

required for activation of *Zic1* upon inhibition of BMP signalling (Tropepe et al., 2006). The expression of *Zic3* was also up-regulated by the inhibition of BMP signalling (Nakata et al., 1997). Therefore, interruption of BMP signalling may activate *Zic1* and *Zic3* to cause neural induction in *Xenopus*. In mouse embryos, *Zic1* was first detected in the neuroectoderm during gastrulation and the *Zic1* null embryo showed cerebellar and dorsal spinal cord hypoplasia (Aruga et al., 1998). Although the *Zic1* null mutant maintained the ability to generate neural tissue, the involvement of *Zic1* in neural induction still could not be completely ruled out because the lost function of *Zic1* may be compensated by *Zic3,* which was also expressed in the neural plate (Elms et al., 2004; Furushima et al., 2000).

Like Zic1 and Zic3, Sip1 (Smad-interacting protein 1) is also involved in vertebrate neural induction (Nitta et al., 2004; Sheng et al., 2003). The *Sip1* encodes a two-handed zinc-finger protein (Verschueren et al., 1999) and is expressed in the prospective neural ectoderm of *Xenopus* embryo (Eisaki et al., 2000; Verschueren et al., 1999). The injection of *Sip1* mRNA into *Xenopus* embryos at the two-cell stage induced the expression of the neural marker *NCAM* in isolated animal caps (Eisaki et al., 2000; Nitta et al., 2004). In contrast, knocking down the expression of *Sip1* by injection of antisense oligos into *Xenopus* embryos inhibited the generation of *NCAM*-expressing neural tissue (Nitta et al., 2004). These results suggested that *Sip1* is involved in neural induction of *Xenopus*. In chick embryo, another zinc-finger protein Churchill was found to bind to the promoter region of *Sip1* and activate its transcription, and both *Churchill* and *Sip1* were expressed in the prospective neural plate (Sheng et al., 2003). When *Churchill* was electroporated into the non-prospective neural ectoderm, the expression of *Sip1* was induced and ectopic *Sox2*-expressing neural tissue was generated. In the prospective neural ectoderm of chick embryo, knocking down the expression of *Churchill* not only inhibited the expression of *Sip1*, but also blocked the formation of neural plate (Sheng et al., 2003). Therefore, *Sip1* also plays a role in neural induction of chick.

During neural differentiation of human ESCs, the expression of the neural progenitor markers *OLIG3*, *SOX1*, and *SIX1* were up-regulated by over-expressing *SIP1*. In contrast, when the expression of *SIP1* was knocked down using shRNA, the expression of *OLIG3*, *SOX1*, and *SIX1* was down-regulated and the expression of the pluripotent genes *OCT4* and *NANOG* was sustained (Chng et al., 2010). These results suggested that *SIP1* promoted neural induction of human ESCs. Using chromatin immunoprecipitation analysis, it had been demonstrated that OCT4 and NANOG proteins bind to the *SIP1* promoter region. Knocking down the expression of *OCT4* or *NANOG* up-regulated the expression of *SIP1* (Chng et al., 2010), suggesting that OCT4 and NANOG proteins negatively regulated the transcription of *SIP1*. Therefore, when the expression of *OCT4* and *NANOG* are down-regulated to initiate germ-layer formation during early embryogenesis, *SIP1* may be up-regulated to promote neural induction. It has been showed that Sip1 proteins bind to the promoter region of *Smad7* (an inhibitor of BMP signallings, see section 1.4.1) and over-expressing *Sip1* up-regulated the expression of *Smad7* (Weng et al., 2012), suggesting that *Sip1* activated the expression of Smad7 to inhibit BMP signalling. In addition, Sip1 proteins were also shown to physically interact with Smad1, Smad2, and Smad5, and then inhibited the function of these Smads (Verschueren et al., 1999; Weng et al., 2012). Smad1/5 and Smad2 are intracellular effectors of BMP and Activin/Nodal signallings respectively (see sections 1.4.1 and 1.5.3). Because BMP and Activin/Nodal signalling needs to be suppressed during neural induction in vertebrates (see sections 1.2, 1.4, and 1.5.3), Sip1 may repress these signalling pathways to promote neural induction.

Similar to Sip1, Zfp521 also plays a crucial role in mouse neural induction (Kamiya et al., 2011). *Zfp521* encodes a zinc-finger protein and is particularly expressed in the neuroectoderm of mouse embryo during gastrulation (Kamiya et al., 2011). During neural differentiation of mouse ESCs, over-expressing *Zfp521* increased the generation of Sox1-expressing neural progenitors while *Zfp521* knock-down decreased the generation of $Sox1^+$ cells (Kamiya et al., 2011). Using chromatin immunoprecipitation

analysis, it had been demonstrated that Zfp521 proteins can bind to the promoter region of *Sox1*, *Sox3*, and *Pax6*, and up-regulate the expression of these neuroectodermal genes (Kamiya et al., 2011), suggesting that *Zfp521* promotes neural induction in mouse ESCs.

From the above it is evident that we are beginning to identify key transcription factors involved in the regulation of neural induction, however, further investigation into the interaction of signalling pathways, transcription factors, and neural inductive genes is still necessary.

1.8 Nnat may be involved in neural induction

As described above, neural induction is a complicated process that cannot simply be a 'default' process as originally hypothesised by Hemmati-Brivanlou and Melton (details see section 1.3, Fig. 1.5; Hemmati-Brivanlou and Melton, 1997a; Stern, 2005; Stern, 2006). Instructive cues, such as Calcium and FGF signalling, are of fundamental importance for neural induction (for details see sections 1.5.1 and 1.5.4). We are interested in understanding the molecular mechanisms regulating the instructive cues involved in this process, using mouse ESCs grown in a monolayer culture as a model system. Thus, we seek to discovery the genes and signalling pathways that are involved in the process of ESCs neural induction and subsequent differentiation.

In order to screen for these genes, Dr. Yuh-Man Sun constructed subtractive cDNA libraries using cDNA collected at different time points during the neural induction and differentiation of ESCs using a monolayer culture system. Dr. Sun found a number of genes up-regulated during the neural induction and differentiation of ESCs into neurons. One of these genes, *Neuronatin* (*Nnat*), was particular interesting because of its putative function and expression pattern both *in vitro* and *in vivo* (during mouse embryogenesis). When mouse ESCs were grown in a monolayer neural differentiation model (Ying et al., 2003), the expression of *Nnat* was up-regulated and remained high until the generation of neurons at differentiation day 12 (Fig. 1.13, analysed by Dr. Sun using real-time PCR).

This suggested that Nnat may be involved in the early neural development of mouse ESCs. Within this thesis, I specifically investigated the role of Nnat in neural induction of mouse ESCs using loss- and gain-of-function experiments in which the expression of *Nnat* had been knocked down or over-expressed (see Chapter 3).

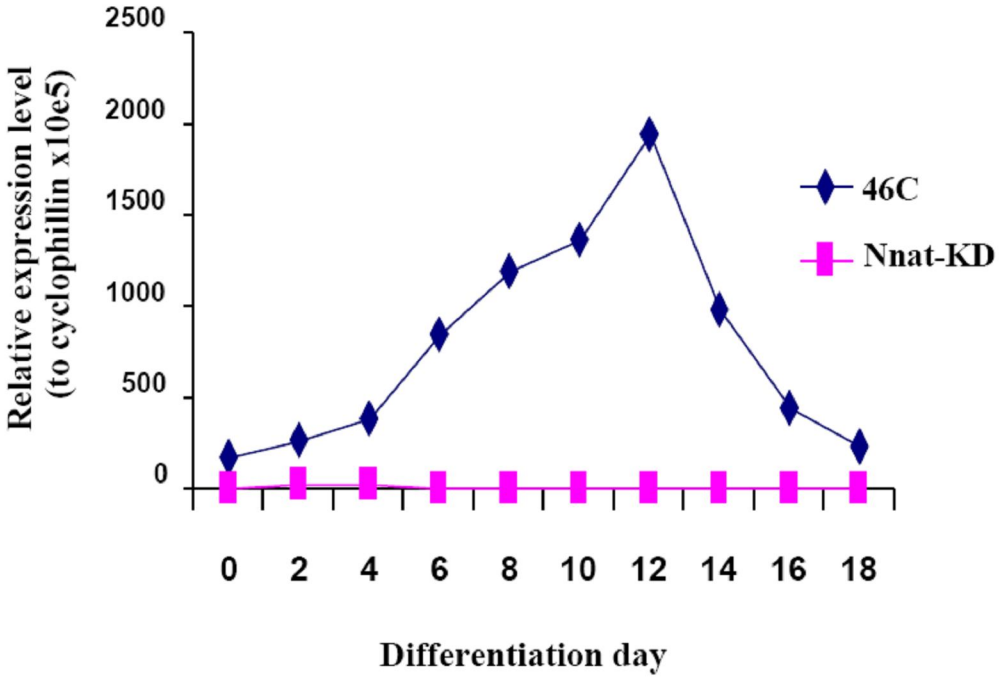

Fig. 1.13. Expression of Nnat during mouse ESC neural differentiation.
46C and Nnat-KD ESCs were grown under differentiating conditions for 18 days and the total RNAs were isolated from the cells after differentiation for 0, 2, 4, 6, 8, 10, 12, 14, 16, and 18. The relative expression of Nnat was analysed using real-time PCR. In 46C cells, the expression of Nnat was low at the ESC stage (Differentiation day 0) and then its expression started to increase until differentiation after day 12 when neurons were generated. In Nnat-KD cells, the expression of Nnat was very low throughout the whole differentiation process. Thus the efficiency of Nnat knock-down was high and persistent during differentiation.
Abbreviations: ES, embryonic stem; Nnat-KD, Nnat-knockdown; PCR, polymerase chain reaction; RNA, ribonucleic acid.
(Adapted from Lin et al., 2010)

1.8.1 The *in vivo* expression pattern of Nnat

Nnat (also known as *Peg5*) expression was first described in the neonatal (3 days) rat and human fetal (18-24 weeks) brain (Joseph et al., 1994). However, its expression was not confined to the brain since Nnat was also expressed, at lower levels, in the adrenal gland, pituitary gland, pancreatic β-cells and adipocytes (Chu and Tsai, 2005; Suh et al., 2005; Wijnholds et

al., 1995). *Nnat* is an imprinted gene and is expressed only from the paternal allele, while the maternal allele is silenced by methylation (John et al., 2001; Kagitani et al., 1997). Most imprinted genes are located in gene clusters, but *Nnat* is not closely linked to other imprinted genes (John et al., 2001). The *Nnat* locus is 1.2 kbp and is located on the distal arm of chromosome 2 in the mouse and chromosome 20 in human (Dou and Joseph, 1996; John et al., 2001; Kagitani et al., 1997). *Nnat* is composed of three exons and two introns (Joe et al., 2008; Joseph et al., 1995; Kikyo et al., 1997) that generate two different isoforms, α and β. Nnatα (81 amino acids) is encoded by all three exons and Nnatβ (54 amino acids) is only encoded by the first and third exons (Joseph et al., 1995).

The neuron-restrictive silencer factor is a zinc-finger protein and the binding of this transcription factor with the neuron-restrictive silencer element can silence the transcription of neuronal promoters in non-neuronal cells (Bessis et al., 1997; Chen et al., 1998). This element had been found in the 5'-flanking region of *Nnat* and this may be the reason that Nnat is more highly expressed in neural tissue than in non-neural tissue (Dou and Joseph, 1996). The promoter region of *Nnat* has also been shown to contain multiple CpG islands that are methylated to different extents in different tissues (Evans et al., 2001). For example, in the pituitary gland 50% of *NNAT* promoter-associated CpG islands were found to be methylated (Revill et al., 2009). However, the expression of NNAT was loss or significantly decreased in pituitary adenoma (a tumor of pituitary gland), and in these cells the methylation of CpG islands increased to 75-100% (Revill et al., 2009), suggesting that the methylation of the *NNAT* promoter region reduced the expression of *NNAT*. In contrast to the repressive effect of neuron-restrictive silencer element and methylation, NeuroD1 is the only known transcription factor to up-regulate *NNAT* expression (Chu and Tsai, 2005; Li et al., 2010). In NeuroD1 null mouse embryo, the expression of Nnat gene and protein was reduced in pancreatic tissue compared with wild type embryos (Chu and Tsai, 2005). Chromatin immunoprecipitation analysis revealed that the NeuroD1 protein bound to the promoter region of *Nnat* in pancreatic β-cells (Chu

and Tsai, 2005), suggesting that the transcription factor NeuroD1 promoted the expression of *Nnat*. However, during neural development, the expression of *NeuroD1* was first detected in the neural epithelium at 8 dpc (after neural plate formation at 7.5 dpc) and was highly expressed throughout the neural tissue at 10 dpc (Cho and Tsai, 2004; Lee et al., 2000a). This suggests that NeuroD1 is not involved in neural induction in mouse embryo, but may promote the expression of Nnat during neurogenesis.

In rat embryos, *Nnatα* is first expressed at 7-10 dpc, when the neural plate is formed, while *Nnatβ* is first expressed at 11-14 dpc, which is concomitant with the period of neural tube closure and neuroepithelial cells proliferation (Joseph et al., 1995). The expression of both isoforms peaks at 16-19 dpc, the height of neurogenesis and declines when neurogenesis is complete (Joseph et al., 1995). According to the data from the Allen Developing Mouse Brain Atlas (http://developingmouse.brain-map.org/data/Nnat.html), at 13.5 dpc *Nnat* is expressed in the germinal zones of many brain regions (cingulate cortex, preoptic, hypothalamic, superior tectal, isthmal, and pontine neuroepithelium) (Fig. 1.14). Its expression is significantly decreased in the brain of adult rat, mouse, and human compared with fetal brains (Dou and Joseph, 1996; Joseph et al., 1994; Joseph et al., 1995; Kikyo et al., 1997). However, in adult mouse brain the expression of *Nnat* is still evident in the subventricular zones (SVZ) of the lateral ventricles and throughout the hippocampal formation, including the dentate gyrus (Fig. 1.14). Both the adult SVZ and the dentate gyrus of the hippocampus, are regions where adult neurogenesis is observed (Doetsch, 2003; Temple, 2001). Thus, according to the reported expression patterns *in vivo*, *Nnat* is present in the correct places and at the correct times to play a role in neural development.

In mouse embryo, *Nnat* was expressed in ectoderm and mesoderm at 7.0 dpc and after that maximal expression was seen in the head fold (Sousa-Nunes et al., 2003). During later embryogenesis, *Nnat* is strongly expressed in the central and peripheral nervous system (Wijnholds et al.,

1995). Although Nnat expression is widespread in the forebrain of mouse embryo at 8.5-9.5 dpc (Sousa-Nunes et al., 2003), Wijnholds et al. (1995) also found Nnat was expressed in rhombomeres 3 and 5 of the hindbrain of mouse embryo at the same period of time. Because rhombomeres 3 and 5 are important for segmentation of the hindbrain (Wijnholds et al., 1995), Nnat may also be involved in this process.

In addition to neural development, it has been demonstrated that Nnat also plays important roles in metabolism (Chu and Tsai, 2005; Joe et al., 2008; Li et al., 2010; Sharma et al., 2011; Suh et al., 2005; Vrang et al., 2010). For example, in a pancreatic β-cell line (MIN6N8 cells), the expression of *Nnat* was increased by the treatment of glucose and this effect was dose dependent (Joe et al., 2008). NIT cells (another pancreatic β-cell line) secrete insulin upon treatment with glucose but this secretion was suppressed when *NNAT* was knocked down in these cells using RNAi treatment (Chu and Tsai, 2005), suggesting that NNAT played a role in the secretion of insulin in pancreatic β-cells. Nnat is also expressed in adipocytes and over-expression of *Nnatα* in pre-adipocytes induced their differentiation and caused lipid accumulation in these cells (Suh et al., 2005). These findings suggest that Nnat may be involved in metabolic regulation.

NNAT is endogenously expressed at low levels in normal human brain tissue (Xu et al., 2012), but is abundantly expressed in some types of tumour, such as medulloblastoma (Siu et al., 2008), glioblastoma multiforme (Xu et al., 2012), and pulmonary non-small cell carcinoma (Uchihara et al., 2007). In medulloblastoma cells, knocking down the expression of *NNAT* using RNAi resulted in a significant decrease in proliferation. In contrast, over-expressing *NNAT* in medulloblastoma cells caused a shift from G1 to G2/M phase in the cell cycle and increased colony formation when cells were grown on soft agar (Siu et al., 2008). Similarly, the expression of NNAT protein was higher in the high grade glioblastoma multiforme than in the low grade glioblastoma multiforme

(Xu et al., 2012). Indeed, over-expressing NNAT in U87 malignant glioma cells caused an increase in proliferation (Xu et al., 2012). These results suggested that NNAT may play a role in cellular proliferation.

The data obtained from the subtractive cDNA libraries suggests a role for Nnat in early neural development (neural induction), while the *in vivo* expression data suggests that Nnat may also be involved in the differentiation of NSCs and NPCs. Thus, Nnat may play more than one role during neural development. Although Nnat also has a role in the metabolic regulation and cellular proliferation, I am specifically interested in its function in neural induction of mouse ESCs. In this thesis, I will investigate whether Nnat is indeed involved in neural induction using loss- and gain-of-function approaches in mouse ESCs that, as described above, can be differentiated into neuroectoderm, neural progenitors, and neurons (see Chapter 3).

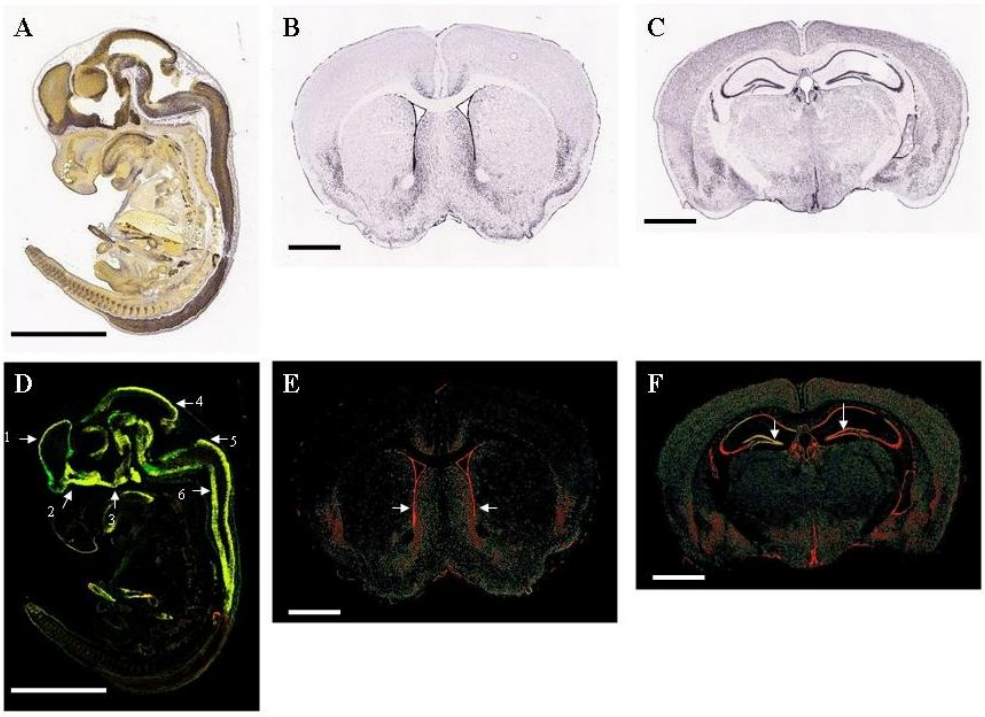

Fig. 1.14. The expression of *Nnat* as shown by *in situ* hybridization in 13.5 dpc mouse embryo and P53 adult mouse brain.
(A, D) A sagittal view of a 13.5 dpc mouse embryo revealed that *Nnat* was expressed in the developing brain and spinal cord. *Nnat* is highly expressed in many germinal zones, including the (1) cingulate cortex, (2) preoptic, (3) hypothalamic, (4) superior tectal, (5) isthmal, and (6) pontine neuroepithelium at 13.5 dpc. Scale bar, 3200 μm. (B, E) A coronal view of a P53 adult mouse brain revealed that *Nnat* was expressed within the subventricular zone (arrow) of the lateral ventricles. Scale bar, 1680 μm. (C, F) A coronal view of a P53 adult mouse brain revealed that *Nnat* was expressed in the hippocampal formation (including the dentate gyrus, arrow). Scale bar, 1680 μm.
Abbreviations: dpc, days post conception.
(Adapted from Allen Brain Atlas, http://www.brain-map.org/)

1.8.2 Putative function of Nnat

The Nnat protein has a hydrophobic domain at N-terminus and hydrophilic domain at C-terminus (Dou and Joseph, 1996; Joseph et al., 1994), suggesting that Nnat is a membrane protein. Using immunocytochemical analysis, it had been demonstrated that the Nnat protein located in the ER (Joe et al., 2008; Oyang et al., 2011; Suh et al., 2005). The precise molecular role of Nnat in neural development is unclear; however, it has been shown that Nnat exhibits 50% homology, at the amino acid level, with phospholamban (Dou and Joseph, 1996). Both Nnat and phospholamban have an α-helical membrane domain and basic cytoplasmic tails (Dou and Joseph, 1996). Phospholamban is an integral

membrane protein of the ER. Studies in muscle cells have shown that under resting state (low $[Ca^{2+}]_i$, see section 1.5.4.4), un-phosphorylated phospholamban interacts with the sarcoendoplasmic reticulum Ca^{2+}-ATPase (Atp2a/SERCA) and this interaction reduces the affinity of Atp2a/SERCA for Ca^{2+} and inhibits the action of the Ca^{2+}-ATPase in pumping cytosolic Ca^{2+} into the ER, resulting in an increase in $[Ca^{2+}]_i$ (James et al., 1989; MacLennan and Kranias, 2003). When phospholamban is phosphorylated by cAMP-dependent protein kinase, it causes the dissociation of the phospholamban-Atp2a/SERCA complex, and then the Atp2a/SERCA pumps cytosolic Ca^{2+} into the ER to decrease the $[Ca^{2+}]_i$ (James et al., 1989; MacLennan and Kranias, 2003). Therefore, it is possible that Nnat may function by modulating $[Ca^{2+}]_i$ through interactions with Atp2a/SERCA (Dou and Joseph, 1996; Joe et al., 2008; Li et al., 2010). In support of this idea, $[Ca^{2+}]_i$ has been shown to be increased in Nnat over-expressed insulinoma cells or hippocampal neurons (Joe et al., 2008; Oyang et al., 2011), suggesting that Nnat may antagonise the action of Apt2a/SERCA resulting in less cytosolic Ca^{2+} being pumped into the ER and an increase in $[Ca^{2+}]_i$.

In vertebrates there are three Apt2a/SERCA genes (for details see section 1.5.4.4). During *Xenopus* embryonic development, Apt2a2/SERCA2 is expressed in the neural plate and neural tube indicating a role for this gene in aspects of neurogenesis (Pegoraro et al., 2011). Apt2a2/SERCA2 is also expressed in human and mouse ESCs (Salomonis et al., 2010). Further to this, Dr. Yuh-Man Sun's unpublished data also revealed that the Atp2a2/SERCA2 is expressed at much higher levels compared to both Apt2a1/SERCA1 and Apt2a3/SERCA3 in mouse ESCs and during ESC neural differentiation (Fig. 1.15). Because of these observations, I hypothesised that Nnat suppresses the action of Apt2a2/SERCA2, which in turn results in the increase in $[Ca^{2+}]_i$ resulting in the initiation of neural induction in mouse ESCs. In this thesis, I have investigated the molecular mechanisms underlying the action of Nnat and tested whether Nnat physically interacts with Apt2a2/SERCA2 (see Chapter 4).

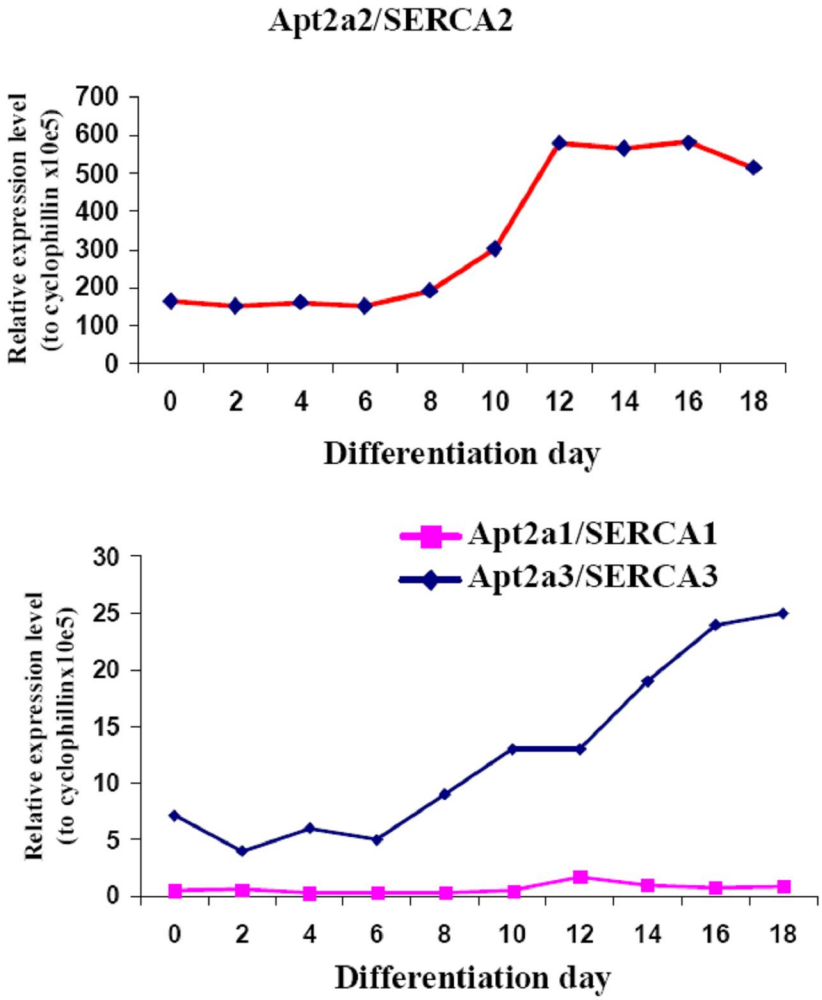

Fig. 1.15. The expression of Atp2a/SERCA genes during the differentiation of mouse ESCs along a neural lineage.

46C ESCs were grown in differentiating conditions for 18 days and the total RNAs were isolated from the cells after differentiation for 0, 2, 4, 6, 8, 10, 12, 14, 16, and 18. In ESCs stage (Differentiation day 0), the expression of Apt2a2/SERCA2 was 10-fold over Apt2a1/SERCA1 and Apt2a3/SERCA3. During differentiation, the expression of Apt2a2/SERCA2 was increased since day 8 and peaked at day 12. The expression of Apt2a1/SERCA1 and Apt2a3/SERCA3 was remained low compared with Apt2a2/SERCA2.

Abbreviations: Atp2a/SERCA, sarcoendoplasmic reticulum Ca^{2+}-ATPase; ES, embryonic stem; RNA, ribonucleic acid.

(Unpublished data from Dr. Yuh-Man Sun)

1.9 Aims of thesis

Neural induction is a process by which unspecified embryonic ectoderm receives signals instructing it to take up a neural fate whereby the ectoderm differentiates into neuroectoderm. Many studies show that signals, such as BMP, FGF, Wnt, Activin/Nodal, and calcium, are involved in neural induction, but the precise molecular mechanisms which underlying this process in higher vertebrates are not fully understood. In order to investigate the molecular mechanisms underlying neural induction in mammals, an ESC-derived neural differentiation model has been widely used. Using this differentiation model, it was found that the expression of Nnat was up-regulated when mouse ESCs differentiated into NSCs and neurons. Further to this, Nnat is highly expressed in developing neural tissue of mouse embryos and it may interact with Apt2a/SERCA to increase $[Ca^{2+}]_i$. In *Xenopus*, an increase in $[Ca^{2+}]_i$ has been demonstrated to be involved in neural induction. However, it is not clear whether calcium plays similar roles in mammalian neural induction. Due to the expression pattern of Nnat and its putative function, I hypothesise that Nnat may play a role in neural induction in mouse ESCs.

The work described in my thesis tests this hypothesis and also attempts to define the molecular mechanisms underlying the action of Nnat in the neural induction of mouse ESCs. Specifically, I investigated:

- Whether the neural specification and differentiation of ESCs were altered when *Nnat* was dysregulated in mouse ESCs.
- Whether Nnat physically interacted with Apt2a2/SERCA2, which in turn increased $[Ca^{2+}]_i$ leading to neural induction in mouse ESCs.
- Whether there are any crosstalks between Nnat and other signalling pathways involved in the neural induction of mouse ESCs.

The experiment described within Chapter 3 studying the effects of Nnat in *Xenopus* was collaboration with Dr. Esther Bell (MRC Centre for Developmental Neurobiology, King's College London). The experiment described within Chapter 4 describing the measurement of $[Ca^{2+}]_i$ was

carried out in collaboration with Dr. Vladimir Snetkov (Department of Asthma, Allergy and Respiratory Science, King's College London). In the rest of this thesis, unless specified, the work presented was carried out independently.

Chapter 2. Materials and Methods

2.0 Materials and methods

2.1 ESC lines and culture

ESCs are derived from the ICM of the blastocyst and are pluripotent so ESCs can differentiate into all the different cell lineages that compose the embryo (Evans and Kaufman, 1981; Murry and Keller, 2008). In this study, the main topic was focused on how Nnat affected the differentiation of mouse ESCs to neural lineages. Loss- and gain-of-function experiments were conducted. In the loss-of-function experiment, Nnat expression was knocked-down in ESCs using shRNA (short hairpin RNA); in the gain-of-function experiment, Nnat was over-expressed in ESCs.

In this study the mouse 46C ESC line was used (a gift from Prof. A. Smith, Cambridge). This cell line was derived by knocking green fluorescent protein (GFP) into the open reading frame of *Sox1*. As Sox1 is the early marker of neuroectoderm this enables the identification of those ESCs committed to a neural fate (Camus et al., 2006; Ying et al., 2003; Zhao et al., 2004).

Nnat-knockdown (Nnat-KD) ESCs were generated from 46C mouse ESCs using shRNA. Nnat shRNA designed to knockdown both *Nnatα* and *β* isoforms was used for gene silencing to create Nnat-KD ESCs; this ESC line was generated by Dr. Yuh-Man Sun.

All ESC lines were maintained in Glasgow minimum essential medium (Sigma) supplemented with 5% foetal bovine serum (PAA), 5% new born calf serum (GIBCO), 2mM L-glutamine (GIBCO), 1× non-essential amino acids (GIBCO), 1mM sodium pyruvate (GIBCO), 100μM 2-mercaptoethanol (GIBCO), and 1000 units/ml leukaemia inhibitory factor (LIF, Chemicon). ESCs were grown on T25 tissue culture flasks coated with 0.1% gelatin (Sigma) and incubated in a humidified incubator at 37°C and an atmosphere of 5% CO_2. The ESC medium was replaced completely everyday. When the cells became 100% confluent, they were passaged to new T75 culture flasks (2×10^7 cells/flask) or frozen and stored at -80°C or in liquid nitrogen.

2.2 Generation of Nnat-over-expression ESC line

2.2.1 Amplification and cloning of Nnat

To clone Nnat, total RNA was isolated from mouse 46C ESCs (for details see section 2.7.1) and cDNA was obtained by reverse transcription (for details see section 2.7.2). The full length coding sequences for *Nnatα* and *β* were obtained by polymerase chain reaction (PCR) using primers (see Table 2.1 for sequences) designed by Dr. Yuh-Man Sun and synthesised by Sigma Genosys. The sequence of NnatS and NantA primers included *Hin*dIII and *Bam*HI restriction sites as well as the Kozak consensus sequence to allow for directional cloning and efficient translation of the resultant PCR product. Amplification of Nnat cDNA was performed with 5µl of 10× buffer, 5µl of 2mM dNTP, 3µl of 10µM NnatS, 3µl of 10µM NnatA, 0.5 µl of Taq DNA polymerase (Stratagene), 0.5µl of Taq extender (Stratagene) and 28µl of water. The PCR cycle parameters were:

94°C × 3 minutes
94°C × 15 seconds
55°C × 20 seconds
68°C × 3 minutes
× 10 cycles
94°C × 15 seconds
65°C × 20 seconds
68°C × 3 minutes
× 25 cycles
72°C × 10 minutes
4°C × 10 minutes

The QIAquick PCR purification kit (Qiagen) was used to purify the PCR product after agarose gel electrophoresis. Purified PCR products were then directionally cloned into the *Hin*dIII and *Bam*HI sites of the vector pNEBR-X1-Hygro (Appendix 1, New England Biolabs). The PCR products were digested with the restriction enzymes and purified from agarose gel using QIAquick PCR purification kit. The digested pNEBR-X1 Hygro vector and Nnat cDNA were ligated using T4 DNA ligase (Roche) and the Rapid DNA Ligation Kit (Roche). The pNEBR-X1-Nnat vector was transformed into the competent *E. coli* strain DH5α (Invitrogen). 50µl of DH5α was mixed with 2µl ligated vector and left on

ice for 30 minutes. The mixture was heat shocked at 42°C for 30 seconds. SOC medium was then added and the transformed cells incubated at 37°C for one hour. 40µl of transformed E. *coli* was then cultured at 37°C on standard Luria Bertani (LB) agar plate supplemented with 100µg/ml ampicillin overnight. The following day colonies were picked and individually inoculated into 3ml LB medium supplemented with 100µg/ml ampicillin. The tubes were placed in a shaker overnight at 37°C. The cultured cells were then taken and centrifuged at 13000 rpm for 5 minutes and the plasmid DNA purified using the Wizard Plus SV Minipreps DNA purification system (Promega). The plasmid DNA was digested with restriction enzyme *Hin*dIII and *Bam*HI to confirm that it contained the Nnat. The digested samples were run on a 1% agarose gel with the appropriate DNA size markers (New England Biolabs).

2.2.2 Sequencing of pNEB-X1-Nnat clones

In order to determine that the isolated clones contained full length Nnat coding sequences with no errors the clones were sequenced. The sequencing reactions were performed using NnatA and RheoSwitch R-X1 sequencing primers. 1µl of the purified plasmid DNA, 1µl of primer, 1µl of BigDye (Applied Biosystems), 2µl of 5× sequencing buffer, and 5µl of water were mixed. The PCR cycle parameters were:

96°C × 1 minute
96°C × 10 seconds
50°C × 15 seconds
60°C × 4 minutes
] × 35 cycles
4°C × 10 minutes

To precipitate the PCR product, 1.5µl of 2M sodium acetate and 25µl of 100% ethanol were applied and incubated on ice for 15 minutes. This mixture was centrifuged at 13000 rpm for 20 minutes at 4°C and then washed with 20µl of 70% ethanol. After the product dried, it was sent to Geneservice Limited (Unit 2 Cambridge Science Park, Milton Road, Cambridge, CB4 0FE) for sequencing. The sequence was analysed using Chromas lite.

2.2.3 Midi preps

The *E. coli* carrying the wild type mouse Nnat DNA was grown on LB agar plates supplemented with 100µg/ml ampicillin overnight. Colonies were picked from the plates and were individually inoculated into 4ml LB medium supplemented with 100µg/ml ampicillin. 100µl of the inoculated LB was added into 100ml of LB medium supplemented with 100µg/ml ampicillin overnight. The following day, plasmid DNA was purified using HiSpeed Midi Kit (Qiagen).

2.2.4 Transfection of ESCs with pNEBR-X1-Nnat Vector

The 46C ESCs were plated in a 6-well plate. When the cells had become 40% confluent, they were transfected with the pNEBR-X1-Nnat Vector using Lipofectamine reagent, using the following protocol. Three micrograms of pNEBR-X1-Nnat DNA was added to 500µl of Optimen (Invitrogen) containing 40µl of Plus Reagent (Invitrogen). 20µl of Lipofectamine (Invitrogen) was added to 500µl of Optimen. Both mixtures were left at room temperature for 10 minutes before being combined and the mixture left for a further 20 minutes at room temperature before adding 2ml of Optimen.. The 46C ESCs were rinsed twice with Phosphate-Buffered Saline (PBS, Invitrogen) and once with Optimen. The final mixed reagent was applied to ESCs and the cells were incubated at 37°C for 6 hours. The reagent was taken off and the cells were cultured with ES medium for 24 hours. Then ESCs were cultured in ES medium supplemented with Hygromycin (200µg/ml; Invitrogen) for 8 days to select the transfected cells. Because the pNEBR-X1 vector contained the Hygromycin-resistance gene, transfected cells should survive after Hygromycin selection. The surviving cells were pooled and re-plated onto gelatine-coated 10-cm culture plates (10 cells/plate). These transfected cells were cultured in ES medium for four days, and then 8 single-cell clones were collected.

2.2.5 Confirmation of over-expression of Nnat in ESCs

To confirm Nnat-overexpression in cells, the isolated ESC clones transfected with pNEBR-X1-Nnat were cultured on gelatin-coated coverslips in ESC medium for two days. Immunocytochemistry was used to detect the expression of Nnat. Nnat primary antibody (1:500; Santa Cruz Biotechnology) was applied to check the over-expression of Nnat (see section 2.4 for details).

2.3 ESCs differentiation

The monolayer and aggregate culture systems were used for the differentiation of ESCs into neural lineage (Abranches et al., 2009; Carpenter et al., 2001; Chambers et al., 2009; Ying et al., 2003). In the monolayer culture, ESCs were cultured with a chemical-defined medium. It is easy to manipulate cells using this system. The monolayer culture was employed to differentiate ESCs towards a neural fate, in this method ESCs were first differentiated into NSCs, then to neural progenitors, and finally into neurons (Ying et al., 2003). In aggregate culture, ESCs were grown in a serum-containing medium to form EBs. This system provides a three-dimensional environment and ESCs could generate three primary germ layers (ectoderm, endoderm, and mesoderm). This aggregate culture is widely used in ESCs differentiation and three primary germ layers formation. To examine the influence of Nnat on the development of three primary germ layers, EBs were formed in 46C, Nnat-KD, and Nnat-OE ESC lines.

2.3.1 Monolayer culture

Coverslips were baked in an oven for 4 hours at 180°C. To gelatinize coverslips, coverslips were put into 24-well plates. 1ml of 0.1% gelatin (Sigma) was applied to each well and left at room temperature for 30 minutes. ESCs were plated onto gelatinized coverslips at a density of 6×10^4 cells/ml. The next day, the ESC medium was replaced with N2B27 differentiation medium, which consisted of a 1:1 mixture of DMEM/F12 medium (Invitrogen) supplemented with N2 and Neurobasal medium supplemented with B27 (Invitrogen). N2 consisted of 25 μg/ml insulin (Sigma), 100 μg/ml apotransferrin (SCIPAC), 6 ng/ml progesterone

(Sigma), 16 μg/ml putrescine (Sigma), 30 nM sodium selenite (Sigma) and 50 μg/ml bovine serum albumin fraction V (GIBCO). The N2B27 medium was changed every other day.

2.3.2 Aggregate culture

To form EBs, ESCs (10^7 cells/dish) were cultured onto 90mm Petri Dishes containing 10 ml of ESC medium without LIF. The medium was changed every other day. In order to avoid removing EBs while changing medium, the dish was tilted so that the EBs would settle and then the old medium was replaced with fresh medium. After cultured for six days, EBs were collected for total RNA isolation and quantitative real-time PCR (see section 2.6 for details).

2.3.3 Chemical manipulation of ESC neural differentiation

Nnat might inhibit Apt2a/SERCAs to increase intracellular calcium and so affect ESC neural differentiation as it has been shown that calcium signalling may be involved in neural induction (Lee et al., 2009). 2,5-Di-t-butyl-1,4-benzohydroquinone (BHQ) and Thapsigargin (Tg) are specific Apt2a/SERCA inhibitors (Johnson and Misler, 2002). 50 μM BHQ (Calbiochem) or 25 nM Tg (Sigma) was used to mimic the function of Nnat and rescue the neural development of Nnat-KD cells. During ESCs differentiation, cells were treated with different drugs to change intracellular calcium level. 2-aminoethoxydiphenyl borate (2-APB), an inhibitor of IP_3R, blocks calcium release from ER into cytoplasm (Lang et al., 2007). 1,2-Bis (2-aminophenoxy) ethane-N,N,N',N'-tetraacetic acid tetrakis (acetoxymethyl ester) (BAPTA-AM) is a membrane permeable Ca^{2+} chelator. Dantrolene is an inhibitor of Ca^{2+} release from ER into cytoplasm through RyR. 75 μM 2-APB (Enzo Life Sciences), 20 μM BAPTA-AM (Calbiochem), or 100 μM Dantrolene (Sigma) was used to treat ESCs to decrease intracellular free Ca^{2+}. ESCs were also cultured with differentiation conditions in the present of 2 mM ethylene glycol tetraacetic acid (EGTA) (Sigma) to chelate the extracellular Ca^{2+} and determine whether extracellular Ca^{2+} was needed for neural induction.

FGF signalling pathway is required for neural induction in chicken and *Xenopus* (Linker and Stern, 2004; Streit et al., 2000). *Fgf4* knockout mouse ESCs are deficient in neural induction (Kunath et al., 2007). 5ng/ml FGF4 (R&D Systems) or 10 ng/ml of FGF5 (R&D Systems) was applied to ESCs to activate FGF signalling pathway. 100ng/ml PD173074 (Sigma), an inhibitor of FGF receptors, and 5μM PD184352 (Axon Medchem), an inhibitor of MEK, were used to block FGF/Erk signalling pathway.

BMP4 is one member of TFG-β superfamily. Active BMP signalling pathway inhibits ectoderm to differentiate into neuroepithelium and leads ectoderm to an epidermal fate (Munoz-Sanjuan and Brivanlou, 2002). Inhibition of BMP signalling pathway induces ectoderm to become neuroepithelium (Hemmati-Brivanlou and Melton, 1997b; Wilson et al., 1997). 10ng/ml BMP4 (R&D Systems) was used to inhibit neural differentiation in ESCs. Chordin, Follistatin, and Noggin are antagonists of BMP (Stern, 2005). 150 or 300ng/ml of Chordin (R&D Systems), 150 or 300ng/ml of Follistatin (R&D Systems), and 100 or 200ng/ml of Noggin (R&D Systems) were used to treat ESCs to induce neural development.

2.4 Immunocytochemistry

ESCs were grown on gelatin-coated coverslips and were fixed in 4% paraformaldehyde (Sigma) for 20 minutes at room temperature, washed three times with PBS, then incubated for one hour in 0.1% Triton X-100 (Sigma) to permeabilise the cell membrane. Primary antibodies were diluted in 0.1% Triton X-100 and applied overnight at 4°C, followed by four washes in PBS. Secondary antibodies were diluted in PBS and applied for one hour at room temperature in the dark. The information of antibodies was listed in Table 2.2. For double staining, two different primary antibodies, which originated from different hosts, were diluted in the same solution and applied to cells at the same time. Corresponding secondary antibodies, which were conjugated with different fluorescent conjugates, were used to distinguish the different primary antigens. The cells were washed four times in PBS and submerged in double distilled water prior to mounting of coverslips onto slides using Vectashield mounting medium (Vector) with

4',6-diamidino-2-phenylindole (DAPI) to stain the nuclei. As a negative control, ESCs were stained with secondary antibody in the absence of primary antibody (see Appendix 2). Generic nail polish was used to seal coverslips to slides. Fluorescent microscopy images were acquired using the AxioImager Z1 (Carl Zeiss) and analysed using AxioVision version 4.5(Carl Zeiss). The ApoTome module (Carl Zeiss) was used to obtain stacks of confocal slices for the cultures.

2.5 Quantification of cell-types

To compare the ability of neural differentiation of Nnat-OE, Nnat-KD, and 46C ESCs, the numbers of Sox1-GFP$^+$/Nestin$^+$ NSCs and NeuN$^+$ neurons in different ESCs were counted. ESCs were plated on gelatin-coated coverslips and differentiated for 6 days or 14 days (see section 2.3.1), and then cultures were fixed in 4% paraformaldehyde for 20 minutes at room temperature, and washed three times with PBS. The expression of Sox1-GFP, Nestin, and NeuN were analysed by immunofluorescence analysis (see section 2.4). NSCs were identified by Sox1-GFP and Nestin, and neurons were identified by NeuN. Each coverslip was examined with a fluorescence microscope at magnification of ×400 and 10 microscopic fields were taken randomly. The percentage of Sox1-GFP$^+$/Nestin$^+$ NSCs and NeuN$^+$ neurons were counted manually and the number of total counted cells of each coverslip was 1000 at least. Three coverslips were counted per condition. All experiments were repeated three times.

2.6 Quantitative real-time PCR

The quantitative real-time PCR is one of the practical ways of both detection and quantification of a gene expression. The expression pattern of genes, which are involved in ESC differentiation, could be detected by this method. During ESC differentiation total RNA was collected at different time points and then first-strand cDNA was synthesised and used for real-time PCR.

2.6.1 Total RNA isolation

Differentiated or undifferentiated ESCs were harvested using trypsin and were washed with PBS, collected in centrifuge tubes, and centrifuged. The supernatant was discarded and the cell pellet lysed in 1 ml TRI Reagent (Sigma) by repeated pipetting up and down. 0.2 ml chloroform was added and the mixture was shaken vigorously for 15 seconds, before being allowed to stand for 5 minutes at room temperature. The mixture was then separated into three phases by centrifuge at 13000 rpm for 15 minutes at 4°C. The bottom phase contained protein, the interphase contained DNA, and the colourless top aqueous phase contained RNA. The top phase was transferred to a new tube and 0.5 ml of isopropanol was added to precipitate the RNA. The sample was centrifuged at 13000 rpm for 15 minutes at 4°C. The RNA pellet was washed with 75% ethanol and centrifuged at 7500 rpm for 5 minutes at 4°C. The RNA pellet was dried and then dissolved in RNase-free water.

2.6.2 cDNA synthesis

SuperScript™ III Reverse Transcriptase (Invitrogen) was used to synthesis first-strand cDNA. The reaction mixture was as followed: 2 µg RNA, 1 µl oligo$(dT)_{20}$ primer (Invitrogen), 1 µl 10 mM dNTP (Sigma), and sterile water to make up a total of 14 µl. The reaction mixture was incubated at 65°C for 5 minutes and then quenched with ice for at least one minute. 4 µl 5X buffer, 1 µl 0.1M DTT, and 1 µl SuperScript™ III Reverse Transcriptase were added and mixed gently. The reaction mixture was then incubated at 42°C for 2 hours before being transferred to a 70°C water bath for 15 minutes to inactivate the enzyme.

2.6.3 Real-time PCR

The following reaction was set up for each sample: 2 µl cDNA, 10 µl iQ™ SYBR® Green Supermix (Bio-Rad), 1 µl sense primer, 1 µl antisense primer, and 6 µl sterile water. Each sample was duplicated and each reaction was repeated three times independently. A Chromo4 Real-Time PCR Detection System (Bio-Rad) was used to carry out the PCR reactions. The following PCR protocol was used:

95°C × 3 minute
95°C × 30 seconds
60°C × 30 seconds
72°C × 30 seconds
] × 44 cycles
Plate read
The melting cure from 50°C to 96°C was read every 1°C.

Gene expression was relative to cyclophilin using the formula $1/2^{\Delta Ct}$, where ΔCt = unknown gene threshold cycle minus cyclophilin threshold cycle. In differentiated or undifferentiated ESCs, the expression level of cyclophilin was consistent throughout the experiments in this study so only this housekeeping gene was used.

2.7 Western blotting

The Western blotting is a widely used to detect specific proteins in tissue or cell populations. Cells were lysed and proteins were released into the lysis buffer. Proteins were separated by gel electrophoresis and transferred to a membrane. The membrane is then blotted with a protein specific antibody to detect the protein.

2.7.1 Sample preparation

Differentiated or undifferentiated ESCs were cultured on 10cm culture dishes, washed twice with ice-cold PBS, then and left on ice. One ml of freshly made ice-cold RIPA lysis buffer (1× protease inhibitor cocktail (Sigma), 1× phosphatase inhibitor cocktail (Sigma), 10 mM sodium fluoride (Sigma), 1 mM sodium orthovanadate (Sigma), and 1 mM β-glycerophosphate (Sigma)) was added to the cells and the cells were then scraped from the surface of the dish. Cell lysates were transferred to a fresh tube, shaken vigorously, and left on ice for 30 minutes. The cell lysates were then centrifuged at 13000 rpm for 20 minutes at 4°C. The supernatant contained protein was aliquoted and stored at -80°C until required. The Qubit™ Protein Assay Kit (Invitrogen) was used to detect the protein concentration according to manufacturer's instructions using a

NanoDrop 3300 Fluorospectrometer (Thermo Scientific) to measure the protein concentration in the samples.

2.7.2 Gel electrophoresis

The SDS polyacrylamide gels were used for proteins separation. Gel polymerization was initiated by the addition of Ammonium Persulfate (Sigma) along with Tetramethylethylenediamine (TEMED, Sigma). The percentage of gel was between 10-20%, which was determined by the relative size of the protein under study. As the size of the Nnatα and β proteins was small (9 and 6 kD respectively), 20% SDS polyacrylamide gels were used to identify Nnat. For other proteins, 10% SDS polyacrylamide gel was used. 100 µg total protein per mini-gel well was mixed with 2× Laemmli sample buffer (Sigma) and was heated at 90°C for 5 minutes to denature proteins. 5 µl Novex® Sharp Protein Standard (Invitrogen) was loaded into a mini-gel well to determine protein size and also to monitor the progress of the electrophoretic run. The gel was run at 125-150V for between 1 to 3 hours, which was again dependent on the size of the protein being analysed.

2.7.3 Electroblotting of proteins

The wet transfer method (MacPhee, 2010) was used to transfer the proteins from the SDS-gels to nitrocellulose membranes. The XCell II™ Blot Module apparatus (Invitrogen) was used to perform the wet transfer, according to manufacturer's instructions, using 0.2 µm pore size Nitrocellulose membranes (Invitrogen). The transfer conditions were at a constant voltage of 25V for 90 minutes at 4°C. To transfer the small-size proteins (Nnatα and β), the transfer condition was changed to a constant voltage of 15V for 30 minutes at 4°C to avoid that the proteins passing through the membrane.

2.7.4 Immunoprobing of Western Blots

The membrane was washed twice with Tris buffered saline (TBS) for five minutes before blocking the membrane with either, non-fat milk or bovine serum albumin (BSA, Cell Signaling). To study phosphor-proteins, the

membranes were blocked in 5% BSA in Tris buffered saline with Tween 20 (TBST) for one hour at room temperature; to study non-phosphor-proteins, 5% non-fat milk in TBST was used to block the membranes. After blocking, the membranes were washed three times with TBST for 10 minutes. The membranes were incubated with primary antibody diluted in the appropriate blocking solution overnight at 4°C. The membranes were then washed three times with TBST for 10 minutes and then incubated with secondary antibody diluted in the blocking solution for one hour at room temperature. The information of antibodies was listed in Table 2.3. The membranes were then washed three times with TBST for 10 minutes and the membranes were then ready for scanning. The Odyssey Infrared Imaging System was used to detect the far-red-fluorescent Alexa Fluor (Invitrogen) labelled secondary antibody bodies. Beta-actin was used as the internal control to ensure that the protein in each lane of the gel had been equally loaded.

2.8 Co-Immunoprecipitation

The molecular mechanisms and physiological functions of Nnat are still unclear (Li et al., 2010). In insulinoma cells, over-expression of Nnat causes increased intracellular calcium (Joe, Lee et al. 2008). The amino acid sequence of Nnat is about 50% homologous to phospholamban (Dou and Joseph, 1996). Therefore, it might function in a similar way to phospholamban, that is, to regulate Apt2a/SERCAs and to cause an increase in intracellular calcium. In order to test this hypothesis, Co-immunoprecipitation (Co-IP) and Duolink *in-situ* proximity ligation assay (see section 2.9) were used to examine whether Nnat directly interacts with Apt2a/SERCAs.

Co-IP is a technique for precipitating a specific protein complex out of a whole cell or tissue protein lysate. The protein complex is precipitated using an antibody that is specific to one of the proteins found within the complex. The other members of the protein complex can then be identified from the immunoprecipitated product. Therefore, Co-IP is a widely used technique to analyse protein-protein interactions. Normally, a non-ionic detergent is used

in the cell lysis buffer so the native protein conformation can be maintained. The Apt2a2/SERCA2 is expressed in mouse ESCs. If Nnat binds to Apt2a2/SERCA2, both will form a protein complex in the cell lysate. This complex could be precipitated using anti-Nnat antibody. Western blotting could be used to confirm that the Apt2a2/SERCA2 is a part of the protein complex.

Co-IP was performed using the Universal magnetic Co-IP kit (Active Motif, www.activemotif.com/), according to the manufacturer's instructions. 46C ESCs were grown in differentiating conditions for 12 days and cultures were lysed with freshly prepared complete whole-cell lysis buffer and incubated on ice for 30 minutes. The sample was centrifuged at 13000 rpm for 20 minutes at 4°C. The supernatant (whole-cell extract) was aliquoted and stored at -80°C. 500 µg whole-cell extract was mixed with 10 µg of three different anti-Nnat antibodies individually (Santa Cruz, goat; Santa Cruz, rabbit; Abcam, rabbit), and incubated for one hour at 4°C on a rotator. 25 µl Protein G Magnetic Beads was added to each sample and incubated for four hours at 4°C on a rotator. The beads were washed with TPST and pulled down by magnetic force. The beads were mixed with 20µl 2× reducing loading buffer and boiled at 90°C for 5 minutes. Western blotting was performed (as described in section 2.7) and the membrane was blotted with anti-Apt2a2/SERCA2 antibody.

2.9 Statistics

All data are presented as the mean ± the standard error (SE) from experiments that have been repeated three times. Student t-test was performed to compare data between two conditions. One-way analysis of variance (ANOVA) was used to identify significant differences between three subjects. All reported *p*-values are two-tailed, and $p < 0.05$ was accepted as significant.

Table 2.1. Primer Sequences

Primer	Sequence
BMP4	5'-TTCCTGGTAACCGAATGCTGA-3' 5'-CCTGAATCTCGGCGACTTTTT-3'
Brachyury	5'-GCTTCAAGGAGCTAACTAACGAG-3' 5'-CCAGCAAGAAAGAGTACATGGC-3'
Cyclophillin	5'-TGGAGCGTTTTGGGTCCAG-3' 5'-AGCTGTCCACAGTCGGAAATG-3'
Fgf4	5'-GTGTGCCTTTCTTTACCGACG-3' 5'-CTGAGGGCCATGAACATACCG-3'
Fgf5	5'-CCGTCTGTGGTTTCTGTTGAGG-3' 5'-ACCCTTTGAGCTTTCTACCC-3'
Hnf4	5'-TCCCAGTGTCCAAAAATTCC-3' 5'-CTGTTGTGTGGGGGTTCTTT-3'
Mesp1	5'-ACCTGACCAAGATCGAGACG-3' 5'-GAGGTTGTCCTCGCTGAGTC-3'
Msx1	5'-GCGCCTCACTCTACAGTGC-3' 5'-CTCTGGACCCACCTAAGTCAG-3'
Msx2	5'-TTCACCACATCCCAGCTTCTA-3' 5'-TTGCAGTCTTTTCGCCTTAGC-3'
Nnat	5'-CGGCTGGCGCCAAGCTTCGCCACCATGGCCGCAGTGGCAGCA-3' 5'-ATTTAAGAATTCGTGGATCCATGACACGGCCGCCCAGG-3'
Otx2	5'-TATCTAAAGCAACCGCCTTACG-3' 5'-AAGTCCATACCCGAAGTGGTC-3'
Sox1	5'-ATACCGCAATCCCCTCTCAG-3' 5'-ACAACATCCGACTCCTCTTCC-3'

Table 2.2. Antibodies used for Immunocytochemistry

Primary antibodies				
Specificity	Supplier (catalogue number)	Dilution	Host	
Brachyury	Chemicon (#04-135)	1:500	Mouse	
CK18	Chemicon (MAB3234)	1:500	Mouse	
MAP2	Abcam (ab24640)	1:400	Rabbit	
Nestin	Chemicon (MAB353)	1:500	Mouse	
NeuN	Chemicon (MAB377)	1:500	Mouse	
Nnat	Abcam (ab27266)	1:500	Rabbit	
Oct4	Santa Cruz Biotechnology (sc-5279)	1:500	Mouse	
RC2	Hybridoma bank	1:500	Mouse	
Apt2a2/SERCA2	Santa Cruz Biotechnology (sc-8094)	1:500	Goat	
Secondary antibodies				
Specificity	Supplier (catalogue number)	Format	Dilution	Host
Mouse IgG	Chemicon (AP124C)	Cy3	1:500	Goat
Mouse IgG	Chemicon (AP124S)	Cy5	1:500	Goat
Rabbit IgG	Chemicon (AP183C)	Cy3	1:500	Goat
Rabbit IgG	Chemicon (AQ132F)	FITC	1:500	Goat
Goat IgG	Chemicon (AP180C)	Cy3	1:500	Donkey

Table 2.3. Antibodies used for Western blotting

Primary antibodies				
Specificity	Supplier (catalogue number)	Dilution	Dilution buffer	Host
β-actin	Sigma (A2228)	1:10000	5% non-fat milk in TPST	Mouse
pErk1/2 (Thr202/Tyr204)	Cell Signaling (#4376)	1:1000	5% BSA in TPST	Rabbit
Nnat	Abcam (ab27266)	1:1000	5% non-fat milk in TPST	Rabbit
Apt2a2/SERCA2	Santa Cruz Biotechnology (sc-8094)	1:1000	5% non-fat milk in TPST	Goat
pSmad1 (Ser463/465)/ Smad5 (Ser463/465)/ Smad8 (Ser426/428)	Cell Signaling (#9511)	1:1000	5% BSA in TPST	Rabbit
pSmad1 (Ser206)	Cell Signaling (#9553)	1:1000	5% BSA in TPST	Rabbit
Secondary antibodies				
Specificity	Supplier (catalogue number)	Dilution	Dilution buffer	Host
Mouse IgG	Invitrogen (A10038)	1:2000	As primary antibody	Donkey
Rabbit IgG	Invitrogen (A10043)	1:2000	As primary antibody	Donkey
Goat IgG	Invitrogen (A21084)	1:2000	As primary antibody	Donkey

Chapter 3. Nnat promotes the neural induction of mouse ESCs

3.0 Nnat promotes the neural induction of mouse ESCs

3.1 Introduction

Neural induction is a process by which unspecified embryonic ectoderm receives signals from the underlying mesoderm instructing it to take up a neural fate (details see section 1.1; Hemmati-Brivanlou and Melton, 1997b; Munoz-Sanjuan and Brivanlou, 2002; Stern, 2005). During gastrulation, the central embryonic ectoderm region acquires neural properties and forms the neural plate (neuroectoderm) while the peripheral embryonic ectoderm forms epidermis. The neural plate then folds creating the neural groove and finally develops into a tubular structure called the neural tube (Clarke et al., 1991; Greene and Copp, 2009). The caudal region of the neural tube gives rise to the spinal cord while the rostral region gives rise to the brain (Downs and Davies, 1993; Greene and Copp, 2009). Therefore neural induction is the initial step in the generation of the vertebrate central nervous system. Within this Chapter, I will describe data showing that the gene Nnat plays an important role in the neural induction of mouse ESCs.

The origin of the neural inductive signals that leads to the differentiation of the central nervous system is a long-standing question in vertebrate embryology. Over the past decades, many studies carried out in amphibian embryos have tried to answer this question (Munoz-Sanjuan and Brivanlou, 2002; Wilson and Edlund, 2001). Based on data obtained from these experiments, the 'default model' of neural induction was developed (see section 1.3). This popular model proposes that ectodermal cells will adopt a neural fate autonomously in the absence of BMP signalling (Hemmati-Brivanlou and Melton, 1997a). However, this default model does not take into account results showing that instructive signals are also required for ectodermal cells to give rise to neuroectodermal cells (see section 1.5). For example, FGF/Erk signalling is active in the developing neural plate of *Xenopus* embryos during gastrulation (Christen and Slack, 1999), and when this signalling is inhibited by culturing *Xenopus* embryos with the FGFR inhibitor (SU5402) the generation of tissue expressing the neural plate marker *NCAM* is reduced (Delaune et al., 2005). This observation suggested that FGF/Erk signalling is an instructive cue for neural induction and,

without the activation of FGF/Erk signalling, neural specification is restricted. In addition to FGF/Erk signalling, an increase in $[Ca^{2+}]_i$ is also required for neural induction of *Xenopus* embryos (see section 1.5.4). Elevated $[Ca^{2+}]_i$ is observed in the prospective neural ectoderm during gastrulation, while no such increase is observed in the prospective non-neural ectoderm (Leclerc et al., 2003; Leclerc et al., 2000), suggesting that an increase in $[Ca^{2+}]_i$ plays a pivotal role in neural induction. Further to this, the treatment of *Xenopus* embryos with a calcium channel blocker to prevent an increase in $[Ca^{2+}]_i$ down-regulated the expression of the early neural genes *Zic3* and *Geminin* (Leclerc et al., 2000). This suggests that an increase in $[Ca^{2+}]_i$ is also an instructive cue for neural induction in *Xenopus* embryos. Therefore, both FGF and calcium are instructive signals for neural induction suggesting that regulation of this process is more complex than originally thought and cannot simply be explained by the 'default' hypothesis.

Many studies on neural induction in vertebrates reveal that BMP, FGF, calcium, Wnt, and Activin/Nodal signals are involved in this process (see sections 1.3, 1.4, and 1.5). Yet, despite extensive research into neural induction, the precise molecular mechanisms that govern this process in higher vertebrates have yet to be fully elucidated. In order to investigate the mechanisms that control neural induction in mouse and humans, *in vitro* neural differentiation models have been created using mouse and human ESCs (see section 1.6.1; Abranches et al., 2009; Chambers et al., 2009; Ying et al., 2003). As part of a larger study carried out by Dr. Yuh-Man Sun to discover genes and signalling pathways that regulate neural induction and subsequent differentiation in mouse ESCs, a number of genes were identified that were up-regulated during the differentiation of ESCs into neural stem cells, and one of these genes, *Nnat*, is the focus of this thesis. Nnat is of particular interesting because of its putative function and expression pattern both *in vitro* and *in vivo* (see section 1.7). During mouse ESCs neural induction *in vitro*, the expression of *Nnat* was up-regulated and remained high throughout the period of neurogenesis. Similarly *in vivo* Nnat is highly expressed in developing neural tissue (see section 1.7.1), suggesting that Nnat may be involved in the early neural development. In

addition to its expression pattern, Nnat shares significant homology with the calcium regulator Phospholamban (an inhibitor of SERCA) and so Nnat may function as an inhibitor of Apt2a/SERCA2, causing an increase in $[Ca^{2+}]_i$ (see section 1.7.2). Because an increase in $[Ca^{2+}]_i$ is known to be an instructive signal for neural induction in *Xenopus* embryos, Nnat, by regulating $[Ca^{2+}]_i$, may provide a similar instructive signal in mouse. The work described in this Chapter tests the hypothesis that Nnat is involved in neural induction of mouse ESCs.

In order to study the role of Nnat in neural induction, loss- and gain-of-function experiments were carried out using ESCs in which the expression of Nnat had been knocked down (Nnat-KD ESCs, generated by Dr. Yuh-Man Sun) or over-expressed (Nnat-OE ESCs, generated as part of my thesis research). According to the data obtained from subtractive cDNA libraries (see section 1.7), Nnat expression is up-regulated during ESC neural differentiation and so it may be required for the differentiation of ESCs towards a neural fate. If this reasoning is correct then ESCs in which Nnat has been knockdown should show an impaired ability to generate neural cells, while over-expression of Nnat in ESCs should promote the generation of neural cells.

Specifically, this chapter describes:

1) The expression of Nnat during ESC-derived neural differentiation
2) The generation of Nnat-OE ESCs
3) The phenotypic changes of Nnat-mutant cells during the neural development
4) The *in vivo* effects of *Nnat* on the neural induction of *Xenopus laevis*

3.2 Results

3.2.1 Neural differentiation of ESCs using an *in vitro* monolayer culture system

Ying et al. (2003) created a monolayer cell-culture system that recapitulates the process of *in vivo* neural development in mouse ESCs; generating NSCs, NPCs, and neurons sequentially. In order to confirm that this model behaves as reported in my hands, immunocytochemistry using stage-specific markers was used to characterise the cell-types generated as ESCs differentiated along the neural pathway. The pluripotent marker Oct4 is a transcription factor that is highly expressed in mouse ESCs (Hwang et al., 2004; Loh et al., 2006), so Oct4 was used to identify undifferentiated ESCs. Sox1 and Nestin were used to identify NSCs (Johansson et al., 1999; Murayama et al., 2002), and the Radial glial cell marker-2 (RC2) used to define radial glial cells (Gates et al., 1995). Neurons were identified by their expression of the Neuronal nuclear antigen (NeuN) or Microtubule-associated protein 2 (MAP2) (Chen et al., 2001). The 46C ESCs used throughout this thesis are *Sox1*-GFP knock-in mouse ESCs, in which GFP is activated concomitantly with *Sox1* expression. As Sox1 is an established early neuroectodermal marker in mammals, GFP can be used as the readout of neuroectodermal cell production (Ying et al., 2003).

To analyse the neural differentiation of 46C ESCs, these cells were plated on gelatin-coated coverslips at a concentration of 6×10^4 cells/ml and cultured in non-differentiating medium supplemented with LIF (1000 units/ml) for one day to allow the cells to adhere to the coverslips (see Material and Methods, section 2.1). To initiate neural differentiation, the medium was switched to differentiating (N2B27) medium (see Material and Methods, section 2.3.1). The ESCs were cultured in differentiating medium for a further 14 days, and the medium was changed every other day. At specific time points during this differentiation process (0, 2, 6, 9, 12, and 14 days), cultures were fixed and analysed to determine the types of neural cells present in the culture using the antibodies described above.

Undifferentiated 46C ESCs highly expressed the pluripotent marker Oct4 (Fig. 3.1A). After 2 days of differentiation, Sox1-GFP expressing neuroectodermal cells (early NSCs) were observed (Fig. 3.1B) and these cells had increased in number by differentiation day 6 (compare Fig. 3.1B to C). Cells expressing Nestin, a NSCs marker, were seen after 6 days of differentiation (Fig. 3.1C) and after 9 days of differentiation, RC2 expressing radial glial cells appeared (Fig. 3.1D). Neurons, as identified by expression of NeuN and MAP2, were observed after 12 days of differentiation (Fig. 3.1E-F). Thus, using cell-type specific markers we observed that upon differentiation 46C cells generated neuroectoderm, NSCs, radial glial, and neurons sequentially, recapitulating the events seen during neural development *in vivo* (Abranches et al., 2009; Ying et al., 2003). From these observations we defined differentiation day 0-1 as being the ES stage, 2-6 as being the NSC stage, 6-12 as being the NPCs stage and from 12 days onwards as the neuronal stage.

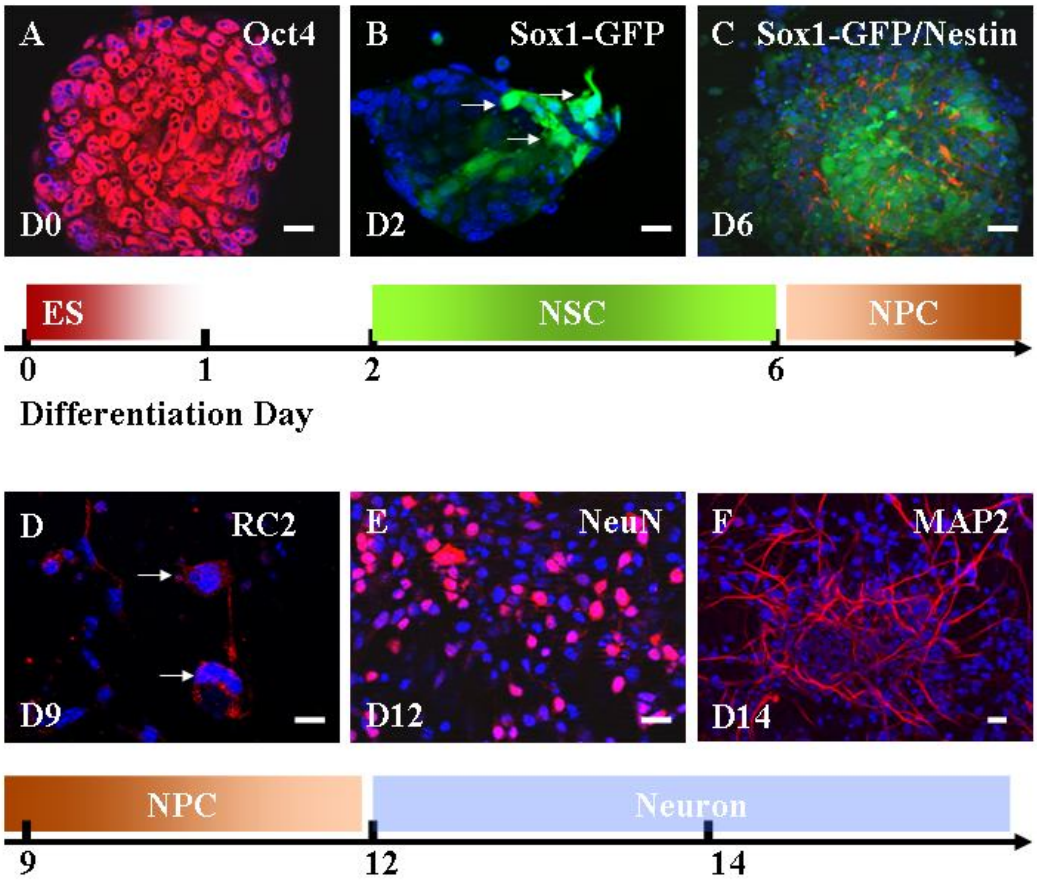

Fig. 3.1. The expression of neural stage-specific markers during ESC-derived neural development *in vitro*.

46C ESCs (Sox1-GFP knock-in mouse ESCs) were plated on gelatin-coated coverslips and cultured in non-differentiating medium for 24 hours after which time the medium was then switched to differentiating medium. After 2, 6, 9, 12, and 14 days of differentiation, cells were fixed to analyse the expression of neural stage-specific markers. (A) Oct4 (red) was highly expressed in undifferentiated ESCs. (B) Sox1-GFP$^+$ neuroectoderm (green, see arrows), (C) Sox1-GFP$^+$ (green) and Nestin$^+$ (red) NSCs, (D) RC2$^+$ radial glial (red, see arrows), (D) NeuN$^+$ neurons (red) and (E) MAP2$^+$ neurons (red) were generated by 2, 6, 9, 12, and 14 days of differentiation respectively, as seen *in vivo*. All nuclei were stained with DAPI (blue). Scale bar, 20 μm.

Abbreviations: DAPI, 4',6-diamidino-2-phenylindole; ESC, embryonic stem cell; GFP, green fluorescent protein; MAP2, microtubule-associated protein 2; NeuN, neuronal nuclear antigen; NSC, neural stem cell; NPC, neural progenitor; RC2, radial glial cell marker-2; Sox1, SRY (sex determining region Y)-box 1.

3.2.2 Nnat expression is up-regulated as ESCs generate NSCs

If Nnat is required for neural development, its expression should correlate with the generation of neural cells. To confirm the hypothesis, the expression of Nnat protein was analysed as ESCs differentiated along a neural pathway.

The expression level of Nnat was observed to be low in ESCs grown under proliferating conditions, compared with cells that had been differentiated for 2 days (Fig. 3.2A-C). Thus, initiating neural differentiation causes the expression of Nnat protein to be up-regulated, which is consistent with the increased expression of Nnat mRNA seen during ESC neural differentiation (see section 1.7). After two days of differentiation, Nnat expression was restricted to Sox1-GFP expressing neuroectodermal cells (Fig. 3.2D-F). At day 6, the NSC stage, Nnat expression co-localised with Nestin (Fig. 3.3A-C), while after 14 days of differentiation, Nnat expression was found in NeuN expressing neurons (Fig. 3.3D-F). At day 14, as expected, NeuN was expressed in the nucleus (Fig. 3.3F, arrow), surrounded by Nnat expression in the cytosol (Fig. 3.3D, arrow), as would be expected if Nnat is located in the ER where it can interact with Atp2a/SERCA (discussed in section 1.7.2). These data showed that up-regulation of Nnat expression correlated well with the generation of cells belonging to the neural lineage. This led us to hypothesise that Nnat may be involved in neural induction as well as functioning at later stages in neural development.

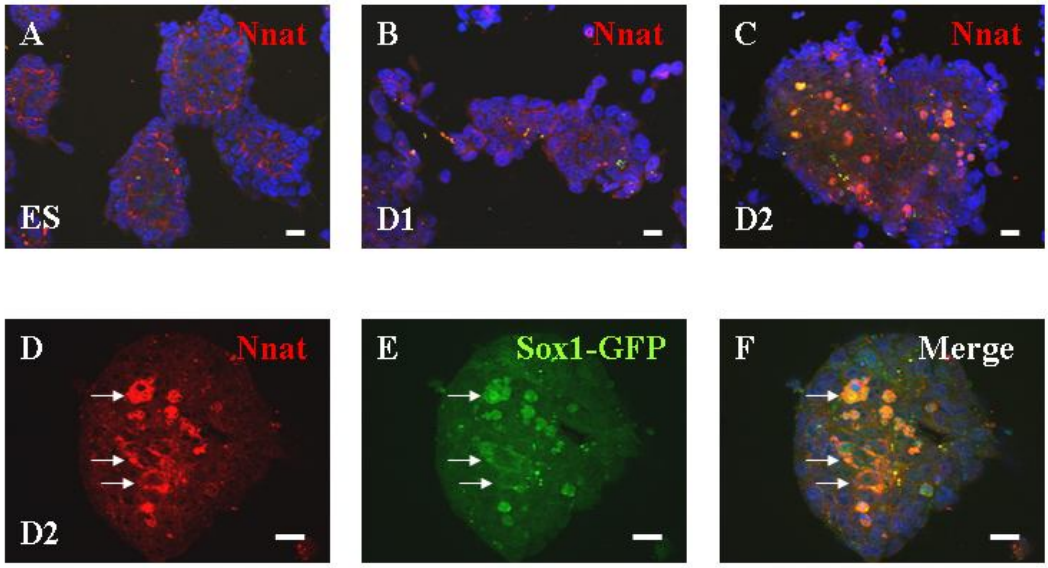

Fig. 3.2. Nnat is expressed in neuroectodermal cells.
46C ESCs were plated on gelatin-coated coverslips and cultured in non-differentiating medium for 24 hours to allow the ESCs to adhere to the coverslips. The medium was then switched to differentiating medium. After 1 or 2 days of differentiation, cells were fixed to analyse the expression of Nnat using immunocytochemistry. (A) The expression of Nnat (red) was low in undifferentiated ESCs. (B) After 1 day of differentiation, the expression of Nnat (red) remained low. (C) After 2 days of differentiation, the expression of Nnat (red) was increased (compare C and D with A and B). (D) Nnat expression (red, arrows) co-localised with (E) Sox1-GFP (green, arrows) expression after 2 days of differentiation, as indicated by (F) the merging of red and green to become orange (arrows). All nuclei were visualised by staining with DAPI (blue). Scale bar, 20 μm.
Abbreviations: D1, 1 day of differentiation; D2, 2 days of differentiation; DAPI, 4',6-diamidino-2-phenylindole; ESC, embryonic stem cell; GFP, green fluorescent protein; NSC, neural stem cell; Sox1, SRY (sex determining region Y)-box 1.

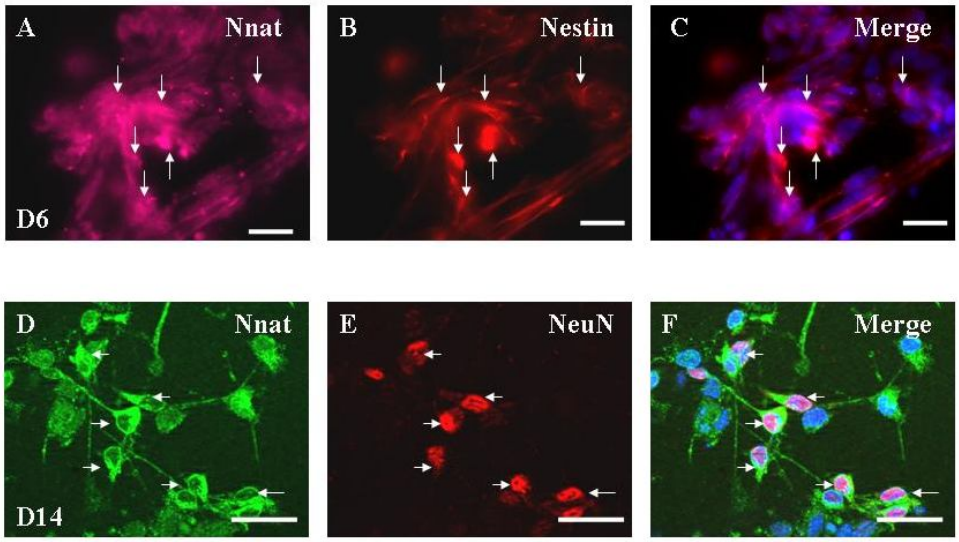

Fig. 3.3. Nnat is expressed in NSCs and neurons.
ESCs were plated on gelatin-coated coverslips and cultured in non-differentiating medium for 24 hours to allow the ESCs to adhere to the coverslips. The medium was then switched to differentiating medium. After 6 or 14 days of differentiation, cells were fixed to analyse the expression of Nnat, Nestin, and NeuN using immunocytochemistry. (A-C) Co-localisation of Nnat (A, pink, arrows) with the NSC marker Nestin (B, red, arrows) was noted after 6 days of differentiation. (D-F) Co-localisation of Nnat (D, green, arrows) with the neuronal marker NeuN (E, red, arrows) was noted after 14 days of differentiation. NeuN was expressed in the nucleus (E, F) and surrounded by Nnat expression in the cytosol (D, arrows). All nuclei were stained with DAPI (blue). Scale bar, 20 µm.
Abbreviations: D6, 6 days of differentiation; D14, 14 days of differentiation; DAPI, 4',6-diamidino-2-phenylindole; ESC, embryonic stem cell; GFP, green fluorescent protein; NeuN, neuronal nuclear antigen; NSC, neural stem cell; Sox1, SRY (sex determining region Y)-box 1.

3.2.3 Nnat over-expressing increases the generation of neural cells

To investigate the function of Nnat during neural development, loss- and gain-of-function approaches were employed. Before my involvement in the Nnat project, our group had already generated the Nnat-KD ESCs (see Material and Methods, section 2.1). In these cells Nnat was knocked down using Nnat short hairpin RNA (shRNA), designed to knock down both *Nnatα* and *Nnatβ* isoforms. To fully elucidate the effect of Nnat on neural development, Nnat-OE ESCs were generated as part of my study (see Material and Methods, section 2.2). If my hypothesis that Nnat is needed during neural development is correct, then I would expect that, Nnat over-expression will promote neural development while Nnat knock down will hinder this process.

3.2.3.1 Generation of Nnat-OE ESC lines

46C ESCs were used to create stably transfected pNEBR-Nnatα or pNEBR-Nnatβ ESCs (see Material and Methods, section 2.2). After Hygromycin selection, 16 single-cell clones were generated. To check whether Nnat was overexpressed in these clones, all clones and 46C ESCs were plated onto gelatinised coverslips and grown in non-differentiating condition for two days. Cultures were fixed with 4% PFA and the expression of Nnat was analysed using immunocytochemical analysis (see Appendix 3). Nnatα-OE clone 7 and Nnatβ-OE clone 4 were chosen to carry out all of the experiments described in this thesis.

To compare Nnat expression by western blot analysis, 46C, Nnat-KD, Nnatα-OE, and Nnatβ-OE ESCs were cultured in non-differentiating medium until 100% confluent and then whole cell lysates were collected for electrophoresis. After gel electrophoresis, proteins were transferred to a nitrocellulose membrane and the presence of Nnat detected by immunoblotting using an anti-Nnat antibody (see Material and Methods, section 2.7). 46C and Nnatβ-OE ESCs expressed Nnatα weakly compared with Nnatα-OE ESCs. Neither 46C nor Nnatα-OE ESCs expressed Nnatβ (Fig. 3.4). According to the expression of Nnat *in vivo*, Nnatα is expressed earlier than Nnatβ (see section 1.7), so 46C ESCs may represent a developmental stage before Nnatβ is expressed. No expression of either isoform was observed in the Nnat-KD ESCs (Fig. 3.4). The results confirmed that Nnat was over-expressed in Nnat-OE ESCs and was knocked down by the Nnat shRNA in Nnat-KD ESCs.

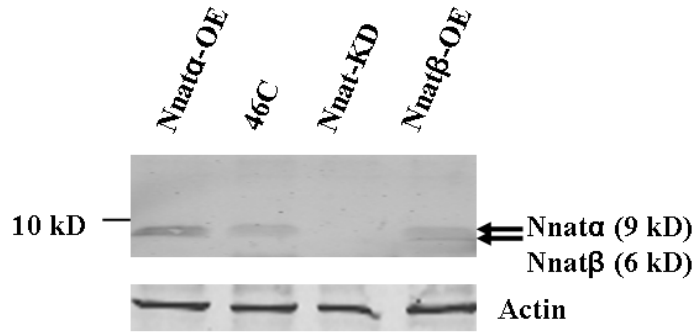

Fig. 3.4. Nnat protein expression in 46C and Nnat-mutant ESCs.
46C, Nnatα-OE, Nnatβ-OE, and Nnat-KD ESCs were cultured under non-differentiating conditions until they reached 100% confluency and then whole cell protein lysates were collected to analyse the expression of Nnat by Western blotting using an antibody that detected both isoforms. 46C ESCs weakly expressed Nnatα and did not expressed Nnatβ. Nnatα-OE ESCs expressed higher Nnatα compared with the parent 46C cells. Nnatβ-OE ESCs not only expressed a low level of Nnatα like 46C, but also expressed Nnatβ. Nnat-KD ESCs did not express Nnatα or Nnatβ. The results confirmed that Nnat was over-expressed or knocked down in Nnat-OE or Nnat-KD ESCs.
Abbreviations: ESC, embryonic stem cell; kD, kiloDalton; Nnat-KD, Nnat-knockdown; Nnatα-OE, Nnatα-overexpression; Nnatβ-OE, Nnatβ-overexpression.

3.2.3.2 Nnat over-expression enhances the generation of NSCs and neurons

To determine whether over-expression of *Nnatα* or *Nnatβ* in ESCs influenced their ability to differentiate into NSCs, 46C, Nnatα-OE and Nnatβ-OE ESCs were cultured under differentiating conditions for 6 days (see sections 2.3.1 and 3.2.1). Sox1 and Nestin are both markers of NSCs (Camus et al., 2006; Murayama et al., 2002; Ying et al., 2003; Zhao et al., 2004). However, Sox1 is also expressed in the lens during gastrulation in mouse embryos (Aubert et al., 2003), and Nestin is also expressed in astrocytes, developing pancreatic cells, and muscle precursors (Clarke et al., 1994; Messam et al., 2000; Selander and Edlund, 2002; Zimmerman et al., 1994). Thus, I stained these with two markers at the same time to verify that these cells were NSCs. After 6 days of differentiation, Nnatα-OE and Nnatβ-OE ESCs generated more Sox1-GFP$^+$/Nestin$^+$ NSCs than did 46C ESCs (Fig. 3.5A-C) indicating that over-expression of Nnat enhanced the generation of NSCs. This observation was confirmed by quantifying the numbers of Sox1-GFP$^+$/Nestin$^+$ NSCs (see Material and Methods, section 2.5), showing

that the percentage of NSCs generated by Nnatα-OE cells was two-fold greater than the percentage generated by 46C cells (Fig. 3.5D, 66.7% v.s. 24.2%, n = 3, $p < 0.01$). Because the effect of NSC generation by Nnatα or Nnatβ over-expression was similar, I did not count the NSCs derived from Nnatβ-OE ESCs.

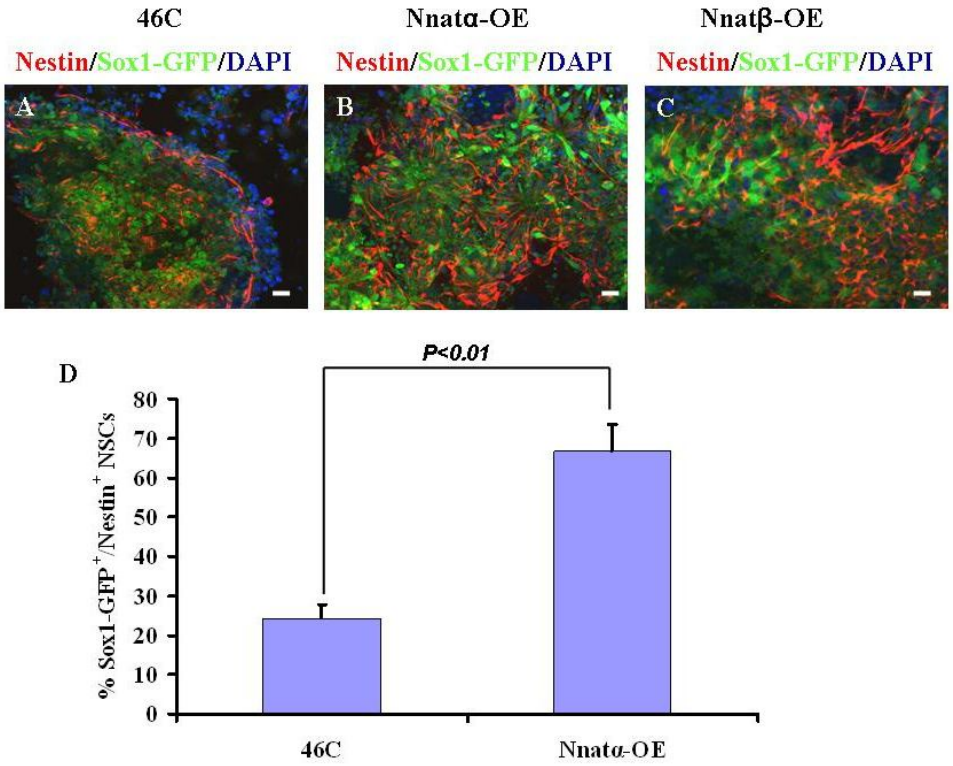

Fig. 3.5. Over-expression of Nnat promotes the generation of NSCs.
46C, Nnatα-OE and Nnatβ-OE ESCs were grown in monolayer culture and differentiated for 6 days. (A) 46C ESCs generated Sox1-GFP$^+$ (green) and Nestin$^+$ (red) NSCs. (B, C) Nnatα-OE and Nnatβ-OE ESCs generated more Sox1-GFP$^+$ and Nestin$^+$ NSCs compared with 46C ESCs. (D) The numbers of both Sox1-GFP and Nestin-expressing NSCs cells were quantified. 46C ESCs generated less NSCs than Nnatα-OE ESCs (24.2 ± 3.6% and 66.7 ± 6.7%, respectively, $p < 0.01$, n=3, two-tailed Student's t test). Thus, the over-expression of Nnat promoted the generation of NSCs. All nuclei were stained with DAPI (blue). Scale bar, 20 μm.
Abbreviations: DAPI, 4',6-diamidino-2-phenylindole; ESC, embryonic stem cell; GFP, green fluorescent protein; Nnatα-OE, Nnatα-overexpression; Nnatβ-OE, Nnatβ-overexpression; NSC, neural stem cell; Sox1, SRY (sex determining region Y)-box 1.

To determine whether over-expression of *Nnatα* or *Nnatβ* in ESCs influenced neuronal differentiation, 46C, Nnatα-OE and Nnatβ-OE ESCs were cultured under differentiating conditions for 14 days (see sections 2.3.1 and 3.2.1) to investigate their ability to generate neurons (identified

by their expression of MAP2). As expected, MAP2 expressing neurons were observed in cultures of differentiated 46C ESCs after 14 days (Fig. 3.6A). However, many more MAP2 expressing neurons were observed in differentiated Nnatα-OE and Nnatβ-OE ES cultures than in differentiated 46C ES cultures (Fig. 3.6B-C). Again this was confirmed by quantification of neuronal numbers (see Material and Methods, section 2.5) after ESCs had been differentiated for 14 days. For quantification, neurons were identified by NeuN instead of MAP2 because NeuN is located in the nucleus and is convenient for cell counting. The number of neurons generated by Nnatα-OE cells was two-fold higher that the number generated by 46C ESCs after 14 days of differentiation (Fig. 3.6D, 60.2% v.s. 21.4%, n = 3, $p < 0.01$).

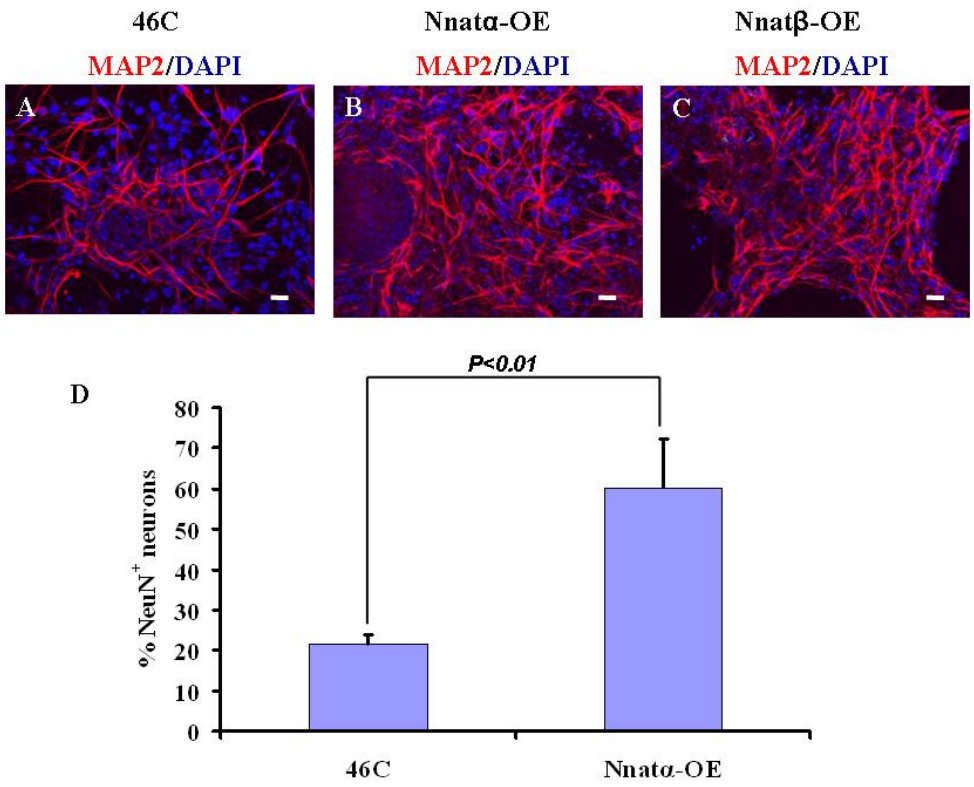

Fig. 3.6. Nnat promotes neuronal development.
46C, Nnatα-OE and Nnatβ-OE ESCs were grown in monolayer culture and differentiated for 14 days. (A) 46C ESCs generated $MAP2^+$ (red) neurons by 14 days. (B, C) Increased numbers of $MAP2^+$ (red) neurons was observed in differentiated Nnatα-OE and Nnatβ-OE ES cultures. (D) After 14 days of differentiation, neurons were identified by NeuN expression and quantified. 46C ESCs generated less neurons than did Nnatα-OE ESCs (21.4 ± 2.5% and 60.2 ± 12.1%, respectively, $p < 0.01$, n=3, two-tailed Student's t test). All nuclei were stained with DAPI (blue). Scale bar, 20 μm. Abbreviations: DAPI, 4',6-diamidino-2-phenylindole; ESC, embryonic stem cell; MAP2, microtubule-associated protein 2; NeuN, neuronal nuclear antigen; Nnatα-OE, Nnatα-overexpression; Nnatβ-OE, Nnatβ-overexpression.

These studies show that over-expressing Nnat enhances the differentiation of ESCs along a neural pathway, resulting in an increase in the generation of NSCs and subsequently neurons. However, these data were obtained using a single clone of Nnatα-OE and Nnatβ-OE ESCs. Therefore, it is potentially possible that a mutation caused by the genomic insertion of the transfected vector resulted in the increased generation of NSCs by Nnat-OE ESCs. Nevertheless, in the next section, I show that the effect of Nnat knockdown results in a reduction in the generation of neural cells, an opposite effect to that observed after Nnat over-expression, providing support for the conclusions I draw from the experiments described in this chapter.

3.2.4 Nnat knocked-down restricts the generation of neural cells

Since Nnat over-expression increased the generation of NSCs and neurons, I hypothesised that Nnat knocked-down would suppress neural induction in ESCs and hence reduce the generation of neurons. To test this hypothesis, the ability of Nnat-KD ESCs to differentiate into NSCs and neurons was evaluated.

3.2.4.1 Nnat-KD cells exhibit protracted Oct4 expression during neural differentiation

Undifferentiated ESCs tend to form compact colonies (Yu et al., 2007). Both undifferentiated 46C and Nnat-KD ESCs did form compact colonies and also highly expressed the pluripotent marker Oct4 (Fig. 3.7A-B). After 6 days of differentiation, 46C cells no longer formed compact colonies and the expression of Oct4 was decreased (Fig. 3.7C). However, Oct4 was still highly expressed in Nnat-KD cells at this stage (Fig. 3.7D). After 12 days of differentiation, Oct4 was no longer expressed in 46C (Fig. 3.7E), but Nnat-KD cells still retained Oct4 expression (Fig. 3.7F). Unlike 46C cells, Nnat-KD colonies maintained a compact morphology, characteristic of undifferentiated ESCs, throughout the differentiation procedure. The observed morphology of Nnat-KD cells together with their Oct4 expression indicated that the majority of Nnat-KD cells retained a pluripotent character.

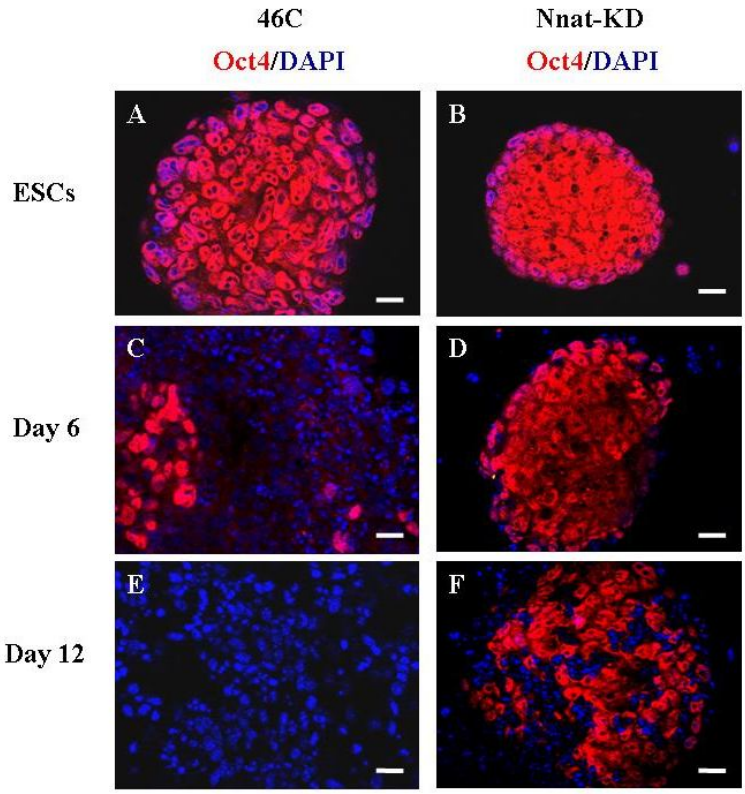

Fig. 3.7. Oct4 expression is protracted in Nnat-KD cells.
46C and Nnat-KD ESCs were grown in monolayer culture under non-differentiating conditions where they form compact colonies. (A, B) The pluripotent marker Oct4 (red) was highly expressed in undifferentiated 46C and Nnat-KD ESCs. (C) After 6 days of differentiation, the expression of Oct4 was down-regulated in 46C cells (compare C with A). and cells within these cultures had spread out. (E) After 12 days of differentiation, 46C cells no longer expressed Oct4. (D) After 6 days of differentiation, Oct4 was still highly expressed in Nnat-KD ESCs and these cells still grew as colonies like undifferentiated ESCs. (F) Even when cultured in differentiating conditions for 12 days, Oct4 expression was retained by Nnat-KD ESCs. All nuclei were stained with DAPI (blue). Scale bar, 20 μm.
Abbreviations: DAPI, 4',6-diamidino-2-phenylindole; ESC, embryonic stem cell; Nnat-KD, Nnat-knockdown.

3.2.4.2 Nnat knock-down curbs neural development

To test whether knocking down Nnat affected ESC differentiation into NSCs and neurons, 46C and Nnat-KD ESCs were plated on gelatin-coated coverslips and then cultured in differentiating conditions for 6 or 14 days (see sections 2.3.1 and 3.2.1). The cells were fixed and analysed for the ability to generate NSCs after 6 days of differentiation (identified using the Sox1-GFP and Nestin) and neurons after 14 days of differentiation (identified using the MAP2 or NeuN). The undifferentiated 46C and Nnat-KD ESCs did not express the NSC markers, Sox1-GFP and Nestin (Fig. 3.8A-B). After 6 days of differentiation, 46C ESCs generated NSCs, whereas the generation of NSCs was significantly reduced in Nnat-KD ESCs (Fig. 3.8C-D), as confirmed by cell counts (Fig. 3.8G, 2.4% v.s. 20.2%, n = 3, $p < 0.01$). In addition, although Nnat-KD cells did generate some Sox1-GFP expressing cells, these did not appear to significantly increase in number from day 6 to day 14 (Fig. 3.8D, F).

As might be expected, after 14 days of differentiation, 46C cells generated neurons, whereas very few such cells were generated by Nnat-KD ESCs (Fig. 3.8E-F). As before, NeuN expression was used for the quantification of neurons in these cultures (see section 3.2.3.3), revealing a significant reduction in the ability of Nnat-KD ESCs to generate these cells compared with 46C ESCs (Fig. 3.8H, 0.8% v.s. 21.4%, n = 3, $p < 0.01$).

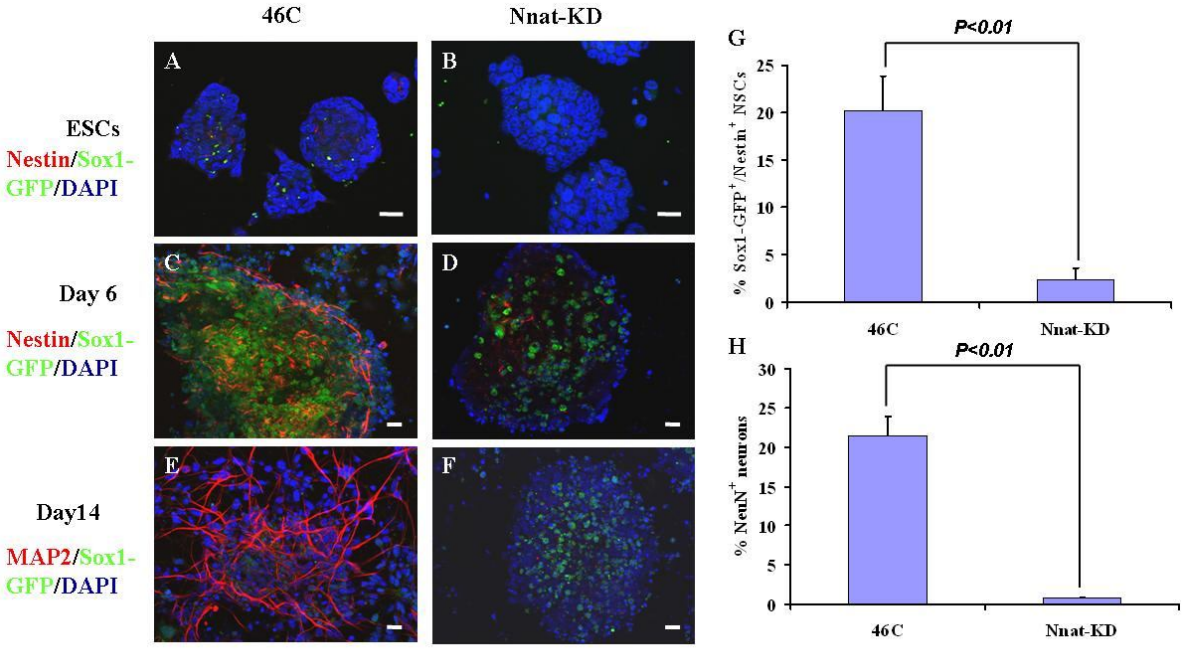

Fig. 3.8. Nnat knocked-down restricted neural development.
46C and Nnat-KD ESCs were grown in monolayer cultures. (A, B) The neuroectodermal marker Sox1 (green) and NSC marker Nestin (red) were not expressed by undifferentiated 46C and Nnat-KD ESCs. (C) After 6 days of differentiation, 46C ESCs generated Sox1-GFP$^+$ and Nestin$^+$ NSCs. (D) The generation of NSCs were significantly reduced in Nnat-KD cells. (G) Quantification of NSCs in Nnat-KD and 46C differentiated cultures (2.4 ± 1.2% and 24.2 ± 3.6%, respectively, $p < 0.01$, n=3, two-tailed Student's t test). (E) After 14 days of differentiation, 46C ESCs generated MAP2$^+$ neurons but (F) Nnat-KD ESCs generated few if any MAP2$^+$ neurons. (H) The percentage of NeuN$^+$ neurons was counted. Nnat-KD cells generated less neurons than did 46C cells (0.8 ± 0.03% and 21.4 ± 2.5%, respectively, $p < 0.01$, n=3, two-tailed Student's t test). This data suggested that Nnat knockdown restricted neural development. All nuclei were stained with DAPI (blue). Scale bar, 20 µm.
Abbreviations: DAPI, 4',6-diamidino-2-phenylindole; ESC, embryonic stem cell; GFP, green fluorescent protein; MAP2, microtubule-associated protein 2; NeuN, neuronal nuclear antigen; Nnat-KD, Nnat-knockdown; SRY (sex determining region Y)-box 1.

In summary, Oct4 expression was protracted in Nnat-KD ESCs even after 12 days of differentiation and the generation of Sox1-GFP$^+$/Nestin$^+$ NSCs and NeuN$^+$ or Map2$^+$ neurons was significantly reduced compared with wild type ESCs. This indicates that Nnat knock-down disturbs the neural induction of ESCs, limiting their ability to generate neural cells.

3.2.5 Nnat re-expression rescues the Nnat-knockdown phenotype

In order to confirm that the knocked-down phenotype described above was not due to off-target RNA interference, Nnat-KD ESCs were transfected with pNEBR-Nnatα or pNEBR-Nnatβ vectors (see Materials and Methods, section 2.2.4) to determine whether *Nnatα* or *Nnatβ* re-expression could rescue the Nnat-KD phenotypes, which manifest as a reduction of the generation of NSCs and hence neurons.

Nnat-KD ESCs were transfected with pNEBR-Nnatα or pNEBR-Nnatβ vectors using Lipofectamine and then stably transfected cell lines were generated (see Materials and Methods, section 2.2). The resultant ES lines were cultured on gelatin-coated coverslips and then differentiated towards NSCs and neurons (see sections 2.3.1 and 3.2.1). The expression of Nnat was analysed by immunofluorescence staining and Nnat-KD/Nnatα or Nnat-KD/Nnatβ ESCs were found to express Nnat protein highly, whereas, as expected, Nnat-KD cells were negative (Fig. 3.9A-C). After 6 days of differentiation, Nnat-KD/Nnatα and Nnat-KD/Nnatβ ESCs were able to generate significantly more Sox1-GFP$^+$/Nestin$^+$ NSCs compared with Nnat-KD ESCs (Fig. 3.9D-F) and similarly, after 14 days of differentiation, they generated significantly more MAP2$^+$ neurons (Fig. 3.9G-I). However, the neuron production by both types of Nnat-KD/Nnat cells was less than that observed when wild type ESCs were differentiated (compare Fig. 3.8 with Fig. 3.9). This may be due to the silencing effect of Nnat shRNA still present in the Nnat-KD cells. These results showed that *Nnatα* or *Nnatβ* re-expression could rescue the ability of Nnat-KD cells to generate neural cells, suggesting that the phenotypic change of Nnat-KD ESCs was caused by *Nnat* knockdown and not due to "off-target" effects.

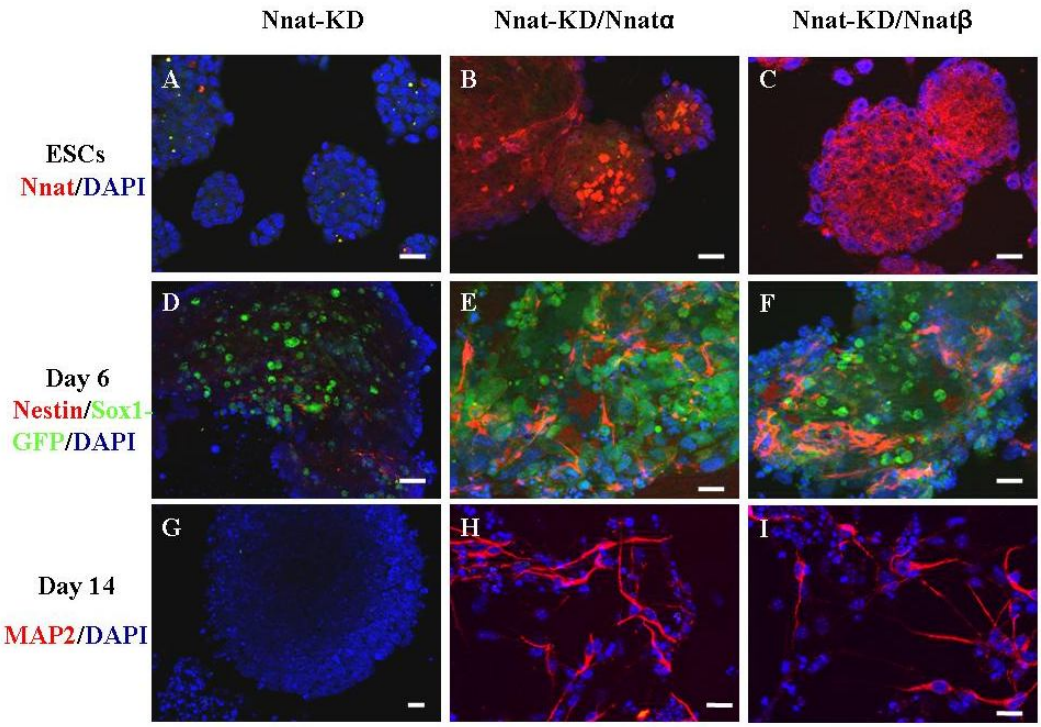

Fig. 3.9. Nnat re-expression rescues the ability of Nnat-KD ESCs to generate neural cells.

Nnatα or Nnatβ stably transfected ESC lines were generated from parent Nnat-KD ESCs. Nnat-KD, Nnat-KD/Nnatα, and Nnat-KD/Nnatβ ESCs were grown in monolayer culture and differentiated for 6 or 14 days. The expression of Nnat, Nestin, and MAP2 in the undifferentiated day 6-differentiated and day 14-differentiated cells were analysed respectively by immunocytochemistry. (A) Nnat (red) was not expressed in the undifferentiated Nnat-KD ESCs. (B) Nnatα (red) was re-expressed in the undifferentiated Nnat-KD/Nnatα ESCs and (C) Nnatβ (red) was re-expressed in the undifferentiated Nnat-KD/Nnatβ ESCs. (D) After 6 days of differentiation, Nnat-KD ESCs only generated a few Sox1-GFP^{+} (green) and Nestin^{+} (red) NSCs. (E, F) After Nnatα or Nnatβ was re-expressed in Nnat-KD cells, the generation of NSCs was increased compared with the parent Nnat-KD cells. (G) After 14 days of differentiation, Nnat-KD ESCs generate few, if any, neurons. (H, I) After Nnatα or Nnatβ re-expression, ESCs regained their ability to generate neurons. All nuclei were stained with DAPI (blue). Scale bar, 20 μm.

Abbreviations: DAPI, 4',6-diamidino-2-phenylindole; ESC, embryonic stem cell; GFP, green fluorescent protein; MAP2, microtubule-associated protein 2; Nnat-KD, Nnat-knockdown; Sox1, SRY (sex determining region Y)-box 1.

3.2.6 Nnat-KD ESCs still have the ability to generate the three primary germ layers

Normally wild type ESCs differentiate into primitive ectoderm and then into the three primary germ layers (ectoderm, mesoderm, and endoderm) (Fig. 10; Desbaillets et al., 2000; Fok and Zandstra, 2005; Keller, 2005; Rathjen et al., 1999). Ectodermal cells will further differentiate into neuroectodermal cells and epithelial cells (Desbaillets et al., 2000; Greber et al., 2010). Nnat-KD ESCs are impaired in their ability to generate neuroectodermal cells, and hence NSCs and neurons (see the section 3.2.4.2). To examine whether this impairment was attributed to the fact that Nnat-KD ESCs simply failed to differentiate efficiently into any of the three primary germ layers or were pushed along a non-neural lineage, 46C, Nnatα-OE, and Nnat-KD ESCs were grown under conditions known to promote differentiation into the three primary germ layers (aggregate culture; Fok and Zandstra, 2005). In this culture system, ESCs differentiate in a three dimensional mode and form EBs, which have the ability to differentiate into the three primary germ layers. The differentiation of EBs mimics early mammalian embryogenesis and provides a platform to study the impact of genetic manipulations, during early embryonic development (Desbaillets et al., 2000; Fok and Zandstra, 2005). After culture for 6 days, EBs were collected for total RNA isolation and quantitative real-time PCR was used to analyse the expression pattern of markers for primitive ectoderm, ectoderm, mesoderm and endoderm. *Fgf5*, a marker of primitive ectoderm, was expressed in 46C and Nnatα-OE cells, but was expressed at much higher levels in Nnat-KD cells (Fig. 3.11A). Thus, Nnat-KD cells may generate more primitive ectoderm than the other cell types. *Brachyury* and *Mesp1* (mesoderm), *Hnf4* (endoderm), and *Otx2* (ectoderm) were also expressed in 46C, Nnatα-OE, and Nnat-KD cells (Fig. 3.11B-E). Thus, Nnat-KD ESCs could differentiate into primitive ectoderm, and the three germ layers like 46C and Nnatα-OE ESCs. As expected, the expression of the neuroectodermal marker *Sox1* was significantly lower in Nnat-KD ESCs compared with 46C and Nnatα-OE ESCs (Fig. 3.11F, $p < 0.05$). Nnatα-OE cells showed an increase in the expression of *Brachyury* compared with 46C ESCs (Fig. 3.11B, $p < 0.05$). A similar result also was

found in *Xenopus* embryos, where over-expression of mouse *Nnatα* or *Nnatβ* increased the expression of the mesodermal marker *nxk2.5* (see section 3.2.7 and Fig. 3.13). These results suggest that Nnat may also promote the generation of mesodermal cells (see section 3.3.3 for a discussion of this observation).

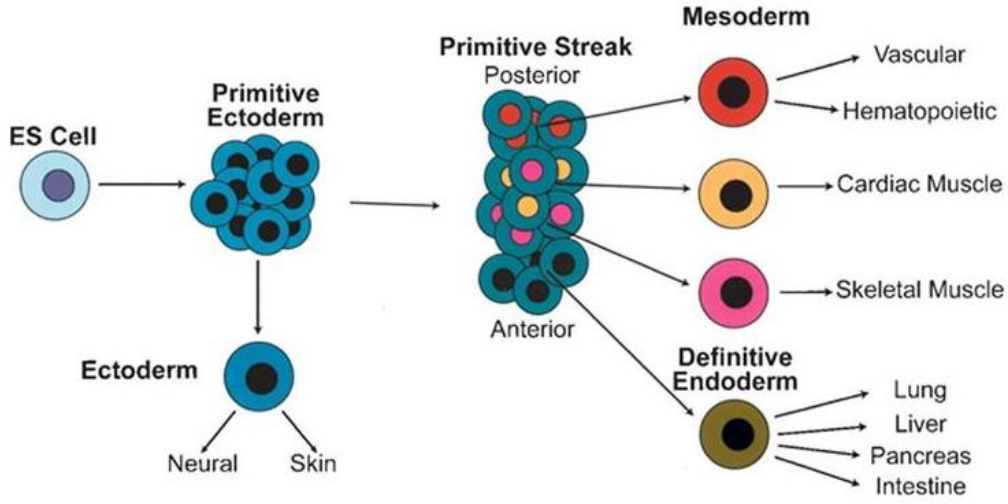

Fig. 3.10. Schematic diagram of ESCs differentiation.
ESCs give rise to primitive ectoderm and the primitive ectoderm generates ectoderm and primitive streak. The ectoderm further differentiates into neuroectoderm and epithelium to generate neural and skin cells, respectively. The primitive streak differentiates into mesoderm and definitive endoderm. The mesoderm forms cardiovascular system and skeletal muscles. The definitive endoderm forms lung, liver, pancreas, and intestine.
Abbreviations: ESC, embryonic stem cell.
(Modified from Keller, 2005)

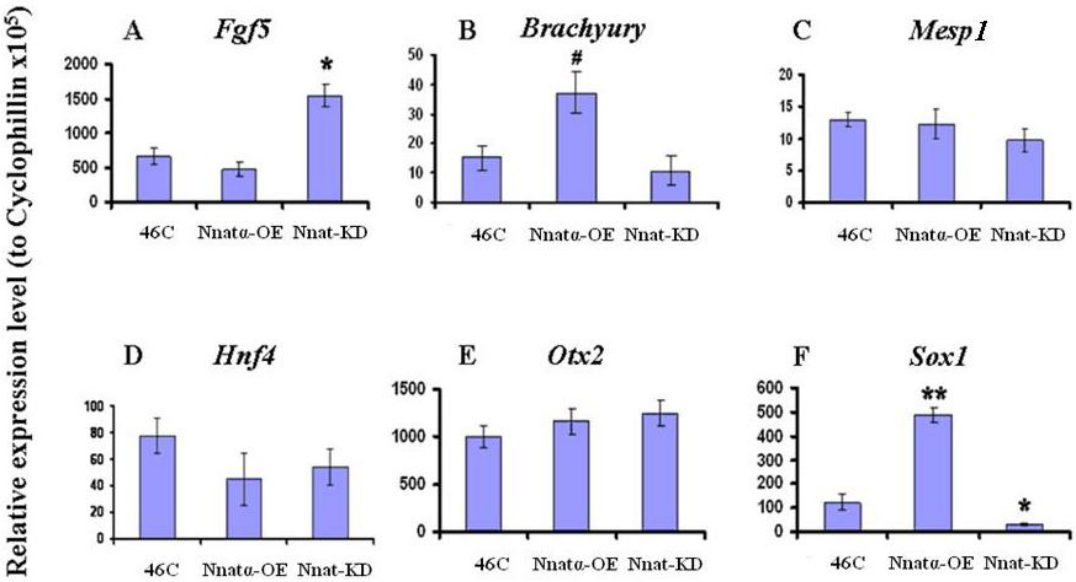

Fig. 3.11. The competence of Nnat-mutant ESCs to give rise to the three primary germ cells.

The generation of neuroectoderm by Nnat-KD ESCs was significantly reduced in the monolayer culture system. In order to rule out the possibility that this impairment of neural development was attributed to the fact that Nnat-KD ESCs simply failed to generate primitive ectoderm and three primary germ layers, 46C, Nnatα-OE, and Nnat-KD ESCs were cultured to form EBs using aggregate culture. After 6 days, EBs were collected to examine the expression of different genes using real-time PCR. (A) 46C, Nnatα-OE, and Nnat-KD ESCs all expressed the primitive ectoderm marker *Fgf5* but expression was significantly higher in Nnat-KD ESCs ($p < 0.05$, one-way ANOVA test). (B) 46C, Nnatα-OE, and Nnat-KD ESCs all expressed the mesoderm marker *Brachyury* with expression being highest in Nnatα-OE ESCs ($p < 0.05$, one-way ANOVA test). 46C, Nnatα-OE, and Nnat-KD ESCs all expressed (C) the mesoderm marker *Mesp1*, (D) the ectodermal marker *Hnf4* and (E) the ectoderm marker *Otx2*. (F) The expression of the neuroectoderm marker *Sox1* was higher in Nnatα-OE ESCs than 46C and Nnat-KD ESCs ($p < 0.01$, one-way ANOVA test), and also 46C expressed higher *Sox1* than did Nnat-KD ESCs ($p < 0.05$, one-way ANOVA test).

Abbreviations: ANOVA, analysis of variance; EB, embryoid body ; ESC, embryonic stem cell; *Fgf*, fibroblast growth factor; *Hnf4*, Hepatocyte Nuclear Factor 4; *Mesp1*, mesoderm posterior 1; Nnat-KD, Nnat-knockdown; Nnatα-OE, Nnatα-overexpression; PCR, polymerase chain reaction; *Sox1*, SRY (sex determining region Y)-box 1.

In order to analyse the protein expression of Brachyury (a marker of mesoderm) and Keratin 18 (a marker of epithelial tissue), EBs were dissociated and re-plated on coverslips for immunocytochemical analysis. 46C, Nnatα-OE, and Nnat-KD ESCs generated Brachyury-expressing mesodermal cells, as expected, and also Keratin 18-expressing epithelial cells (Fig. 3.12). Therefore, the impairment of Nnat-KD ESCs to generate neuroectodermal cells is not attributable to the fact that Nnat-KD ESCs fail to differentiate into the primitive ectoderm or the three primary germ layers.

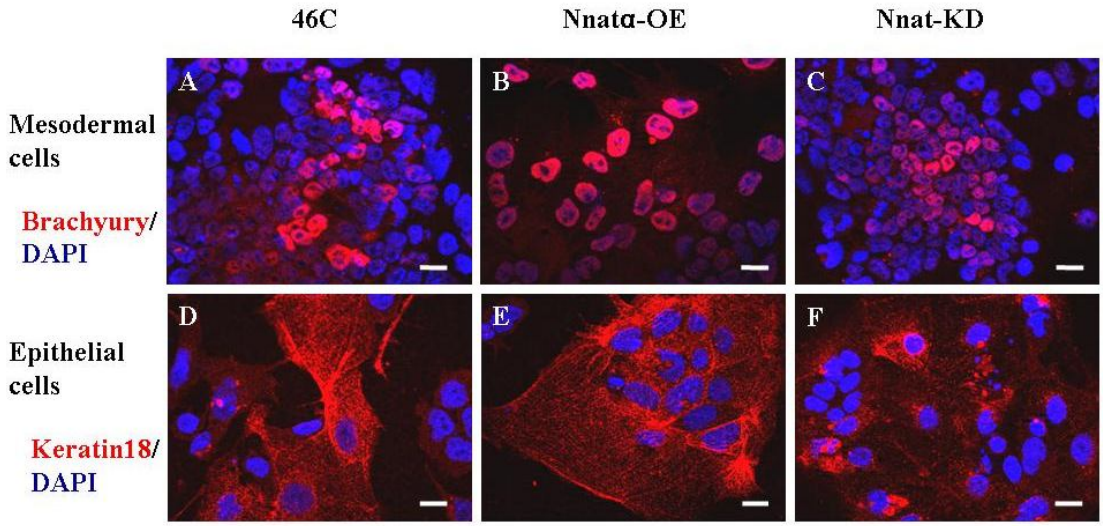

Fig. 3.12. Nnat-mutant ESCs generate mesodermal and epithelial cells in the same way as do wild-type ESCs.
46C, Nnatα-OE, and Nnat-KD ESCs were cultured to form EBs. After 6 days, EBs were dissociated with trypsin and re-plated on coverslips. After being cultured for 24 hours, the expression of the mesodermal marker Brachyury and epithelial marker Keratin 18 were analysed by immunocytochemistry. (A-C) 46C, Nnatα-OE, and Nnat-KD ESCs all generated Brachyury-expressing mesoderm. (D-F) 46C, Nnatα-OE, and Nnat-KD ESCs all generated Keratin 18-expressing epithelial cells. All nuclei were stained with DAPI (blue). Scale bar, 20 μm.
Abbreviations: DAPI, 4',6-diamidino-2-phenylindole; EB, embryoid body ; ESC, embryonic stem cell; Nnat-KD, Nnat-knockdown; Nnatα-OE, Nnatα-overexpression.

It is possible that the anti-keratin antibody may cross react with actin and/or collagen (Baboonian et al., 1991). In order to rule out any false positive effects from using this antibody, 46C and Nnatα-OE ESCs were grown in differentiating conditions for 4 days with or without the treatment with BMP4 (10 ng/ml for four days). BMP4 is an epidermal

inducer and neural inhibitor (Wilson and Hemmati-Brivanlou, 1995), so treatment of 46C ESCs with BMP4 suppressed the generation of Sox1-GFP$^+$ neural progenitors (see section 5.2.5), but induced the generation of Keratin 18$^+$ epidermal cells, acting as a positive control for the anti-keratin antibody. However, BMP4 treated Nnatα-OE ESCs still preserved the ability to generate Sox1-GFP$^+$ neural progenitors (see section 5.2.5). If the anti-Keratin 18 antibody cross reacted with actin, the Sox1-GFP$^+$ cells should be stained with the antibody. After fixation, immunocytochemical analysis was performed and the same anti-keratin 18 antibody was applied. The Sox1-GFP$^+$ neural progenitors were not stained with Keratin 18 while the BMP4 treated cells generated large Sox1-GFP^{--}/keratin 18$^+$ cells, suggesting that the anti-keratin antibody did not bind non-specifically (see Appendix 4).

3.2.7 Nnat over-expression neuralises ectoderm in *Xenopus laevis*

As showed in the previous sections, Nnat over-expression promoted mouse ESCs differentiation towards a neural fate *in vitro*. However, the results of *in vitro* experiments do not always correlate with the *in vivo* situation. To examine whether Nnat over-expression also affects neural development *in vivo*, we collaborated with Dr. Esther Bell (MRC Centre for Developmental Neurobiology, King's College London) to look at the effects of Nnat over-expression in *Xenopus laevis.* These experiments were carried out by Dr. Esther Bell and her group. Her results are shown for the completeness of my thesis.

The *Xenopus* neural induction model is a widely used and well-established model (Bell et al., 2003; Munoz-Sanjuan and Brivanlou, 2002). To over-express *Nnat* in *Xenopus* embryos, *Nnatα* or *Nnatβ* mRNAs were injected into the embryos at the 2-cell stage and the embryos left to develop to early tadpole stage. *Nnatα* or *Nnatβ* over-expression resulted in enlarged brain tissue and expansion of the expression domain of the neural marker *NCAM* at the early tadpole stage (Fig. 3.13A-C). The animal cap assay (see section 1.3) also demonstrated that mouse *Nnat* over-expression caused neural induction in *Xenopus*. The isolated animal cap explants have

the potential to differentiate into the three primary germ layers, so are used to study the factors that direct differentiation along different lineages (Agius et al., 2000; Sasai et al., 1996). The isolated animal caps give rise to neural cells after treatment with neural inducers (Grunz and Tacke, 1989; Munoz-Sanjuan and Brivanlou, 2002). In the animal cap assay, the mouse *Nnat* mRNA was injected into *Xenopus* embryos at the 2-cell stage and then animal cap explants were cut at the blastula stage (before neural induction occurs in the gastrula stage, see section 1.3) and cultured *in vitro*. Explants were harvested at last gastrula stage and the neural and mesodermal markers were analysed by RT-PCR (reverse transcriptase PCR) (Fig. 3.13D). *Nnatα* or *Nnatβ* over-expression up-regulated the neural plate marker *nrp1*. Therefore, *Nnat* overexpression neuralises animal cap explants in *Xenopus*. *Nnatα* or *Nnatβ* over-expression also increased the expression of *nxk2.5* (a heart/mesoderm marker). This result was similar to the increased expression of the mesoderm marker *Brachyury* in Nnatα-OE cells (Fig. 3.11B) with both *Xenopus* and mouse systems showing that Nnat also increases mesoderm production. These *in vivo* results revealed that Nnat plays a conserved role in *Xenopus* and mouse ESCs.

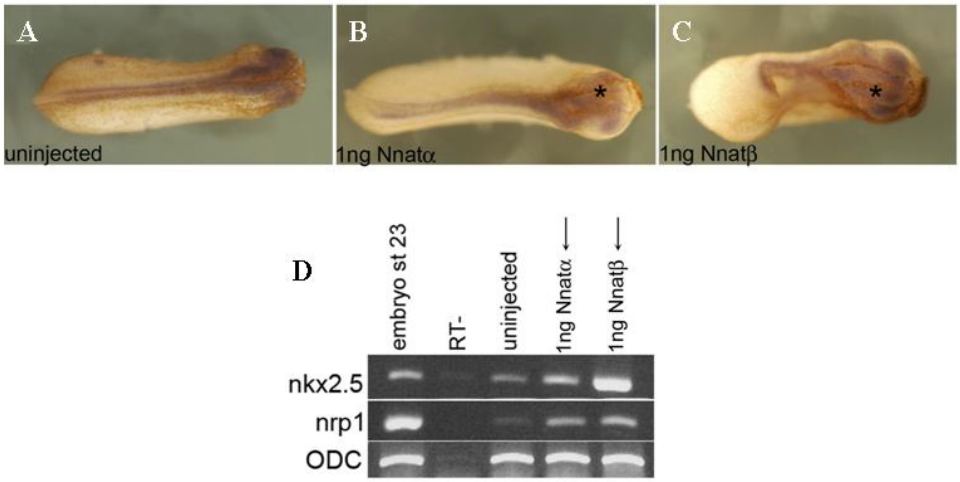

Fig. 3.13. The effects of *Nnatα* and *Nnatβ* on neural induction in *Xenopus*.
(A-C) To determine whether Nnat causes neural induction *in vivo*, 1 ng *Nnatα* or *Nnatβ* mRNA was injected into *Xenopus* embryos at the 2-cell stage, and then embryos were left to develop to the early tadpole stage. (A) In un-injected embryos, the neural marker *NCAM* (blue) was expressed in neural tissue of the tadpole. (B, C) Injecting *Nnatα* or *Nnatβ* enlarged the brain tissue and the expression domain of *NCAM* in the injection side (*). (D) In animal cap assay, 1ng *Nnat* mRNA was injected into the embryos at the 2-cell stage and then animal cap explants were cut at blastula stage and cultured *in vitro*. Explants were harvested at last gastrula stage and the neural (*nrp1*) and mesodermal (*nkx2.5*) markers were analysed by RT-PCR. Embryos at stage 23 and RT- (no reverse transcriptase) were the positive and negative control, respectively. *Nkx2.5* and *nrp1* were up-regulated in the injected explants compared with un-injected explants. *ODC* was used as a loading control.
Abbreviations: *NCAM*, neural cell adhesion molecule; *ODC*, ornithine decarboxylase; RT-, no reverse transcriptase; RT-PCR, reverse transcription polymerase chain reaction.
(Adapted from Lin et al., 2010)

3.3 Discussion

3.3.1 Summary of main findings

In summary, Nnat expression is up-regulated when ESCs begin to differentiate along the neural lineage *in vitro*. Gain- and loss-of-function experiments show that ESCs in which Nnat expression had been knocked-down have a dramatically decreased ability to generate NSCs, and subsequently neurons, while ESCs in which Nnat is over-expressed generate an excess of NSCs and hence neurons. These *in vitro* results were consistent with the *in vivo* experiments showing that microinjecting *Nnat* mRNA into *Xenopus* embryos increased the generation of neural cells. Thus, these results suggest that Nnat is needed for the neural induction and subsequent neural development of mouse ESCs.

3.3.2 Nnat is an intrinsic factor for neural induction

During gastrulation, ectoderm will be induced to give rise to neural tissue by molecules that are called neural inducers (Harland, 1994). Neural inducers also cause the neuralisation of isolated animal cap explants (Pera et al., 2003; Stern, 2005). The known neural inducers include BMP antagonists (Noggin, Chordin, and Follistatin), Wnt antagonist (Dickkopf-1), and FGFs (Ang et al., 1994; Doniach, 1995; Glinka et al., 1998; Holley et al., 1995; Kuroda et al., 2005; Lee et al., 2006; Slack, 1994). BMP antagonists are secreted by the organiser region which is a part of the mesoderm (see section 1.3; Gaulden and Reiter, 2008; Lebreton and Jones, 2006; Leyns et al., 1997). The treatment of *Xenopus* embryos with BMP antagonists (Noggin, Follistatin or Chordin) induces the generation of neural cells from embryonic ectoderm (Batut et al., 2005; Hemmati-Brivanlou et al., 1994; Knecht et al., 1995; Lamb et al., 1993; Sasai et al., 1995). During early gastrulation, the Wnt antagonist, Dickkopf-1, is first expressed in the organiser region of *Xenopus*, and in the animal cap assay, Dickkopf-1 induces the expression of the neural marker *NCAM* (Glinka et al., 1998). These results suggest that BMP and Wnt antagonists are not generated within the prospective neural ectoderm during early neural development, so these antagonists could be regarded as extrinsic factors that regulate neural induction.

The expression of Nnat in mammalian embryos was first seen before the formation of the neural plate and maximal expression was seen in neural tissue during gastrulation (details see section 1.7; Sousa-Nunes et al., 2003), suggesting that Nnat may have a role in neural induction. Gain- and loss-of function experiments (see sections 3.2.3 and 3.2.4) showed that Nnat knocked-down in mouse ESCs suppressed the generation of neural cells, and conversely Nnat over-expression in mouse ESCs enhanced the formation of neural cells. These results suggest that Nnat expression is needed for the neural induction of mouse ESCs, and Nnat promotes ESCs differentiation along the neural lineage. Further to this, injecting mouse *Nnat* mRNA into *Xenopus* embryos increased the generation of neural tissue in *Xenopus* embryos and up-regulated neural plate markers in animal cap explants (see section 3.2.7), suggesting that Nnat has the property of a neural inducer. However, unlike BMP and Wnt antagonists, which are secreted by the organiser region, Nnat is highly expressed within the developing neural tissue (see section 1.7). My work also revealed that Nnat is expressed in cells that belong to the neural lineage when mouse ESCs differentiate along a neural differentiation pathway (see section 3.2.2). Furthermore, Nnat is a membrane protein localised within the ER (Dou and Joseph, 1996; Joe et al., 2008), and so far, there is no evidence that cells can secrete Nnat. These findings suggest that Nnat initiates neural development of mouse ESCs internally and it can therefore be considered as an intrinsic regulator of neural induction.

When *BMP4* was electroporated into the prospective neural plate of chick embryos *in vivo*, the expression of the neural plate markers *Sox2* and *Sox3* in the normal neural domain were inhibited (Linker and Stern, 2004), suggesting that BMP is a negative cue for neural induction (see sections 1.2, 1.3, and 1.4). In contrast, the injection of *Fgf8* mRNA into *Xenopus* embryos to activate FGF signalling induced ectopic neural tissue (Pera et al., 2003), suggesting that FGF acts as a positive cue for neural induction (see section 1.5.1). Within this Chapter, gain- and loss-of-function experiments revealed that the generation of NSCs was increased when

Nnat was over-expressed in mouse ESCs, and conversely the generation of NSCs was reduced significantly when Nnat expression was knocked-down, suggesting that Nnat has a positive effect on neural induction in mouse ESCs. Similarly, *Fgf4*$^{-/-}$ mouse ESCs have been shown to generate significantly fewer Nestin-expressing NSCs than wild type ESCs after 6 days of differentiation - the same differentiating condition used in my study (Kunath et al., 2007). At the same time, over 90% of *Fgf4*$^{-/-}$ mouse ESCs still express the pluripotent marker Oct4 after 6 days of differentiation. My results also show that the generation of NSCs was reduced and the expression of Oct4 was protracted in the Nnat-KD ESCs even after 12 days of differentiation (see section 3.2.4). Thus, like FGF, Nnat is a positive cue that promotes the neural induction of mouse ESCs.

3.3.3 Nnat may also affect the generation of primitive ectoderm and early mesoderm

ESCs have the ability to differentiate into primitive ectoderm and then into the three primary germ layers sequentially (Fok and Zandstra, 2005; Keller, 2005; Rathjen et al., 1999). My experiments show that when wild type and Nnat-mutant ESCs were grown in suspension culture to form EBs, they expressed markers representative of primitive ectoderm and all three germ layers (*Fgf5*, primitive ectoderm marker; Brachyury, mesodermal marker; and Keratin 18 epithelial marker) (see section 3.2.6). These results imply that knocking down Nnat does not inhibit the formation of ectodermal cells. Thus, the reduction of Nnat-KD ESCs to generate neuroectodermal cells which are generated from ectodermal cells is not due to the fact that Nnat-KD ESCs fail to differentiate into ectodermal cells. However, as shown in Figure 3.11A, Nnat-KD cells express higher levels of *Fgf5* in EBs than either 46C or Nnatα-OE cells (see section 3.2.6). This may be due to the up-regulation of BMP4 expression observed in Nnat-KD ESCs that in turn promotes the expression of *Fgf5*. Indeed, I will go on to show in Chapter 5 that Nnat knocked-down resulted in an increased expression of BMP4. The disruption of growth differentiation factor-3 (GDF3, a BMP inhibitor) expression by gene trap in mouse ESCs causes *Fgf5* up-regulation in EBs (Levine and Brivanlou, 2006). This suggests that the

activation of BMP signalling, by inhibiting the expression of GDF3, increases the expression of *Fgf5*. Compared with 46C and Nnatα-OE ESCs, Nnat-KD ESCs expresses higher level of BMP4 and its target genes (see section 5.2.6). Thus, the up-regulation of *Fgf5* in Nnat-KD cells may be due to the fact that BMP signalling is up-regulated in Nnat-KD cells. Conversely, however, Zhang et al. (2010) showed that BMP4-treatment decreased *Fgf5* expression in EBs (Zhang et al., 2010). This opposite result may be due to the difference between the two culture conditions. In the latter study, EBs were cultured in serum free medium supplement with 10 ng/ml BMP4 for two days. In my experiments, EBs were cultured with serum containing medium for 6 days, conditions similar to those used by Levine and Brivanlou who obtained results similar to mine.

Brachyury is an early marker of mesoderm induction (Smith et al., 1991; Wilson et al., 1995). The expression of *Brachyury* is increased in animal cap explants exposed to FGF2 compared with untreated explants (Smith et al., 1991). Conversely, the injection of *Xenopus* embryos with a dominant-negative FGF receptor to inhibit FGF signalling reduces the expression of *Brachyury* (Schulte-Merker and Smith, 1995). These results suggest that the activation of FGF signalling up-regulates the expression of the mesodermal marker *Brachyury*. In Fig. 3.11B, Nnatα-OE cells express a higher level of *Brachyury* than do 46C and Nnat-KD cells. This may be due to the FGF/Erk signalling being activated by Nnat. In Chapter 4 and 5, I will show that Nnat increases cytosolic calcium levels and this results in the activation of FGF/Erk signalling. Thus, *Brachyury* may be up-regulated in Nnatα-OE cells because of the activation of FGF/Erk signalling. As shown in Fig. 3.13D, injecting *Nnat* mRNA into *Xenopus* embryos increased the expression of the mesodermal marker *nkx2.5* in animal cap explants. Therefore, Nnat may also be involved in mesoderm induction. However, further study would be required to confirm this observation.

3.3.4 Nnat plays different roles in different stages of neural development

The *in vivo* expression pattern of Nnat (see section 1.7) shows that Nnat is expressed from the beginning of neural induction to the end of neurogenesis. Neural induction is the initial step of neural development whereby the ectoderm differentiates into NSCs (Wilson and Edlund, 2001). Nnat knocked-down significantly reduces the generation of NSCs from mouse ESCs. In contrast, Nnat over-expression increases the generation of NSCs. These results suggest that Nnat plays a pivotal role in the neural induction of mouse ESCs. Neurogenesis is the process by which neurons are generated from NSCs and NPCs, so neural induction is followed by neurogenesis during neural development (Gaspard and Vanderhaeghen, 2010). In our *in vitro* model, Nnat is still expressed in NSCs, NPCs, and neurons (see sections 1.7 and 3.2.2). Therefore, after neural induction, Nnat may have other roles during neurogenesis. Although more neurons are generated from Nnat-OE ESCs, it is not clear whether this is due to the fact that Nnat actively promotes neurogenesis or simply due to the fact that Nnat-OE cells produce more NSCs. In order to determine the role of Nnat throughout neurogenesis, another two experiments could be carried out. First, Nnat conditional knocked-down ESCs could be generated. After ESCs differentiate into NSCs, Nnat could then be knocked down. Alternatively, Nnat could be simply knocked down in NSCs by transfection of RNAi (RNA interference). If Nnat expression is required for further neural development then the generation of neurons will be reduced. Second, Sox1-expressing NSCs could be sorted out (by fluorescence activated cell sorting) from Nnat-OE, Nnat-KD, and wild type ESCs after 6 days of differentiation, and then equal numbers of NSCs generated from different ESCs could be re-plated and differentiated into neurons. If Nnat expression is required for neurogenesis, fewer neurons would be generated in Nnat-KD cells. Using these two approaches, the function of Nnat in neurogenesis could be further analysed.

During development, as well as generating neurons, neural progenitor cells also generate glial cells (astrocytes and oligodendrocytes) (Kornblum,

2007; Raff et al., 1983). Within my thesis, I focused on the role of Nnat in neural induction, NPC formation and neuronal development, thus, I did not analyze the generation of glial cells. So far, it is unknown whether glial cells express Nnat or not; however, as mention in the introduction (section 1.8.1) NNAT was shown to be highly expressed in glioblastoma multiforme, the most malignant variant of human glial tumors (Xu et al., 2012). Furthermore, increasing expression of NNAT in malignant glioma cells promoted their proliferation, suggesting that Nnat may affect the self-renewal of glial cells.

3.3.5 Flow cytometry and cell counting

In this chapter, the numbers of Sox1-GFP$^+$/Nestin$^+$ NSCs and NeuN$^+$ neurons were counted manually. Compared with this, flow cytometry may be considered a more efficient way to quantify NSCs and neurons. Flow cytometry is a biophysical technology frequently used in cell counting and biomarker detection (Davey and Kell, 1996; Fukuda et al., 2006; Lyons and Parish, 1994). Indeed, flow cytometry was initially used to count the Sox1-GFP$^+$/Nestin$^+$ NSCs and NeuN$^+$ neurons; however, it was observed that the percentages of Nestin or NeuN-expressing cells determined using this method was decreased compared with manual counting, although the proportion of each cell-types remained similar. Also, when compared with previous report where the same ESCs and differentiation method was used as in my experiments (Kunath et al., 2007), the percentage of Nestin$^+$ cells in my experiments when analysed by flow cytometry appeared to be significantly underestimated. One possible reason for these lower cell counts could be due to the formation of cell aggregates. Both Nestin and NeuN are intracellular proteins, so permeabilisation was required for intracellular staining. Permeabilised cells can become sticky and aggregate to form cell clumps (Gujral et al., 2009) and such clumps would be filtered out prior to flow cytometry. This could potentially result in decreased numbers of Nestin or NeuN-expressing cells in the sample. In addition, low cell counts may also be due to the large fluorochrome which was conjugated to the secondary antibody. A Cy3-labeled secondary antibody was used in my experiments. Cy3 is a large molecular weight

fluorochrome and according to the applications guide of fluorochrome conjugates for flow cytometry (www.caltagmedsystems.co.uk/downloads/Caltag_Fluorochromes.pdf), this large molecular weight fluorochrome will reduce antibody motility and thus its entry into cells, resulting in a weak fluorescence intensity. Therefore, low molecular weight fluorochrome, such as Allophycocyanin and R-Rhycoerythrin, should be used to detect intracellular proteins.

3.3.6 The role of NNAT in neural induction of human ESCs

As shown in section 3.2.7, the ability of *Nnat* over-expression to promote neural development is conserved in *Xenopus* and mouse ESCs. If the mechanisms of neural induction are similar in all vertebrates, then NNAT may also be needed for the neural induction of human ESCs. According to the NCBI protein database, there is only one amino acid difference between human and mouse Nnat proteins (http://www.ncbi.nlm.nih.gov/protein/?term=Nnat). Thus to test the hypothesis that NNAT may also play a role in the neural induction of human ESCs, similar loss- and gain-of-function experiments to those described in this chapter could carried out using human ESCs.

Chapter 4. Nnat promotes neural development by modulating intracellular calcium levels

4.0 Nnat promotes neural development by modulating intracellular calcium levels

4.1 Introduction

As shown in Chapter 3, mouse ESCs grown in a monolayer differentiation system sequentially differentiated into neuroectodermal cells, NSCs, NPCs, and neurons. Nnat expression was up-regulated when mouse ESCs began to differentiate along this neural lineage. Furthermore, experiments showed that mouse ESCs in which Nnat expression had been knocked-down were restricted in their ability to generate NSCs, and subsequently neurons, while ESCs that over-expressed Nnat generated an excess of NSCs and hence neurons. Therefore, these results suggested that Nnat is needed for the neural induction and subsequent neuronal differentiation of mouse ESCs.

Although the precise molecular mechanisms underlying Nnat action is unknown, it has been shown that Nnat exhibits a 50% amino acid sequence homology with phospholamban, suggesting that these proteins may have similar functions (Dou and Joseph, 1996). Phospholamban is an inhibitor of Atp2a/SERCA which pumps cytosolic Ca^{2+} into the ER to decrease $[Ca^{2+}]_i$ (James et al., 1989), so Nnat may also antagonise the action of Apt2a/SERCA to cause an increase in $[Ca^{2+}]_i$ (details see section 1.7.2). In vertebrates, there are three Apt2a/SERCA genes (details see section 1.5.4.4). During *Xenopus* embryonic development, Apt2a2/SERCA2 is prominently expressed in the neural plate and neural tube, indicating a role for this gene in aspects of neurogenesis (Pegoraro et al., 2011). Further to this, Dr. Yuh-Man Sun's unpublished data also revealed that the Atp2a2/SERCA2 is expressed at much higher levels compared to both Apt2a1/SERCA1 and Apt2a3/SERCA3 in mouse ESCs and during ESCs neural differentiation (see section 1.7.2). Because of these observations, I hypothesised that Nnat acts by suppressing the action of Apt2a2/SERCA2, which in turn causes an increase in $[Ca^{2+}]_i$ resulting in the initiation of neural induction in mouse ESCs.

As detailed in section 1.5.4, an increase in $[Ca^{2+}]_i$ is known to play a pivotal role in neural induction in *Xenopus* (Batut et al., 2005; Moreau et al., 2008).

During *Xenopus* gastrulation, frequent increases in $[Ca^{2+}]_i$ are observed in the prospective neural ectoderm, and the treatment of *Xenopus* embryos with calcium channel blockers to prevent the increase in $[Ca^{2+}]_i$ suppressed the neural specification of ectoderm (Leclerc et al., 2003; Leclerc et al., 2000). This finding implied that an increase in $[Ca^{2+}]_i$ is needed for neural induction of *Xenopus* embryos. However, it is unknown whether or not neural induction in mammals requires an increase in $[Ca^{2+}]_i$. In this chapter, I will report novel data suggesting that Nnat interacts with Apt2a2/SERCA2 to modulate cytosolic Ca^{2+} levels and promote the neural differentiation of mouse ESCs.

In order to investigate the molecular mechanisms underlying the action of Nnat, Co-IP and Duolink *in-situ* PLA experiments were carried out to test whether Nnat physically interacts with Apt2a/SERCA. We reasoned that if Nnat interacts with Apt2a/SERCA to suppress the function of Apt2a/SERCA, resulting in an increase of $[Ca^{2+}]_i$, then a specific inhibitor of Apt2a/SERCA should function like Nnat and restore the ability of Nnat-KD ESCs to generate neural cells. In contrast, preventing an increase in $[Ca^{2+}]_i$ of wild type ESCs should reduce the generation of NSCs from wild type ESCs.
Specifically, this chapter describes:

1) The protein-protein interaction of Nnat and Apt2a2/SERCA2
2) The effect of Nnat on the $[Ca^{2+}]_i$ of mouse ESCs
3) That Nnat acts as an inhibitor of Apt2a/SERCA
4) That an increase in $[Ca^{2+}]_i$ is required for neural induction in mouse ESCs
5) The source of cytosolic Ca^{2+} for neural induction

4.2 Results

4.2.1 Nnat interacts with Atp2a2/SERCA2 in mouse ESCs

Because Nnat shares a high degree of homology with phospholamban (Dou and Joseph, 1996), a known interacting partner for Atp2a/SERCA, I hypothesise that Nnat physically interacts with Atp2a/SERCA to regulate $[Ca^{2+}]_i$ in mouse ESCs. Since Atp2a2/SERCA2 is the Atp2a/SERCA family member that is most highly expressed in mouse ESCs and their neural derivatives (see section 1.7), I focused on studying the interaction of Nnat with Apt2a2/SERCA2 using various methods - immunocytochemical analysis, Co-IP and Duolink *in-situ* PLA.

4.2.1.1 Nnat colocalises with Atp2a2/SERCA2

Nnat and Atp2a2/SERCA2 should colocalise within cells if Nnat physically interacts with Apt2a2/SERCA2. To determine whether this is the case I employed immunocytochemistry.

46C ESCs were plated onto gelatin-coated coverslips and cultured under non-differentiating conditions for two days (see Material and Methods, section 2.1). After fixation in 4% PFA, cells were stained with primary antibodies for Nnat and Atp2a2/SERCA2 and each primary antibody was visualised using a secondary antibody tagged with a fluorochrome. This revealed that some ESCs expressed Nnat (Fig. 4.1A, arrows) and most cells expressed Apt2a/SERCA2 (Fig. 4.1B). Both Nnat and Atp2a2/SERCA2 were located in the cytosol and Nnat staining colocalised with the staining of Atp2a2/SERCA2 (Fig. 4.1D, arrows), suggesting that these proteins occupy the same cellular location. However, this result is not, in itself, evidence of a physical interaction between the two proteins. To prove that a protein-protein interaction exists between Nnat and Atp2a2/SERCA2 a more sophisticated method of analysis is needed.

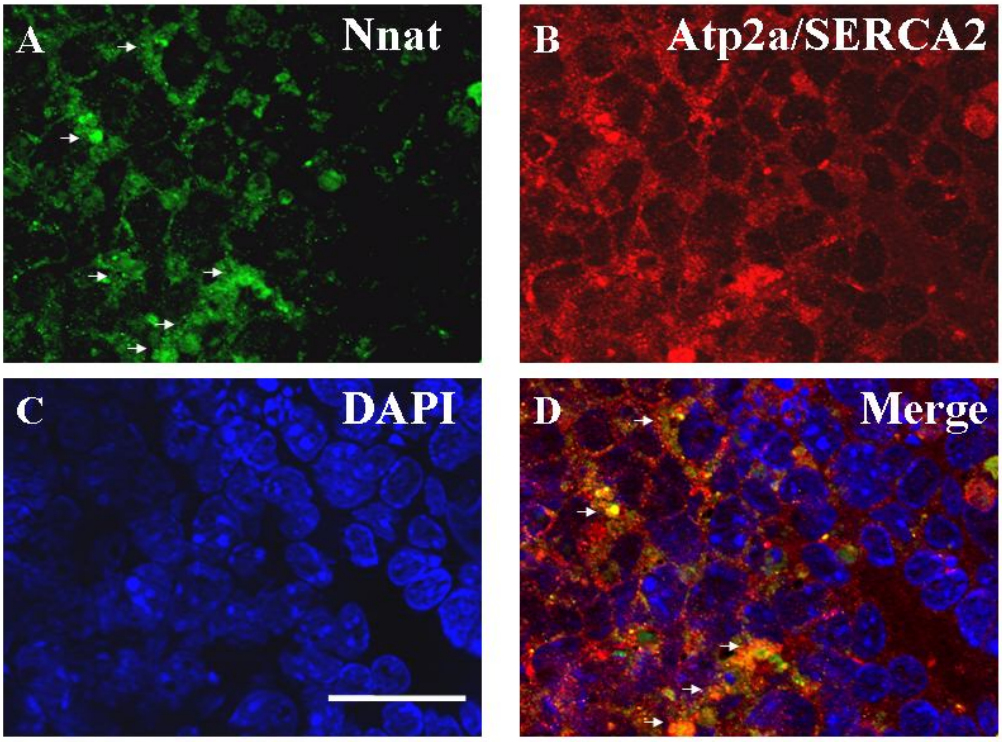

Fig. 4.1. Colocalisation of Nnat with Atp2a2/SERCA2.

46C ESCs were plated on gelatin-coated coverslips and cultured in non-differentiating conditions for two days. After fixation in 4% PFA, immunocytochemistry was carried out using primary antibodies for Nnat and Apt2a2/SERCA2, (A) Nnat (green, arrows) and (B) Apt2a2/SERCA2 (red) were located in the cytosol. (C) The nuclei were stained with DAPI (blue). (D) The overlay is shown in orange (arrows) indicates that Nnat colocalised with Apt2a2/SERCA2. Scale bar, 50 μm.

Abbreviations: Atp2a/SERCA, sarcoendoplasmic reticulum Ca^{2+}-ATPase; DAPI, 4',6-diamidino-2-phenylindole; ESC, embryonic stem cell; PFA, paraformaldehyde.

4.2.1.2 Nnat physically interacts with Apt2a2/SERCA2

In order to investigate whether or not Nnat and Apt2a2/SERCA2 physically interact with each other, Co-IP and Duolink *in-situ* PLA were used.

Although Co-IP is frequently used in the detection of protein-protein interaction, a disadvantage of this technique is that relatively high concentrations of proteins are needed to facilitate detection (Hou et al., 2002). As discussed in section 1.7, the expression of Nnat is low in un-differentiated 46C ESCs, and its expression is increased when ESCs differentiate along a neural pathway, peaking at differentiation day 12. Similarly, the expression of Apt2a2/SERCA2 peaks at differentiation day 12 (see Fig. 1.15). Therefore, in order to facilitate the detection of interactions between Nnat and Apt2a2/SERCA2 proteins, 46C cells were plated on gelatin-coated 10cm culture dishes and cultured under differentiating conditions for 12 days. To carry out the Co-IP experiments (Fig. 4.2), whole cell lysates were prepared from differentiated 46C cells (see Material and Methods, section 2.8) and mixed with anti-Nnat antibodies. If Nnat physically interacts with Apt2a2/SERCA2, then these proteins will form a complex that can be recognised by an anti-Nnat antibody. Protein G Magnetic Beads were then mixed with the samples to precipitate the protein/protein-antibodies complexes. The precipitated products were analysed by Western blotting using an anti-Apt2a2/SERCA2 antibody to examine whether the protein complex contains Apt2a2/SERCA2 (Fig. 4.3).

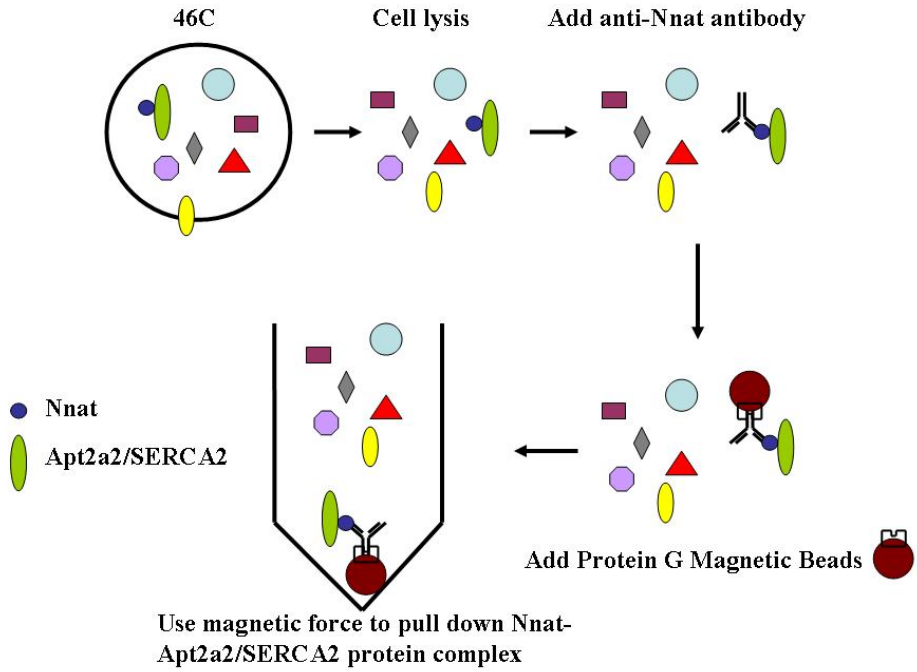

Fig. 4.2. Schematic representation of Co-IP experiments.
46C cells were grown in differentiating conditions for 12 days, at time when the expression of Nnat (blue) and Apt2a2/SERCA2 (green) proteins is maximal. The differentiated 46C cells were lysed, and then an anti-Nnat antibody was mixed with the whole cell lysate. If Nnat physically interacts with Apt2a2/SERCA2, then Nnat, Apt2a2/SERCA2, and the anti-Nnat antibody would form a protein complex allowing the protein G Magnetic Beads (brown) to bind with the anti-Nnat antibody and pull the protein complex down by magnetic force. The precipitated products were then analysed by immunoblotting using an anti-Apt2a2/SERCA2 antibody to examine whether the protein complex contains Apt2a2/SERCA2.
Abbreviations: Atp2a2/SERCA2, sarcoendoplasmic reticulum Ca^{2+}-ATPase 2; Co-IP, co-immunoprecipitation; Nnat, neuronatin.

In Figure 4.3, Lane A (input) represented 5% of the whole cell lysate used in the Co-IP experiment, and revealed that Atp2a2/SERCA2 was expressed in 46C cells and thus could be considered as a positive control. For a negative control Co-IP was carried out using 10µg of rabbit IgG (Santa Cruz) and under these conditions no Atp2a2/SERCA2 specific band was observed. Samples in Lane B-D represented Co-IP products using 10µg of three different anti-Nnat antibodies individually (B: Santa Cruz, goat; C: Santa Cruz, rabbit; D: Abcam, rabbit), and the three lanes all revealed a band at 100 kD, the expected size of Atp2a2/SERCA2, when the blot was probed with an anti-Atp2a2/SERCA2 antibody. Thus, Atp2a2/SERCA2 could be precipitated by anti-Nnat antibodies indicating that Nnat physically

interacts with Apt2a2/SERCA2 and forms a protein complex. As well as the Atp2a2/SERCA2 specific band at 100 kD, a second broader band was observed at 110 kD in lanes B-D. This band may represent a modified Apt2a2/SERCA2. For example, it has been reported that Apt2a2/SERCA2 protein could be modified through glutathionylation, non-enzymatic glycation, and glycosylation, resulting in a protein of increased molecular weight (Belke and Dillmann, 2004; Gallogly and Mieyal, 2007; Li and Camacho, 2004). In addition, the possibility could not be ruled out that this band resulted from some proteins in the cell lysate attaching to the Protein G Magnetic Beads non-specifically and then being pulled down in the Co-IP experiments because they contained a similar amino acid sequence to that targeted by the anti-Apt2a2/SERCA2 antibody (a non-specific interaction).

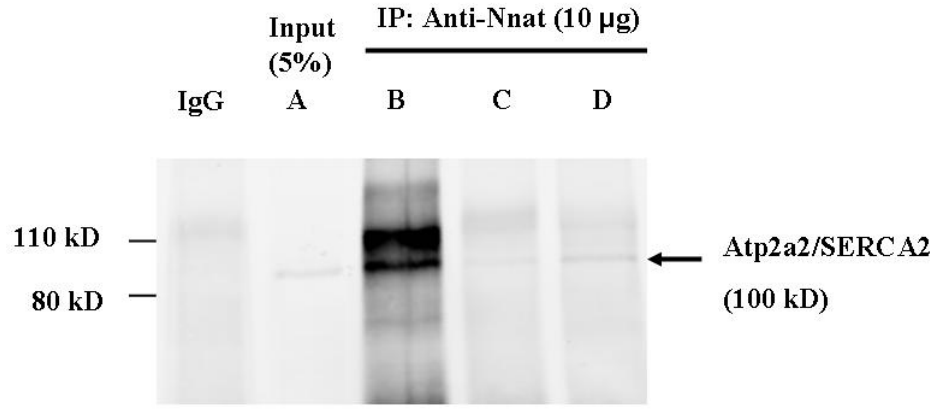

Fig. 4.3. Nnat physically interacts with Atp2a2/SERCA2.
46C ESCs were plated on gelatin-coated 10cm culture dishes and grown in differentiating conditions for 12 days. 46C cells were lysed to prepare whole cell lysates. 10µg of rabbit IgG (Santa Cruz) was used in IP as a negative control. (B-D) 10µg of three different anti-Nnat antibodies (B: Santa Cruz, goat; C: Santa Cruz, rabbit; D: Abcam, rabbit) were used to IP Nnat proteins. The IP products were examined by Western blotting using an anti-Atp2a2/SERCA2 antibody (Santa Cruz, goat). (A) The input, representing 5% of the whole cell lyate used in the Co-IP experiment. Lanes A-D all revealed a band at 100 kD specific for the Atp2a2/SERCA2 protein. Thus, Atp2a2/SERCA2 could be pulled down by anti-Nnat antibodies indicating that Nnat physically interacts with Atp2a2/SERCA2.
Abbreviations: Atp2a/SERCA, sarcoendoplasmic reticulum Ca^{2+}-ATPase; ESC, embryonic stem cell; Co-IP, co-immunoprecipitation; IgG, Immunoglobulin G; IP, immunoprecipitate; kD, kiloDalton.

4.2.2 Nnat acts as an inhibitor of Apt2a/SERCA to increase $[Ca^{2+}]_i$ in mouse ESCs

The Apt2a/SERCA is a calcium ATPase located in the ER that pumps Ca^{2+} from the cytosol into the ER keeping $[Ca^{2+}]_i$ low. Although the results obtained from Co-IP and Duolink *in-situ* PLA experiments indicate that Nnat physically interacts with Apt2a2/SERCA2, they do not address whether this interaction influences the activity of Apt2a2/SERCA2, and if so whether the $[Ca^{2+}]_i$ is increased or not after this interaction. Since Nnat has 50% amino acid sequence homology with phospholamban (Dou and Joseph, 1996), an inhibitor of the Apt2a/SERCA, I hypothesised that Nnat may also act in this manner. Further support for this hypothesis comes from the observations that over-expression of Nnat in insulinoma or 3T3 cells causes $[Ca^{2+}]_i$ to increase (Joe et al., 2008; Suh et al., 2005), suggesting that Nnat may inhibit the Apt2a/SERCA resulting in less cytosolic Ca^{2+} being pumped into the ER and an increase in $[Ca^{2+}]_i$.

To determine whether Nnat inhibits the Apt2a2/SERCA2 to cause an increase in $[Ca^{2+}]_i$, the $[Ca^{2+}]_i$ of ESCs was measured in collaboration with Dr. Vladimir Snetkov (Department of Asthma, Allergy and Respiratory Science, King's College London). 46C, Nnatα-OE, and Nnat-KD ESCs were cultured to confluence on laminin-coated glass coverslips, and then the $[Ca^{2+}]_i$ of ESCs with different Nnat expression levels were recorded. Gelatine was used to prepare coverslips throughout my thesis except in experiments of $[Ca^{2+}]_i$ measurement, because I followed the protocol provided by Dr. Vladimir Snetkov (Snetkov et al., 2010) that used laminin as a substrate. If Nnat inhibits the action of Apt2a2/SERCA2, then Nnatα-OE ESCs should have higher $[Ca^{2+}]_i$ than wild type and Nnat-KD ESCs. Before the $[Ca^{2+}]_i$ of the various ESC lines were measured, 46C, Nnatα-OE, and Nnat-KD ESCs were incubated with a Ca^{2+} sensitive indicator (Fura PE-3/AM) in the dark for 40 minutes. Then coverslips were mounted in an imaging chamber and continuously perfused with a physiological salt solution. Calcium imaging was carried out using an inverted microscope equipped with a

microspectrofluorimeter and the $[Ca^{2+}]_i$ was represented by fluorescence intensity. In Figure 4.4A-C, calcium imaging revealed that the $[Ca^{2+}]_i$ of Nnatα-OE ESCs was higher than that of 46C and Nnat-KD ESCs. The histogram (Fig. 4.4D) of calcium imaging experiments showed that the peak of fluorescence intensity of Nnatα-OE (pink arrow) ESCs was shifted to the right toward higher fluorescent values compared with wild type (blue arrow) ESCs, and conversely the peak of Nnat-KD (green arrow) ESCs was left-shifted towards lower values. This result suggested that the over-expression of Nnatα increases the $[Ca^{2+}]_i$ of ESCs. Thus, these results fit with my hypothesis that Nnat inhibits Apt2a2/SERCA2 resulting in an increase in $[Ca^{2+}]_i$.

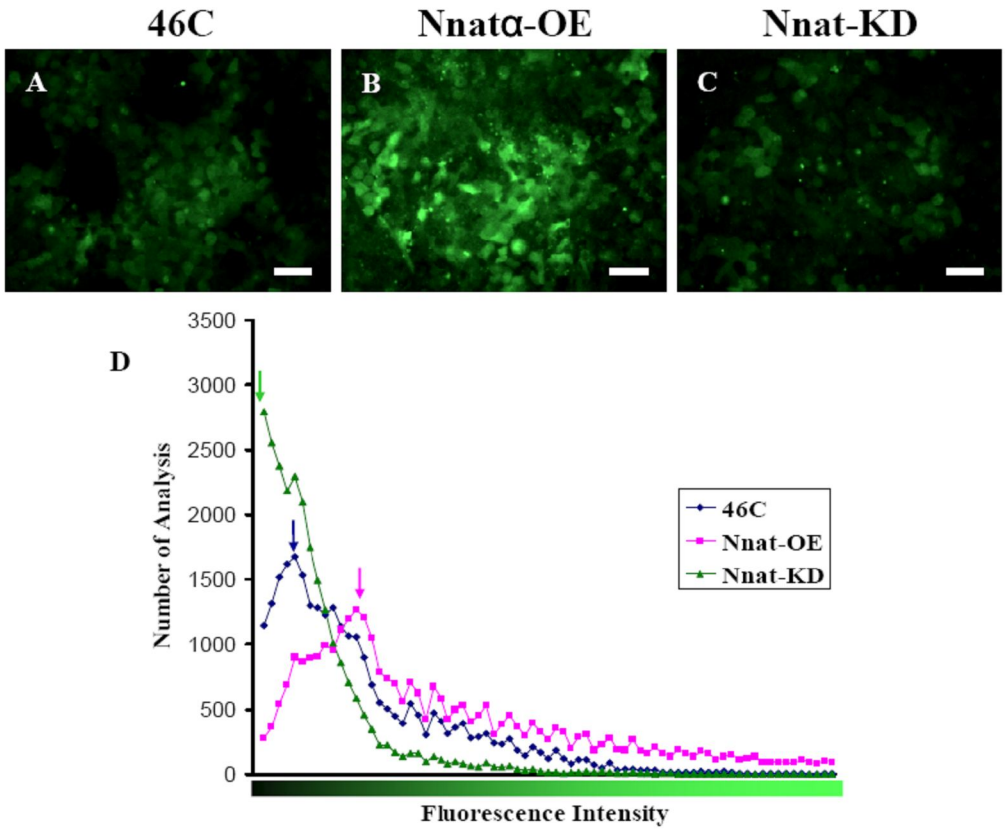

Fig. 4.4. Nnat over-expression increases $[Ca^{2+}]_i$.

46C, Nnatα-OE, and Nnat-KD ESCs were cultured to confluence on laminin-coated glass coverslips. Coverslips were rinsed twice with HEPES-buffered PSS, and incubated with 0.5 μM Fura PE-3/AM in the dark for 40 minutes. Coverslips were mounted in the imaging chamber and placed on the inverted microscope equipped with a microspectrofluorimeter to measure $[Ca^{2+}]_i$. The $[Ca^{2+}]_i$ of (A) 46C, (B) Nnatα-OE, and (C) Nnat-KD ESCs were monitored with the Ca^{2+} sensitive indicator (Fura PE-3/AM). The $[Ca^{2+}]_i$ was represented according to fluorescence intensity. The $[Ca^{2+}]_i$ of Nnatα-OE ESCs was higher than Nnat-KD and 46C ESCs. (D) The graph showed that the peak of fluorescence intensity of Nnatα-OE ESCs (pink arrow) was right-shifted to higher values compared with wild type ESCs (blue arrow). In contrast, the peak of Nnat-KD ESCs (green arrow) was left-shifted to lower values, suggesting that over-expression Nnatα increases the $[Ca^{2+}]_i$ of ESCs. Scale bar, 20 μm.

Abbreviations: $[Ca^{2+}]_i$, cytosolic Ca^{2+} concentration, ESC, embryonic stem cell; HEPES, (4-(2-hydroxyethyl)-1-piperazineethanesulfonic acid); Nnatα-OE, Nnatα-overexpression; Nnat-KD, Nnat-knockdown; PSS, physiological salt solution.

(Provided by Dr. Vladimir Snetkov)

4.2.3 Specific inhibitors of Apt2a/SERCA mimic the function of Nnat

The results obtained from Co-IP, Duolink *in-situ* PLA experiments (see section 4.2.1) and calcium imaging (see section 4.2.2) suggest that Nnat physically interacts with Apt2a2/SERCA2 and antagonises the action of Apt2a2/SERCA2 to decrease cytosolic Ca^{2+} movement into the ER, thus increasing $[Ca^{2+}]_i$. As shown in Chapter 3, the knocked-down of Nnat in ESCs (Nnat-KD ESCs) markedly decreased the ability of these cells to generate NSCs compared with wild type ESCs (see section 3.2.4.). This ability was restored by re-expressing Nnat (see section 3.2.5). If my hypothesis that Nnat inhibits Apt2a2/SERCA2 to increase $[Ca^{2+}]_i$ is correct, then specific inhibitors of Apt2a/SERCA should, like Nnat, act to rescue the generation of neural cells from Nnat-KD ESCs. Thus, in this section, I will show evidence that specific inhibitors of Apt2a/SERCA increase $[Ca^{2+}]_i$ in Nnat-KD ESCs, and mimic the function of Nnat to restore the ability of Nnat-KD ESCs to generate neural cells.

Thapsigargin (Tg) and 2,5-Di-t-butyl-1,4-benzohydroquinone (BHQ) are specific inhibitors of Apt2a/SERCA (Lopez et al., 2008; Lytton et al., 1991). To determine what concentration and the duration of the Tg or BHQ treatment to use, Nnat-KD ESCs were plated onto gelatin-coated coverslips and allowed to adhered before being treated with different concentrations of Tg or BHQ for different times under differentiating conditions. 100, 50, 25, and 5 nM of Tg was added into the culture medium for 0.5, 2, 4, and 24 hours. Concentrations of Tg above 25 nM and exposure times lasting longer than 30 minutes caused cell death. Tg is an irreversible inhibitor of Apt2a/SERCA, but the interaction of BHQ with Apt2a/SERCA is reversible (Lytton et al., 1991; Shimazaki et al., 1999; Tse et al., 1994). Thus the suppressive action of Tg is still continued even after Tg is removed from the medium (Doutheil et al., 1999), and conversely, the function of Apt2a/SERCA is restored once BHQ has been removed (Shimazaki et al., 1999; Tse et al., 1994). Therefore, BHQ should be present over the whole time course of inhibition. 100, 50, 25, and 5 μM of BHQ were added into the culture

medium for 1 and 2 days. Concentrations of BHQ above 50 μM and exposure times over 1 day caused cell death. Therefore, 25 nM Tg for 30 minutes or 50 μM BHQ for 24 hours was used to treat Nnat-KD ESCs to investigate their effects on $[Ca^{2+}]_i$ and their ability to rescue the neural phenotype of Nnat-KD ESCs.

4.2.3.1 Specific inhibitors of Apt2a/SERCA increase $[Ca^{2+}]_i$

Atp2a/SERCA is located in the ER and pumps cytosolic Ca^{2+} into the ER to reduce $[Ca^{2+}]_i$, so inhibiting Atp2a/SERCA will increase $[Ca^{2+}]_i$. Although the specific Apt2a/SERCA inhibitors Tg and BHQ have been shown to increase $[Ca^{2+}]_i$ in many different cell-types, such as 3T3, cardiac, COS, DRG, muscle, pancreatic, PC12 and CCE mouse ESCs (Dolnikov et al., 2006; Krause et al., 1996; Lytton et al., 1991; Razani-Boroujerdi et al., 1994; Sauer et al., 1998), I wanted to show that 25 nM Tg or 50 μM BHQ also increases $[Ca^{2+}]_i$ in Nnat-KD ESCs. To do this, the $[Ca^{2+}]_i$ of Nnat-KD ESCs were measured after 25 nM Tg or 50 μM BHQ treatment. These $[Ca^{2+}]_i$ measurements were carried out by my collaborator Dr. Vladimir Snetkov (Department of Asthma, Allergy and Respiratory Science, King's College London).

For these measurements, Nnat-KD ESCs were cultured to confluence on laminin-coated glass coverslips. We observed that after a 25 nM Tg or 50 μM BHQ treatment, the $[Ca^{2+}]_i$ of Nnat-KD ESCs increased within 2 minutes (Fig. 4.5A-B). Even when cells were left in calcium-free medium, Tg and BHQ treatment still elevated the $[Ca^{2+}]_i$, but the potency and duration of this response were diminished (Fig. 4.5C-D), indicating that the source of cytosolic Ca^{2+} was not only from the extracellular fluid but also from the internal calcium store.

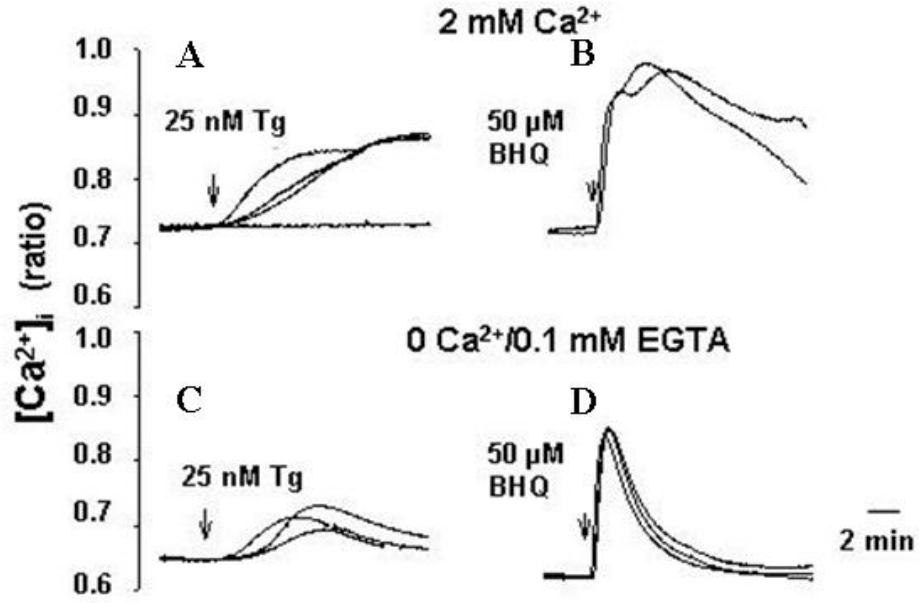

Fig. 4.5. Specific Apt2a/SERCA inhibitors, Tg and BHQ, increase $[Ca^{2+}]_i$ levels in Nnat-KD ESCs.

Nnat-KD ESCs were cultured to confluence on laminin-coated glass coverslips. The ESCs were treated with specific Apt2a/SERCA inhibitors and $[Ca^{2+}]_i$ were measured. In calcium-containing medium, (A) 25 nM Tg or (B) 50 μM BHQ treatment increased $[Ca^{2+}]_i$ of Nnat-KD ES within 2 minutes when compared to cells that had not received any treatment. In 0.1 mM EGTA calcium-free medium, (C) 25 nM Tg and (D) 50 μM BHQ treatment still elevated $[Ca^{2+}]_i$, but the potency and duration were diminished. The results reveal that specific Apt2a/SERCA inhibitors, Tg and BHQ, increased $[Ca^{2+}]_i$ levels in Nnat-KD ESCs.

Abbreviations: BHQ, 2,5-Di-t-butyl-1,4-benzohydroquinone; $[Ca^{2+}]_i$, cytosolic Ca^{2+} concentration; EGTA, ethylene glycol tetraacetic acid; ESC, embryonic stem cell; Nnat-KD, Nnat-knockdown; Atp2a/SERCA, sarcoendoplasmic reticulum Ca^{2+}-ATPase; Tg, thapsigargin.

(Adapted from Lin et al., 2010)

4.2.3.2 Specific inhibitors restore the ability of Nnat-KD ESCs to generate NSCs and neurons

If Nnat interacts with Apt2a2/SERCA2 and suppresses its activity, then specific inhibitors of Apt2a/SERCA should act to rescue the generation of NSCs from Nnat-KD ESCs. In order to prove this assumption, Nnat-KD ESCs were treated with 25 nM Tg for 30 min or 50 μM BHQ for 24 hr on the first day of differentiation and the ability of Nnat-KD ESCs to generate NSCs was analysed after 6 days of differentiation. If Tg and BHQ restore the production of NSCs and neurons from Nnat-KD ESCs, this suggests that these specific Apt2a/SERCA inhibitors mimic the action of Nnat during neural induction.

As shown in Chapter 3, 46C ESCs generated Sox1-GFP and Nestin-expressing NSCs after being differentiated for 6 days while Nnat-KD ESCs did not (Fig. 4.6A-B, also see section 3.2.4.). However, after treatment with Tg or BHQ, the Nnat-KD cells regained the ability to generate Sox1-GFP and Nestin-expressing NSCs (Fig. 4.6C-D). Because the efficiency of Tg or BHQ to rescue Nnat-KD cells was similar, I chose to quantify the results obtained from Tg only. Quantification of these results revealed that the generation of $Nestin^{+}/Sox1\text{-}GFP^{+}$ NSCs in Nnat-KD ESCs was significantly increased from 3.2% to 21.4% after Tg treatment ($n = 3$, $p < 0.05$) (Fig. 4.6E).

These results indicate that the generation of NSCs by Nnat-KD ESCs can be restored by treatment with Tg and BHQ, specific inhibitors of Apt2a/SERCA, suggesting that Tg and BHQ act in a similar fashion to Nnat during neural induction. These results help confirm the hypothesis that Nnat acts as an inhibitor of Apt2a/SERCA to increase $[Ca^{2+}]_i$ in ESCs.

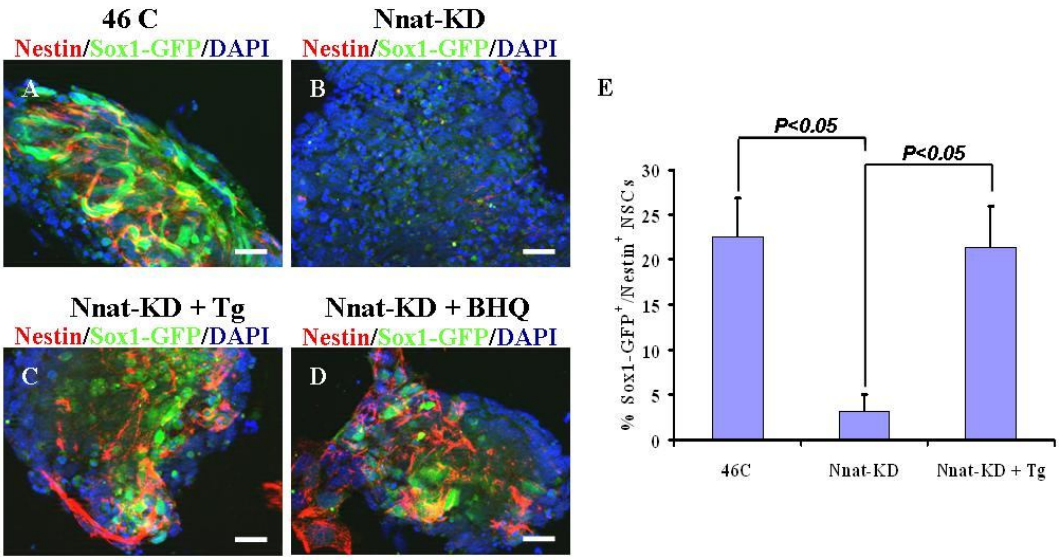

Fig. 4.6. Tg and BHQ treatment rescue the generation of NSCs from Nnat-KD ESCs. 46C or Nnat-KD ESCs were differentiated for 6 days. On the first day, Nnat-KD ESCs were treated with 25 nM Tg for 30 minutes or 50 μM BHQ for 24 hours, and then the culture medium was replaced with fresh medium without Tg or BHQ. After fixation, cultures were stained with the NSC marker Nestin (red). (A) 46C ESCs could generate Sox1/GFP$^+$ and Nestin$^+$ NSCs after differentiation for 6 days. (B) The generation of Nestin$^+$ NSCs declined in Nnat-KD ESCs. (C) With 25 nM Tg treatment or (D) 50 μM BHQ treatment, the ability of Nnat-KD ESCs to generate Sox1/GFP$^+$ and Nestin$^+$ NSCs was restored. (E) The percentage of both Sox1-GFP and Nestin positive NSCs cells was counted. Nnat-KD cells generated significantly fewer NSCs than 46C ESCs (3.2 ± 1.8% vs. 22.6 ± 4.2%, $p < 0.05$, two-tailed Student's t test), and the generation of NSCs in Nnat-KD ESCs was significantly increased to 21.4 ± 4.6% after Tg treatment (n = 3, $p < 0.05$, two-tailed Student's t test). There was no difference in the percentage of NSC between 46C and Tg treated Nnat-KD ESCs. All nuclei were stained with DAPI (blue). Scale bar, 20 μm.
Abbreviations: BHQ, 2,5-Di-t-butyl-1,4-benzohydroquinone; DAPI, 4',6-diamidino-2-phenylindole; ESC, embryonic stem cell; GFP, green fluorescent protein; Nnat-KD, Nnat-knockdown; NSCs, neural stem cells; Sox1, sex determining region Y-box 1; Tg, thapsigargin.

To determine whether the effect of Tg and BHQ in restoring the ability of Nnat-KD cells to generate Nestin-expressing NSC resulted in the subsequent development of neurons in these cultures, the same experiments were carried out as described above, but cultures were allowed to differentiate for 14 days instead of 6 days. After this time 46C ESCs generated many NeuN expressing neurons, while Nnat-KD ESCs, as expected, did not (Fig. 4.7A-B, also see section 3.2.4.). After treatment with Tg or BHQ, the ability of Nnat-KD cells to generate NeuN expressing neurons was restored (Fig. 4.7C-D), but the number of neurons observed was fewer than seen in wild type cultures. Quantification of these results revealed that the generation of NeuN expressing neurons from Nnat-KD ESCs was significantly increased after Tg treatment from 2.1% to 11.0% (n = 3, $p < 0.05$) (Fig. 4.7E), but not to the levels seen in differentiated 46C ESCs (20.8%, n = 3, $p < 0.05$). Since there was no difference in the percentage of NSCs between the 46C and Tg treated Nnat-KD ESCs after 6 days differentiation (Fig. 4.6E), one might presume that similar numbers of neurons would be generated under these conditions. This difference in neuronal number observed may be due to the fact that only a single dose of Tg was given on the first day of differentiation and its effects were not fully sustained through the whole course of neurogenesis. The *in vivo* and *in vitro* expression patterns of Nnat reveal that Nnat is still highly expressed after neuroectoderm is formed (see sections 1.7 and 3.2.2). This implies that Nnat may be still be required when neuroectodermal cells differentiate into neurons, thus I conclude that administration of Tg only on the first day of differentiation of Nnat-KD cells was not sufficient to restore neuronal levels to that seen in differentiated wild type 46C cell. Therefore, this observation revealed that, in addition to the early role in neural induction, Nnat might also play another role in the later neurogenesis.

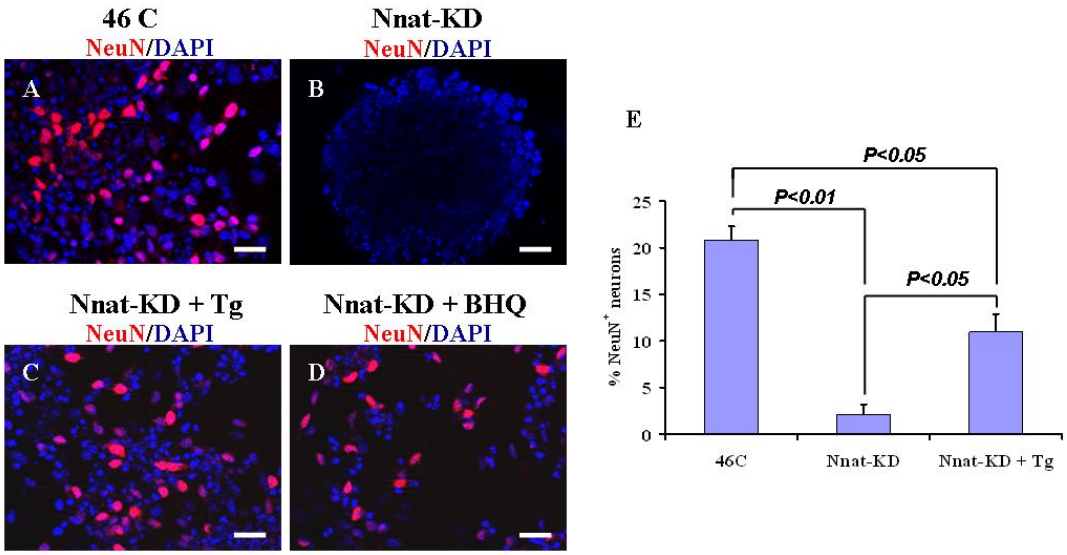

Fig. 4.7. Tg or BHQ exposure rescue the ability of Nnat-KD ESCs to generate neurons.

46C or Nnat-KD ESCs were differentiated for 14 days. On the first day of differentiation, Nnat-KD ESCs were treated with 25 nM Tg for 30 minutes or 50 µM BHQ for 24 hours, and then the culture medium was replaced with fresh medium without Tg or BHQ. After fixation, cultures were stained with the nuclear neuronal marker NeuN (red). (A) 46C ESCs could generate $NeuN^+$ neurons after 14 days of differentiation. (B) The generation of $NeuN^+$ neurons was significantly decreased in Nnat-KD ESCs. (C) With 25 nM Tg or (D) 50 µM BHQ treatment the ability of Nnat-KD ESCs to generate $NeuN^+$ neurons was restored. (E) The percentage of $NeuN^+$ neurons was counted. Nnat-KD cells generated significantly fewer neurons than 46C ESCs (2.1 ± 1.1% vs. 20.8 ± 1.5%, $p < 0.01$, two-tailed Student's t test). The generation of neurons in Nnat-KD ESCs was significantly increased to 11.0 ± 1.9% after Tg treatment (n = 3, $p < 0.05$, two-tailed Student's t test), but did not reach the level observed in differentiated 46C ESC cultures ($p < 0.05$, two-tailed Student's t test). All nuclei were stained with DAPI (blue). Scale bar, 20 µm.

Abbreviations: BHQ, 2,5-Di-t-butyl-1,4-benzohydroquinone; DAPI, 4',6-diamidino-2-phenylindole; ESC, embryonic stem cell; NeuN, neuronal nuclei; Nnat-KD, Nnat-knockdown; Tg, thapsigargin.

4.2.4 Intracellular Ca^{2+} is important for the neural induction of ESCs

An elevation in $[Ca^{2+}]_i$ has been demonstrated to be important for neural induction in *Xenopus* (Batut et al., 2005; Moreau et al., 2008), but whether calcium is similarly involved in neural induction in mammals is still unknown. To test the involvement of calcium in the neural induction of mouse ESCs, 46C ESCs were grown under monolayer differentiation conditions in the presence of BAPTA-AM, a membrane permeable calcium chelator that chelates both intracellular and extracellular Ca^{2+} (Bouchard et al., 2001; Collatz et al., 1997; van Der Luit et al., 1999). If calcium is necessary for mouse ESCs to differentiate along a neural lineage, the generation of NSCs by 46C should be inhibited by the presence of the calcium chelator.

To decide the concentration and duration of BAPTA-AM treatment to use, 46C ESCs were cultured in differentiating conditions and were treated with 80, 60, 40, 30, 20, 15, or 10 μM BAPTA-AM for 4, 6, 8, 24, or 48 hours. Concentrations of BAPTA-AM above 10 μM and treatment durations of over 24 hours caused cell death. Thus, I used 10 μM BAPTA-AM for 24 hours to treat 46C ESCs.

In order to determine whether BAPTA-AM blocks the neural induction of 46C ESCs, these cells were cultured under differentiating conditions for 3 days. On the first day, cultures were treated with 10 μM BAPTA-AM for 24 hours, and then the medium was replaced (without BAPTA-AM) and cultured for a further 2 days. Normally the NSC marker Sox1-GFP is first expressed in 46C cells after differentiation for 2 days (see section 3.2.1), but it is more apparent after differentiation for 3 days. Thus I fixed cells after 3 days and analysed the expression of Sox1-GFP. As shown in Figure 4.8, the generation of Sox1-GFP-expressing NSCs was dramatically reduced by the treatment of 46C cells with BAPTA-AM, suggesting that Ca^{2+} is required on the first day of differentiation for neural induction to occur.

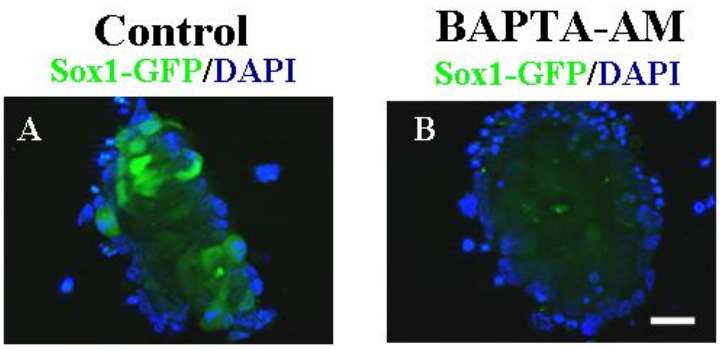

Fig. 4.8. BAPTA-AM restricts the generation of NSCs.
46C ESCs were differentiated for 3 days. On the first day, experimental cultures were treated with 10 μM BAPTA-AM (a membrane permeable calcium chelator) for 24 hours and then the culture medium was replaced with fresh medium without BAPTA-AM. Control cultures did not receive any BAPTA-AM. After differentiation for 3 days, cells were fixed to check for expression of Sox1-GFP, a marker of NSCs. (A) 46C ESCs generated Sox1-GFP$^+$ NSCs after differentiation for 3 days. (B) Following BAPTA-AM treatment, the generation of Sox1-GFP$^+$ NSCs was restricted in 46C ESCs, suggesting that Ca^{2+} is required on the first day of differentiation for neural induction of mouse ESCs. All nuclei were stained with DAPI (blue). Scale bar, 20 μm.
Abbreviations: BAPTA-AM, 1,2-Bis (2-aminophenoxy) ethane-N,N,N',N'-tetraacetic acid tetrakis (acetoxymethyl ester) ; DAPI, 4',6-diamidino-2-phenylindole; ESC, embryonic stem cell; GFP, green fluorescent protein; NSCs, neural stem cells; Sox1, sex determining region Y-box 1.

Because BAPTA-AM chelates both intracellular and extracellular Ca^{2+}, the results described above could not determine which source of Ca^{2+} is important for neural induction. In order to solve this question, 46C ESCs were grown under monolayer differentiation conditions in the presence of EGTA to chelate the extracellular Ca^{2+} and determine whether extracellular Ca^{2+} was needed for neural induction. EGTA is a membrane impermeable calcium chelator and is used to bind extracellular Ca^{2+} (Artursson and Magnusson, 1990; Tsien et al., 1982). The Ca^{2+} concentration of solution containing EGTA can be calculated accurately using a special equation (Bers, 1982). Using this equation, I calculated that, under my differentiating condition, the addition of EGTA to a final concentration of 2 mM would chelate 99.9% of the Ca^{2+} within the differentiation medium. 46C ESCs were cultured in differentiating conditions for 3 days. On the first day, the cells were treated with 2 mM EGTA, in differentiation medium, for 24 hours, then the medium was replaced with fresh medium lacking EGTA and cultures were maintained

for a further 2 days. The cells were then fixed to check for their ability to generate Sox1-GFP-expressing NSCs. Under these conditions 46C ESCs still generated Sox1-GFP expressing NSCs (Fig. 4.9). This indicates that extracellular Ca^{2+} is not necessary for the neural induction of mouse ESCs. As shown in Figure 4.8, the exposure of 46C cells to BAPTA-AM (chelates both intracellular and extracellular Ca^{2+}) on the first day of differentiation reduced the expression of Sox1-GFP, but when 46C cells were exposed to EGTA (only chelates extracellular Ca^{2+}) on the first day of differentiation, the generation of Sox1-GFP-expressing cells was not inhibited. This suggests that calcium released from intracellular stores is pivotal for the neural induction of mouse ESCs.

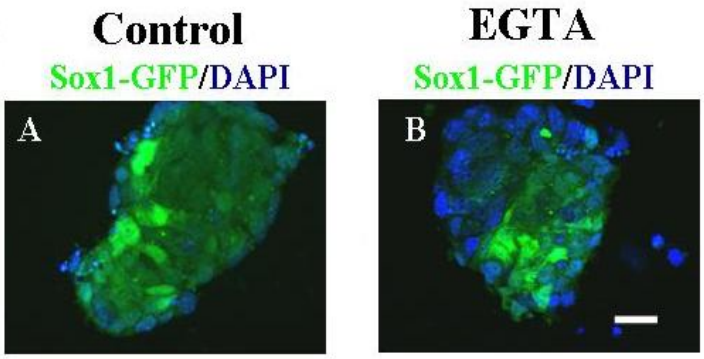

Fig. 4.9. Extracellular Ca^{2+} removal does not inhibit neural development.
46C ESCs were grown in monolayer culture and differentiated for 3 days. On the first day, experimental cultures were treated with 2 mM of EGTA (a membrane non-permeable calcium chelator) for 24 hours, while control cultures did not receive any EGTA. Cultures were then maintained in differentiating conditions without EGTA for a further 2 days before being fixed to check for expression of Sox1-GFP, a marker of NSCs. (A) 46C ESCs generated Sox1-GFP^+ NSCs after 3 days in differentiation medium. (B) Following EGTA treatment to chelate extracellular Ca^{2+}, the generation of Sox1-GFP^+ NSCs was preserved, suggesting that Ca^{2+} from internal stores is sufficient to activate neural induction of mouse ESCs. All nuclei were stained with DAPI (blue). Scale bar, 20 μm.
Abbreviations: DAPI, 4',6-diamidino-2-phenylindole; EGTA, ethylene glycol tetraacetic acid; ER, endoplasmic reticulum; ES, embryonic stem; GFP, green fluorescent protein; NSCs, neural stem cells; Sox1, sex determining region Y-box 1.

4.2.5 Calcium release from the ER is necessary for neural induction of ESCs

As shown above, an increase in $[Ca^{2+}]_i$ is needed for neural induction of mouse ESCs. However, when a cell is in a basal state, the $[Ca^{2+}]_i$ is kept low because Ca^{2+} is pumped into the ER, or pushed out of cells into the extracellular fluid (Clapham, 2007). The source of Ca^{2+} for increasing $[Ca^{2+}]_i$ is either the extracellular fluid or the ER, or both. However, preventing the influx of Ca^{2+} from extracellular fluid by treating 46C ESCs with EGTA did not inhibit neural induction (see section 4.2.4), suggesting that the source of Ca^{2+} for neural induction may be the ER. In order to confirm this hypothesis, 46C ESCs were grown under differentiating conditions and treated with an inhibitor of IP_3R or RyR. These receptors are located in the ER and it is through them that Ca^{2+} leaves the ER and enters the cytosol (see section 1.5.4.4). Thus inhibiting these receptors will block Ca^{2+} release from the ER, and if this inhibition blocks the generation of NSCs, then the source of cytosolic Ca^{2+} for neural induction is the ER.

2-aminoethoxydiphenyl borate (2-APB) blocks Ca^{2+} release from the ER into the cytosol through inhibition of IP_3R (Lang et al., 2007), and Dantrolene blocks Ca^{2+} release from the ER through inhibition of the RyR (Charles et al., 1993). Thus, both of these chemicals can be used to prevent an increase in $[Ca^{2+}]_i$ by inhibiting its release from the ER and can therefore be used to test whether this is the source of Ca^{2+} used to generate the increase in $[Ca^{2+}]_i$ required for neural induction.

To decide the concentration of 2-APB and Dantrolene to be used in these experiments, 46C ESCs were cultured in differentiating conditions and were exposed to 150, 75, or 25 μM 2-APB or 200, 100, 50, or 25 μM Dantrolene for 24 hours. The highest concentration of 2-APB and Dantrolene used was found to cause cell death. Thus 75 μM 2-APB or 100 μM Dantrolene was used in these experiments. On the first day of differentiation, ESCs were treated with 75 μM 2-APB or 100 μM Dantrolene for 24 hours, and then the medium was replaced with fresh

medium without 2-APB or Dantrolene. After differentiation for 3 days, cells were fixed to check for expression of Sox1-GFP. As shown in Figure 4.10, the generation of Sox1-GFP-expressing NSCs were inhibited by 2-APB or Dantrolene treatment, suggesting that Ca^{2+} released from the ER on the first day of differentiation is necessary for neural induction. I also treated 46C ESCs with 75 μM 2-APB plus 100 μM Dantrolene for 24 hours, but this caused cell death, suggesting that inhibition of both RyR and IP_3R together is too harsh and cells fail to survive under this condition. Maybe when the action of only one of these receptors is blocked, some Ca^{2+} still can be released form the ER through the un-blocked receptor but this is not enough to trigger neural induction in ESCs.

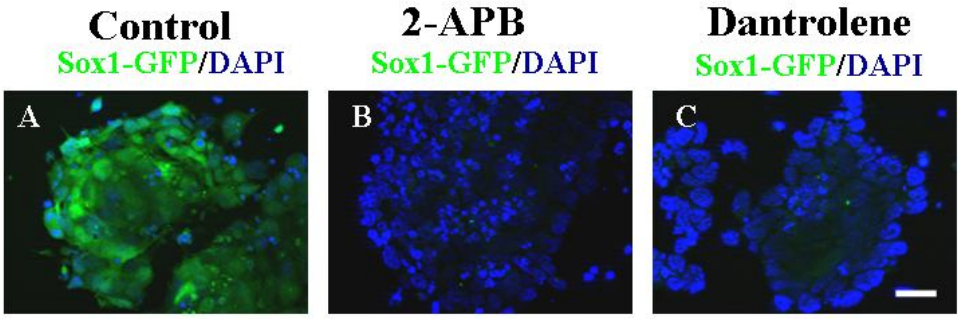

Fig. 4.10. Inhibition of Ca^{2+} release from the ER blocks neural development.
46C ESCs were grown in monolayer culture under differentiated conditions. On the first day, experimental cultures were treated with 75 μM 2-APB (an inhibitor of IP_3R) or 100 μM Dantrolene (an inhibitor of RyR) for 24 hours, and then the culture medium was replaced with fresh one without 2-APB or Dantrolene, while control cells received no such treatments. After a further 2 days, cultures were fixed to check for the expression of Sox1-GFP, a marker of NSCs. (A) In the absence of inhibitors, 46C ESCs generated Sox1-GFP^+ NSCs after differentiated for 3 days. (B,C) Following 2-APB or Dantrolene treatment, the generation of Sox1-GFP^+ NSCs was inhibited in 46C ESCs. This suggests that the inhibition of calcium releasing from the ER through IP_3R or RyR on the first day of differentiation blocked neural development. All nuclei were stained with DAPI (blue). Scale bar, 20 μm.
Abbreviations: 2-APB, 2-aminoethoxydiphenyl borate; DAPI, 4',6-diamidino-2-phenylindole; ER, endoplasmic reticulum; ESC, embryonic stem cell; GFP, green fluorescent protein; IP_3R, Inositol 1,4,5-trisphosphate receptor; Nnatα-OE, Nnatα-overexpression; NSCs, neural stem cells; RyR, ryanodine receptor; Sox1, sex determining region Y-box 1.

4.2.6 Nnat initiates neural induction via increasing $[Ca^{2+}]_i$

As shown in Figure 4.6 and 4.7, exposure of Nnat-KD ESCs to Tg and BHQ rescued the ability of Nnat-KD cells to generate NSCs and subsequently neurons (see section 4.2.3). Furthermore, the treatment of Nnat-KD ESCs with Apt2a/SERCA inhibitors Tg and BHQ caused an increase in $[Ca^{2+}]_i$ (see section 4.2.3.1). These data suggest that the Apt2a/SERCA inhibitor rescues the generation of neural cells from Nnat-KD ESCs via an increase in $[Ca^{2+}]_i$. If this is the case, then the membrane permeable calcium chelator, BAPTA-AM, should prevent the increase in $[Ca^{2+}]_i$ in Tg treated Nnat-KD ESCs and inhibit the generation of NSCs.

To test the above hypothesis, Nnat-KD ESCs were treated with 25 nM of Tg or 10 μM of BAPTA-AM alone or in combination for 30 minutes on the first day of differentiation, and then the medium was replaced with fresh medium without Tg and/or BAPTA-AM. After differentiation for 3 days, the cells were fixed to check for expression of Sox1-GFP. Without BAPTA-AM treatment, the treatment of Nnat-KD ESCs with 25 nM of Tg for 30 minutes rescued the development of Sox1-GFP expressing NSCs (Fig. 4.11A-C). However, following BAPTA-AM treatment, Tg failed to rescue the ability of Nnat-KD ESCs to generate these cells (Fig. 4.11C-D). This confirms that Tg rescue is via the increase in $[Ca^{2+}]_i$ of Nnat-KD ESCs.

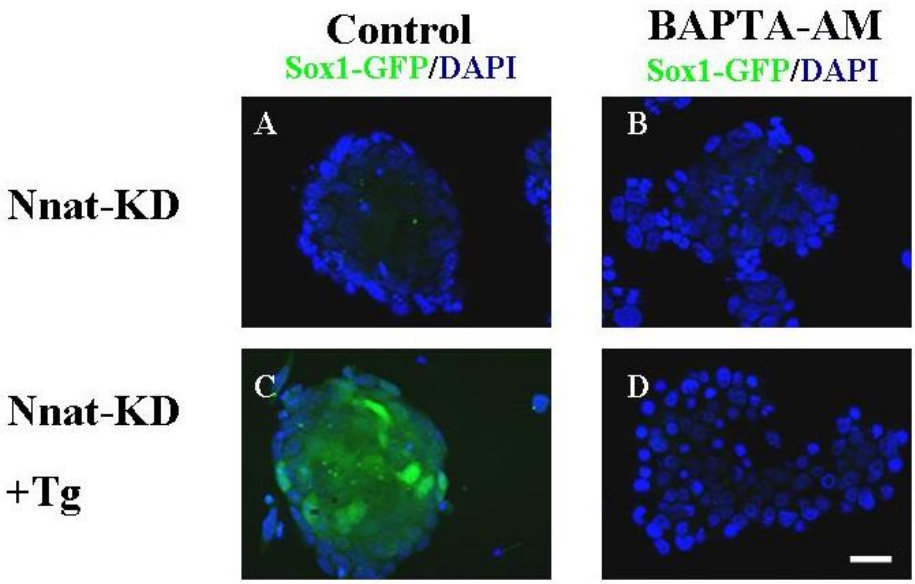

Fig. 4.11. BAPTA-AM prevents Tg rescuing the ability of Nnat-KD ESCs to generate NSCs.

Nnat-KD ESCs were grown in monolayer culture under differentiation conditions. On the first day, experimental cultures were treated with 25nM Tg or 10 μM BAPTA-AM (a membrane permeable calcium chelator) for 30 minutes, and then the culture medium was replaced with fresh medium without Tg and/or BAPTA-AM while control cells received no such treatment. After a further 2 days, cultures were fixed to check for the expression of Sox1-GFP, a marker of NSCs. (A) Without or (B) with the BAPTA-AM treatment, Nnat-KD ESCs did not generate Sox1-GFP$^+$ NSCs. (C) With the Tg treatment, Nnat-KD ESCs could generate Sox1-GFP$^+$ NSCs. (D) When Tg treatment was carried out in the presence of BAPTA-AM, the generation of Sox1-GFP$^+$ NSCs was prevented, suggesting that Tg rescued the generation of Sox1-GFP$^+$ NSCs from Nnat-KD ESCs via an increase in $[Ca^{2+}]_i$. All nuclei were stained with DAPI (blue). Scale bar, 20 μm.

Abbreviations: BAPTA-AM, 1,2-Bis (2-aminophenoxy) ethane-N,N,N',N'-tetraacetic acid tetrakis (acetoxymethyl ester) ; DAPI, 4',6-diamidino-2-phenylindole; ESC, embryonic stem cell; GFP, green fluorescent protein; Nnat-KD, Nnat-knockdown; NSCs, neural stem cells; Sox1, sex determining region Y-box 1; Tg, thapsigargin.

4.3 Discussion

4.3.1 Summary of main findings

In summary, my results indicate that Nnat physically interacts with Apt2a2/SERCA2 and causes an increase in $[Ca^{2+}]_i$. Furthermore, I reveal that Tg and BHQ, inhibitors of Atp2a/SERCA, mimic the action of Nnat to rescue the ability of Nnat-KD ESCs to generate neural cells. Using a membrane permeable calcium chelator (BAPTA-AM) to prevent an increase in $[Ca^{2+}]_i$, on the first day of differentiation, reduced the generation of NSCs from wild type mouse ESCs, and also abolished the Tg-restored neural induction in Nnat-KD ESCs. Thus, I have confirmed my theory that Nnat antagonises the action of Apt2a2/SERCA2, which in turn increases $[Ca^{2+}]_i$ and leads to neural induction in mouse ESCs.

4.3.2 Nnat physically interacts with Apt2a2/SERCA2 to increase $[Ca^{2+}]_i$ and initiate neural induction of mouse ESCs

Apt2a/SERCA is a Ca^{2+} ATPase pump that sits in the membrane of the ER and pumps cytosolic Ca^{2+} back to the ER to maintain a stable and low $[Ca^{2+}]_i$ (Slusarski and Pelegri, 2007; Zhong and Inesi, 1998). Under this basal condition, the inhibition of Apt2a/SERCA induces an increase in $[Ca^{2+}]_i$ (James et al., 1989; MacLennan and Kranias, 2003). There are three members of the Apt2a/SERCA gene family, Atp2a2/SERCA2 is expressed at much higher levels compared to Apt2a1/SERCA1 and Apt2a3/SERCA3 in mouse ESCs and during ESC neural differentiation (see section 1.7). My novel findings obtained from Co-IP and Duolink *in-situ* PLA experiments revealed that Nnat physically interacts with Apt2a2/SERCA2 in mouse undifferentiated ES or differentiated cells (see section 4.2.1.2). I also found that over-expressing Nnat increased $[Ca^{2+}]_i$, whereas knocking down Nnat reduced $[Ca^{2+}]_i$ (see section 4.2.2). My findings fit well with the idea that Nnat inhibits the action of Apt2a2/SERCA2, resulting in an increase in $[Ca^{2+}]_i$, which in turn leads to neural induction in ESCs. These findings were corroborated using blockers of Apt2a/SERCA, Tg and BHQ. Without the treatment of Nnat-KD ESCs with Tg or BHQ, Nnat-KD ESCs generated less neural cells compared with wild type ESCs. Treatment of Nnat-KD ESCs with Tg or BHQ

caused an increase in $[Ca^{2+}]_i$ and recued the ability of Nnat-KD ESCs to generate neural cells (see section 4.2.3). This suggests that the function of Nnat mimics that of the Apt2a/SERCA inhibitors. This rescue could be disrupted by the treatment of Tg treated Nnat-KD ESCs with a membrane permeable calcium chelator BAPTA-AM, suggesting the rescue is via an increase in $[Ca^{2+}]_i$ (see section 4.2.6). These results show that Nnat acts to inhibit the action of Apt2a2/SERCA2 resulting in an increase in $[Ca^{2+}]_i$ that initiates neural induction in mouse ESCs. Thus, the increase in $[Ca^{2+}]_i$ is important for neural induction in mouse ESCs as well as in *Xenopus*.

4.3.3 Nnat modulating $[Ca^{2+}]_i$ plays a role in neurogenesis of NSCs

Previously, Yu et al. (2008) had reported that the movement of intracellular Ca^{2+} is important in neurogenesis of mouse ESCs. In this report, ESCs isolated from the RyR2 null mouse embryo were employed to investigate the role of RyR2 in neuronal differentiation. As already mentioned, RyR is a Ca^{2+} channel located in the ER and upon activation RyR releases Ca^{2+} from the ER into the cytosol. In RyR2 null ESCs, the expression of the neuronal transcription factor NeuroD and generation of MAP2 positive neurons were reduced (Yu et al., 2008a). Although this report highlights the importance of Ca^{2+} release from the ER through RyR2 during ESC neural differentiation, it does not show whether the observed reduction in neurogenesis is due to the inhibition of neural induction in ESCs or the inhibition of NSCs to generate NPCs and neurons. My experiments expand the observation made by Yu et al., by showing that Nnat modulates $[Ca^{2+}]_i$ by regulating Apt2a2/SERCA2 and Nnat-knockdown prevents neural induction of mouse ESCs (see section 3.2.4). Although an increase in cytosolic Ca^{2+} plays a pivotal role in neural induction of mouse ESCs, this does not rule out the possibility that Ca^{2+} release from the ER is also important in the neuronal generation from neural progenitors. In line with this, treatment of the developing neocortex (isolated from mouse embryos at 16 dpc) with Suramin (an ATP receptor antagonist) *in vitro* to suppress the generation of IP_3 and reducing IP_3-mediated Ca^{2+} release from the ER, repressed the proliferation of radial glial cells (neural progenitors) in the ventricular zone (Weissman et al.,

2004). The antiproliferative effect of Suramin could be rescued in the presence of PMT (a PLC activator) to induce the generation of IP_3. Further, the treatment of radial glial cells with 2-APB, an inhibitor of IP_3R, disrupted the proliferation of these neural progenitors, while treatment with the extracellular calcium chelator EGTA (2mM) had no effects. These results suggests that the Ca^{2+} released from the ER, resulting in an increase in $[Ca^{2+}]_i$, is also important in the proliferation of NPCs (Weissman et al., 2004).

In addition to neural induction, Nnat, by regulating $[Ca^{2+}]_i$, may also play a role in controlling the generation of NPCs and neurons from NSCs. As shown in section 4.2.3, when $[Ca^{2+}]_i$ of Nnat-KD ESCs is increased by exposure to Tg, on the first day of the differentiation process, Nnat-KD ESCs generate similar numbers of NSCs as wild type ESCs. Thus, one might presume that similar numbers of neurons would be generated under these conditions, if Nnat regulation of $[Ca^{2+}]_i$ was not needed during neurogenesis. However, these Tg-treated Nnat-KD ESCs generated less neuron than their wild type counterparts (see Fig. 4.7E). Therefore, the assumption that Nnat regulation of $[Ca^{2+}]_i$ was not needed during neurogenesis appeared not to be correct. In order to prove this, Tg could be administered to Nnat-KD ESCs not only on the first day of differentiation, but also at the sixth day of differentiation after the formation of NSCs. If Tg treatment after the formation of NSCs can increase the generation of neurons, this will indicate that the regulation of $[Ca^{2+}]_i$ by Nnat also plays a role in neurogenesis.

4.3.4 Ca^{2+} releasing from the ER is crucial for neural induction of mouse ESCs

As discussed in section 1.5.4.4, the source of cytosolic Ca^{2+} in cells is either from the extracellular fluid through the calcium channels in the plasma membrane or from the ER through IP_3R or RyR. As shown in section 4.2.4 and 4.2.5, an increase in $[Ca^{2+}]_i$ was required on the first day of differentiation for the neural induction of mouse ESCs, and when this Ca^{2+} release from the ER was blocked in wild type ESCs using antagonist

of IP_3R or RyR, the generation of NSCs was reduced. In contrast, removing extracellular Ca^{2+} on the first day of differentiation of mouse ESCs, using EGTA, did not inhibit the generation of NSCs. Thus, the source of cytosolic Ca^{2+} required for neural induction is from the ER. In *Xenopus* embryos, neural induction was suppressed when embryos were cultured with an L-type calcium channel blocker, R(+)BayK, to inhibit Ca^{2+} influx from extracellular fluids into the cytosol through the L-type calcium channels in the plasma membrane (see section 1.5.4.2). At present, there is no data suggesting that Ca^{2+} release from the ER is required for neural induction in *Xenopus* embryos. However, from my studies it appears that extracellular Ca^{2+} is not as important for neural induction in mouse ESCs as it is in *Xenopus* embryos.

4.3.5 How cytosolic Ca^{2+} elevation initiates neural induction in mouse ESCs

When a membrane permeable calcium chelator BAPTA-AM was added into the culture medium to reduce the concentration of free Ca^{2+} in the cytosol of mouse ESCs, cultures failed to generation NSCs (see section 4.2.4). In contrast, if a specific Apt2a/SERCA inhibitor Tg was added into the culture medium to increase $[Ca^{2+}]_i$ of Nnat-KD ESCs, the ability to generate NSCs was restored (see section 4.2.3). Therefore, an increase in cytosolic Ca^{2+} is pivotal for neural induction of mouse ESCs. It has been demonstrated that an increase in $[Ca^{2+}]_i$ by treatment with Tg activates Ras through the exchange of bound GDP for GTP, and this in turn activates Erk1/2 (see section 1.5.4.3; Agell et al., 2002; Ebinu et al., 1998; Kupzig et al., 2005). Since the activation of Erk signalling is required for neural induction in mouse ESCs (see section 1.5.1), it is possible that the treatment of Nnat-KD ESCs with Tg rescues the ability of Nnat-KD ESCs to generate neural cells via the activation of Erk signalling. The interaction between calcium and Erk signalling will be investigated in the next chapter.

Chapter 5. Nnat promotes neural induction in mouse ESCs by increasing positive signalling and attenuating negative signalling

5.0 Nnat promotes neural induction in mouse ESCs by increasing positive signalling and attenuating negative signalling

5.1 Introduction

During *Xenopus* gastrulation, FGF/Erk signalling is active in the forming neural plate (Christen and Slack, 1999), and the injection of *Fgf8* mRNA into *Xenopus* embryos in order to activate Erk signalling has been shown to induce the generation of ectopic neural tissue (Pera et al., 2003). Similarly the implantation of FGF4 soaked beads into the embryonic ectoderm of chick embryos induced the formation of ectopic neural tissue (Rodriguez-Gallardo et al., 1997). Conversely culturing *Xenopus* embryos with the FGFR inhibitor (SU5402) suppressed neural plate formation (Delaune et al., 2005), and the expression of the neural plate makers *ERNI* and *Sox3* were suppressed when SU5402 soaked beads were implanted into the prospective neural plate of chick embryos (Streit et al., 2000). Thus, these results suggested that FGF/Erk signalling is required for neural induction in *Xenopus* and chick embryos (see section 1.5.1).

In addition to FGF/Erk signalling, BMP signalling also plays an important role in neural induction, but the action of BMP is opposite to that of FGF/Erk in that BMP is a negative cue (details see sections 1.2 and 1.4). During gastrulation, the organiser region of *Xenopus* embryos secrets BMP antagonists, such as Noggin, Chordin, and Follistatin, to induce the neural specification of dorsal ectoderm (Hemmati-Brivanlou et al., 1994; Sasai et al., 1994; Smith and Harland, 1992), and the injection of *Noggin*, *Chordin* or *Follistatin* mRNAs into *Xenopus* embryos induced the generation of a second neural axis and expanded neural tissue (Iemura et al., 1998; Pera et al., 2003; Piccolo et al., 1996; Sasai et al., 1994). These results imply that inhibition of BMP signalling induces neural induction in *Xenopus* embryos. Further, similar observations have also been found in other vertebrates (see section 1.4; Di-Gregorio et al., 2007; Wilson et al., 2000).

As discussed, both FGF/Erk and BMP signallings play pivotal roles in neural induction, and data reveals that there is crosstalk between these two pathways (details see section 1.5.1.4; Kuroda et al., 2005; Pera et al., 2003).

The activation of BMP signalling caused the phosphorylation of Smad1 at the C-terminus (Massague and Chen, 2000), enabling the C-ter-p-Smad1 to activate target genes and inhibit neural induction in *Xenopus* embryos (Pera et al., 2003; Phippard et al., 1996; Suzuki et al., 1997). However, the activation of FGF/Erk signalling induced phosphorylation of Smad1 at the linker region, inhibiting the action of C-ter-p-Smad1 and promoting neural specification (Kuroda et al., 2005; Pera et al., 2003). This finding suggested that the ability of BMP signalling to block neural induction in *Xenopus* was repressed by the activation of FGF/Erk signalling, but these experiments did not exclude the possibility that FGF/Erk signalling also provided an instructive cue to induce neural induction. For example, the injection of *Smad7* mRNA into *Xenopus* embryos to inhibit BMP signalling induced ectopic neural tissue, and this ectopic neural induction was enhanced by the activation of FGF signalling (Wawersik et al., 2005). This finding implies that FGF signalling not only acts by inhibiting BMP signalling, but also provides an instructive signal to the ectoderm of *Xenopus* to develop along a neural pathway (Aruga and Mikoshiba, 2011).

In this chapter, I will show that Nnat affects both pathways to facilitate neural induction of mouse ESCs. As shown in Chapter 3 and 4, Nnat is required for the neural induction of mouse ESCs, and this is brought about by Nnat's ability to increase $[Ca^{2+}]_i$ by regulating Atp2a/SERCA. Here, I will demonstrate that an increase in $[Ca^{2+}]_i$ activates FGF/Erk signalling, and may also down-regulate the expression of *BMP4*, thus initiating neural induction.

Specifically, this chapter describes experiments that show:

1) How FGF/Erk signalling is needed in the neural induction of mouse ESCs
2) An increase in $[Ca^{2+}]_i$ by a specific Atp2a/SERCA inhibitor Tg activates FGF/Erk signalling, and the activation of FGF/Erk signalling restores the generation of neural cells from Nnat-KD ESCs
3) Activation of BMP signalling inhibits neural induction of mouse ESCs
4) Nnat may down-regulate the expression of *BMP4*

5.2 Results

5.2.1 The inhibition of FGF/Erk signalling prevents ESCs from undergoing neural induction

To test the requirement of FGF/Erk signalling in the neural induction of mouse ESCs, 46C ESCs were grown under monolayer differentiation conditions in the presence of PD173074 (a FGFR inhibitor), or PD184352 (a MEK inhibitor) to block FGF/Erk signalling. If FGF/Erk signalling is necessary for mouse ESCs to differentiate along a neural pathway, the generation of NSCs from 46C ESCs should be inhibited by the presence of FGFR or MEK inhibitors.

To carry out experiments in this Chapter, I established the differentiation paradigm represented in Fig. 5.1. ESCs were plated on gelatin-coated coverslips and cultured in non-differentiating condition for 24 hours to let ESCs adhere to the coverslips, and then the medium was switched to differentiation medium. As shown in section 3.2.1, Sox1-GFP-expressing neuroectodermal cells developed when wild type ESCs were grown in this differentiation conditions for two days. This suggests that the first 2 days of differentiation represent a crucial time window for neural induction of mouse ESCs. Thus, the ESCs were treated with PD173074 or PD184352 for the first 2 days (in experiments described later in this chapter treatments with growth factors were similarly carried out, see Fig. 5.1). The medium was then replaced with fresh medium lacking PD173074 or PD184352 and the cells cultured for a further 4 days. The cells were then fixed to check for their ability to generate Sox1-GFP and Nestin-expressing NSCs.

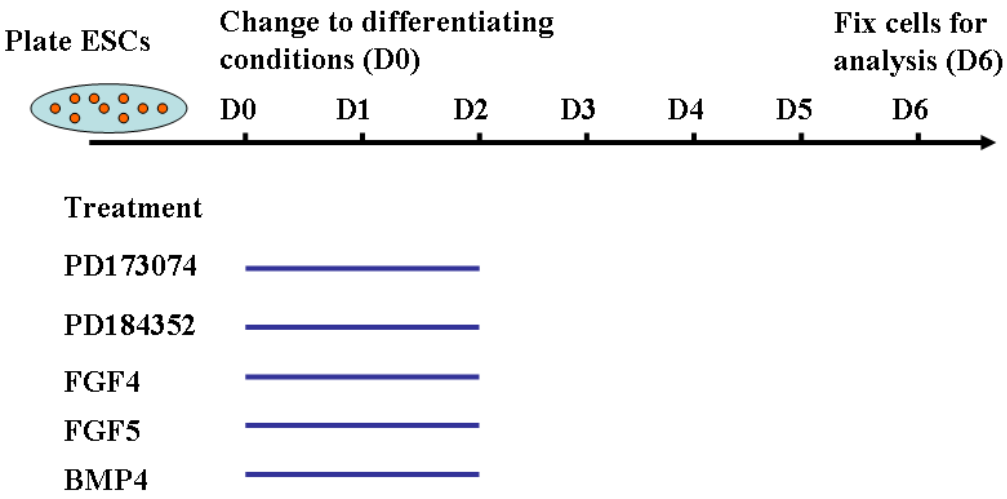

Fig. 5.1. Treatment with growth factors or inhibitors during ESCs neural differentiation. ESCs were plated and adhered to gelatin-coated coverslips in non-differenitating conditions. At D0, culture medium was changed to differentiating medium. On D2, wild type ESCs generated Sox1-GFP^{+} neuroectodermal cells, suggesting that the first 2 days of differentiation represent a crucial time window for neural induction of mouse ESCs. Thus ESCs were treated with FGF4, FGF5, BMP4, PD173074 (an inhibitor of FGFR) or PD184352 (an inhibitor of MEK) on the first 2 days, and then the medium was replaced with fresh medium lacking growth factors or inhibitors and the cells cultured for a further 4 days. On D6, cultures were fixed for immunocytochemical analysis to check for expression of the NSC marker Nestin.
Abbreviations: BMP, Bone morphogenetic protein; D, differentiation day; ESC, embryonic stem cell; FGF, Fibroblast growth factor; FGFR, FGF receptor; GFP, green fluorescent protein; MEK, Mitogen-activated Protein/Extracellular Signal-regulated Kinase Kinase; NSC, neural stem cell; Sox1, SRY (sex determining region Y)-box 1.

PD173074 and PD184352 are selective inhibitors of FGFR kinase and MEK activity respectively, and both reduce the phosphorylation of Erk1/2 and suppress Erk signalling (Grand et al., 2004; Yao et al., 2003). 100 ng/ml PD173074 can inhibit Erk1/2 phosphorylation in 46C ESCs (Stavridis et al., 2007), and the same ESCs were used in my experiments, so the same concentration of this inhibitor was used here. To determine the concentration of PD184352 to use, 46C ESCs were treated with different concentrations under differentiating conditions. 10, 5, and 1 μM PD184352 were applied to the cells for 2 days as shown in Figure 5.1; 10 μM PD184352 caused severe cell death. However, treating 46C ESCs with 5 ng/ml of FGF4 and 5 μM PD184352 together, showed that the FGF4-induced phosphorylation of Erk1/2 was inhibited by PD184352 (as assayed by Western blotting, Appendix 5). Thus, 5 μM PD184352 was used in my experiments to inhibit the activation of Erk1/2.

46C ESCs were grown under differentiation conditions (see section 3.2.1 for details) for six days and 100 ng/ml PD173074 or 5 μM PD184352 was added into the culture medium for the first two days. After 6 days of differentiation, 46C cells were fixed and analysed for expression of NSC markers, Sox1-GFP and Nestin. As expected (see sections 3.2.1 and 3.2.3), wild type ESCs generated many Sox1-GFP and Nestin-expressing NSCs (Fig. 5.2A). However, few, if any, of Sox1-GFP and Nestin-expressing NSCs were observed when 46C cells were exposed to PD173074 or PD184352 for the first two days of differentiation. Thus, the activation of FGF/Erk signalling is needed for the neural induction of mouse ESCs.

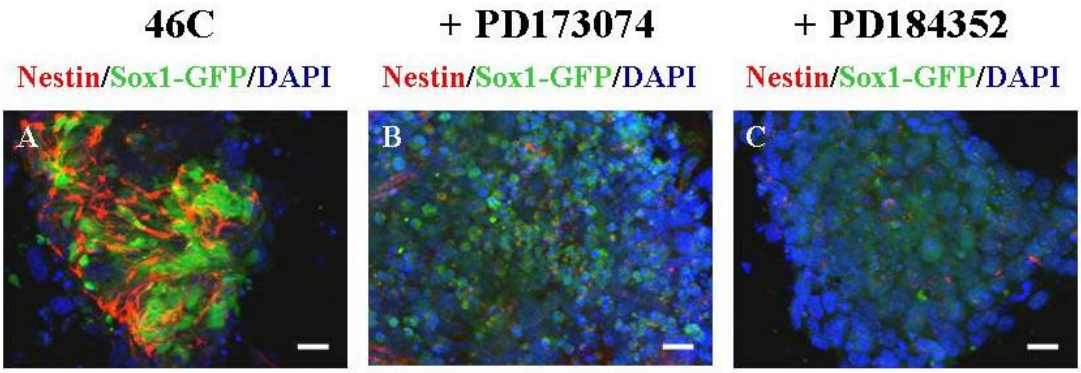

Fig. 5.2. The activation of FGF/Erk signalling is required for neural induction of mouse ESCs.

46C ESCs were differentiated for 6 days. Cells were exposed to 100 ng/ml PD173074 (an inhibitor of FGFR) or 5 μM PD184352 (an inhibitor of MEK) for the first two days of differentiation to inhibit the FGF/Erk signalling. After six days of differentiation, 46C cells were fixed and analysed for expression of the NSC markers, Sox1-GFP and Nestin. (A) 46C ESCs generated Sox1-GFP$^+$ (green) and Nestin$^+$ (red) NSCs. (B, C) Only a few Sox1-GFP$^+$ and Nestin$^+$ NSCs were observed when 46C cells were exposed to PD173074 or PD184352 for the first two days of differentiation. Thus, the activation of FGF/Erk signalling is needed for the neural induction of mouse ESCs. All nuclei were stained with DAPI (blue). Scale bar, 20 μm

Abbreviations: DAPI, 4',6-diamidino-2-phenylindole; Erk, Extracellular Signal-regulated Kinase; ESC, embryonic stem cell; FGF, Fibroblast growth factor; FGFR, FGF receptor; GFP, green fluorescent protein; MEK, Mitogen-activated Protein/Extracellular Signal-regulated Kinase Kinase; NSC, neural stem cell; Sox1, SRY (sex determining region Y)-box 1.

5.2.2 FGF4 and FGF5 rescue the ability of Nnat-KD ESCs to generate NSCs and neurons

If Nnat functions by increasing $[Ca^{2+}]_i$ that in turn activates FGF/Erk signalling to initiate neural induction, then directly activating FGF/Erk signalling should bypass the need to increase $[Ca^{2+}]_i$ and restore the ability of Nnat-KD ESCs to generate NSCs and neurons. 5 ng/ml of FGF4 or 10 ng/ml of FGF5 has been used to activate FGF/Erk signalling in the same mouse ESCs used in my experiments (Kunath et al., 2007). Therefore, to test whether or not activation of FGF/Erk signalling restored the ability of Nnat-KD ESCs to generate NSCs, 5 ng/ml of FGF4 or 10 ng/ml of FGF5 was used to treat Nnat-KD ESCs over the first 2 days of differentiation (Fig. 5.1). Cells were fixed after 6 days of differentiation for immunocytochemical analysis. As shown in section 3.2.4.2, Nnat knocked-down in 46C ESCs significantly reduced the formation of NSCs (Fig. 5.3A-B). Treatment with FGF4 or FGF5 restored the ability of Nnat-KD ESCs to generate Sox1-GFP$^+$/Nestin$^+$ NSCs (Fig. 5.3C-D). Quantification of these results revealed that the generation of Nestin$^+$/Sox1-GFP$^+$ NSCs in Nnat-KD ESCs was significantly increased from 5.6% to 14.4% and 15.6% after FGF4 or FGF5 treatment for the first two days of differentiation respectively ($n = 3$, $p < 0.05$, Fig. 5.3E). These results suggest that activating FGF signalling restores the ability of Nnat-KD ESCs to generate NSCs.

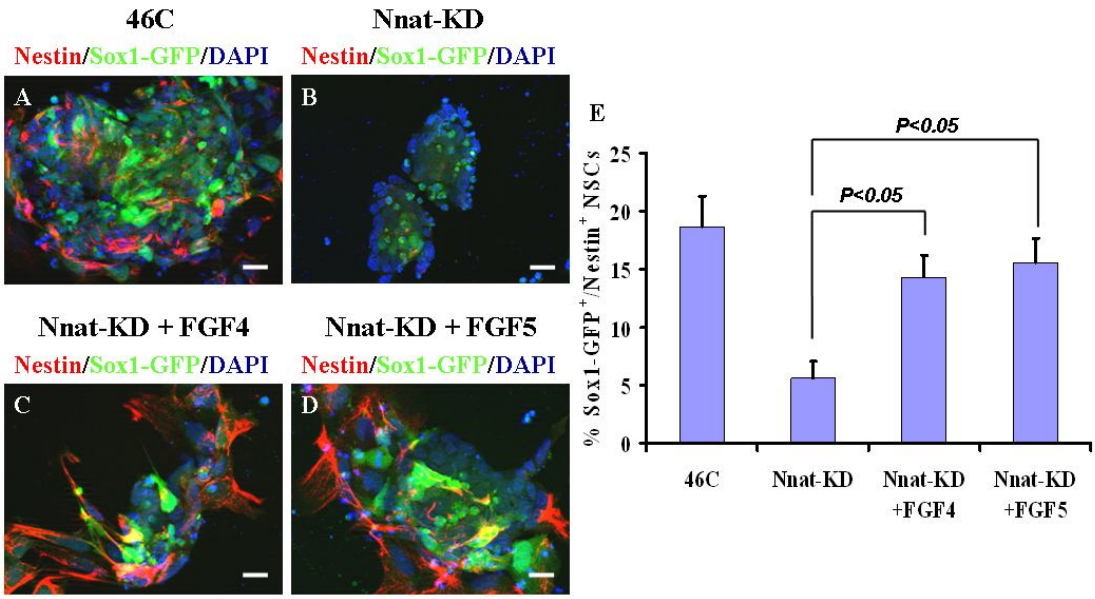

Fig. 5.3. FGF4 and FGF5 restore the ability of Nnat-KD ESCs to generate NSCs

46C or Nnat-KD ESCs were differentiated for 6 days. On the first two days of differentiation, Nnat-KD ESCs were exposed to 5 ng/ml of FGF4 or 10 ng/ml of FGF5. After differentiation for 6 days, the cells were fixed and stained with the NSC marker Nestin (red). (A) 46C ESCs could generate Sox1/GFP$^+$ and Nestin$^+$ NSCs after differentiation for 6 days. (B) The generation of Nestin$^+$ NSCs was reduced in Nnat-KD ESCs. (C) With 5 ng/ml of FGF4 treatment or (D) 10 ng/ml of FGF5 treatment, the ability of Nnat-KD ESCs to generate Sox1/GFP$^+$ and Nestin$^+$ NSCs was restored. (E) The percentage of both Sox1-GFP and Nestin-expressing NSCs was counted. Nnat-KD cells generated significantly fewer NSCs than 46C ESCs (5.6 ± 1.5% vs. 18.7 ± 2.6%, $p < 0.05$, two-tailed Student's t test), and the generation of NSCs in Nnat-KD ESCs was significantly increased to 14.4 ± 1.9% and 15.6 ± 2.1% after FGF4 or FGF5 treatment respectively (n = 3, $p < 0.05$, two-tailed Student's t test). There was no significant difference in the percentage of NSC generated between 46C and FGF4 or FGF5 treated Nnat-KD ESCs. All nuclei were stained with DAPI (blue). Scale bar, 20 μm.

Abbreviations: DAPI, 4',6-diamidino-2-phenylindole; ESC, embryonic stem cell; FGF, Fibroblast growth factor; GFP, green fluorescent protein; Nnat-KD, Nnat-knockdown; NSC, neural stem cell; Sox1, SRY (sex determining region Y)-box 1.

To determine whether FGF4- or FGF5-restored Sox1-GFP$^+$/Nestin$^+$ NSCs can give rise to neurons, the same experimental procedures were carried out as described above, but now the cultures were allowed to differentiate for 14 days to enable the generation of neurons. As shown in section 3.2.4, Nnat knock-down in 46C ESCs significantly reduced the formation of neurons (Fig. 5.4A-B). The exposure of Nnat-KD cells to 5 ng/ml of FGF4 or 10 ng/ml of FGF5 for the first two days of differentiation restored the ability of these cells to generate NeuN-expressing neurons (Fig. 5.4C-D). Quantified data revealed that the generation of NeuN-expressing neurons from Nnat-KD ESCs was significantly increased after FGF4 or FGF5 treatment from 2.4% to 12.2% or 11.8% (n = 3, $p < 0.05$) (Fig. 5.4E), but not to the levels seen in differentiated wild type 46C ESCs (23.1%, n = 3, $p < 0.05$). The difference observed between 46C and Nnat-KD ESCs may be due to the fact that the cells were only treated with FGF4 or FGF5 for the first two days of differentiation (at a time when ESCs are generating NSCs, see section 3.2.1) and not during the time when these cells go on to differentiate into NPCs and neurons. This could suggest that FGF4 or FGF5 only compensates for the early action of Nnat in neural induction (the first 2 days of differentiation), because of the time period of FGF treatments. However, the *in vivo* and *in vitro* expression patterns of Nnat reveal that this protein is still highly expressed after the neuroectoderm is formed (see section 1.7), suggesting that Nnat may be still required when neuroectodermal cells differentiate into NPCs and neurons.

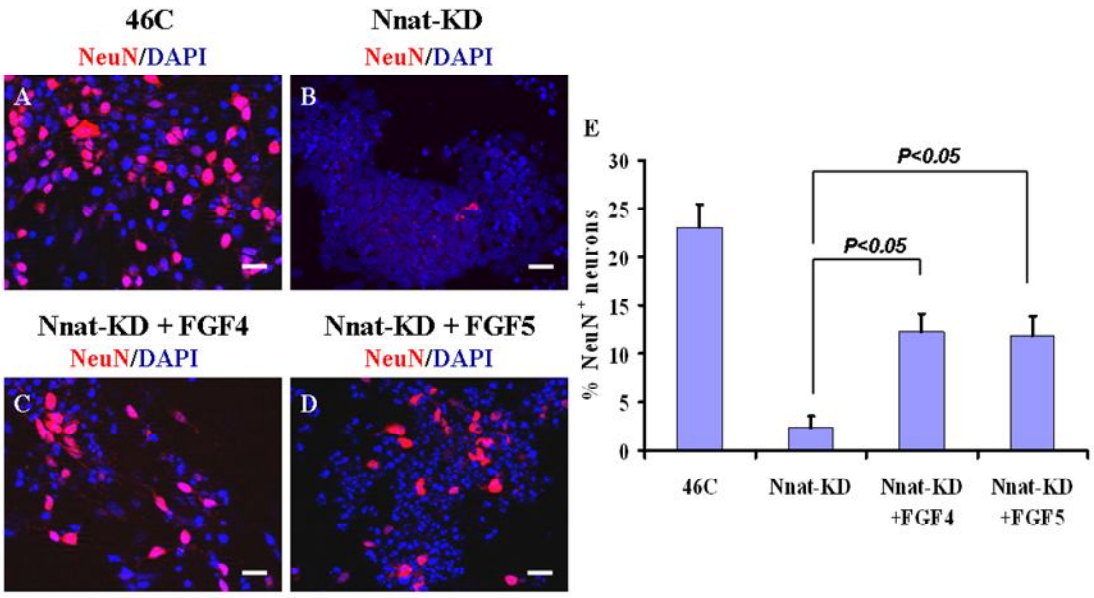

Fig. 5.4. FGF4 and FGF5 restore the ability of Nnat-KD ESCs to generate neurons.
46C or Nnat-KD ESCs were differentiated for 14 days. On the first two days of differentiation, Nnat-KD ESCs were exposed to 5 ng/ml of FGF4 or 10 ng/ml of FGF5. After differentiated for 14 days, the cells were fixed and stained with the nuclear neuronal marker NeuN (red). (A) 46C ESCs generated $NeuN^+$ neurons after 14 days of differentiation. (B) The generation of $NeuN^+$ neurons was significantly decreased in Nnat-KD ESCs. (C) With 5 ng/ml of FGF4 treatment or (D) 10 ng/ml of FGF5 treatment, the ability of Nnat-KD ESCs to generate $NeuN^+$ neurons was restored. (E) The percentage of $NeuN^+$ neurons was counted. Nnat-KD cells generated significantly fewer neurons than 46C ESCs (2.4 ± 1.2% vs. 23.1 ± 2.3%, $p < 0.01$, two-tailed Student's t test). The generation of neurons in Nnat-KD ESCs was significantly increased to 12.2 ± 1.9% and 11.8 ± 2.1% after FGF4 or FGF5 treatment respectively (n = 3, $p < 0.05$, two-tailed Student's t test), but could not reach the level of 46C ESCs ($p < 0.05$, two-tailed Student's t test). All nuclei were stained with DAPI (blue). Scale bar, 20 μm.
Abbreviations: DAPI, 4',6-diamidino-2-phenylindole; ESC, embryonic stem cell; FGF, Fibroblast growth factor; GFP, green fluorescent protein; NeuN, neuronal nuclei; Nnat-KD, Nnat-knockdown.

5.2.3 Blocking p-Erk signalling abolished Tg-restored the capacity of neural specification in Nnat-KD ESCs

As shown in sections 5.2.1 and 5.2.2, the FGF/Erk pathway plays a crucial role in neural induction in wild type ESCs and also rescues the impairment in neural cell production of Nnat-KD ESCs. Next, I wanted to establish whether the FGF/Erk pathway is involved in Tg-restored neural specification in Nnat-KD ESCs. To do this, Nnat-KD ESCs were first treated with 25 nM Tg for 30 minutes on the first day of differentiation to restore the ability of these cells to generate NSCs (as described previously in section 4.2.3). Then, to test whether or not this restored ability to generate NSCs was reduced by the inhibition of FGF/Erk signalling, the Tg-treated Nnat-KD ESCs were also exposed to 100 ng/ml PD173074 or 5 μM PD184352 for the first 2 days of differentiation. As expected (see section 4.2.3.2), after 6 days of differentiation, Tg restored the ability of Nnat-KD ESCs to generate Sox1-GFP and Nestin-expressing NSCs cells (Fig. 5.5A-B). However, this ability was dramatically reduced when FGF/Erk signalling was suppressed by addition of PD173074 or PD184352 (Fig. 5.5C-D). Therefore, the FGF/Erk pathway is involved in Tg-mediated neural induction in Nnat-KD ESCs.

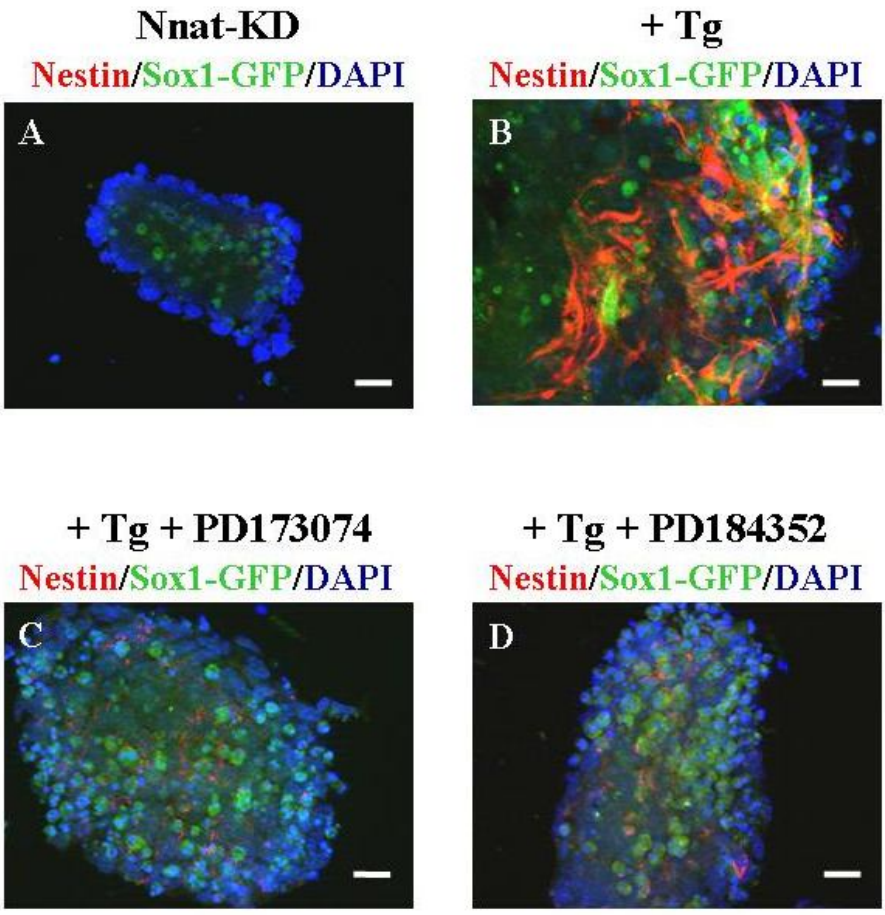

Fig. 5.5. The inhibition of FGF/Erk signalling restricts the ability of Tg to rescue the generation of NSCs from Nnat-KD ESCs.

Nnat-KD ESCs were differentiated for 6 days. On the first day of differentiation, cells were treated with 25 nM Tg (an inhibitor of Apt2a/SERCA) for 30 minutes to restore their ability to generate NSCs. Cells were also exposed to 100 ng/ml PD173074 (an inhibitor of FGFR) or 5 μM PD184352 (an inhibitor of MEK) for the first two days of differentiation to inhibit FGF/Erk signalling. After six days of differentiation, Nnat-KD cells were fixed and analysed for expression of the NSC markers, Sox1-GFP and Nestin. (A, B) Tg rescued the ability of Nnat-KD ESCs to generate Sox1-GFP$^+$ (green) and Nestin$^+$ (red) NSCs. (C, D) Only a few Sox1-GFP$^+$ and Nestin$^+$ NSCs were observed when Tg-treated Nnat-KD cells were exposed to PD173074 or PD184352 for the first two days of differentiation. Thus, the activation of FGF/Erk signalling is required for the Tg rescue of Nnat-KD ESCs to generate NSCs. All nuclei were stained with DAPI (blue). Scale bar, 20 μm.

Abbreviations: Apt2a/SERCA, sarcoendoplasmic reticulum Ca^{2+}-ATPase; DAPI, 4',6-diamidino-2-phenylindole; Erk, Extracellular Signal-regulated Kinase; ESC, embryonic stem cell; FGF, Fibroblast growth factor; FGFR, FGF receptor; GFP, green fluorescent protein; MEK, Mitogen-activated Protein/Extracellular Signal-regulated Kinase Kinase; Nnat-KD, Nnat-knockdown; NSC, neural stem cell; Sox1, SRY (sex determining region Y)-box 1; Tg, Thapsigargin.

5.2.4 Increasing $[Ca^{2+}]_i$ activates Erk signalling

I have shown above that Erk signalling is involved in the Tg-restored neural induction in Nnat-KD ESCs. The next question I would like to find out is whether the increase in $[Ca^{2+}]_i$ caused by the treatment of Nnat-KD ESCs with Tg (pivotal for restoring NSC development, see section 4.2.3.2) triggers the activation of Erk signalling. To answer this question, I employed Western blotting to analyse whether Erk1/2 were activated by Tg treatment in Nnat-KD ESCs. First, I established the effect of different concentrations of Tg on the p-Erk1/2 levels. To this end, Nnat-KD ESCs were plated out onto gelatin-coated plates in non-differentiating conditions and the next day 25, 100, or 1000 nM Tg was added into the culture medium for 5 minutes before cells were immediately collected and lysates prepared for analysis. The cell lysates were run on a gel, transferred to a nitrocellulose membrane and the membrane blotted with anti-p-Erk1/2 antibodies (for details of Western blotting see section 2.7). If treatment of Nnat-KD ESCs with Tg activates Erk signalling, then the active form of Erk1/2, p-Erk1/2, should be increased. In Figure 5.6A, p-Erk1/2 was increased in cultures treated with all three concentrations of Tg, with a Tg concentration as low as 25 nM being sufficient to activate Erk signalling in Nnat-KD ESCs. This may explain why 25 nM Tg can rescue the defective neural induction in Nnat-KD ESCs. Further, to determine when the peak of p-Erk activity was observed, Nnat-KD ESCs samples were collected after 5, 10, 20, and 60 minutes of 25 nM Tg treatments. The results showed that the activation of Erk1/2 peaked at 10 minutes and declined thereafter (Fig. 5.6B). Therefore, from experiments described in section 4.2.3.2 and above, I hypothesise that Tg causes an increase in $[Ca^{2+}]_i$ which then activates Erk1/2; so it is likely that Nnat has a similar function, as we know that Tg imitates the action of Nnat (see section 4.2.3).

Thus, my data suggests that Tg increases $[Ca^{2+}]_i$, which leads to the activation of Erk signalling that then mediates neural induction in Nnat-KD ESCs. There is a question as to whether Tg activates Erk signalling at the level of FGFRs, which are upstream elements of the Erk pathway. To answer this question, I adopted a biochemical approach together with

Western blotting. Prior to treatment with Tg, Nnat-KD ESCs were treated with the FGFR inhibitor PD173074 (100 ng/ml for 2 hours), and then Nnat-KD ESCs were cultured with 25 nM Tg and PD173074 for 10 minutes together. After treatment, Nnat-KD ESCs were collected and the level of p-Erk1/2 analysed using immunoblotting (Fig. 5.6C). The level of p-Erk1/2 observed in Lane 1, represents basal activity under undifferenitating conditions without Tg or PD173074 treatments. As expected, p-Erk1/2 was increased after Tg treatment (Fig. 5.6C, compare lane 1 with lane 2), and was decreased by the treatment of PD173074 (Fig. 5.6C, compare lane 1 with lane 3). This result suggested that as well as FGF, other signals also activated Erk1/2 in mouse ESCs. For example, EGFR (epidermal growth factor receptor) is expressed by the ICM in mouse and is active throughout preimplantation and gastrulation (Adamson, 1990; Brison and Schultz, 1996), so EGFR may also be active in mouse ESCs. Like FGFR, EGFR is also a receptor tyrosine kinase (RTK) that activates the Erk1/2 pathway (Xia et al., 2002). Thus, EGF/Erk may be active in mouse ESCs. Similarly, PDGFR (platelet-derived growth factor receptor) is another RTK that has also been shown to be active in the ICM of vertebrates (Artus et al., 2010; Karpova et al., 1997; Osterlund et al., 1996), suggesting that Erk1/2 may also be phosphorylated by the activation of PDGFR in mouse ESCs.

When FGFR were inhibited by PD173074, p-Erk1/2 was still increased by treatment with Tg (Fig. 5.6C, compare lane 3 with lane 4). These observations suggest that FGF/Erk signalling and Tg-mediated Erk signalling represent two different pathways that converge at the level of Erk1/2. It has previously been demonstrated in Hela, human mesenchymal stem, and Jurkat T-cells that an increase in $[Ca^{2+}]_i$ caused by Tg administration activates RasGRP, which in turn activates Ras and Raf/MEK/Erk protein kinase cascade (for details see section 1.5.4.3) (Denys et al., 2004; Kupzig et al., 2005; Riddle et al., 2006). Therefore my results are consistent with this observation that Tg-mediated Erk signalling is not via the activation of FGFR.

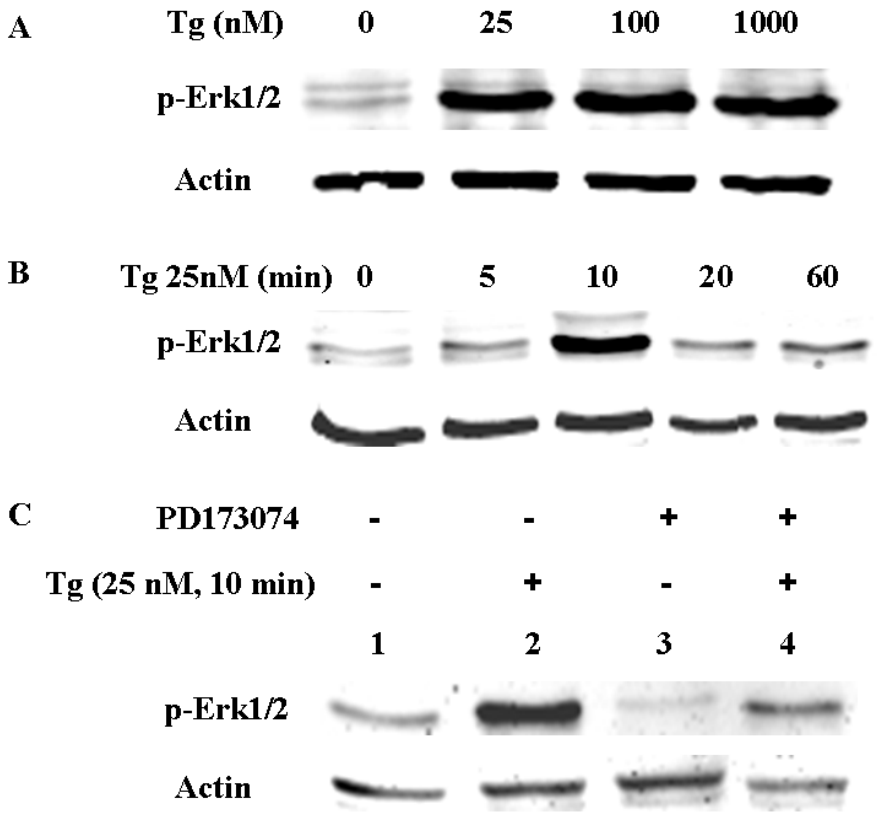

Fig. 5.6. FGFR is not involved in the activation of Tg-mediated Erk signalling.
Nnat-KD ESCs were cultured in non differentiating culture conditions. After different treatments, the protein levels of p-Erk1/2 were analysed by Western blotting using an anti-p-Erk1/2 antibody. (A) After Nnat-KD ESCs were exposed to 25, 100, or 1000 nM Tg for five minutes, the levels of p-Erk/12 were increased in all conditions. (B) Nnat-KD ESCs were treated with 25 nM Tg for 5, 10, 20, and 60 minutes to activate Erk1/2. The activation of Erk1/2 peaked at 10 minutes and declined thereafter. (C) To verify whether FGFR was involved in the activation of Tg-mediated Erk signalling, Nnat-KD ESCs were treated with the FGFR inhibitor (100 ng/ml PD173074) for 2 hours first followed by a 10 min treatment with 25 nM Tg to activate Erk1/2 in the presence of PD173074. Lane 1 shows the basal level of p-Erk1/2 under culture condition without Tg or PD173074. As expected, p-Erk1/2 was increased by treatment with Tg (compare lane 1 with lane 2), and p-Erk1/2 was decreased by the treatment of PD173074 (compare lane 1 with lane 3). When Nnat-KD ESCs were treated with PD173074 and Tg together, p-Erk1/2 was still increased by treatment with Tg (compare lane 3 with lane 4), suggesting that the FGFR is not involved in the activation of Tg-mediated Erk signalling.
Abbreviations: Erk, Extracellular Signal-regulated Kinase; ESC, embryonic stem cell; FGFR, Fibroblast growth factor receptor; Nnat-KD, Nnat-knockdown; p-Erk1/2, phosphorylated Erk1/2; Tg, Thapsigargin.

As shown in Chapter 4, Nnat acts to inhibit the movement of cytosolic Ca^{2+} into the ER by antagonising Apt2a/SERCA, which then causes an increase in $[Ca^{2+}]_i$. This action of Nnat resembles that of Tg, a specific blocker of Apt2a/SERCA. As shown in Figure 5.6, the treatment of Nnat-KD ESCs with Tg increases p-Erk1/2, and the Tg-mediated phosphorylation of Erk1/2 is not abrogated by exposure to the FGFR inhibitor PD173074. These results suggest that Tg is not acting at the level of FGFRs to cause the phosphorylation of Erk1/2. I propose that Nnat may act in the same manner to activate Erk signalling and initiate neural induction in mouse ESCs.

46C and Nnatα-OE ESCs were cultured in the presence or absence of 100 ng/ml PD173074 or 5 μM PD184352 for the first two days (Fig. 5.1). Cell samples were collected after 6 days of differentiation, and cells were analysed for Sox1-GFP and Nestin-expressing NSCs. 46C and Nnatα-OE ESCs generated NSCs as usual after 6 days of differentiation (Fig. 5.7A and D). As shown in section 5.2.1, the generation of NSCs was reduced in the PD173074 treated 46C ESCs (Fig. 5.7B). Interestingly, NSCs were still generated from the PD173074 treated Nnatα-OE ESCs (Fig. 5.7E), but the number of NSCs generated by these cells were fewer that were generated by untreated Nnatα-OE ESCs (Fig. 5.7, compare D with E). This result suggests that FGFs that are secreted from ESCs and act in an autocrine or paracrine manner also play a part in the neural induction of Nnatα-OE ESCs. Although PD173074 treatment reduced the generation of NSCs in both Nnatα-OE and wild type ESCs, the reduction was more severe in wild type compared with Nnatα-OE ESCs (Fig. 5.7, compare B with E), suggesting that the over-expression of Nnatα partially compensates for the loss of activation of FGFRs during neural induction. The treatment of Nnatα-OE ESCs with the MEK inhibitor PD184352 to inhibit the activation of Erk1/2 almost abolished the production of NSCs (Fig. 5.7F). Similarly results were observed for PD184352 treated 46C ESCs (Fig. 5.7C). This data suggest that Nnat-mediated neural induction occurs via the activation of Erk signalling.

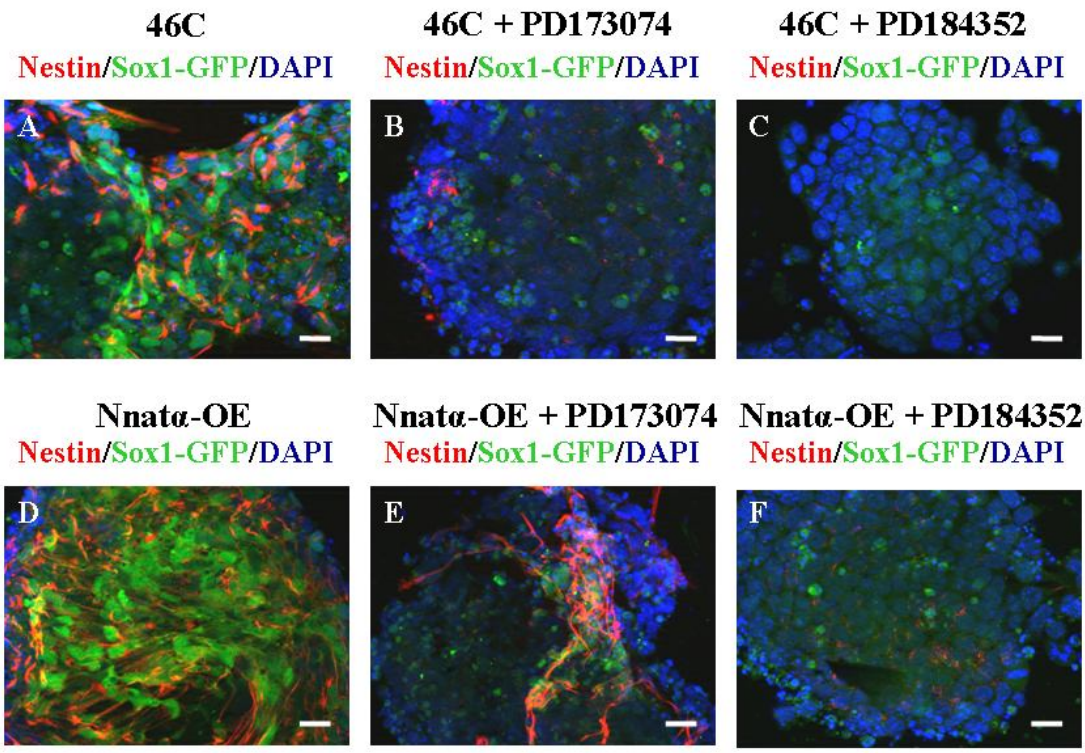

Fig. 5.7. The activation of Erk signalling plays a crucial role in Nnat-mediated neural induction.

46C and Nnatα-OE ESCs were differentiated for six days. Cells were exposed to 100 ng/ml PD173074 (an inhibitor of FGFR) or 5 μM PD184352 (an inhibitor of MEK) for the first two days of differentiation to inhibit the FGF/Erk signalling. After six days of differentiation, 46C and Nnatα-OE cells were fixed and analysed for expression of the NSC markers, Sox1-GFP and Nestin. (A,D) Nnatα-OE ESCs generated more Sox1-GFP$^+$ (green) and Nestin$^+$ (red) NSCs than 46C ESCs. (B) The treatment of 46C ESCs with PD173074 significantly reduced the generation of NSCs, suggesting that the endogenous FGF is pivotal for neural induction in wild type ESCs. (E) However, some NSCs were still generated when Nnatα-OE cells were exposed to PD173074 for the first two days of differentiation, suggesting that the over-expression of Nnatα partially compensates the generation of NSCs for loss of action of endogenous FGF during neural induction, and the FGFR is not involved in the Nnat-mediated neural induction. (C,F) When 46C or Nnatα-OE cells were exposed to PD184352 for the first two days of differentiation, very few NSCs were observed. Therefore the activation of Erk1/2 dose play a crucial role in both FGF and Nnat-mediated neural induction. All nuclei were stained with DAPI (blue). Scale bar, 20 μm.

Abbreviations: DAPI, 4',6-diamidino-2-phenylindole; Erk, Extracellular Signal-regulated Kinase; ESC, embryonic stem cell; FGF, Fibroblast growth factor; FGFR, FGF receptor; GFP, green fluorescent protein; MEK, Mitogen-activated Protein/Extracellular Signal-regulated Kinase Kinase; Nnatα-OE, Nnatα-overexpression; NSC, neural stem cell; Sox1, SRY (sex determining region Y)-box 1.

5.2.5 The activation of BMP signalling prevents ESCs differentiating along a neural pathway

As BMP signalling suppresses neural induction in vertebrates, it is likely that neural induction in mouse ESCs will be inhibited by activating BMP signalling (see sections 1.4 and 1.6.2). I adopted an immunocytochemical analysis to explore the effects of BMP signalling on neural induction in 46C, Nnat-KD, and Nnatα-OE ESCs. 46C, Nnat-KD, and Nnatα-OE ESCs were differentiated for six days, with the Nnat-KD ESCs being treated with 25 nM Tg for 30 minutes on the first day to restore their ability to generate NSCs (see section 4.2.3). In 46C ESCs, 10 ng/ml of BMP4 activates BMPR causing phosphorylation of Smad1 at its C-terminus to activate dowstream signalling (Stavridis et al., 2007; Ying et al., 2003). Because the first two days of differentiation is the time during which neural induction occurs (see section 3.2.1), 10 ng/ml BMP4 was added into the culture medium over this time period to see if the generation of NSCs was inhibited. After 6 days of differentiation, cells were fixed and analysed for the expression of the NSC markers, Sox1-GFP and Nestin. Exposure to BMP4 reduced the generation of NSCs from 46C ESCs (Fig. 5.8A-B). As reported previously (see section 4.2.3), Tg restored the ability of Nnat-KD ESCs to generate NSCs, but the number of NSCs generated under these 'Tg-rescue' conditions was reduced by BMP4 administration (Fig. 5.8C-E). Although BMP4 also decreased the generation of NSCs from Nnatα-OE ESCs, the suppressive effect in Nnatα-OE ESCs was not as severe as in wild type ESCs (Fig. 5.8F-G). Thus, the activation of BMP signalling markedly reduced the ability of wild type mouse ESCs to differentiate along a neural pathway, and when Nnatα was over-expressed, the repressive ability of BMP signalling was reduced. When BMP4 was administered on the third day of differentiation (avoiding the first two days), BMP4 no longer suppressed the ability of 46C, Tg-treated Nnat-KD, or Nnatα-OE ESCs to generate of NSCs. Thus the first two days of differentiation is the crucial time for neural induction in mouse ESCs.

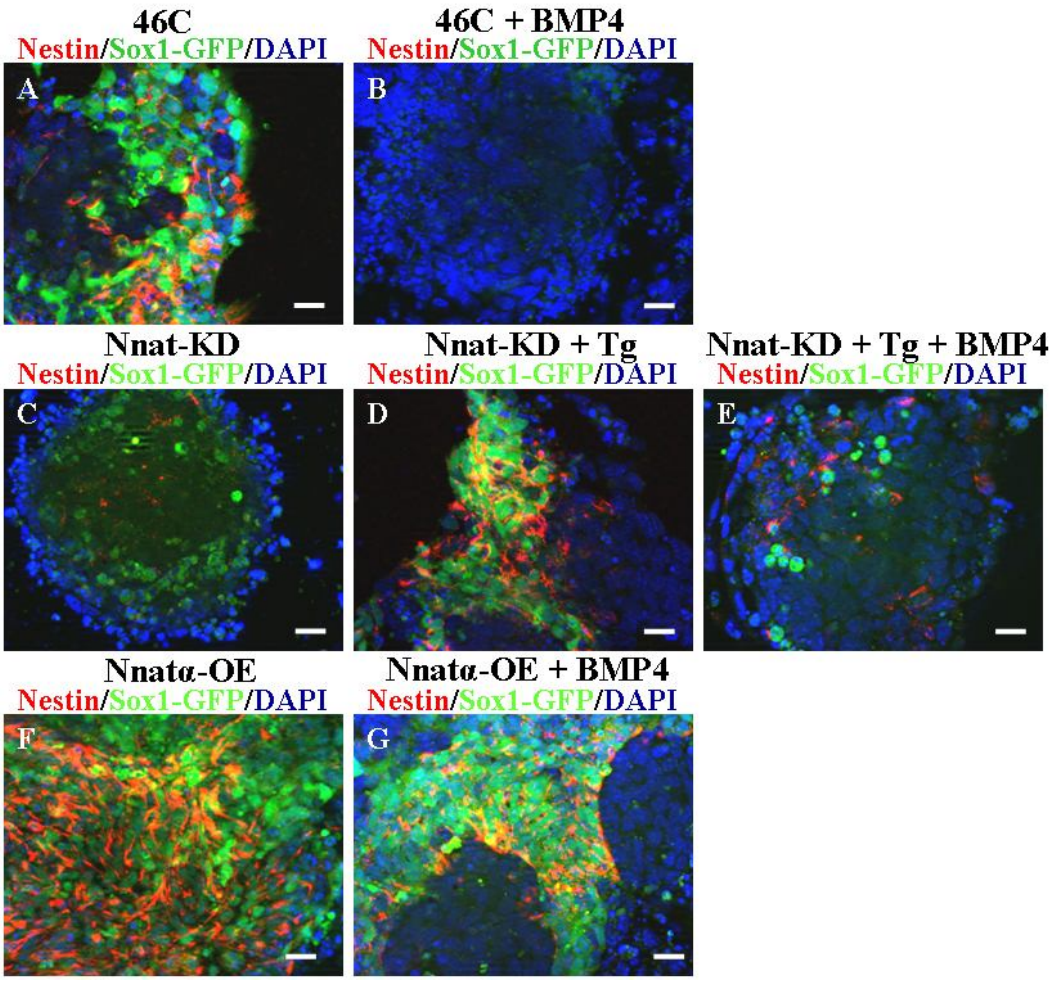

Fig. 5.8. Nnat may compete with BMP signalling during the neural induction of ESCs. 46C, Nnat-KD, and Nnatα-OE ESCs were differentiated for six days. Cells were exposed to 10 ng/ml BMP4 for the first two days of differentiation. After six days of differentiation, cells were fixed and analysed for expression of the NSC markers, Sox1-GFP and Nestin. (A) 46C ESCs generated Sox1-GFP^{+} (green) and Nestin^{+} (red) NSCs. (B) The administration of BMP4 restricted the generation of NSCs from 46C ESCs. (C) The generation of NSCs was reduced in Nnat-KD ESCs. (D) When Nnat-KD ESCs were exposed to 25nM Tg for 30 minutes on the first day of differentiation, the ability of Nnat-KD ESCs to generate NSCs was regained. (E) The generation of NSCs from Tg-treated Nnat-KD ESCs was suppressed when cells were exposed to BMP4. (F) Nnatα-OE ESCs generated more NSCs than 46C ESCs. (G) BMP4 treatment only partially reduced the generation of NSCs from Nnatα-OE ESCs. These results suggested that activation of BMP signalling markedly reduced the ability of wild type mouse ESCs to differentiate along a neural pathway, and when Nnat is over-expressed, the repressive ability of BMP signalling is reduced. Thus, Nnat and BMP may compete with each other during the neural induction of ESCs. All nuclei were stained with DAPI (blue). Scale bar, 20 μm.
Abbreviations: BMP, Bone morphogenetic protein; DAPI, 4',6-diamidino-2-phenylindole; Erk, Extracellular Signal-regulated Kinase; ESC, embryonic stem cell; GFP, green fluorescent protein; Nnat-KD, Nnat-knockdown; Nnatα-OE, Nnatα-overexpression; NSC, neural stem cell; Sox1, SRY (sex determining region Y)-box 1; Tg, Thapsigargin.

5.2.6 Nnat may down-regulate the transcription of *BMP4* and its target genes, *Msx1* and *Msx2*

The expression of *BMP4* and its target genes, *Msx1* and *Msx2*, are up-regulated in embryonic ectoderm as it differentiates along an epidermal fate, but are down-regulated in neuroectoderm (see section 1.4). In order to determine whether Nnat-mediated signalling down-regulates the expression of *BMP4*, *Msx1* and *Msx2* in mouse ESCs to promote a neural fate, the expression of *BMP4*, *Msx1* and *Msx2* were evaluated in 46C, Nnatα-OE, and Nnat-KD ESCs using quantitative real-time PCR.

46C, Nnatα-OE, and Nnat-KD ESCs were grown on gelatin-coated plates and cultured in non-differentiating conditions until they reached 100% confluency. Then the ESCs were collected for analysing the expression levels of *BMP4*, *Msx1*, and *Msx2* using real-time PCR. The expression of *BMP4, Msx1 and Msx2* were found to be up-regulated in Nnat-KD ESCs as compared with 46C and Nnatα-OE ESCs (Fig. 5.9). Thus it appeared that Nnat may down-regulate the expression of *BMP4* and its target genes, so the increase in expression of *BMP4* in Nnat-KD ESCs may restrict their neural differentiation through increased expression of its target genes *Msx1* and *Msx2*. However, the above results did not show that Nnat directly inhibits BMP signalling. To test this possibility a luciferase reporter gene assay could be used. Using this assay, the expression of target genes could be analysed by quantitative determination of firefly luciferase activity in transfected cells (Brasier et al., 1989). For instance, the vector contains a luciferase reporter gene with an upstream multiple cloning site for introducing the promoter region of *BMP4*, *Msx1*, or *Msx2*. *Nnat* is then sub-cloned into another expression vector and both vectors co-transfected into 3T3 cells and the luciferase activity analysed. If Nnat directly inhibited BMP signalling, then the luciferase activity with a promoter of *BMP4*, *Msx1*, or *Msx2* would be reduced.

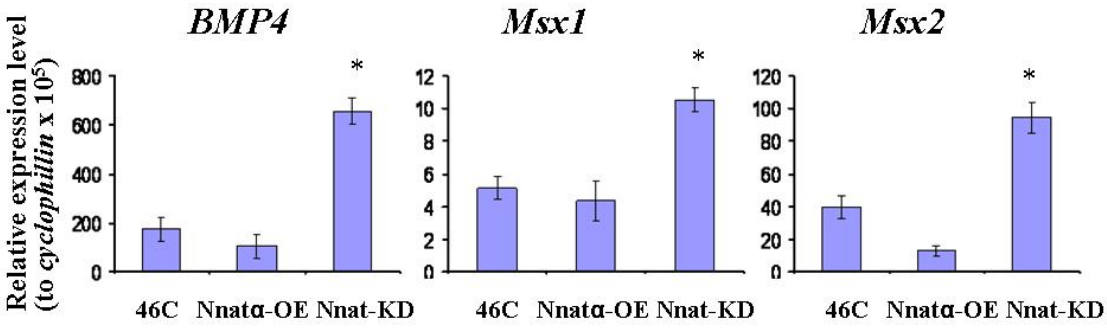

Fig. 5.9. Nnat may down-regulate the expression of *BMP4* and its target genes *Msx1* and *Msx2* in ESCs.

The expression of *BMP4* and its target genes, *Msx1* and *Msx2*, are up-regulated when embryonic ectoderm differentiates along an epidermal pathway, but was down-regulated in neuroectoderm. In order to determine whether Nnat-mediated signalling down-regulates the expression of *BMP4*, *Msx1* and *Msx2* in mouse ESCs to promote a neural fate, the expression of the message for these proteins were evaluated in 46C, Nnatα-OE, and Nnat-KD ESCs using quantitative real-time PCR. The expression of *BMP4*, *Msx1*, and *Msx2* were up-regulated in Nnat-KD ESCs compared with 46C and Nnatα-OE ESCs ($p < 0.05$, one-way ANOVA test). Thus Nnat may down-regulate the expression of *BMP4* and its target genes to facilitate ESCs to differentiate along a neural pathway.

Abbreviations: ANOVA, analysis of variance; *BMP4*, *Bone morphogenetic protein 4*; ES, embryonic stem; Nnat-KD, Nnat-knockdown; Nnatα-OE, Nnatα-overexpression; PCR, polymerase chain reaction.

The above data shows that Nnat may down-regulate the expression of *BMP4*, so may influence BMP signalling by reducing the availability of this ligand. The binding of BMP to its receptor activates Smad1 and causes the phosphorylation of Smad1 at its C-terminus, and then the C-ter-p-Smad1 is translocated to the nucleus where it activates its target genes *Msx1* and *Msx2* (see section 1.4.1). It is undetermined whether Nnat can down-regulate the expression of *Msx1* and *Msx2* by suppressing C-ter-p-Smad1. As discussed, in *Xenopus* activation of FGF/Erk signalling causes the degradation of C-ter-p-Smad1 and inhibits BMP signalling thus enabling neural induction to occur (see the section 1.5.1.4; Fuentealba et al., 2007; Kuroda et al., 2005; Pera et al., 2003). Furthermore, I have shown that increasing $[Ca^{2+}]_i$ activates Erk signalling in Nnat-KD ESCs (see section 5.2.4). Thus, increasing $[Ca^{2+}]_i$ may induce the degradation of C-ter-p-Smad1 via Erk signalling. To examine this hypothesis, Nnat-KD cells were treated with BMP4 to increase C-ter-p-Smad1, and then $[Ca^{2+}]_i$ (and hence activated Erk1/2) was increased by Tg treatment to determine

whether C-ter-p-Smad1 was reduced by the activation of Tg-mediated Erk signalling.

In 46C ESCs, the phosphorylation of Smad1 at its C-terminus induced by BMP4 peaks 60 minutes after 10 ng/ml BMP4 treatment (Ying et al., 2003). Nnat-KD ESCs are generated from 46C ESCs, so Nnat-KD ESCs were pretreated with 10 ng/ml BMP4 for 60 minutes to reach the peak of phosphorylation. Then 25 nM Tg was added into the culture medium with BMP4 for another 10, 30, and 60 minutes to activate Erk1/2. After BMP4 and Tg treatment, cells were lysed to prepare whole cell lysates and the levels of C-ter-p-Smad1 analysed by Western blotting using an anti-C-ter-p-Smad1 antibody (Fig. 5.10). The base level of C-ter-p-Smad1 in Nnat-KD ESCs was shown in Lane 1 (Fig. 5.10). After BMP4 treatment for 70 minutes, C-ter-p-Smad1 was increased (Fig. 5.10, compare lane 1 with lane 2), and it was not decreased when cells were exposed to Tg for 10 minutes, which is the peak of Tg-mediated Erk1/2 phosphorylation (Fig. 5.10, compare lane 2 with lane 3). The activation of Smad1 declined after 90 and 120 minutes of BMP4 treatment (Fig. 5.10, compare lanes 2, 4, with 6), and at these same time points the C-ter-p-Smad1 was not decreased by Tg (Fig. 5.10, compare lanes 4 with 5, and 6 with 7). Therefore adding Tg after exposing cells to BMP4 did not decrease the C-ter-p-Smad1. Therefore, Tg-treatment did not decrease BMP4 induced C-ter-p-Smad1 expression in mouse ESCs, so Nnat may not be repressing BMP signalling through the reduction of C-ter-p-Smad1.

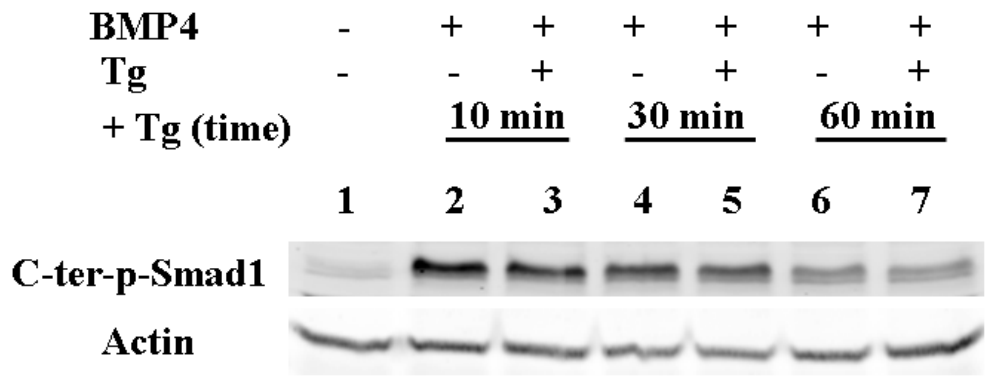

Fig. 5.10. Activation of Erk signalling does not decrease C-ter-p-Smad1 in mouse ESCs. In *Xenopus*, activation of Erk signalling decreases C-ter-p-Smad1 to promote neural induction. To determine whether the Tg-mediated Erk signalling decreased the C-ter-p-Smad1 in mouse ESCs Nnat-KD ESCs were treated with 10 ng/ml BMP4 for 60 minutes to increase the C-ter-p-Smad1, and then 25 nM Tg was added into the culture medium with BMP4 for another 10, 30, and 60 minutes to activate Erk1/2. After BMP4 and Tg treatment, the levels of C-ter-p-Smad1 were analysed by Western blotting using an anti-C-ter-p-Smad1 antibody. Lane 1 revealed the base level of C-ter-p-Smad1 in Nnat-KD ESCs. After BMP4 treatment for 70 minutes, C-ter-p-Smad1 was increased (compare lane 1 with 2), and it was not decreased when cells were exposed to Tg for 10 minutes (compare lane 2 with 3). The activation of Smad1 declined at 90 and 120 minutes of BMP4 treatment (compare lane 2, 4, with 6), and at the same time points the C-ter-p-Smad1 was not decreased by Tg (compare lane 4 with 5, and 6 with 7). The results show that Tg-treatment does not decrease BMP4 induced C-ter-p-Smad1 expression in mouse ESCs, so the activation of Erk signalling may not inhibit C-ter-p-Smad1 in mouse ESCs. Abbreviations: BMP, Bone morphogenetic protein; C-ter-p-Smad1, C-terminal phosphorylated Smad1; Erk, Extracellular Signal-regulated Kinase; ESC, embryonic stem cell; Nnat-KD, Nnat-knockdown; Tg, Thapsigargin.

5.2.7 BMP antagonists do not restore the generation of neuroectoderm from Nnat-KD ESCs

My research indicates that Nnat increases $[Ca^{2+}]_i$ which activates Erk signalling and initiates neural induction in mouse ESCs. Furthermore, Nnat may also down-regulate the expression of *BMP4* and its target genes. Both activating Erk signalling and suppressing BMP signalling are pivotal in neural induction (details see sections 1.4 and 1.5). To test whether BMP inhibition is sufficient to induce the neural differentiation of Nnat-KD ESCs, BMP antagonists were used to suppress BMP signalling in these cells and the ability of these cells to generate neuroectoderm was evaluated.

100 ng/ml Noggin, 150 ng/ml Chordin, or 150 ng/ml Follistatin has

previously been used to antagonise BMP signaling in cultured ESCs (Gerrard et al., 2005; Hosseinkhani et al., 2007; Naito et al., 2006; Suzuki et al., 2006; Yuasa et al., 2005). These ESCs are different from 46C ESCs used in my experiments and there is no evidence that the reported concentrations of Chordin or Follistatin will inhibit BMP signalling in a monolayer differentiation model of 46C ESCs; however, such evidence does exist for 100 ng/ml Noggin (Stavridis et al., 2007). Therefore different concentrations of BMP antagonists were applied to Nnat-KD ESCs to see if the generation of neuroectoderm was rescued (Noggin (100 or 200 ng/ml), Chordin (150 or 300 ng/ml) or Follistatin (150 or 300 ng/ml)). Because Sox1-expressing neuroectodermal cells are generated after 2-3 days of differentiation (see section 3.2.1), Nnat-KD ESCs were grown under differentiating conditions in the presence of BMP antagonists for four days before being fixed, to allow the generation of sufficient Sox1-GFP-expressing neuroectodermal cells, which is an indication of neural induction having taken place. 46C cells differentiated in the absence of antagonists were included as a positive control for the generation of Sox1-GFP$^+$ neuroectodermal cells, as were Nnat-KD cells treated with 25nM Tg for 30 minutes on the first day of differentiation to rescue their ability to generate NSCs (details see section 4.2.3.2).

As expected, after 4 days of differentiation 46C ESCs generated Sox1-GFP$^+$ neuroectodermal cells (Fig. 5.11A), as did Tg-treated Nnat-KD ESCs (Fig. 5.11B and C). Interestingly, when Nnat-KD ESCs were treated either with Noggin (100 or 200 ng/ml), Chordin (150 or 300 ng/ml) or Follistatin (150 or 300 ng/ml) throughout the 4-day differentiation period, Nnat-KD ESCs still failed to undergo neural induction (Fig. 5.11D-F). Even when these cells were cultured with a combination of 200 ng/ml Noggin, 300 ng/ml Chordin, and 300 ng/ml Follistatin for 4 days, the ability of Nnat-KD ESCs to generate neuroectodermal cells was still not restored (Fig. 5.11G). Thus simply inhibiting BMP signalling was not sufficient to cause neural induction in Nnat-KD ESCs. The results suggest that Nnat may not only down-regulate the expression of BMP4, but also affect other pathways, such as increasing cytosolic Ca^{2+} which in turn

leads to activate Erk signalling (see sections 4.2.2 and 5.2.4), to initiate neural induction.

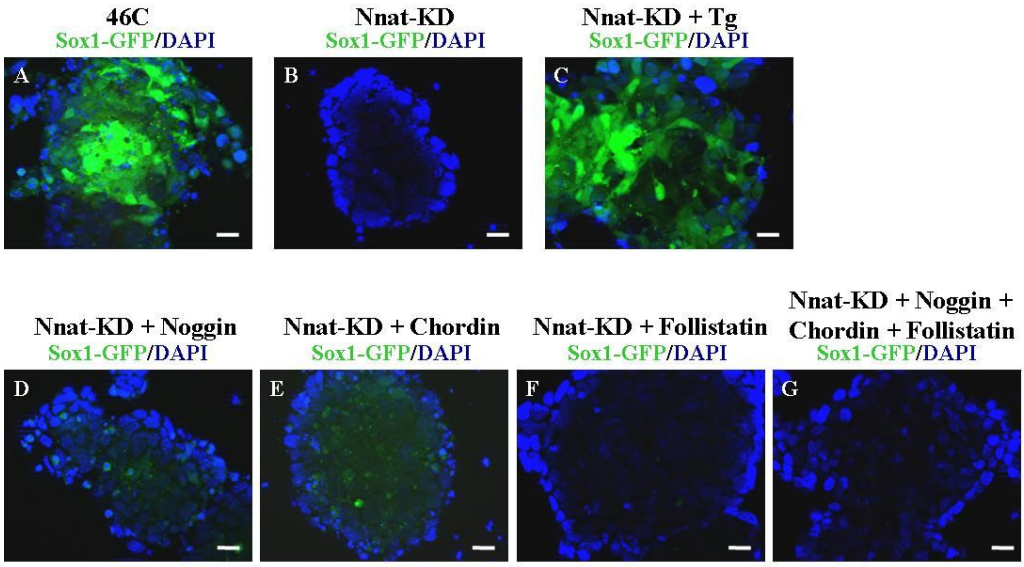

Fig. 5.11. BMP antagonists do not restore the ability of Nnat-KD ESCs to generate neuroectoderm.

46C and Nnat-KD ESCs were grown under differentiation conditions for four days and then were fixed to analyse the generation of Sox1-GFP$^+$ neuroectodermal cells. (A) After 4 days of differentiation, 46C ESCs generated Sox1-GFP$^+$ cells. (B) The generation of neuroectodermal cells was significantly reduced in Nnat-KD ESCs. (C) 25 nM Tg was applied to Nnat-KD ESCs for 30 minutes on the first day of differentiation and this restored their ability to generate Sox1-GFP$^+$ cells. When Nnat-KD ESCs were exposed to (D) 200 ng/ml Noggin, (E) 300 ng/ml Chordin, or (F) 300 ng/ml Follistatin throughout the 4-day differentiation period, the generation of Sox1-GFP$^+$ cells was not regained. (G) Even Nnat-KD ESCs were cultured with a combination of 200 ng/ml Noggin, 300 ng/ml Chordin, and 300 ng/ml Follistatin; the ability of Nnat-KD ESCs to generate neuroectodermal cells was still not restored. Thus, simply inhibiting BMP signalling by BMP antagonists was not sufficient to cause neural induction in Nnat-KD ESCs. All nuclei were stained with DAPI (blue). Scale bar, 20 μm.

Abbreviations: BMP, Bone morphogenetic protein; DAPI, 4',6-diamidino-2-phenylindole; ESC, embryonic stem cell; GFP, green fluorescent protein; Nnat-KD, Nnat-knockdown; Sox1, SRY (sex determining region Y)-box 1; Tg, Thapsigargin.

5.3 Discussion

5.3.1 Summary of main findings

In summary, I have shown that activation of FGF/Erk signalling is required for the neural induction of mouse ESCs, and my work confirms that of others showing that inhibition of FGF/Erk signalling dramatically reduces the ability of ESCs to generate NSCs (Cohen et al., 2010; Tropepe et al., 2001). Nnat functions by increasing $[Ca^{2+}]_i$ (see section 4.2.3) which in turn causes activation of Erk signalling leading to neural induction, and this action of Nnat is a novel finding of my research. Furthermore, the treatment of mouse ESCs with BMP4 suppressed neural induction. The expression of *BMP4* and its target genes were found to be up-regulated by Nnat knocked-down, suggesting that Nnat may also promote neural induction by down-regulation of BMP transcription. However, the treatment of Nnat-KD ESCs with BMP antagonists did not rescue the generation of neuroectoderm. This result implies that the inhibition of BMP signalling alone is insufficient for neural induction to occur. In line with this, I suggest that Nnat may act not only by down-regulation of BMP transcription, but also by activating the Erk pathway to initiate neural induction in mouse ESCs.

5.3.2 The activation of Erk1/2 is crucial to FGF and Nnat induced neural induction of mouse ESCs

Mouse ESCs are derived from the ICM of the blastocyst of mouse embryos and *Fgf4* is expressed in the ICM (Blagovic et al., 2011; Niswander and Martin, 1992; Rappolee et al., 1994), suggesting that *Fgf4* is expressed in mouse ESCs too. Using real-time PCR, I have confirmed the expression of *Fgf4* by 46C, Nnat-KD, and Nnatα-OE ESCs, and no difference was observed in the expression levels of *Fgf4* in these three ESC types (see Appendix 6). Thus, although mouse ESCs were grown in differentiating conditions without the addition of exogenous FGFs, FGFs generated by ESCs were present in these cultures. As shown in section 5.2.1, the treatment of 46C ESCs with the FGFR inhibitor PD173074 significantly reduced the generation of NSCs from 46C ESCs, so FGF signalling is pivotal for the neural induction of wild type (Nnat intact)

mouse ESCs, confirming work published by Tropepe et al. (2001). Without the inhibition of FGF signalling, knocking down Nnat expression also reduces the generation of NSCs (see section 3.2.4), so both Nnat and FGF are required for the neural induction of mouse ESCs. Further, when Nnatα was over-expressed, ESCs exposed to the FGFR inhibitor still generated NSCs (see section 5.2.4), suggesting that the over-expression of Nnatα compensates for the loss of action of FGF during neural induction. In contrast, the activation of FGF signalling by treating Nnat-KD ESCs with FGF4 or FGF5 rescued the ability of Nnat-KD ESCs to generate NSCs (see section 5.2.2). These results suggest that Nnat and FGF act in parallel to promote neural induction, and Nnat and FGF can compensate for one another.

Tg (a specific inhibitor of Apt2a/SERCA) mimics the function of Nnat to increase $[Ca^{2+}]_{i,}$ and an increase in $[Ca^{2+}]_i$ leads to the activation of Erk1/2 in Nnat-KD ESCs (see section 5.2.4), so Nnat inhibits the Apt2a/SERCA to cause an increase in $[Ca^{2+}]_i$ which in turn activates Erk1/2. Further, the activation of Erk1/2 is required for neural induction, as the MEK inhibitor PD184352, which blocks the phosphorylation of Erk1/2 by MEK, suppresses neural induction in wild type, and Nnatα-OE ESCs (details see sections 5.2.1, and 5.2.4). However, the FGFR inhibitor PD173074 significantly reduces the generation of NSCs from wild type ESCs, but only partially reduces the generation from Nnatα-OE ESCs (see section 5.2.4). My data suggest that Nnat activates Erk1/2 to initiate neural induction in mouse ESCs, and the activation of Erk signalling is not via the activation of FGFR (Fig. 5.12). Thus the activation of Erk1/2 is crucial for FGF and Nnat induced neural induction, and Nnat may cooperate with FGF to activate Erk signalling in the neural induction of wild type ESCs *in vitro*.

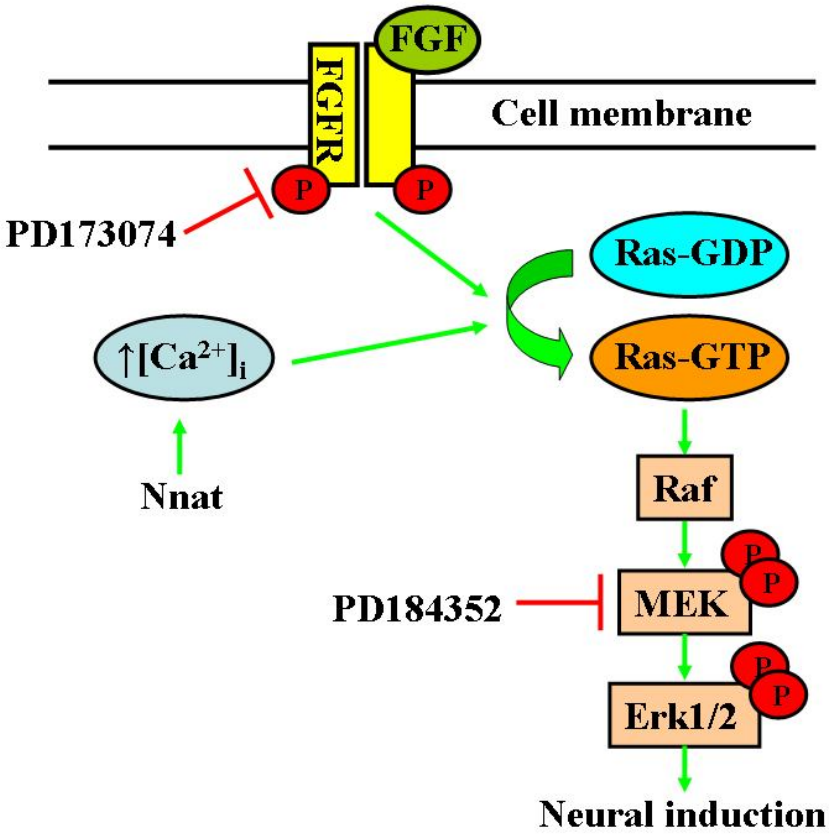

Fig. 5.12. The action of Nnat and FGF are parallel to activate Erk signalling in neural induction of ESCs.
In mouse ESCs, Nnat causes an increase in $[Ca^{2+}]_i$ which in turn activates Ras through the exchange of bound GDP for GTP. At the same time, the binding of FGF with FGFRs also activates Ras, and in turn Ras-GTP activates the Raf/MEK/Erk protein kinase cascade to promote neural induction. Either the treatment of ESCs with PD173074 (an inhibitor of FGFR) or Nnat knocked-down in ESCs significantly suppressed neural induction in ESCs. Thus both the action of Nnat and FGF are required for neural specification in wild type ESCs. When Nnatα was over-expressed in ESCs, the generation of NSCs was partially reduced by PD173074, but almost abolished by PD184352 (an inhibitor of MEK), suggesting that the action of Nnat and FGF act in parallel to activate Erk signalling causing neural induction of ESCs.
Abbreviations: Erk, Extracellular Signal-regulated Kinase; ESC, embryonic stem cell; FGF, Fibroblast growth factor; FGFR, FGF receptor; GDP, Guanosine diphosphate; GTP, Guanosine triphosphate; MEK, Mitogen-activated Protein/Extracellular Signal-regulated Kinase Kinase; NSC, neural stem cell.

The above discussion leads to the idea that in order to initiate neural induction, the level of p-Erk1/2 needs to reach a certain threshold. In wild type ESCs, both Nnat and FGF induce the phosphorylation of Erk1/2 (Fig. 5.12), enabling levels of p-ERK1/2 to reach the threshold needed to enable ESCs to generate neuroectodermal cells. When Nnat was knocked-down in ESCs, the generation of NSCs was significantly reduced (see section

3.2.4.2), suggesting that the p-Erk1/2 activated by FGF does not reach the required threshold. In contrast, when the action of FGF was blocked by PD173074, the formation of NSCs was also suppressed in wild type ESCs (see section 5.2.1), suggesting that the levesl of p-Erk1/2 activated by Nnat also does not reach the required threshold. Furthermore, the over-expression of Nnatα compensated for the loss of FGFR activation in PD173074 treated Nnatα-OE ESCs, resulting in neural specification of Nnatα-OE ESCs (see section 5.2.4). This result implies that even without the activation of FGFR, the levels of p-Erk1/2 generated by the over-expression of Nnatα is sufficient to reach the required threshold. Similarly, the treatment of Nnat-KD ESCs with FGF4 also compensated for the Nnat knock-down inducing the generation of NSCs (see section 5.2.2), suggesting that even without the action of Nnat, the levels of p-Erk1/2 caused by the presence of exogenous FGFs again reached the required threshold for neural induction. If the hypothesis that p-Erk1/2 needs to reach a certain threshold for neural induction to occur is correct, then an increase in p-Erk1/2 should also induce neural induction. The binding of IGF2 (insulin-like growth factor 2) to its receptor activates the Raf/MEK/Erk protein kinase cascade (Desbois-Mouthon et al., 2006). The injection of *Xenopus* embryos with IGF2 increased p-Erk1/2 and also induced the ectopic neural tissue (Pera et al., 2003). This result fits with my hypothesis, but further confirmation is still required. For example, Nnat-KD ESCs could be treated with different concentrations of FGF4 and the levels of p-Erk1/2 evaluated using immunoblotting. If the hypothesis is true, then the treatment of Nnat-KD ESCs with FGF4 will induce the generation of NSCs after p-Erk1/2 passes certain level.

5.3.3 Nnat may down-regulate the expression of *BMP* and activate Erk signalling to facilitate the generation of neuroectoderm from mouse ESCs

When mouse ESCs were exposed to BMP4, the generation of neuroectoderm was reduced (see section 5.2.5). Thus my work confirms previous reports that the activation of BMP signalling inhibits neural induction in ESCs (details see section 1.6; Finley et al., 1999; LaVaute et

al., 2009; Stavridis et al., 2007; Tropepe et al., 2001). Conversely the inhibition BMP signalling is required for neural induction (see sections 1.2 and 1.3). As shown in section 5.2.5, Nnat may down-regulate the expression of *BMP4* and its target genes, *Msx1* and *Msx2*. However, using BMP antagonists, such as Noggin, Chordin, and Follistatin, to inhibit BMP signalling did not restore the ability of Nnat-KD ESCs to generate neuroectodermal cells (see section 5.2.7). Therefore, as well as down-regulating the expression of *BMP*, Nnat must also affect other signals to initiate neural induction. I have shown that Nnat physically interacts with Apt2a/SERCA and inhibits Apt2a/SERCA pumping cytosolic Ca^{2+} into the ER, and thus causes an increase in $[Ca^{2+}]_i$ (see sections 4.2.1, 4.2.2, and 4.2.3). An increase in $[Ca^{2+}]_i$ activates Erk signalling (see section 5.2.4) and the activation of Erk signalling is essential for neural induction of mouse ESCs (see section 5.2.1). Therefore, Nnat, via its ability to elevate $[Ca]_i$, activates the instructive Erk signal to facilitate the generation of neuroectodermal cells from mouse ESCs.

Therefore, it appears that these positive (such as FGF/Erk and Nnat) and negative (such as BMP) signals compete with each other to decide the lineage fates of mouse ESCs. When wild type ESCs were exposed to BMP4, to repress neural induction, the generation of NSCs was significantly reduced (see section 5.2.5). However, this suppressive effect of BMP4 on neural induction was partially reversed when the positive cue Nnat is augmented. For example, when Nnatα was over-expressed in ESCs, the treatment of Nnatα-OE ESCs with BMP4 could not completely inhibit the generation of NSCs from Nnatα-OE ESCs (see section 5.2.5). This result suggests that increasing expression of a positive cue (Nnat) can push ESCs towards a neural fate even in the presence of a negative signal (BMP). However, the popular 'default model' for neural induction proposes that ectodermal cells give rise to neural cells autonomously in the absence of BMP activation (details see section 1.3). My observation that Nnatα-OE ESCs still generate neural cells in the presence of BMP4 does not fit with the default model.

If the default model is correct, then the process of neural induction should not need any positive cue in the absence of BMP activation. Thus the treatment of Nnat-KD ESCs with BMP antagonists should let ESCs take up their default fate - to differentiate into neural cells. My observation that such treatments did not induce the generation of neuroectoderm from Nnat-KD ESCs contradict this assumption (see section 5.2.7). Certainly, neural induction is not as simple as the default model implies. The insufficiency of the default model is also raised by many other studies (details see section 1.5), suggesting that in addition to the inhibition of the negative signal (BMP), positive cues are required (such as FGF/Erk and Nnat) to let the neural induction occur.

5.3.4 The activation of Erk signalling may not inhibit C-ter-p-Smad1 in mouse ESCs

As discussed in section 1.5.1.4, BMP signalling is inhibited by Erk signalling in *Xenopus* neural induction. The activation of BMP signalling causes the phosphorylation of Smad1 at its C-terminus and the resulting C-ter-p-Smad1 is translocated into the nucleus where it activates epidermal genes, such as *Msx1*, *Cytokeratin*, and *Vent2* (Pera et al., 2003). The activation of Erk signalling phosphorylates C-ter-p-Smad1 at a linker region to induce degradation of C-ter-p-Smad1, which results in the inhibition of BMP signalling facilitating neural induction (Fuentealba et al., 2007; Kuroda et al., 2005). Furthermore, it has been demonstrated that the same interaction between C-ter-p-Smad1 and p-Erk1/2 occurs in mouse and human cell lines (Aubin et al., 2004; Fuentealba et al., 2007; Kretzschmar et al., 1997; Sapkota et al., 2007). Therefore Nnat-mediated Erk signalling may also suppress the C-ter-p-Smad1 to inhibit BMP signalling in mouse ESCs.

In this chapter, I have demonstrated that Tg can induce the phosphorylation of Erk1/2 in Nnat-KD ESCs (see section 5.2.4), but the results shown in section 5.2.6 revealed that the activation of Erk1/2 by the treatment of Nnat-KD ESCs with Tg did not reduce the C-ter-p-Smad1. Although C-ter-p-Smad1 is not reduced, it does not mean that the linker

region of C-ter-p-Smad1 is not phosphorylated by p-Erk1/2. To clarify this, I have tried to determine whether the activation of Erk signalling caused the phosphorylation of Smad1 at the linker region. If the linker region is phosphorylated by p-Erk1/2, then the Linker-p-Smad1 should be increased after Tg treatment. Linker-p-Smad1 was analysed by Western blotting using an anti-Linker-p-Samd1 antibody, but I failed to identify this protein because there was no specific band in my immunoblotting analysis. Because I did not have a suitable positive control for the expression of Linker-p-Samd1, it was possible that the anti-Linker-p-Samd1 antibody used in immunoblotting was not good enough to detecting Linker-p-Samd1. Thus, at present, it is not clear whether or not the linker region of Smad1 is phosphorylated by p-Erk1/2 in mouse ESCs.

Studies in HEK293 cells have shown that when the linker region is phosphorylated by p-Erk1/2, C-ter-pSmad1 is inactivated through polyubiquitination or interaction with Smurf1 that C-ter-pSmad1 is kept in the cytosol and not degraded immediately (Sapkota et al., 2007). Although my data did not show that the activation of Tg-mediated Erk signalling reduced C-ter-p-Smad1 (see section 5.2.5), the cytosolic retention of C-ter-p-Smad1 could not be ruled out. To solve this problem, subcellular fractionation could be used to separate the cytosolic and nuclear fractions from the whole cell lysate. Because C-ter-p-Smad1 will relocate to nucleus to activate target genes, the C-ter-p-Smad1 in the nuclear fraction could be considered as the active form. In my experiments, I analysed the C-ter-p-Smad1 using whole cell lysate, so I could not determine the proportion of nuclear to cytosolic C-ter-p-Smad1. If the C-ter-p-Smad1 is just retained in the cytosol after the phosphorylation of linker region, the amount of C-ter-p-Smad1 in whole cell lysate will not be changed so there will be no observable differences between Tg-treated ESCs and no Tg treatment. Using the subcellular fractionation techniques, the proportion of C-ter-p-Smad1 in the nuclear fraction will be detected. If it is the case that the activation of Tg-mediated Erk signalling decreases the proportion of C-ter-p-Smad1 in the nuclear fraction and increases C-ter-p-Smad1 in the

cytosolic fraction, then the activation of Tg-mediated Erk signalling may inactivate C-ter-p-Smad1 by cytosolic retention.

5.3.5 What are the downstream target genes activated by p-Erk1/2 in neural induction?

The activation of Erk signalling is pivotal for the neural induction of mouse ESCs, but most of its downstream target genes are still unknown. Erk1/2 is a protein kinase and the active form (p-Erk1/2) will physically interact with various transcription factors, such as NF-κB, Bcl2, cAMP-responsive element-binding protein, GATA, GAB, c-Myc, Ets, AP1, and Sp1, and in turn these transcription factors activate different genes (Chang et al., 2003; Chotteau-Lelievre et al., 2001; Dajee et al., 2003; Karin, 1995; Liu et al., 2005; Milanini-Mongiat et al., 2002; Pages, 2007; Yeh et al., 2004; Ying et al., 2002), but which transcription factors are responsible for up-regulating genes to initiate neural induction still needs to be elucidated.

Recently, Yoo et al. (2011) found that the poly (ADP-ribose) polymerase 1 (PARP-1), which modifies nuclear proteins by polymerization of ADP-ribose units, is a substrate for p-Erk1/2 and is responsible for neural specification of human ESCs. It has been demonstrated that PARP-1 is directly phosphorylated by p-Erk1/2 (Kauppinen et al., 2006), and the activity of PARP-1 is increased during human ESCs neural differentiation, and reduced by treatments with the FGFR inhibitor SU5402, the MEK inhibitor U0126, or the PARP-1 specific inhibitor PJ34 (Yoo et al., 2011). The treatment of ESCs with PJ34 significantly reduced the generation of SOX2 or PAX6-expressing neural progenitors, suggesting that the activation of PARP-1 promotes neural induction in human ESCs. Using chromatin immunoprecipitation analysis, the promoter region of PAX6 was observed in the precipitated chromatin DNA using a anti-PARP-1 antibody (Yoo et al., 2011), suggesting that the PARP-1 is involved in the activation of PAX6. Thus Erk/PARP-1 signalling is involved in neural induction of human ESCs, but this does not rule out the possibility that other p-Erk1/2 substrates are also involved in the process of neural

induction. For example, Erm is a transcription factor of the Ets family (substrate of p-Erk1/2) and is expressed in the neural plate of mouse and chicken embryos (Chotteau-Lelievre et al., 2001; Stavridis et al., 2007). It has been shown that Erm is involved in the neuronal fate decision of neural crest stem cells (Paratore et al., 2002), but it is unknown whether Erm is required in neural induction. Similarly Sp1, another substrate of p-Erk1/2, is expressed in neuroectoderm, hematopoietic cells, and giant trophoblast cells of mouse embryos at 8.5 dpc (Saffer et al., 1991). The human early neural marker *SOX3* and mouse *Sox2* promoters contain binding sites for Sp1 (Archer et al., 2010; Kovacevic Grujicic et al., 2005; Wiebe et al., 2000), and Sp1 is also a positive regulator of the NSC marker *Nestin* in mouse (Cheng et al., 2004). Therefore, FGF/Erk signalling may cause the phosphorylation of Sp1 that in turn activates *Sox2* and *Nestin* to promote neural induction, but more experiments are needed to verify this.

Chapter 6. Discussion

6.0 Discussion

6.1 Summary of main findings

This thesis focused upon elucidating the role of Nnat in the neural induction; using mouse ESCs as a model system in conjunction with loss- and gain-of-function approaches. I found that Nnat was expressed in neuroectodermal cells, neural progenitors, and neurons during ESCs neural differentiation (see section 3.2.2, Fig. 3.2 and 3.3), suggesting that Nnat may play a role in neural development. This hypothesis was confirmed since Nnat-OE ESCs generated an excess of NSCs and neurons (see section 3.2.3, Fig. 3.5 and 3.6), while Nnat-KD ESCs generated significantly fewer neuroectodermal cells, NSCs, and subsequently neurons (see section 3.2.4.2, Fig. 3.8). These results implied that Nnat was required for neural induction in mouse ESCs. However, these observations could not be explained by Nnat-KD ESCs simply failing to differentiate efficiently into any of the three primary germ layers (see section 3.2.6, Fig. 3.11), rather that these ESCs did not give rise to neuroectodermal cells efficiently. Indeed, when mouse *Nnat* mRNA was injected into *Xenopus* embryos, the domain of neural plate marker *NCAM*-expressing cells was expanded and similarly, in animal cap assays, the expression of the neural plate marker *Nrp1* was up-regulated (see section 3.2.7, Fig. 3.13), suggesting that the neural inductive effect of Nnat is conserved in *Xenopus* and mouse ESCs.

At the amino acid level Nnat shows 50% homology with Phospholamban (an inhibitor of Apt2a/SERCA) and this suggests that Nnat may act to increase $[Ca^{2+}]_i$ by inhibiting the action of Apt2a/SERCA, a Ca^{2+} ATPase located in the membrane of ER that transports cytosolic Ca^{2+} into the ER to decrease $[Ca^{2+}]_i$ (see section 1.7.2). Further to this, I demonstrate that Nnat physically interacts with Apt2a2/SERCA2 (see section 4.2.1.2). Apt2a2/SERCA2 was the member of Apt2a/SERCA family which was most highly expressed in mouse ESCs and during differentiation along the neural pathway (see section 1.7.2, Fig. 1.15). If Nnat inhibits the pumping of cytosolic Ca^{2+} into the ER by Apt2a2/SERCA2, then the consequences of Nnat binding to Apt2a2/SERCA2 should increase cytosolic Ca^{2+}. As expected the $[Ca^{2+}]_i$ in Nnat-OE ESCs was higher than in wild type and Nnat-KD ESCs (see section

4.2.2, Fig. 4.4). This assumption was also confirmed using the specific inhibitors of Apt2a/SERCA (Tg and BHQ), by reasoning that if Nnat inhibits Apt2a2/SERCA2 to cause an increase in $[Ca^{2+}]_i$, then these inhibitors should mimic the action of Nnat - cause an increase in $[Ca^{2+}]_i$ (see section 4.2.3.1, Fig. 4.5) and restore the ability of Nnat-KD cells to generate NSCs and subsequently neurons. Indeed, this was shown to be the case (see section 4.2.3.2, Fig. 4.6 and 4.7). Together these observation indicated that Nnat inhibits the Apt2a2/SERCA2 to cause an increase in $[Ca^{2+}]_i$ and this in turn induces neural specification. Prior to my experiments, there is no data of the role of Ca^{2+} in neural induction of higher vertebrates. My data is the first to reveal that Nnat causes an increase in $[Ca^{2+}]_i$ of mouse ESCs and this is required for neural induction in mouse ESCs. I also showed that the converse was true, namely that preventing the increase in $[Ca^{2+}]_i$ of wild type ESCs using BAPTA-AM (a membrane permeable calcium chelator) suppressed the ability of these ESCs to generate neuroectodermal cells (see section 4.2.4, Fig. 4.8). Thus, an increase in $[Ca^{2+}]_i$ is required for neural induction in mouse ESCs and this increase in $[Ca^{2+}]_i$ is brought about by the action of Nnat.

I have shown that the main function of Nnat in neural induction is to increase $[Ca^{2+}]_i$, the next step was to try and identify the downstream consequences of this increase in $[Ca^{2+}]_i$ in relation to neural development. Since the treatment of Nnat-KD ESCs with the Atp2a/SERCA inhibitor Tg caused an increase in $[Ca^{2+}]_i$ and also activated Erk1/2 (see sections 1.5.4.3 and 5.2.4, Fig. 5.6), it is feasible that this kinase may act downstream of Nnat. In fact, the activation of Erk signalling in Nnat-KD ESCs using FGF4 or FGF5 also rescued the generation of NSCs and neurons (see section 5.2.2, Fig. 5.3 and 5.4). However, when Erk signalling was inhibited by PD184352 (a MEK inhibitor), the treatment of Nnat-KD ESCs with Tg could no longer rescue the generation of neural cells (see section 5.2.3, Fig. 5.5). Thus, this result is due to the fact that an increase in $[Ca^{2+}]_i$ activates Erk signalling to induce neural specification in mouse ESCs. Furthermore, the activation of BMP signalling inhibited neural induction in mouse ESCs (see section 5.2.5, Fig. 5.8) and the expression of *BMP4* and its target genes was increased in

Nnat-KD ESCs compared with wild type and Nnat-OE ESCs (see section 5.2.6, Fig. 5.9), suggesting that Nnat may down-regulate BMP signalling.

In summary, my thesis described a novel function for Nnat in regulating neural induction in mouse ESCs. To do this, Nnat may not only down-regulate BMP signalling, but also antagonise the action of Apt2a/SERCA to cause an increase in $[Ca^{2+}]_i$ which in turn activates Erk signalling to help mouse ESCs give rise to neuroectodermal cells and neural progenitor cells. Nnat plays a pivotal role in enabling ESCs to differentiate along a neural lineage.

6.2 The regulation of Nnat expression

Since Nnat has a crucial role in neural development, how the expression of Nnat is regulated will be interesting. The promoter region of *Nnat* contains the neuron-restrictive silencer element (Dou and Joseph, 1996) that could bind the neuron-restrictive silencer factor and inhibit the expression of pro-neural genes in non-neural cells (Bessis et al., 1997; Chen et al., 1998). This may be the reason that the expression of *Nnat* was sustained in developing neural tissue and suppressed in most non-neural tissue. In addition, *Nnat* is a maternal imprinted gene and the maternal origin-specific DNA of *Nnat* is methylated throughout embryonic development (John et al., 2001; Kagitani et al., 1997). Thus, DNA methylation and the neuron-restrictive silencer factor could act to restrict the expression of *Nnat*.

Another transcription factors that could influence Nnat expression is NeuroD1, a basic helix-loop-helix transcription factor (Poulin et al., 1997), expressed in central nervous system and pancreas of the mouse embryo (Lee et al., 2000a). The binding of NeuroD1 to the promoter region of *Nnat* has been demonstrated in pancreatic β-cells using chromatin immunoprecipitation analysis, and the expression of *Nnat* was decreased in *NeuroD1* null mutants (Chu and Tsai, 2005), suggesting that the transcription factor NeuroD1 bound to the promoter of *Nnat* and activated the transcription of *Nnat*. However, at present, NeuroD1 is the only known

transcription factor to up-regulate *Nnat* expression. Using bio-informatics analysis, Li et al. (2010) found some possible transcription factors (*PPARγ, Rreb1, Klf15, Irf1, Krox20, Gata3, Mlxipl, Srebp1c, Foxo1,* and *Tcf7l2*) with binding sites in the promoter of *Nnat* but whether these actually influence Nnat expression has yet to be confirmed. Interestingly, the involvement of *PPARγ, Klf15, Krox20, Gata3, Foxo1,* and *Tcf7l2* in neural development had been reported (Cho and Dressler, 1998; Giudicelli et al., 2001; Ohtsuka et al., 2011; Paik et al., 2009; Pandolfi et al., 1995; Wada et al., 2006).

PPARγ is highly expressed in the embryonic mouse brain and NSCs (Wada et al., 2006). Knocking down the expression of *PPARγ* in mouse NSCs decreased the generation of neurospheres and the treatment of NSCs with an antagonist of PPARγ induced apoptosis (Wada et al., 2006). In contrast, the treatment of NSCs with an agonist of PPARγ increased the generation of neurospheres (Wang et al., 2009), suggesting that PPARγ activation increased the proliferation of NSCs. *Klf15* is expressed in the ventricular zone of the telencephalon at 11.5-17.5 dpc, and *Klf15* knockdown in NSCs promoted neuronal differentiation, suggesting that Klf15 was involved in the self-renewal of NSCs (Ohtsuka et al., 2011). *Krox20* is expressed in the hindbrain of mouse and chick embryos, and plays a crucial role in the segregation of embryonic hindbrain (Giudicelli et al., 2001; Graham and Lumsden, 1996). *Gata3* was expressed in the central nervous system, somites and embryonic kidney of mammalian embryo (Debacker et al., 1999; George et al., 1994). Although the *Gata3* knockout was lethal and embryos died at 11 dpc, the *Gata3* null mutant showed a reduced thickness of the neuroepithelium and a distorted neural tube (Pandolfi et al., 1995), suggesting the involvement of *Gata3* in neurogenesis. *Foxo1* was expressed in the developing mouse brain and the dentate gyrus of the hippocampus (Hoekman et al., 2006). *Foxo1* was shown to be involved in the cellular proliferation, differentiation, and oxidative defense of NSCs (Paik et al., 2009). *Tcf7l2* is a Wnt signalling related gene that is highly expressed in the developing CNS and limb buds (Cho and Dressler, 1998), suggesting that Tcf7l2 may play a role in neural and limb development.

In summary, transcription factors - neuron-restrictive silencer factor, PPARγ, Klf15, Krox20, Gata3, Foxo1, and Tcf7l2, may be involved in the regulation of the transcription of *Nnat* during neural development. In order to validate the interaction of the above transcription factors with the *Nnat* promoter a Luciferase assay could be used to test whether the expression of Nnat is activated or suppressed by these transcription factors.

6.3 Nnat is a positive instructive cue for neural induction of mouse ESCs

The data presented in sections 3.2.4 and 3.2.7 revealed that Nnat is required for neural induction in mouse ESCs and can enhance the neural specification of embryonic ectoderm in *Xenopus*. Thus, Nnat can be considered as a positive instructive cue for neural induction. Furthermore, it has been demonstrated that FGFs also have the ability to induce neural induction in *Xenopus*, chick, and mouse (see sections 1.5.1). For instance, the injection of *Fgf8* mRNA into *Xenopus* embryos induced the generation of ectopic neural tissue (see section 1.5.1.1; Pera et al., 2003), and the implantation of FGF4 soaked beads into the prospective non-neural ectoderm of the chick embryos induced the formation of ectopic neural tissue (section 1.5.1.1; Rodriguez-Gallardo et al., 1997). During gastrulation, the injection of FGF8b into mouse embryos promoted the generation of NSCs (Dang and Tropepe, 2010). Therefore, both Nnat and FGF are positive instructive cues for neural induction. Using a microfluidic system to remove autocrine or paracrine FGF4 from the culture medium, the ability of mouse ESCs to generate neuroectodermal cells was suppressed, suggesting that FGF4 acts as the autocrine or paracrine signalling to help ESCs neural specification (Blagovic et al., 2011). Although Nnat is not a secretory protein (Dou and Joseph, 1996; Joe et al., 2008), my data revealed that Nnat was expressed in cells that belong to the neural lineage when mouse ESCs differentiate along a neural differentiation pathway (see section 3.2.2). These findings suggested that Nnat initiates neural development of mouse ESCs internally. Thus, Nnat and FGF are intrinsic and extrinsic factors of neural induction in mouse ESCs respectively.

My research suggests that Nnat causes an increase in $[Ca^{2+}]_i$ via its ability to inhibit the action of Apt2a2/SERCA2 (see sections 4.2.1, 4.2.2, and 4.2.3). The increase in $[Ca^{2+}]_i$ is a positive instructive cue for neural induction in *Xenopus* embryos (see section 1.5.4.1; Batut et al., 2005; Leclerc et al., 2003; Moreau et al., 2008). Although the role of Ca^{2+} in neural induction of mammals is unknown, my data revealed that Nnat and an increase in $[Ca^{2+}]_i$ were required for neural induction in mouse ESCs (see sections 3.2.4 and 4.2.4). Therefore, an increase in $[Ca^{2+}]_i$ may be also a positive cue for neural induction in mammals. In addition, my results revealed that an increase in $[Ca^{2+}]_i$, induced by Tg treatment, in mouse ESCs activated Erk signalling (see section 5.2.4). A similar finding has been reported in other cells where an increase in $[Ca^{2+}]_i$ activates RasGRP, and in turn activates Ras and the Raf/MEK/Erk protein kinase cascade (details see section 1.5.4.3; Denys et al., 2004; Kupzig et al., 2005; Riddle et al., 2006). Therefore it seems a reasonable assumption that Nnat increases $[Ca^{2+}]_i$ and activates Erk signalling through this pathway.

Furthermore, Erk is the effector of FGF signalling and FGF/Erk signalling is important for neural induction in vertebrates (see section 1.5.1.3; Kuroda et al., 2005; Stavridis et al., 2007; Yoo et al., 2011). Thus, these positive instructive cues (Nnat, an increase in $[Ca^{2+}]_i$, and FGF) activate Erk signalling to promote neural induction. My work also confirmed that from other laboratories showing that inhibition of Erk signalling dramatically reduces the ability of ESCs to generate NSCs (see sections 5.2.1 and 5.2.4; Cohen et al., 2010; Stavridis et al., 2007; Tropepe et al., 2001). Therefore, the activation of Erk signalling is important for these positive instructive cues in neural induction.

6.4 Challenge of default model of neural induction

According to the results of experiments investigating neural induction in amphibians, the default model was proposed to explain the molecular mechanisms of neural induction (for details see section 1.2 and 1.3). This popular model suggests that, in the absence of BMP signalling, ectodermal

cells autonomously give rise to neuroectoderm (Hemmati-Brivanlou and Melton, 1997a). However, I have shown that the expression of Nnat is required for neural induction in mouse ESCs (see section 3.2.4). The formation of neuroectodermal cells was significantly reduced in Nnat-KD ESCs and this reduction was not due to the inability of Nnat-KD ESCs to generate ectodermal cells (see section 3.2.6). Thus, Nnat was needed during the differentiation of ectodermal cells into neuroectodermal cells. Further, when Nnat-KD ESCs were cultured with BMP antagonists, the ability of Nnat-KD ESCs to generate neuroectodermal cells was not restored (see section 5.2.7). Thus, even in absence of BMP signalling, Nnat-KD ESCs do not give rise to neural cells autonomously. Therefore, neural induction in mouse ESCs requires not only the inhibition of BMP signalling, but also other signals, at least one of which is the instructive cue Nnat.

In addition to Nnat, I showed that inhibiting FGFR function in wild type ESCs suppressed the formation of neuroectodermal cells (see section 5.2.1), suggesting that the activation of FGF is required for the process of neural specification in mouse ESCs. Similar findings were also noted in vertebrate embryos (see section 1.5.1.2). For example, when *Xenopus* embryos were cultured with the FGFR inhibitor (SU5402), the generation of the neural plate marker *NCAM*-expressing cells was inhibited (Delaune et al., 2005). Further to this, I also showed that preventing an increase in $[Ca^{2+}]_i$ in mouse ESCs using the membrane permeable calcium chelator (BAPTA-AM) also suppressed the generation of neuroectodermal cells (see section 4.2.4). Similarly, the treatment of *Xenopus* embryos with an L-type calcium channel blocker, R(+)BayK, to prevent the increase in $[Ca^{2+}]_i$ suppressed neural induction (see section 1.5.4.2). Thus the instructive cues Nnat (via its ability to increase $[Ca^{2+}]_i$) and FGF are pivotal for neural induction in mouse ESCs, showing that the default model of neural induction is far too simple.

However, the default model does provide an important insight into one important molecular mechanism required for neural induction, that being, the inhibition of BMP signalling. For example, electroporation of the prospective neural ectoderm of chick embryos with *BMP4* inhibited the

expression of the neural plate markers *Sox2* and *Sox3* (Linker and Stern, 2004), suggesting that the activation of BMP signalling repressed the neural specification of ectodermal cells. Similarly, within my thesis, I have shown that exposure of mouse ESCs to BMP4 suppressed the generation of neuroectodermal cells (see section 5.2.5) and treatment of Nnat-KD ESCs with BMP antagonists did not rescue the ability of Nnat-KD cells to generate neuroectodermal cells (see section 5.2.7). Thus simply inhibiting BMP signalling is not enough to induce the neural specification of Nnat-KD ESCs. BMP antagonists have also been shown to be unable to induce the generation of neural tissue in the prospective non-neural ectoderm of chick embryos (see section 1.5.1; Streit et al., 1998). However, when FGF8 and Chordin (a BMP antagonist) were applied to the prospective non-neural ectoderm of chick embryos together, the neural plate markers *ERNI* and *Sox3* were induced (Stern, 2005). This leads to the idea that the inhibition of BMP signalling only makes ectodermal cells competent to differentiate into neural cells and a further instructive cue, such as FGF, Nnat, and calcium, is required to commit ectoderm to a neuroectodermal fate.

6.5 There is competition between neural and non-neural fates

As shown in section 3.2.3.2, over-expression of Nnat in mouse ESCs promoted neural specification, suggesting that Nnat is a positive cue in neural induction. However, the exposure of mouse ESCs to BMP4 inhibited the generation of NSCs (see section 5.2.5). When Nnatα was over-expressed in mouse ESCs, the treatment of BMP4 could not completely inhibit the generation of Sox1-expressing neuroectodermal cells (see section 5.2.5). This result suggests that the over-expression of the positive cue, Nnat, overcomes the negative cue BMP4 to allow mouse ESCs to differentiate into neural cells. Thus the positive and negative signals compete with each other to determine the lineage differentiation of mouse ESCs. Similarly, animal caps of *Xenopus* embryos consist of ectodermal cells that express BMP4 causing the animal caps to take up an epidermal fate rather than a neural fate (Hemmati-Brivanlou and Melton, 1997b; Wilson et al., 1997). However, the injection of mouse *Nnat* into *Xenopus* embryos increased the expression of the neural plate marker *Nrp1* in animal caps (see section 3.2.7), again

suggesting that the positive cue, Nnat, overrides the negative cue, BMP4, in *Xenopus* ectoderm. The above findings lead to the idea that neural induction in mouse ESCs is like a seesaw: when positive signals are greater than negative signals, then ectodermal cells differentiate along a neural fate. In contrast, if negative signals are greater than positive signals, then cells differentiate along a non-neural fate.

In addition to the BMP signalling, the activation of Wnt or Activin/Nodal signalling in the ectoderm of vertebrates represses the generation of neuroectodermal cells (see sections 1.4, 1.5.2, and 1.5.3). For example, when *Smad2* mRNA was injected into *Xenopus* embryos to activate Activin/Nodal signalling, the expression of the neural markers *Sox2* and *Sox3* in the neural plate was inhibited (Chang and Harland, 2007). Similarly, during ESCs differentiation, the activation of BMP, Wnt, or Activin/Nodal signalling also suppressed the generation of neural progenitors (see section 1.6.2; Aubert et al., 2002; Chambers et al., 2009; Gerrard et al., 2005; LaVaute et al., 2009). These findings show that Wnt, or Activin/Nodal signalling as well as BMP signalling can act as negative cues to repress the neural induction. Conversely, as mentioned above, Nnat, an increase in $[Ca^{2+}]_i$, and FGF act as positive cues to promote neural specification of vertebrate ectodermal cells. In considering how these positive and negative signallings interact, some research provides evidence in that field (Fuentealba et al., 2007; Kuroda et al., 2005; Pera et al., 2003). For instance, the prospective non-neural ectoderm in *Xenopus* expresses BMP4 which activates the intracellular mediator Smad1, and target genes *Msx1* and *Msx2*, resulting in the ectodermal cells giving rise to epidermal cells (Hemmati-Brivanlou and Melton, 1997a; Khadka et al., 2006; Kretzschmar et al., 1997b; Suzuki et al., 1997). When *Fgf8* mRNA was injected into *Xenopus* embryos, ectopic neural tissue was generated from the prospective non-neural ectoderm (details see section 1.5.1.4; Kuroda et al., 2005; Pera et al., 2003). The result suggests that the negative cue (endogenous BMP4) is overwhelmed by the positive cue (exogenous *Fgf8*) in ectodermal cells so the cells go on to adopt a neural fate.

Within Chapter 5, I showed that Nnat may down-regulate the expression of *BMP4* and its target genes *Msx1* and *Msx2* in mouse ESCs (see section 5.2.5). Nnat also antagonised the action of Apt2a2/SERCA2 to cause an increase in $[Ca^{2+}]_i$ of ESCs (see sections 4.2.1 and 4.2.2). The increase in $[Ca^{2+}]_i$ of ESCs is a positive neural inductive cue and activates Erk signalling (see section 5.2.4) to promote neural specification in mouse ESCs. Thus, Nnat may not only down-regulate the BMP signalling a negative cue, but also enhance the positive cues (Calcium and Erk signalling) to initiate neural induction in mouse ESCs. Thus positive and negative cues must interact during neural induction. For example, during *Xenopus* gastrulation, ectodermal cells generate BMP4 which causes the phosphorylation of Smad1 at the C-terminus, and the C-ter-p-Smad1 goes on to activate target genes, such as *Msx1*, *Msx2*, and *Vent2* which inhibit neural induction (Fig. 6.1; for details see section 1.5.1.4; Pera et al., 2003; Phippard et al., 1996; Suzuki et al., 1997). FGF/Erk signalling is active in the prospective neural ectoderm (Christen and Slack, 1999), and activated Erk1/2 phosphorylates the linker region of Smad1 to suppress the action of Smad1 and promote neural induction in *Xenopus* (Pera et al., 2003). Therefore, the positive cue FGF/Erk signalling suppresses the negative cue BMP signalling to induce the neural specification of ectodermal cells in *Xenopus* embryos (Fig. 6.1). Similarly, the linker region of Smad1 contains the phosphorylation site of GSK3 (Glycogen synthase kinase 3) and the phosphorylation of Smad1 by GSK3 induces polyubiquitinylation and a decrease in Smad1 activity in *Xenopus* embryos (Fuentealba et al., 2007). Because the activity of GSK3 is reduced by Wnt3a, the BMP-mediated Smad1 activation can be prolonged by activation of Wnt signalling (Fuentealba et al., 2007; McManus et al., 2005). Thus the negative cues, Wnt and BMP signalling, work together to suppress neural induction in *Xenopus* (Fig. 6.1). In my study, I found that both Nnat and FGF are positive cues for neural induction in mouse ESCs because loss of the action of either Nnat or FGF significantly reduced the generation of NSCs from ESCs (see sections 3.2.4 and 5.2.1). As shown in sections 4.2.2, and 5.2.4, Nnat caused an increase in $[Ca^{2+}]_i$ in ESCs, resulting in activation of Erk1/2 and inhibition of BMP signalling to promote neural induction. Furthermore, my results (see section 5.2.1) and a previous

report (Stavridis et al., 2007) showed that the activation of FGF/Erk signalling is required for neural induction in mouse ESCs. Thus the positive cues Nnat and FGF activate Erk signalling and allow neural induction to occur (Fig. 6.1).

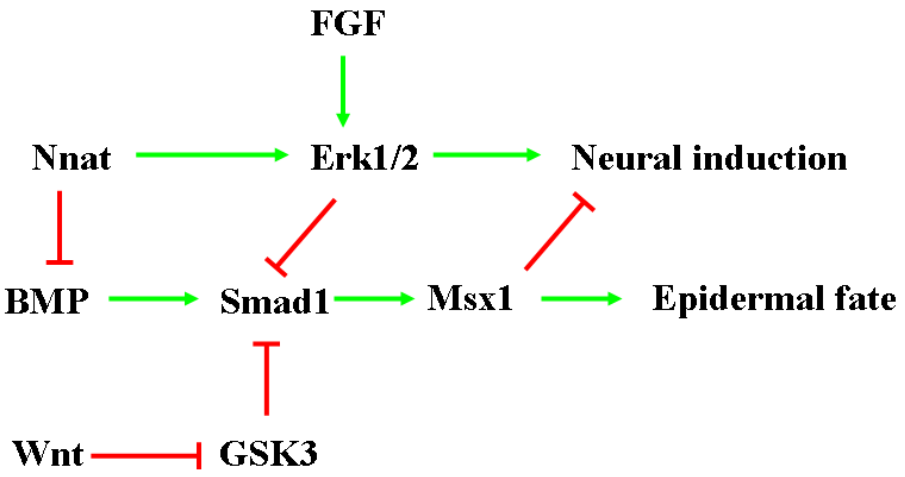

Fig. 6.1. Schematic representation of the positive and negative cues in neural induction.
The negative cue BMP induces the phosphorylation of Smad1 at C-terminus and in turn activates the target gene Msx1 to promote an epidermal fate and inhibit neural induction. The positive cue FGF activates Erk1/2 and induces neural induction. Both active Erk1/2 and GSK3 phosphorylate Smad1 at linker region to cause the polyubiquitinylation of Smad1 and inhibits the epidermal development. The activation of Wnt signalling inhibits GSK3 and prolongs the action of Smad1 to promote epidermal development, suggesting that Wnt is a negative cue for neural induction. Nnat not only suppresses the expression of BMP4 and Msx1, but also cause an increase in $[Ca^{2+}]_i$ to activate Erk1/2. Thus Nnat is a positive cue for neural induction.
Abbreviations: BMP, Bone morphogenetic protein; $[Ca^{2+}]_i$, concentration of cytosolic Ca^{2+}; Erk1/2, Extracellular Signal-regulated Kinase 1/2; FGF, Fibroblast growth factor; GSK3, Glycogen synthase kinase 3.

The exposure of human ESCs to FGF2 and SB431542 (an inhibitor of Activin/Nodal signalling) induced the generation of neuroectodermal cells, and conversely exposure of human ESCs to FGF2 and Activin significantly reduced (over 80%) the expression of the neural plate marker *NCAM* (Vallier et al., 2009), suggesting that the negative cue Activin represses neural induction in human ESCs. However, at present, it is not known whether there are any interactions or crosstalk between Activin/Nodal and FGF pathways during neural induction. To test whether Activin directly suppresses the FGF/Erk pathway, mouse ESCs could be treated with Activin and FGF at the same time and then the levels of p-Erk1/2 analysed to see if

FGF-mediated Erk signalling is suppressed by Activin.

6.6 Nnat plays roles in neural induction and neurogenesis

The expression of Nnat has been shown to be increased from the beginning of differentiation until the formation of neurons during mouse ESCs neural differentiation (see sections 1.7 and 3.2.2). *In vivo* data also showed that Nnat is not only expressed during early neural development but also in the adult NSCs where neurogenesis occurs (see section 1.7.1). These results suggest that Nnat plays roles in both neural induction (the first step of neural development) and neurogenesis (the process by which neurons are generated). This assumption can help to explain the observation that treatment of Nnat-KD ESCs with Tg (to mimic Nnat and increase $[Ca^{2+}]_i$ and hence activate Erk1/2) or FGF4 at the beginning of differentiation rescued their ability to NSCs, with the same numbers being generated as from wild type ESCs, but only partially restored their ability to generate neurons (see sections 4.2.3.2 and 5.2.2). Here, many fewer neurons were generated compared with wild type ESCs. If Nnat was only required for neural induction, then similar numbers of neurons would be expected to be seen. These observations suggest that the effects of Tg or FGF4 are not sustained through the whole course of neurogenesis, and in addition to the early role played by Nnat in neural induction, this protein also plays another role during the neurogenesis of NSCs.

6.7 Neural induction is conserved in vertebrates

Within my thesis, I have demonstrated that Nnat is required for neural induction in mouse ESCs (see section 3.2.4), and that the injection of mouse *Nnat* mRNA into *Xenopus* embryos induced neural specification (see section 3.2.7). These results suggested that the role of Nnat in neural induction is conserved in mouse ESCs and *Xenopus*. This finding leads to an assumption that the key molecular mechanisms underlying neural induction are conserved cross species in vertebrates. Some published data in which the organiser induces neural tissue in different species support this assumption. For example, Hensen's node is the chick equivalent of the *Xenopus* organiser (Yuan and Schoenwolf, 1998), and when Hensen's node was isolated and

sandwiched between two *Xenopus* animal cap explants, it induced the generation of neural tissue in these animal caps (Kintner and Dodd, 1991). Thus, the organiser of chick embryos can direct *Xenopus* ectodermal cells along a neural fate. Similarly 'the node' which is the organiser in mouse embryos, is located at the anterior end of the primitive streak (Beddington, 1994; Kinder et al., 2001), and when the anterior portion of primitive streak is isolated and transplanted into the ventral side of the blastocoel (prospective non-neural ectoderm) of a host *Xenopus* embryos, it can induce ectopic neural tissue, too (Blum et al., 1992). Thus, the organiser of mouse embryos can also induce neural tissue in *Xenopus* embryos. Finally, the transplantation of the organiser - equivalent of rabbit embryo into chick embryos induced ectopic *Sox3*-expressing neural tissue (Knoetgen et al., 1999). This cross-species neural inductive ability of the organiser suggests that the molecular mechanisms of neural induction are conserved in the vertebrates.

Both my experiments and previously published studies (see section 1.6.2 and 5.2.5) showed that the activation of BMP signalling suppresses neural induction in ESCs. These results are consistent with the findings in *Xenopus*, chick, and mouse embryos where BMP signalling inhibits neural specification during gastrulation (see section 1.4). From this point of view, the role of BMP signalling is conserved in ESCs and vertebrates. Similarly the activation of FGF/Erk signalling is required for neural induction in ESCs, *Xenopus*, chick, and mouse embryos (see sections1.5.1 and 1.6.2). Thus**,** the role of FGF/Erk signalling is also conserved in ESCs and vertebrates. In addition to BMP and FGF/Erk signals, the activation of Wnt or Activin/Nodal signalling represses neural induction not only in ESCs, but also in vertebrate embryos during gastrulation (see sections 1.5.2, 1.5.3, and 1.6.2). Therefore, the roles of these key signals are similar in neural induction of ESCs and vertebrate embryos, suggesting that the molecular mechanisms of neural induction are conserved. This means that since ESCs are easier to manipulate than mammalian embryos, studies on the molecular mechanisms underlying neural induction can be carried out using ESCs first, and then these *in vitro* finding could be tested *in vivo*. For example, my *in*

vitro findings revealed that Nnat is needed for neural specification of mouse ESCs (see section 3.2.4). If the role of Nnat is conserved in ESCs and mouse embryo, then it would be worth creating Nnat inducible knockout mouse in the future to study its role in neural induction of mouse embryos *in vivo*.

6.8 Nnat/Erk may interact with Sp1 to activate the transcription of *Sox2* in neural induction

Within Chapter 4 and 5, I showed that Nnat caused an increase in $[Ca^{2+}]_i$ and in turn this increase in $[Ca^{2+}]_i$ activated Erk1/2. The activation of Erk signalling is pivotal for the neural induction of mouse ESCs (see section 5.2.1). Erk1/2 is a protein kinase and the active form (p-Erk1/2) physically interacts with various transcription factors (Chang et al., 2003; Dajee et al., 2003; Karin, 1995; Pages, 2007; Yeh et al., 2004). Sp1 is one of these transcription factors (Milanini-Mongiat et al., 2002). It is a zinc-finger protein that is expressed in neuroectoderm, hematopoietic cells, and giant trophoblast cells of mouse embryos at 8.5 dpc (Saffer et al., 1991). The human early neural marker *SOX3* and mouse *Sox2* promoters contain binding sites for Sp1 (Archer et al., 2010; Kovacevic Grujicic et al., 2005; Wiebe et al., 2000), and Sp1 is also a positive regulator of the NSC marker *Nestin* in mouse (Cheng et al., 2004). Therefore, Nnat-mediated Erk signalling may cause the phosphorylation of Sp1 that in turn activates *Sox2* and *Nestin* to promote neural induction, but more experiments are needed to verify this.

6.9 A better understanding of neural induction facilitates the future usage of ESCs in cell replacement therapy for neurodegenerative disorders

Neurodegenerative disorders are diseases where neurons are progressively lost; examples include Parkinson's, Alzheimer's and Huntington's diseases, and amyotrophic lateral sclerosis (Mattson, 2000). Parkinson's disease is a well-known condition caused by the death of dopaminergic neurons in the substantia nigra of the midbrain (Lotharius and Brundin, 2002). The transplantation of human embryonic dopaminergic neurons into the brains of patients with Parkinson's disease has been used to improve the symptoms

and signs of this disease (Freed et al., 2001). However, the dopaminergic neurons used for transplantation are isolated from human embryos. Thus the source of transplanted cells is an important issue because a limited number of dopaminergic neurons were isolated from each embryo (Kim et al., 2002). As discussed in section 1.6.1, ESCs are pluripotent and able to differentiate into all the cell types of the adult body. Therefore ESCs could be used as a source of different tissue-specific cells (Dang and Tropepe, 2006; Kim et al., 2002; Williams et al., 1988; Wu et al., 2007). This implies that ESCs have a great therapeutic promise for cell replacement therapies and regenerative medicine. Further, the transplantation of ESC-derived dopaminergic neurons into an animal model of Parkinson's disease improved the symptoms of this disease (Kim et al., 2002; Kriks et al., 2011). Similarly behavioural improvements in Parkinsonian rats were noted after human ESC-derived neural progenitors were transplanted into the striatum (Ben-Hur et al., 2004). In addition to Parkinson's disease, ESCs-derived neural cells has been transplanted into the cortex of a mouse model of Alzheimer's disease to improve memory disruption of diseased mice (Wang et al., 2006). These results suggested that transplantation of ESC-derived neural cells is a possible strategy in the treatment of Neurodegenerative disorders. However, the long-term safety of transplanted cells is a crucial issue. For instance, tumour formation is a common theme of ESCs based cell replacement therapy (Brederlau et al., 2006; Kim et al., 2002). Although the studies cited above did not show that the transplantation of ESC-derived neural cells induced the tumour formation in animals (Ben-Hur et al., 2004; Brederlau et al., 2006; Kim et al., 2002; Kriks et al., 2011), these animals were sacrificed for analysis at 12-20 weeks after transplantation. Therefore, it is uncertain whether or not teratomas will be found in a long-term follow-up.

In addition to tumour formation, it is hard to generate pure tissue-specific cells form ESCs and this has become another obstacle to their therapeutic uses (Dang and Tropepe, 2006). Cell replacement therapy is based on the fact that stem cells have the potential to be precisely directed to differentiate along different cell lineages, producing different tissue-specific progenitor cells that can be used for transplantation (Brederlau et al., 2006; Brustle et

al., 1999; Keller, 2005). A better understanding of the molecular mechanisms of neural development will help develop protocols that will enable the routine generation of neural progenitor cells or neurons from ESCs for therapeutic purposes *in vitro* (Suter and Krause, 2008). My study focused on the mechanisms by which Nnat promotes neural induction, which is the fist step of neural development. The data I have presented within this thesis demonstrate that Nnat modulates cytosolic Ca^{2+} levels to activate Erk signalling and suppress BMP signalling, resulting in promotion of neural induction. Although my study is basic research, it may help us to understand the mechanisms regulating ESCs differentiation into therapeutically relevant cells and facilitate the future usage of ESCs in cell replacement therapy for neurodegenerative disorders.

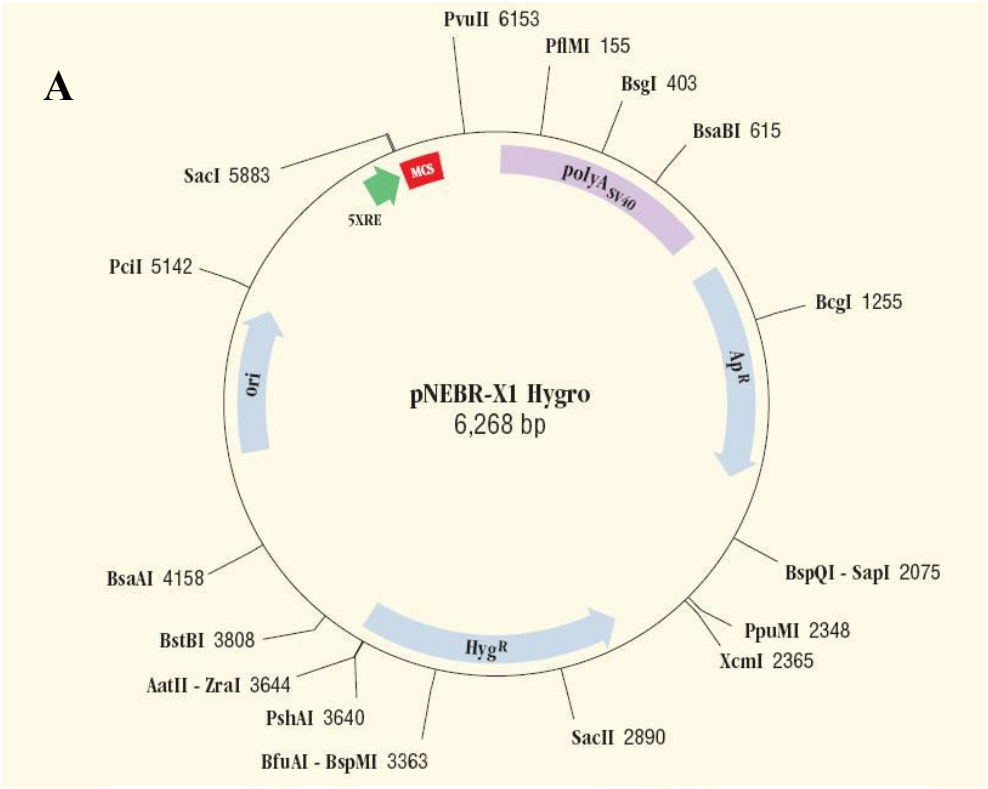

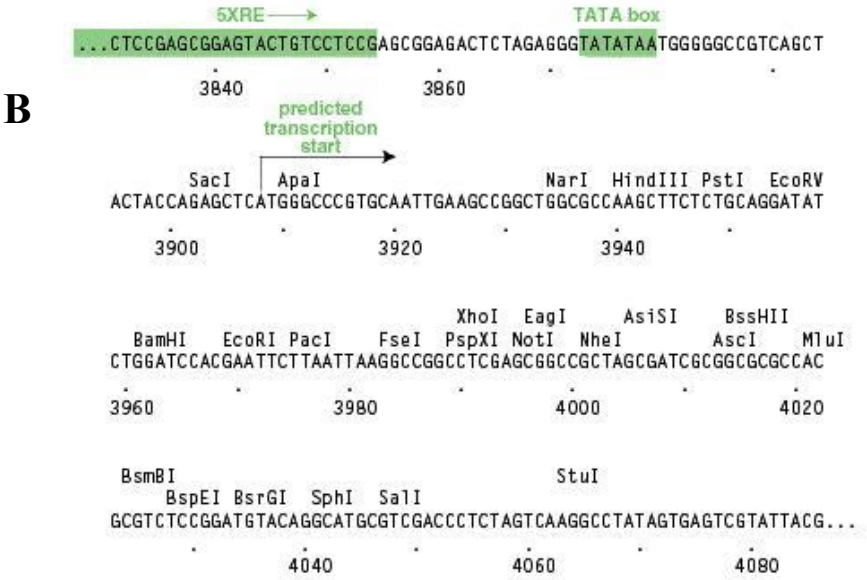

Appendix 1. Schematic vector map of pNEBR-X1-Hygro.
(A) The vector pNEBR-X1-Hygro (New England Biolabs) contains Amp^R, Hyg^R, ori, and MCS downstream of 5 copies of GAL4 RE (5XRE) and a minimal promoter. (B) The MCS contains a sequence that can be recognised by *Hin*dIII and *Bam*HI. Nnat was cloned into the *Hin*dIII and *Bam*HI sites and the vector was transfected into ESCs to generate Nnat-OE ESCs. Hygromycin was used to select the transfected cells.
Abbreviations: Amp^R, Ampicillin-resistance gene; ESCs, embryonic stem cells; Hyg^R, Hygromycin-resistance gene; MCS, multiple cloning site; ori, origin of replication; RE, response element. (Adapted from http://www.neb.com/nebecomm/tech_reference).

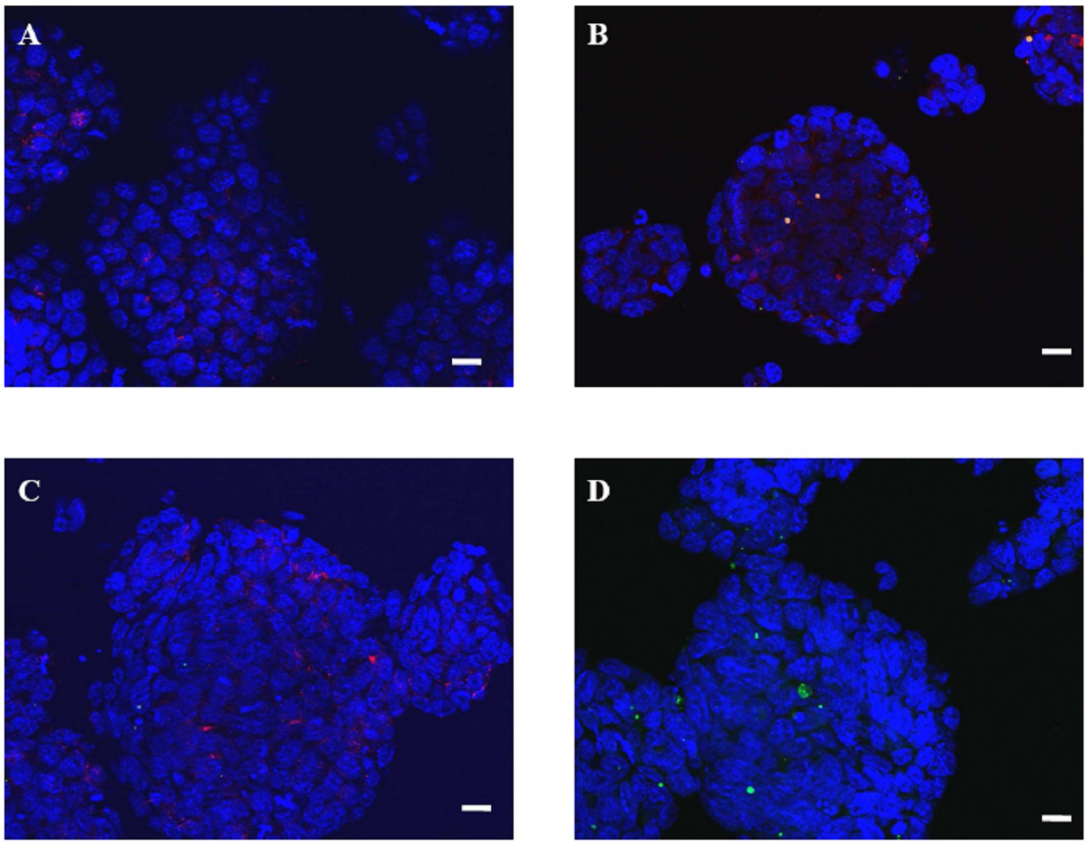

Appendix 2. Negative controls for immunocytochemical analysis.
46C ESCs were grown on gelatine-coated coverslips in non-differentiation condition for two days. After fixation and permeabilization, (A) Cy3-conjugated mouse, (B) Cy3-conjugated rabbit, (C) Cy3-conjugated rat, (D) FITC-conjugated rabbit secondary antibodies were applied at room temperature for one hour. Cells were then washed four times in PBS and submerged in double distilled water prior to mounting of coverslips onto slides using mounting medium with DAPI to stain the nuclei. Fluorescent microscopy images were acquired and no Cy3 or FITC fluorescence was observed in the absence of primary antibody. Scale bar, 20 μm.
Abbreviations: Cy3, Cyanine 3; DAPI, 4',6-diamidino-2-phenylindole; ESC, embryonic stem cell; FITC, Fluorescein isothiocyanate; PBS, Phosphate-buffered saline.

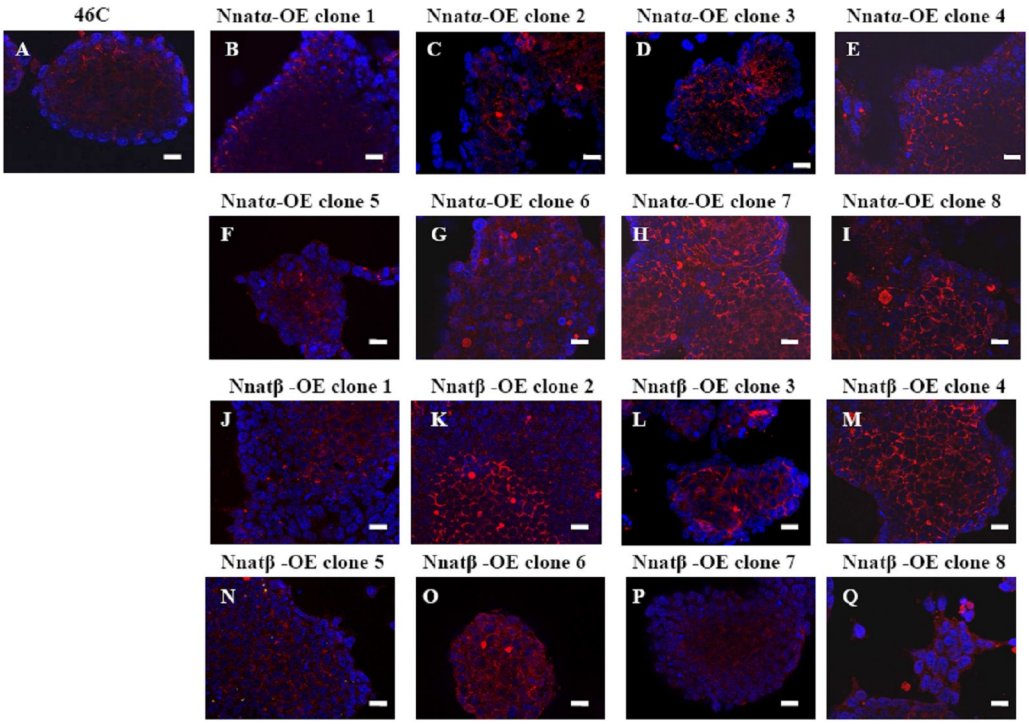

Appendix 3. Nnat expression in Nnatα-OE, Nnatβ-OE, and 46C ESCs.
The selected Nnat-OE clones and 46C ESCs were grown on gelatine-coated coverslips and cultured in non-differentiating condition for two days. After fixation, the expression of Nnat was detected by immunocytochemical analysis using the primary antibody against both Nnatα and Nnatβ. (A) The basal expression of Nnat (red) in 46C ESCs was revealed. (B-I) The expression of Nnat was increased in clones 4, 7, and 8 of Nnatα-OE ESCs. (J-Q) The expression of Nnat was increased in clones 2 and 4 of Nnatβ-OE ESCs. All nuclei were stained with DAPI (blue). Scale bar, 20 μm.
Abbreviations: DAPI, 4',6-diamidino-2-phenylindole; ESC, embryonic stem cell; Nnat, Neuronatin.

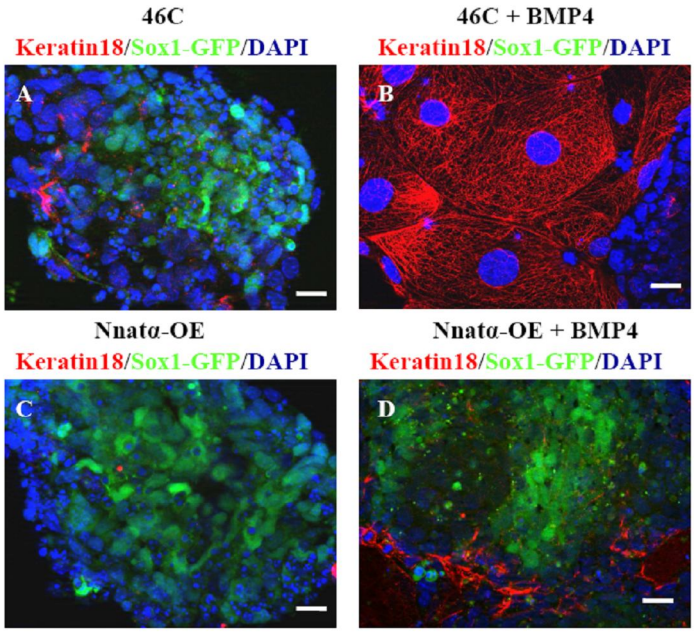

Appendix 4. Anti-Keratin 18 antibody did not bind non-specifically.

The 46C and Nnatα-OE ESCs were grown on gelatine-coated coverslips and cultured in differentiating conditions with/without BMP4 (10 ng/ml) treatment for 4 days. After fixation, the expression of the epidermal marker Keratin 18 was detected by immunocytochemical analysis. If the anti-Keratin 18 antibody cross reacted with actin and/or collagen, then the Sox1-GFP$^+$ cells should be stained with the antibody. (A,C) 46C and Nnatα-OE ESCs generated Sox1-GFP$^+$ neuroectodermal cells after 4 days of differentiation. (B) BMP4 is an epidermal inducer and neural inhibitor, so the treatment of 46C ESCs with BMP4 suppressed the generation of Sox1-GFP$^+$ neural progenitors and induced the generation of Keratin 18$^+$ epidermal cells (red), which could be a positive control for anti-keratin antibody. (D) After treatment with BMP4, Nnatα-OE ESCs still generated Sox1-GFP$^+$ cells and the expression of Keratin 18 was reduced. In Figure A, C, and D, Keratin 18 was not expressed in these Sox1-GFP$^+$ cells, suggesting that the anti-Keratin 18 antibody did not cross react with actin and/or collagen. All nuclei were stained with DAPI (blue). Scale bar, 20 μm.

Abbreviations: BMP, Bone morphogenetic protein; DAPI, 4',6-diamidino-2-phenylindole; ESC, embryonic stem cell; GFP, green fluorescent protein; Nnat, Neuronatin; Sox1, SRY (sex determining region Y)-box 1.

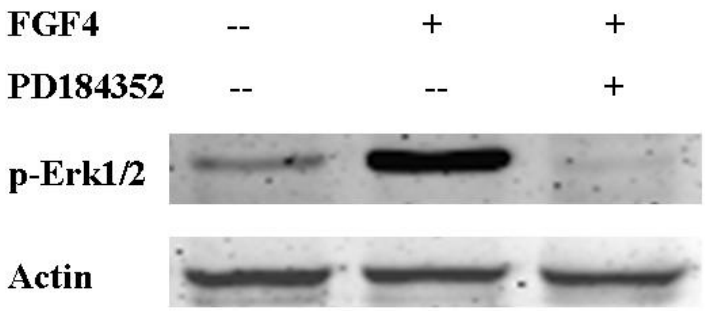

Appendix 5. 5 μM PD184352 suppresses FGF4-induced phosphorylation of Erk1/2.
46C ESCs were treated with 5 ng/ml of FGF4 and/or 5 μM PD184352 for one hour and then the protein levels of p-Erk1/2 were analysed by Western blotting using an anti-p-Erk1/2 antibody. The exposure of FGF4 increased p-Erk1/2, and the activation of Erk1/2 was inhibited by the MEK inhibitor PD184352.
Abbreviations: Erk, Extracellular Signal-regulated Kinase; ESC, embryonic stem cell; FGF4, Fibroblast growth factor 4; MEK, Mitogen-activated Protein/Extracellular Signal-regulated Kinase Kinase; p-Erk1/2, phosphorylated Erk1/2.

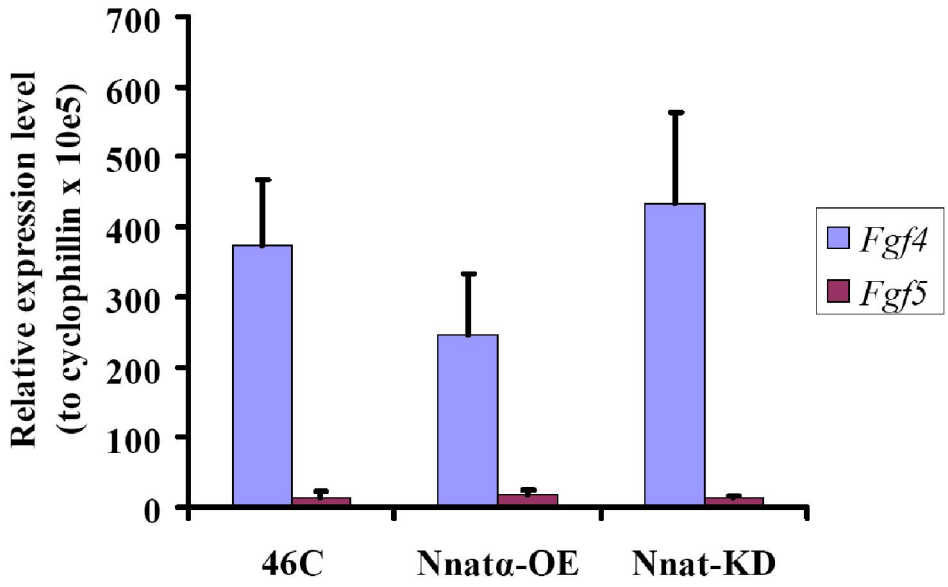

Appendix 6. Mouse ESCs express *Fgf4* in non-differentiating conditions.

The ability of wild type mouse ESCs to generate NSCs in the monolayer culture system was suppressed by PD173074 (a FGFR inhibitor) treatment, suggesting that FGF plays a role in neural induction of mouse ESCs. *Fgf4* is the first expressed gene of FGF family during mouse embryogenesis. *Fgf4* is expressed in ICM and mouse ESCs are generated from ICM, so *Fgf4* should be also expressed in ESCs. 46C, Nnatα-OE, and Nnat-KD ESCs were grown in non-differentiating conditions, and cultures were collected to examine the expression of genes using real-time PCR. 46C, Nnatα-OE, and Nnat-KD ESCs all expressed *Fgf4* and there was no significantly difference between these ESCs ($p > 0.05$, one-way ANOVA test). *Fgf5* is the marker of primitive ectoderm and it is not expressed in ESCs. As expected, these mouse ESCs did not express *Fgf5*.

Abbreviations: ANOVA, analysis of variance; ESC, embryonic stem cell; *Fgf*, fibroblast growth factor; Nnat-KD, Nnat-knockdown; Nnatα-OE, Nnatα-overexpression; PCR, polymerase chain reaction.

Appendix 7. Published Papers

Lin, H. H., Bell, E., Uwanogho, D., Perfect, L. W., Noristani, H., Bates, T. J., Snetkov, V., Price, J. and Sun, Y. M. (2010). Neuronatin promotes neural lineage in ESCs via Ca^{2+} signaling. *Stem Cells* **28**, 1950-60.

Sun, Y. M., Cooper, M., Finch, S., Lin, H. H., Chen, Z. F., Williams, B. P. and Buckley, N. J. (2008). Rest-mediated regulation of extracellular matrix is crucial for neural development. *PLoS One* **3**, e3656.

Reference List:

Abranches, E., Silva, M., Pradier, L., Schulz, H., Hummel, O., Henrique, D. and Bekman, E. (2009). Neural differentiation of embryonic stem cells in vitro: a road map to neurogenesis in the embryo. *PLoS One* **4**, e6286.

Adamson, E. D. (1990). EGF receptor activities in mammalian development. *Mol Reprod Dev* **27**, 16-22.

Agell, N., Bachs, O., Rocamora, N. and Villalonga, P. (2002). Modulation of the Ras/Raf/MEK/ERK pathway by Ca(2+), and calmodulin. *Cell Signal* **14**, 649-54.

Agius, E., Oelgeschlager, M., Wessely, O., Kemp, C. and De Robertis, E. M. (2000). Endodermal Nodal-related signals and mesoderm induction in Xenopus. *Development* **127**, 1173-83.

Alexander, K. A., Wakim, B. T., Doyle, G. S., Walsh, K. A. and Storm, D. R. (1988). Identification and characterization of the calmodulin-binding domain of neuromodulin, a neurospecific calmodulin-binding protein. *J Biol Chem* **263**, 7544-9.

Alvarez, I. S., Araujo, M. and Nieto, M. A. (1998). Neural induction in whole chick embryo cultures by FGF. *Dev Biol* **199**, 42-54.

Aoki, T. O., David, N. B., Minchiotti, G., Saint-Etienne, L., Dickmeis, T., Persico, G. M., Strahle, U., Mourrain, P. and Rosa, F. M. (2002). Molecular integration of casanova in the Nodal signalling pathway controlling endoderm formation. *Development* **129**, 275-86.

Araujo, M. and Nieto, M. A. (1997). The expression of chick EphA7 during segmentation of the central and peripheral nervous system. *Mech Dev* **68**, 173-7.

Archer, T. C., Jin, J. and Casey, E. S. (2010). Interaction of Sox1, Sox2, Sox3 and Oct4 during primary neurogenesis. *Dev Biol* **350**, 429-40.

Argentin, G., Cicchetti, R. and Nicoletti, B. (1993). Mouse chondrocytes in monolayer culture. *In Vitro Cell Dev Biol Anim* **29A**, 603-6.

Arnold, S. J. and Robertson, E. J. (2009). Making a commitment: cell lineage allocation and axis patterning in the early mouse embryo. *Nat Rev Mol Cell Biol* **10**, 91-103.

Artursson, P. and Magnusson, C. (1990). Epithelial transport of drugs in cell culture. II: Effect of extracellular calcium concentration on the paracellular transport of drugs of different lipophilicities across monolayers of intestinal epithelial (Caco-2) cells. *J Pharm Sci* **79**, 595-600.

Artus, J., Panthier, J. J. and Hadjantonakis, A. K. (2010). A role for PDGF signaling in expansion of the extra-embryonic endoderm lineage of the mouse blastocyst. *Development* **137**, 3361-72.

Aruga, J. and Mikoshiba, K. (2011). Role of BMP, FGF, calcium signaling, and Zic proteins in vertebrate neuroectodermal differentiation. *Neurochem Res* **36**, 1286-92.

Aruga, J., Minowa, O., Yaginuma, H., Kuno, J., Nagai, T., Noda, T. and Mikoshiba, K. (1998). Mouse Zic1 is involved in cerebellar development. *J Neurosci* **18**, 284-93.

Ashworth, R., Zimprich, F. and Bolsover, S. R. (2001). Buffering intracellular calcium disrupts motoneuron development in intact zebrafish embryos. *Brain Res Dev Brain Res* **129**, 169-79.

Aubert, J., Dunstan, H., Chambers, I. and Smith, A. (2002). Functional gene screening in embryonic stem cells implicates Wnt antagonism in neural differentiation. *Nat Biotechnol* **20**, 1240-5.

Aubert, J., Stavridis, M. P., Tweedie, S., O'Reilly, M., Vierlinger, K., Li, M., Ghazal, P., Pratt, T., Mason, J. O., Roy, D. et al. (2003). Screening for mammalian neural genes via fluorescence-activated cell sorter purification of neural precursors from Sox1-gfp knock-in mice. *Proc Natl Acad Sci U S A* **100 Suppl 1**, 11836-41.

Avilion, A. A., Nicolis, S. K., Pevny, L. H., Perez, L., Vivian, N. and Lovell-Badge, R. (2003). Multipotent cell lineages in early mouse development depend on SOX2 function. *Genes Dev* **17**, 126-40.

Baboonian, C., Venables, P. J., Williams, D. G., Williams, R. O. and Maini, R. N. (1991). Cross reaction of antibodies to a glycine/alanine repeat sequence of Epstein-Barr virus nuclear antigen-1 with collagen, cytokeratin, and actin. *Ann Rheum Dis* **50**, 772-5.

Bachiller, D., Klingensmith, J., Kemp, C., Belo, J. A., Anderson, R. M., May, S. R., McMahon, J. A., McMahon, A. P., Harland, R. M., Rossant, J. et al. (2000). The organizer factors Chordin and Noggin are required for mouse forebrain development. *Nature* **403**, 658-61.

Bain, G., Kitchens, D., Yao, M., Huettner, J. E. and Gottlieb, D. I. (1995). Embryonic stem cells express neuronal properties in vitro. *Dev Biol* **168**, 342-57.

Batut, J., Vandel, L., Leclerc, C., Daguzan, C., Moreau, M. and Neant, I. (2005). The Ca2+-induced methyltransferase xPRMT1b controls neural fate in amphibian embryo. *Proc Natl Acad Sci U S A* **102**, 15128-33.

Beddington, R. S. (1994). Induction of a second neural axis by the mouse node. *Development* **120**, 613-20.

Belke, D. D. and Dillmann, W. H. (2004). Altered cardiac calcium handling in diabetes. *Curr Hypertens Rep* **6**, 424-9.

Ben-Hur, T., Idelson, M., Khaner, H., Pera, M., Reinhartz, E., Itzik, A. and Reubinoff, B. E. (2004). Transplantation of human embryonic stem cell-derived neural progenitors improves behavioral deficit in Parkinsonian rats. *Stem Cells* **22**, 1246-55.

Berridge, M. J., Lipp, P. and Bootman, M. D. (2000). The versatility and universality of calcium signalling. *Nat Rev Mol Cell Biol* **1**, 11-21.

Bers, D. M. (1982). A simple method for the accurate determination of free [Ca] in Ca-EGTA solutions. *Am J Physiol* **242**, C404-8.

Bessis, A., Champtiaux, N., Chatelin, L. and Changeux, J. P. (1997). The neuron-restrictive silencer element: a dual enhancer/silencer crucial for patterned expression of a nicotinic receptor gene in the brain. *Proc Natl Acad Sci U S A* **94**, 5906-11.

Blagovic, K., Kim, L. Y. and Voldman, J. (2011). Microfluidic perfusion for regulating diffusible signaling in stem cells. *PLoS One* **6**, e22892.

Blum, M., Gaunt, S. J., Cho, K. W., Steinbeisser, H., Blumberg, B., Bittner, D. and De Robertis, E. M. (1992). Gastrulation in the mouse: the role of the homeobox gene goosecoid. *Cell* **69**, 1097-106.

Boehning, D., Patterson, R. L., Sedaghat, L., Glebova, N. O., Kurosaki, T. and Snyder, S. H. (2003). Cytochrome c binds to inositol (1,4,5) trisphosphate receptors, amplifying calcium-dependent apoptosis. *Nat Cell Biol* **5**, 1051-61.

Borisy, F. F., Ronnett, G. V., Cunningham, A. M., Juilfs, D., Beavo, J. and Snyder, S. H. (1992). Calcium/calmodulin-activated phosphodiesterase expressed in olfactory receptor neurons. *J Neurosci* **12**, 915-23.

Boros, J., O'Donnell, A., Donaldson, I. J., Kasza, A., Zeef, L. and Sharrocks, A. D. (2009). Overlapping promoter targeting by Elk-1 and other divergent ETS-domain transcription factor family members. *Nucleic Acids Res* **37**, 7368-80.

Borowiak, M., Maehr, R., Chen, S., Chen, A. E., Tang, W., Fox, J. L., Schreiber, S. L. and Melton, D. A. (2009). Small molecules efficiently direct endodermal differentiation of mouse and human embryonic stem cells. *Cell Stem Cell* **4**, 348-58.

Bottcher, R. T. and Niehrs, C. (2005). Fibroblast growth factor signaling during early vertebrate development. *Endocr Rev* **26**, 63-77.

Bouchard, M. J., Wang, L. H. and Schneider, R. J. (2001). Calcium signaling by HBx protein in hepatitis B virus DNA replication. *Science* **294**, 2376-8.

Boyce, S. T. and Ham, R. G. (1983). Calcium-regulated differentiation of normal human epidermal keratinocytes in chemically defined clonal culture and serum-free serial culture. *J Invest Dermatol* **81**, 33s-40s.

Brasier, A. R., Tate, J. E. and Habener, J. F. (1989). Optimized use of the firefly luciferase assay as a reporter gene in mammalian cell lines. *Biotechniques* **7**, 1116-22.

Brison, D. R. and Schultz, R. M. (1996). RT-PCR-based method to localize the spatial expression of genes in the mouse blastocyst. *Mol Reprod Dev* **44**, 171-8.

Camus, A., Perea-Gomez, A., Moreau, A. and Collignon, J. (2006). Absence of Nodal signaling promotes precocious neural differentiation in the mouse embryo. *Dev Biol* **295**, 743-55.

Carballada, R., Yasuo, H. and Lemaire, P. (2001). Phosphatidylinositol-3 kinase acts in parallel to the ERK MAP kinase in the FGF pathway during Xenopus mesoderm induction. *Development* **128**, 35-44.

Carpenter, M. K., Inokuma, M. S., Denham, J., Mujtaba, T., Chiu, C. P. and Rao, M. S. (2001). Enrichment of neurons and neural precursors from human embryonic stem cells. *Exp Neurol* **172**, 383-97.

Carroll, J. and Swann, K. (1992). Spontaneous cytosolic calcium oscillations driven by inositol trisphosphate occur during in vitro maturation of mouse oocytes. *J Biol Chem* **267**, 11196-201.

Casellas, R. and Brivanlou, A. H. (1998). Xenopus Smad7 inhibits both the activin and BMP pathways and acts as a neural inducer. *Dev Biol* **198**, 1-12.

Chadwick, K., Wang, L., Li, L., Menendez, P., Murdoch, B., Rouleau, A. and Bhatia, M. (2003). Cytokines and BMP-4 promote hematopoietic differentiation of human embryonic stem cells. *Blood* **102**, 906-15.

Chambers, I., Silva, J., Colby, D., Nichols, J., Nijmeijer, B., Robertson, M., Vrana, J., Jones, K., Grotewold, L. and Smith, A. (2007). Nanog safeguards pluripotency and mediates germline development. *Nature* **450**, 1230-4.

Chambers, S. M., Fasano, C. A., Papapetrou, E. P., Tomishima, M., Sadelain, M. and Studer, L. (2009). Highly efficient neural conversion

of human ES and iPS cells by dual inhibition of SMAD signaling. *Nat Biotechnol* **27**, 275-80.

Chang, C. and Harland, R. M. (2007). Neural induction requires continued suppression of both Smad1 and Smad2 signals during gastrulation. *Development* **134**, 3861-72.

Chang, F., Steelman, L. S., Lee, J. T., Shelton, J. G., Navolanic, P. M., Blalock, W. L., Franklin, R. A. and McCubrey, J. A. (2003). Signal transduction mediated by the Ras/Raf/MEK/ERK pathway from cytokine receptors to transcription factors: potential targeting for therapeutic intervention. *Leukemia* **17**, 1263-93.

Charles, A. C., Dirksen, E. R., Merrill, J. E. and Sanderson, M. J. (1993). Mechanisms of intercellular calcium signaling in glial cells studied with dantrolene and thapsigargin. *Glia* **7**, 134-45.

Chen, J., Li, Y., Wang, L., Zhang, Z., Lu, D., Lu, M. and Chopp, M. (2001). Therapeutic benefit of intravenous administration of bone marrow stromal cells after cerebral ischemia in rats. *Stroke* **32**, 1005-11.

Chen, Z. F., Paquette, A. J. and Anderson, D. J. (1998). NRSF/REST is required in vivo for repression of multiple neuronal target genes during embryogenesis. *Nat Genet* **20**, 136-42.

Cheng, L., Jin, Z., Liu, L., Yan, Y., Li, T., Zhu, X. and Jing, N. (2004). Characterization and promoter analysis of the mouse nestin gene. *FEBS letters* **565**, 195-202.

Chin, D. and Means, A. R. (2000). Calmodulin: a prototypical calcium sensor. *Trends Cell Biol* **10**, 322-8.

Chng, Z., Teo, A., Pedersen, R. A. and Vallier, L. (2010). SIP1 mediates cell-fate decisions between neuroectoderm and mesendoderm in human pluripotent stem cells. *Cell Stem Cell* **6**, 59-70.

Cho, E. A. and Dressler, G. R. (1998). TCF-4 binds beta-catenin and is expressed in distinct regions of the embryonic brain and limbs. *Mech Dev* **77**, 9-18.

Cho, J. H. and Tsai, M. J. (2004). The role of BETA2/NeuroD1 in the development of the nervous system. *Mol Neurobiol* **30**, 35-47.

Cholfin, J. A. and Rubenstein, J. L. (2007). Patterning of frontal cortex subdivisions by Fgf17. *Proc Natl Acad Sci U S A* **104**, 7652-7.

Chotteau-Lelievre, A., Dolle, P., Peronne, V., Coutte, L., de Launoit, Y. and Desbiens, X. (2001). Expression patterns of the Ets transcription factors from the PEA3 group during early stages of mouse development. *Mech Dev* **108**, 191-5.

Christen, B. and Slack, J. M. (1999). Spatial response to fibroblast growth factor signalling in Xenopus embryos. *Development* **126**, 119-25.

Chu, K. and Tsai, M. J. (2005). Neuronatin, a downstream target of BETA2/NeuroD1 in the pancreas, is involved in glucose-mediated insulin secretion. *Diabetes* **54**, 1064-73.

Clapham, D. E. (2007). Calcium signaling. *Cell* **131**, 1047-58.

Clarke, J. D., Holder, N., Soffe, S. R. and Storm-Mathisen, J. (1991). Neuroanatomical and functional analysis of neural tube formation in notochordless Xenopus embryos; laterality of the ventral spinal cord is lost. *Development* **112**, 499-516.

Clarke, S. R., Shetty, A. K., Bradley, J. L. and Turner, D. A. (1994). Reactive astrocytes express the embryonic intermediate neurofilament nestin. *Neuroreport* **5**, 1885-8.

Cohen, M. A., Itsykson, P. and Reubinoff, B. E. (2010). The role of FGF-signaling in early neural specification of human embryonic stem cells. *Dev Biol* **340**, 450-8.

Collatz, M. B., Rudel, R. and Brinkmeier, H. (1997). Intracellular calcium chelator BAPTA protects cells against toxic calcium overload but also alters physiological calcium responses. *Cell Calcium* **21**, 453-9.

Cornell-Bell, A. H., Finkbeiner, S. M., Cooper, M. S. and Smith, S. J. (1990). Glutamate induces calcium waves in cultured astrocytes: long-range glial signaling. *Science* **247**, 470-3.

Cotrina, M. L., Lin, J. H., Alves-Rodrigues, A., Liu, S., Li, J., Azmi-Ghadimi, H., Kang, J., Naus, C. C. and Nedergaard, M. (1998). Connexins regulate calcium signaling by controlling ATP release. *Proc Natl Acad Sci U S A* **95**, 15735-40.

Coumoul, X. and Deng, C. X. (2003). Roles of FGF receptors in mammalian development and congenital diseases. *Birth Defects Res C Embryo Today* **69**, 286-304.

Cross, D. A., Alessi, D. R., Cohen, P., Andjelkovich, M. and Hemmings, B. A. (1995). Inhibition of glycogen synthase kinase-3 by insulin mediated by protein kinase B. *Nature* **378**, 785-9.

Cross, M. J. and Claesson-Welsh, L. (2001). FGF and VEGF function in angiogenesis: signalling pathways, biological responses and therapeutic inhibition. *Trends Pharmacol Sci* **22**, 201-7.

Dajee, M., Lazarov, M., Zhang, J. Y., Cai, T., Green, C. L., Russell, A. J., Marinkovich, M. P., Tao, S., Lin, Q., Kubo, Y. et al. (2003). NF-kappaB blockade and oncogenic Ras trigger invasive human epidermal neoplasia. *Nature* **421**, 639-43.

Dang, L. and Tropepe, V. (2006). Neural induction and neural stem cell development. *Regen Med* **1**, 635-52.

Dang, L. T. and Tropepe, V. (2010). FGF dependent regulation of Zfhx1b gene expression promotes the formation of definitive neural stem cells in the mouse anterior neurectoderm. *Neural Dev* **5**, 13.

Dang, L. T., Wong, L. and Tropepe, V. (2012). Zfhx1b Induces a Definitive Neural Stem Cell Fate in Mouse Embryonic Stem Cells. *Stem Cells Dev*.

Daniels, M., Shimizu, K., Zorn, A. M. and Ohnuma, S. (2004). Negative regulation of Smad2 by PIASy is required for proper Xenopus mesoderm formation. *Development* **131**, 5613-26.

Davey, H. M. and Kell, D. B. (1996). Flow cytometry and cell sorting of heterogeneous microbial populations: the importance of single-cell analyses. *Microbiol Rev* **60**, 641-96.

Davis, S., Vanhoutte, P., Pages, C., Caboche, J. and Laroche, S. (2000). The MAPK/ERK cascade targets both Elk-1 and cAMP response element-binding protein to control long-term potentiation-dependent gene expression in the dentate gyrus in vivo. *J Neurosci* **20**, 4563-72.

De Koninck, P. and Schulman, H. (1998). Sensitivity of CaM kinase II to the frequency of Ca2+ oscillations. *Science* **279**, 227-30.

De Robertis, E. M. and Kuroda, H. (2004). Dorsal-ventral patterning and neural induction in Xenopus embryos. *Annu Rev Cell Dev Biol* **20**, 285-308.

Debacker, C., Catala, M. and Labastie, M. C. (1999). Embryonic expression of the human GATA-3 gene. *Mech Dev* **85**, 183-7.

del Barco Barrantes, I., Davidson, G., Grone, H. J., Westphal, H. and Niehrs, C. (2003). Dkk1 and noggin cooperate in mammalian head induction. *Genes Dev* **17**, 2239-44.

Delaune, E., Lemaire, P. and Kodjabachian, L. (2005). Neural induction in Xenopus requires early FGF signalling in addition to BMP inhibition. *Development* **132**, 299-310.

Derda, R., Laromaine, A., Mammoto, A., Tang, S. K., Mammoto, T., Ingber, D. E. and Whitesides, G. M. (2009). Paper-supported 3D cell culture for tissue-based bioassays. *Proc Natl Acad Sci U S A* **106**, 18457-62.

Desbois-Mouthon, C., Cacheux, W., Blivet-Van Eggelpoel, M. J., Barbu, V., Fartoux, L., Poupon, R., Housset, C. and Rosmorduc, O. (2006). Impact of IGF-1R/EGFR cross-talks on hepatoma cell sensitivity to gefitinib. *Int J Cancer* **119**, 2557-66.

Di-Gregorio, A., Sancho, M., Stuckey, D. W., Crompton, L. A., Godwin, J., Mishina, Y. and Rodriguez, T. A. (2007). BMP signalling inhibits premature neural differentiation in the mouse embryo. *Development (Cambridge, England)* **134**, 3359-69.

Di Leva, F., Domi, T., Fedrizzi, L., Lim, D. and Carafoli, E. (2008). The plasma membrane Ca2+ ATPase of animal cells: structure, function and regulation. *Arch Biochem Biophys* **476**, 65-74.

Doetsch, F. (2003). A niche for adult neural stem cells. *Curr Opin Genet Dev* **13**, 543-50.

Dou, D. and Joseph, R. (1996). Cloning of human neuronatin gene and its localization to chromosome-20q 11.2-12: the deduced protein is a novel "proteolipid'. *Brain Res* **723**, 8-22.

Doukas, J., Blease, K., Craig, D., Ma, C., Chandler, L. A., Sosnowski, B. A. and Pierce, G. F. (2002). Delivery of FGF genes to wound repair cells enhances arteriogenesis and myogenesis in skeletal muscle. *Mol Ther* **5**, 517-27.

Doutheil, J., Treiman, M., Oschlies, U. and Paschen, W. (1999). Recovery of neuronal protein synthesis after irreversible inhibition of the endoplasmic reticulum calcium pump. *Cell Calcium* **25**, 419-28.

Downs, K. M. and Davies, T. (1993). Staging of gastrulating mouse embryos by morphological landmarks in the dissecting microscope. *Development* **118**, 1255-66.

Dufort, D., Schwartz, L., Harpal, K. and Rossant, J. (1998). The transcription factor HNF3beta is required in visceral endoderm for normal primitive streak morphogenesis. *Development* **125**, 3015-25.

Ebinu, J. O., Bottorff, D. A., Chan, E. Y., Stang, S. L., Dunn, R. J. and Stone, J. C. (1998). RasGRP, a Ras guanyl nucleotide- releasing protein with calcium- and diacylglycerol-binding motifs. *Science* **280**, 1082-6.

Eisaki, A., Kuroda, H., Fukui, A. and Asashima, M. (2000). XSIP1, a member of two-handed zinc finger proteins, induced anterior neural markers in Xenopus laevis animal cap. *Biochem Biophys Res Commun* **271**, 151-7.

Ellis, P., Fagan, B. M., Magness, S. T., Hutton, S., Taranova, O., Hayashi, S., McMahon, A., Rao, M. and Pevny, L. (2004). SOX2, a persistent marker for multipotential neural stem cells derived from embryonic stem cells, the embryo or the adult. *Dev Neurosci* **26**, 148-65.

Elms, P., Scurry, A., Davies, J., Willoughby, C., Hacker, T., Bogani, D. and Arkell, R. (2004). Overlapping and distinct expression domains of Zic2 and Zic3 during mouse gastrulation. *Gene Expr Patterns* **4**, 505-11.

Engelman, J. A. (2009). Targeting PI3K signalling in cancer: opportunities, challenges and limitations. *Nat Rev Cancer* **9**, 550-62.

Evans, H. K., Wylie, A. A., Murphy, S. K. and Jirtle, R. L. (2001). The neuronatin gene resides in a "micro-imprinted" domain on human chromosome 20q11.2. *Genomics* **77**, 99-104.

Evans, M. J. and Kaufman, M. H. (1981). Establishment in culture of pluripotential cells from mouse embryos. *Nature* **292**, 154-6.

Fainsod, A., Deissler, K., Yelin, R., Marom, K., Epstein, M., Pillemer, G., Steinbeisser, H. and Blum, M. (1997). The dorsalizing and neural inducing gene follistatin is an antagonist of BMP-4. *Mech Dev* **63**, 39-50.

Faucourt, M., Houliston, E., Besnardeau, L., Kimelman, D. and Lepage, T. (2001). The pitx2 homeobox protein is required early for endoderm formation and nodal signaling. *Dev Biol* **229**, 287-306.

Feijen, A., Goumans, M. J. and van den Eijnden-van Raaij, A. J. (1994). Expression of activin subunits, activin receptors and follistatin in postimplantation mouse embryos suggests specific developmental functions for different activins. *Development* **120**, 3621-37.

Feldman, B., Poueymirou, W., Papaioannou, V. E., DeChiara, T. M. and Goldfarb, M. (1995). Requirement of FGF-4 for postimplantation mouse development. *Science* **267**, 246-9.

Ferezou, I., Cauli, B., Hill, E. L., Rossier, J., Hamel, E. and Lambolez, B. (2002). 5-HT3 receptors mediate serotonergic fast synaptic excitation of neocortical vasoactive intestinal peptide/cholecystokinin interneurons. *J Neurosci* **22**, 7389-97.

Ferri, A. L., Cavallaro, M., Braida, D., Di Cristofano, A., Canta, A., Vezzani, A., Ottolenghi, S., Pandolfi, P. P., Sala, M., DeBiasi, S. et al. (2004). Sox2 deficiency causes neurodegeneration and impaired neurogenesis in the adult mouse brain. *Development* **131**, 3805-19.

Fok, E. Y. and Zandstra, P. W. (2005). Shear-controlled single-step mouse embryonic stem cell expansion and embryoid body-based differentiation. *Stem Cells* **23**, 1333-42.

Fong, H., Hohenstein, K. A. and Donovan, P. J. (2008). Regulation of self-renewal and pluripotency by Sox2 in human embryonic stem cells. *Stem Cells* **26**, 1931-8.

Freed, C. R., Greene, P. E., Breeze, R. E., Tsai, W. Y., DuMouchel, W., Kao, R., Dillon, S., Winfield, H., Culver, S., Trojanowski, J. Q. et al. (2001). Transplantation of embryonic dopamine neurons for severe Parkinson's disease. *N Engl J Med* **344**, 710-9.

Fuentealba, L. C., Eivers, E., Ikeda, A., Hurtado, C., Kuroda, H., Pera, E. M. and De Robertis, E. M. (2007). Integrating patterning signals: Wnt/GSK3 regulates the duration of the BMP/Smad1 signal. *Cell* **131**, 980-93.

Fujimi, T. J., Mikoshiba, K. and Aruga, J. (2006). Xenopus Zic4: conservation and diversification of expression profiles and protein function among the Xenopus Zic family. *Dev Dyn* **235**, 3379-86.

Fukuda, H., Takahashi, J., Watanabe, K., Hayashi, H., Morizane, A., Koyanagi, M., Sasai, Y. and Hashimoto, N. (2006). Fluorescence-activated cell sorting-based purification of embryonic stem cell-derived neural precursors averts tumor formation after transplantation. *Stem Cells* **24**, 763-71.

Furdui, C. M., Lew, E. D., Schlessinger, J. and Anderson, K. S. (2006). Autophosphorylation of FGFR1 kinase is mediated by a sequential and precisely ordered reaction. *Mol Cell* **21**, 711-7.

Furushima, K., Murata, T., Matsuo, I. and Aizawa, S. (2000). A new murine zinc finger gene, Opr. *Mech Dev* **98**, 161-4.

Gage, F. H. (2000). Mammalian neural stem cells. *Science* **287**, 1433-8.

Gallogly, M. M. and Mieyal, J. J. (2007). Mechanisms of reversible protein glutathionylation in redox signaling and oxidative stress. *Curr Opin Pharmacol* **7**, 381-91.

Gambaro, K., Aberdam, E., Virolle, T., Aberdam, D. and Rouleau, M. (2006). BMP-4 induces a Smad-dependent apoptotic cell death of mouse embryonic stem cell-derived neural precursors. *Cell Death Differ* **13**, 1075-87.

Gammill, L. S. and Bronner-Fraser, M. (2003). Neural crest specification: migrating into genomics. *Nat Rev Neurosci* **4**, 795-805.

Gaspard, N. and Vanderhaeghen, P. (2010). Mechanisms of neural specification from embryonic stem cells. *Curr Opin Neurobiol* **20**, 37-43.

Gates, M. A., Thomas, L. B., Howard, E. M., Laywell, E. D., Sajin, B., Faissner, A., Gotz, B., Silver, J. and Steindler, D. A. (1995). Cell and molecular analysis of the developing and adult mouse subventricular zone of the cerebral hemispheres. *J Comp Neurol* **361**, 249-66.

Gaulden, J. and Reiter, J. F. (2008). Neur-ons and neur-offs: regulators of neural induction in vertebrate embryos and embryonic stem cells. *Human molecular genetics* **17**, R60-6.

George, K. M., Leonard, M. W., Roth, M. E., Lieuw, K. H., Kioussis, D., Grosveld, F. and Engel, J. D. (1994). Embryonic expression and cloning of the murine GATA-3 gene. *Development* **120**, 2673-86.

Gerrard, L., Rodgers, L. and Cui, W. (2005). Differentiation of human embryonic stem cells to neural lineages in adherent culture by blocking bone morphogenetic protein signaling. *Stem Cells* **23**, 1234-41.

Gille, H., Kortenjann, M., Thomae, O., Moomaw, C., Slaughter, C., Cobb, M. H. and Shaw, P. E. (1995). ERK phosphorylation potentiates Elk-1-mediated ternary complex formation and transactivation. *EMBO J* **14**, 951-62.

Giudicelli, F., Taillebourg, E., Charnay, P. and Gilardi-Hebenstreit, P. (2001). Krox-20 patterns the hindbrain through both cell-autonomous and non cell-autonomous mechanisms. *Genes Dev* **15**, 567-80.

Glassy, M. C., Tharakan, J. P. and Chau, P. C. (1988). Serum-free media in hybridoma culture and monoclonal antibody production. *Biotechnol Bioeng* **32**, 1015-28.

Glinka, A., Wu, W., Delius, H., Monaghan, A. P., Blumenstock, C. and Niehrs, C. (1998). Dickkopf-1 is a member of a new family of secreted proteins and functions in head induction. *Nature* **391**, 357-62.

Glister, C., Kemp, C. F. and Knight, P. G. (2004). Bone morphogenetic protein (BMP) ligands and receptors in bovine ovarian follicle cells: actions of BMP-4, -6 and -7 on granulosa cells and differential modulation of Smad-1 phosphorylation by follistatin. *Reproduction* **127**, 239-54.

Goetz, R., Dover, K., Laezza, F., Shtraizent, N., Huang, X., Tchetchik, D., Eliseenkova, A. V., Xu, C. F., Neubert, T. A., Ornitz, D. M. et al. (2009). Crystal structure of a fibroblast growth factor homologous factor (FHF) defines a conserved surface on FHFs for binding and modulation of voltage-gated sodium channels. *J Biol Chem* **284**, 17883-96.

Goldbeter, A., Dupont, G. and Berridge, M. J. (1990). Minimal model for signal-induced Ca2+ oscillations and for their frequency encoding through protein phosphorylation. *Proc Natl Acad Sci U S A* **87**, 1461-5.

Graham, A. and Lumsden, A. (1996). Interactions between rhombomeres modulate Krox-20 and follistatin expression in the chick embryo hindbrain. *Development* **122**, 473-80.

Grand, E. K., Chase, A. J., Heath, C., Rahemtulla, A. and Cross, N. C. (2004). Targeting FGFR3 in multiple myeloma: inhibition of t(4;14)-positive cells by SU5402 and PD173074. *Leukemia* **18**, 962-6.

Grapin-Botton, A., Bonnin, M. A. and Le Douarin, N. M. (1997). Hox gene induction in the neural tube depends on three parameters: competence, signal supply and paralogue group. *Development* **124**, 849-59.

Gratsch, T. E. and O'Shea, K. S. (2002). Noggin and chordin have distinct activities in promoting lineage commitment of mouse embryonic stem (ES) cells. *Dev Biol* **245**, 83-94.

Greene, N. D. and Copp, A. J. (2009). Development of the vertebrate central nervous system: formation of the neural tube. *Prenat Diagn* **29**, 303-11.

Grose, R. and Dickson, C. (2005). Fibroblast growth factor signaling in tumorigenesis. *Cytokine Growth Factor Rev* **16**, 179-86.

Grunz, H. and Tacke, L. (1989). Neural differentiation of Xenopus laevis ectoderm takes place after disaggregation and delayed reaggregation without inducer. *Cell Differ Dev* **28**, 211-7.

Guillemot, F. (2007). Spatial and temporal specification of neural fates by transcription factor codes. *Development* **134**, 3771-80.

Gujral, S., Tembhare, P., Badrinath, Y., Subramanian, P. G., Kumar, A. and Sehgal, K. (2009). Intracytoplasmic antigen study by flow cytometry in hematolymphoid neoplasm. *Indian J Pathol Microbiol* **52**, 135-44.

Haegele, L., Ingold, B., Naumann, H., Tabatabai, G., Ledermann, B. and Brandner, S. (2003). Wnt signalling inhibits neural differentiation of embryonic stem cells by controlling bone morphogenetic protein expression. *Mol Cell Neurosci* **24**, 696-708.

Hannon, K., Smith, C. K., 2nd, Bales, K. R. and Santerre, R. F. (1992). Temporal and quantitative analysis of myogenic regulatory and growth factor gene expression in the developing mouse embryo. *Dev Biol* **151**, 137-44.

Hardwick, J. C., Kodach, L. L., Offerhaus, G. J. and van den Brink, G. R. (2008). Bone morphogenetic protein signalling in colorectal cancer. *Nat Rev Cancer* **8**, 806-12.

Harland, R. M. (1994). Neural induction in Xenopus. *Curr Opin Genet Dev* **4**, 543-9.

Harland, R. M. and Grainger, R. M. (2011). Xenopus research: metamorphosed by genetics and genomics. *Trends Genet* **27**, 507-15.

Hart, A. H., Hartley, L., Ibrahim, M. and Robb, L. (2004). Identification, cloning and expression analysis of the pluripotency promoting Nanog genes in mouse and human. *Dev Dyn* **230**, 187-98.

Hata, A., Lagna, G., Massague, J. and Hemmati-Brivanlou, A. (1998). Smad6 inhibits BMP/Smad1 signaling by specifically competing with the Smad4 tumor suppressor. *Genes Dev* **12**, 186-97.

Haub, O. and Goldfarb, M. (1991). Expression of the fibroblast growth factor-5 gene in the mouse embryo. *Development* **112**, 397-406.

He, Q., Dent, E. W. and Meiri, K. F. (1997). Modulation of actin filament behavior by GAP-43 (neuromodulin) is dependent on the phosphorylation status of serine 41, the protein kinase C site. *J Neurosci* **17**, 3515-24.

Heasman, J. (2006). Patterning the early Xenopus embryo. *Development* **133**, 1205-17.

Hebert, J. M., Basilico, C., Goldfarb, M., Haub, O. and Martin, G. R. (1990). Isolation of cDNAs encoding four mouse FGF family members and characterization of their expression patterns during embryogenesis. *Dev Biol* **138**, 454-63.

Hebert, J. M., Rosenquist, T., Gotz, J. and Martin, G. R. (1994). FGF5 as a regulator of the hair growth cycle: evidence from targeted and spontaneous mutations. *Cell* **78**, 1017-25.

Heinzel, B., John, M., Klatt, P., Bohme, E. and Mayer, B. (1992). Ca2+/calmodulin-dependent formation of hydrogen peroxide by brain nitric oxide synthase. *Biochem J* **281 (Pt 3)**, 627-30.

Heldin, C. H., Miyazono, K. and ten Dijke, P. (1997). TGF-beta signalling from cell membrane to nucleus through SMAD proteins. *Nature* **390**, 465-71.

Helmchen, F., Imoto, K. and Sakmann, B. (1996). Ca2+ buffering and action potential-evoked Ca2+ signaling in dendrites of pyramidal neurons. *Biophys J* **70**, 1069-81.

Hemmati-Brivanlou, A., Kelly, O. G. and Melton, D. A. (1994). Follistatin, an antagonist of activin, is expressed in the Spemann organizer and displays direct neuralizing activity. *Cell* **77**, 283-95.

Hemmati-Brivanlou, A. and Melton, D. (1997a). Vertebrate embryonic cells will become nerve cells unless told otherwise. *Cell* **88**, 13-7.

Hemmati-Brivanlou, A. and Melton, D. (1997b). Vertebrate neural induction. *Annu Rev Neurosci* **20**, 43-60.

Henrique, D., Tyler, D., Kintner, C., Heath, J. K., Lewis, J. H., Ish-Horowicz, D. and Storey, K. G. (1997). cash4, a novel achaete-scute homolog induced by Hensen's node during generation of the posterior nervous system. *Genes Dev* **11**, 603-15.

Hoekman, M. F., Jacobs, F. M., Smidt, M. P. and Burbach, J. P. (2006). Spatial and temporal expression of FoxO transcription factors in the developing and adult murine brain. *Gene Expr Patterns* **6**, 134-40.

Hongo, I., Kengaku, M. and Okamoto, H. (1999). FGF signaling and the anterior neural induction in Xenopus. *Dev Biol* **216**, 561-81.

Hosseinkhani, M., Hosseinkhani, H., Khademhosseini, A., Bolland, F., Kobayashi, H. and Gonzalez, S. P. (2007). Bone morphogenetic protein-4 enhances cardiomyocyte differentiation of cynomolgus monkey ESCs in knockout serum replacement medium. *Stem Cells* **25**, 571-80.

Hou, Y., Chang, V. and Gautam, N. (2002). Determining G protein heterotrimer formation. *Methods Enzymol* **344**, 505-12.

Hough, S. R., Clements, I., Welch, P. J. and Wiederholt, K. A. (2006). Differentiation of mouse embryonic stem cells after RNA interference-mediated silencing of OCT4 and Nanog. *Stem Cells* **24**, 1467-75.

Huang, H. M., Huang, C. J. and Yen, J. J. (2000). Mcl-1 is a common target of stem cell factor and interleukin-5 for apoptosis prevention activity via MEK/MAPK and PI-3K/Akt pathways. *Blood* **96**, 1764-71.

Hulstrand, A. M., Schneider, P. N. and Houston, D. W. (2010). The use of antisense oligonucleotides in Xenopus oocytes. *Methods* **51**, 75-81.

Husson, M., Enderlin, V., Alfos, S., Boucheron, C., Pallet, V. and Higueret, P. (2004). Expression of neurogranin and neuromodulin is affected in the striatum of vitamin A-deprived rats. *Brain research Molecular brain research* **123**, 7-17.

Hwang, W. S., Ryu, Y. J., Park, J. H., Park, E. S., Lee, E. G., Koo, J. M., Jeon, H. Y., Lee, B. C., Kang, S. K., Kim, S. J. et al. (2004). Evidence of a pluripotent human embryonic stem cell line derived from a cloned blastocyst. *Science* **303**, 1669-74.

Iemura, S., Yamamoto, T. S., Takagi, C., Uchiyama, H., Natsume, T., Shimasaki, S., Sugino, H. and Ueno, N. (1998). Direct binding of follistatin to a complex of bone-morphogenetic protein and its receptor inhibits ventral and epidermal cell fates in early Xenopus embryo. *Proceedings of the National Academy of Sciences of the United States of America* **95**, 9337-42.

Imamura, T., Takase, M., Nishihara, A., Oeda, E., Hanai, J., Kawabata, M. and Miyazono, K. (1997). Smad6 inhibits signalling by the TGF-beta superfamily. *Nature* **389**, 622-6.

Ishimura, A., Maeda, R., Takeda, M., Kikkawa, M., Daar, I. O. and Maeno, M. (2000). Involvement of BMP-4/msx-1 and FGF pathways in neural induction in the Xenopus embryo. *Dev Growth Differ* **42**, 307-16.

Itoh, N. and Ornitz, D. M. (2004). Evolution of the Fgf and Fgfr gene families. *Trends Genet* **20**, 563-9.

Itoh, N. and Ornitz, D. M. (2011). Fibroblast growth factors: from molecular evolution to roles in development, metabolism and disease. *J Biochem* **149**, 121-30.

Iwafuchi-Doi, M., Yoshida, Y., Onichtchouk, D., Leichsenring, M., Driever, W., Takemoto, T., Uchikawa, M., Kamachi, Y. and Kondoh, H. (2011). The Pou5f1/Pou3f-dependent but SoxB-independent regulation of conserved enhancer N2 initiates Sox2 expression during epiblast to neural plate stages in vertebrates. *Dev Biol* **352**, 354-66.

James, P., Inui, M., Tada, M., Chiesi, M. and Carafoli, E. (1989). Nature and site of phospholamban regulation of the Ca2+ pump of sarcoplasmic reticulum. *Nature* **342**, 90-2.

Janknecht, R., Ernst, W. H., Pingoud, V. and Nordheim, A. (1993). Activation of ternary complex factor Elk-1 by MAP kinases. *EMBO J* **12**, 5097-104.

Ji, Q. S., Winnier, G. E., Niswender, K. D., Horstman, D., Wisdom, R., Magnuson, M. A. and Carpenter, G. (1997). Essential role of the tyrosine kinase substrate phospholipase C-gamma1 in mammalian growth and development. *Proc Natl Acad Sci U S A* **94**, 2999-3003.

Joe, M. K., Lee, H. J., Suh, Y. H., Han, K. L., Lim, J. H., Song, J., Seong, J. K. and Jung, M. H. (2008). Crucial roles of neuronatin in insulin secretion and high glucose-induced apoptosis in pancreatic beta-cells. *Cell Signal* **20**, 907-15.

Johansson, B. M. and Wiles, M. V. (1995). Evidence for involvement of activin A and bone morphogenetic protein 4 in mammalian mesoderm and hematopoietic development. *Molecular and cellular biology* **15**, 141-51.

Johansson, C. B., Momma, S., Clarke, D. L., Risling, M., Lendahl, U. and Frisen, J. (1999). Identification of a neural stem cell in the adult mammalian central nervous system. *Cell* **96**, 25-34.

John, R. M., Aparicio, S. A., Ainscough, J. F., Arney, K. L., Khosla, S., Hawker, K., Hilton, K. J., Barton, S. C. and Surani, M. A. (2001). Imprinted expression of neuronatin from modified BAC transgenes reveals regulation by distinct and distant enhancers. *Dev Biol* **236**, 387-99.

Joseph, R., Dou, D. and Tsang, W. (1994). Molecular cloning of a novel mRNA (neuronatin) that is highly expressed in neonatal mammalian brain. *Biochem Biophys Res Commun* **201**, 1227-34.

Joseph, R., Dou, D. and Tsang, W. (1995). Neuronatin mRNA: alternatively spliced forms of a novel brain-specific mammalian developmental gene. *Brain Res* **690**, 92-8.

Kagitani, F., Kuroiwa, Y., Wakana, S., Shiroishi, T., Miyoshi, N., Kobayashi, S., Nishida, M., Kohda, T., Kaneko-Ishino, T. and Ishino, F. (1997). Peg5/Neuronatin is an imprinted gene located on sub-distal chromosome 2 in the mouse. *Nucleic Acids Res* **25**, 3428-32.

Kamiya, D., Banno, S., Sasai, N., Ohgushi, M., Inomata, H., Watanabe, K., Kawada, M., Yakura, R., Kiyonari, H., Nakao, K. et al. (2011). Intrinsic transition of embryonic stem-cell differentiation into neural progenitors. *Nature* **470**, 503-9.

Karaulanov, E., Knochel, W. and Niehrs, C. (2004). Transcriptional regulation of BMP4 synexpression in transgenic Xenopus. *EMBO J* **23**, 844-56.

Karin, M. (1995). The regulation of AP-1 activity by mitogen-activated protein kinases. *J Biol Chem* **270**, 16483-6.

Karpova, A. Y., Abe, M. K., Li, J., Liu, P. T., Rhee, J. M., Kuo, W. L. and Hershenson, M. B. (1997). MEK1 is required for PDGF-induced ERK activation and DNA synthesis in tracheal myocytes. *Am J Physiol* **272**, L558-65.

Kaufman, R. J. (1999). Stress signaling from the lumen of the endoplasmic reticulum: coordination of gene transcriptional and translational controls. *Genes Dev* **13**, 1211-33.

Kauppinen, T. M., Chan, W. Y., Suh, S. W., Wiggins, A. K., Huang, E. J. and Swanson, R. A. (2006). Direct phosphorylation and regulation of poly(ADP-ribose) polymerase-1 by extracellular signal-regulated kinases 1/2. *Proc Natl Acad Sci U S A* **103**, 7136-41.

Keller, G. (2005). Embryonic stem cell differentiation: emergence of a new era in biology and medicine. *Genes Dev* **19**, 1129-55.

Kengaku, M. and Okamoto, H. (1993). Basic fibroblast growth factor induces differentiation of neural tube and neural crest lineages of cultured ectoderm cells from Xenopus gastrula. *Development* **119**, 1067-78.

Khadka, D., Luo, T. and Sargent, T. D. (2006). Msx1 and Msx2 have shared essential functions in neural crest but may be dispensable in epidermis and axis formation in Xenopus. *Int J Dev Biol* **50**, 499-502.

Khokha, M. K., Yeh, J., Grammer, T. C. and Harland, R. M. (2005). Depletion of three BMP antagonists from Spemann's organizer leads to a catastrophic loss of dorsal structures. *Dev Cell* **8**, 401-11.

Kikyo, N., Williamson, C. M., John, R. M., Barton, S. C., Beechey, C. V., Ball, S. T., Cattanach, B. M., Surani, M. A. and Peters, J. (1997). Genetic and functional analysis of neuronatin in mice with maternal or paternal duplication of distal Chr 2. *Dev Biol* **190**, 66-77.

Kim, H. J., Kim, J. H., Bae, S. C., Choi, J. Y. and Ryoo, H. M. (2003). The protein kinase C pathway plays a central role in the fibroblast growth factor-stimulated expression and transactivation activity of Runx2. *J Biol Chem* **278**, 319-26.

Kim, J. H., Auerbach, J. M., Rodriguez-Gomez, J. A., Velasco, I., Gavin, D., Lumelsky, N., Lee, S. H., Nguyen, J., Sanchez-Pernaute, R., Bankiewicz, K. et al. (2002). Dopamine neurons derived from embryonic stem cells function in an animal model of Parkinson's disease. *Nature* **418**, 50-6.

Kinder, S. J., Tsang, T. E., Wakamiya, M., Sasaki, H., Behringer, R. R., Nagy, A. and Tam, P. P. (2001). The organizer of the mouse gastrula is composed of a dynamic population of progenitor cells for the axial mesoderm. *Development* **128**, 3623-34.

Kintner, C. R. and Dodd, J. (1991). Hensen's node induces neural tissue in Xenopus ectoderm. Implications for the action of the organizer in neural induction. *Development* **113**, 1495-505.

Kintner, C. R. and Melton, D. A. (1987). Expression of Xenopus N-CAM RNA in ectoderm is an early response to neural induction. *Development* **99**, 311-25.

Kishi, M., Mizuseki, K., Sasai, N., Yamazaki, H., Shiota, K., Nakanishi, S. and Sasai, Y. (2000). Requirement of Sox2-mediated signaling for differentiation of early Xenopus neuroectoderm. *Development (Cambridge, England)* **127**, 791-800.

Kispert, A., Ortner, H., Cooke, J. and Herrmann, B. G. (1995). The chick Brachyury gene: developmental expression pattern and response to axial induction by localized activin. *Dev Biol* **168**, 406-15.

Klee, C. B., Crouch, T. H. and Krinks, M. H. (1979). Calcineurin: a calcium- and calmodulin-binding protein of the nervous system. *Proc Natl Acad Sci U S A* **76**, 6270-3.

Klipp, E. and Liebermeister, W. (2006). Mathematical modeling of intracellular signaling pathways. *BMC Neurosci* **7 Suppl 1**, S10.

Knecht, A. K., Good, P. J., Dawid, I. B. and Harland, R. M. (1995). Dorsal-ventral patterning and differentiation of noggin-induced neural tissue in the absence of mesoderm. *Development* **121**, 1927-35.

Knoetgen, H., Viebahn, C. and Kessel, M. (1999). Head induction in the chick by primitive endoderm of mammalian, but not avian origin. *Development* **126**, 815-25.

Kornblum, H. I. (2007). Introduction to neural stem cells. *Stroke* **38**, 810-6.

Kouhara, H., Hadari, Y. R., Spivak-Kroizman, T., Schilling, J., Bar-Sagi, D., Lax, I. and Schlessinger, J. (1997). A lipid-anchored Grb2-binding protein that links FGF-receptor activation to the Ras/MAPK signaling pathway. *Cell* **89**, 693-702.

Kovacevic Grujicic, N., Mojsin, M., Krstic, A. and Stevanovic, M. (2005). Functional characterization of the human SOX3 promoter: identification of transcription factors implicated in basal promoter activity. *Gene* **344**, 287-97.

Kretzschmar, M., Liu, F., Hata, A., Doody, J. and Massague, J. (1997). The TGF-beta family mediator Smad1 is phosphorylated directly and activated functionally by the BMP receptor kinase. *Genes Dev* **11**, 984-95.

Kroll, K. L., Salic, A. N., Evans, L. M. and Kirschner, M. W. (1998). Geminin, a neuralizing molecule that demarcates the future neural plate at the onset of gastrulation. *Development* **125**, 3247-58.

Kunath, T., Saba-El-Leil, M. K., Almousailleakh, M., Wray, J., Meloche, S. and Smith, A. (2007). FGF stimulation of the Erk1/2 signalling cascade triggers transition of pluripotent embryonic stem cells from self-renewal to lineage commitment. *Development* **134**, 2895-902.

Kupzig, S., Walker, S. A. and Cullen, P. J. (2005). The frequencies of calcium oscillations are optimized for efficient calcium-mediated activation of Ras and the ERK/MAPK cascade. *Proc Natl Acad Sci U S A* **102**, 7577-82.

Kuroda, H., Fuentealba, L., Ikeda, A., Reversade, B. and De Robertis, E. M. (2005). Default neural induction: neuralization of dissociated Xenopus cells is mediated by Ras/MAPK activation. *Genes Dev* **19**, 1022-7.

Kuroda, H., Wessely, O. and De Robertis, E. M. (2004). Neural induction in Xenopus: requirement for ectodermal and endomesodermal signals via Chordin, Noggin, beta-Catenin, and Cerberus. *PLoS Biol* **2**, E92.

Lamb, T. M. and Harland, R. M. (1995). Fibroblast growth factor is a direct neural inducer, which combined with noggin generates anterior-posterior neural pattern. *Development* **121**, 3627-36.

Lang, R. J., Hashitani, H., Tonta, M. A., Suzuki, H. and Parkington, H. C. (2007). Role of Ca2+ entry and Ca2+ stores in atypical smooth muscle cell autorhythmicity in the mouse renal pelvis. *Br J Pharmacol* **152**, 1248-59.

Lanner, F., Lee, K. L., Sohl, M., Holmborn, K., Yang, H., Wilbertz, J., Poellinger, L., Rossant, J. and Farnebo, F. (2010). Heparan sulfation-

dependent fibroblast growth factor signaling maintains embryonic stem cells primed for differentiation in a heterogeneous state. *Stem Cells* **28**, 191-200.

Launay, C., Fromentoux, V., Shi, D. L. and Boucaut, J. C. (1996). A truncated FGF receptor blocks neural induction by endogenous Xenopus inducers. *Development* **122**, 869-80.

Lawlor, M. A., Mora, A., Ashby, P. R., Williams, M. R., Murray-Tait, V., Malone, L., Prescott, A. R., Lucocq, J. M. and Alessi, D. R. (2002). Essential role of PDK1 in regulating cell size and development in mice. *EMBO J* **21**, 3728-38.

Lea, R., Papalopulu, N., Amaya, E. and Dorey, K. (2009). Temporal and spatial expression of FGF ligands and receptors during Xenopus development. *Dev Dyn* **238**, 1467-79.

Leclerc, C., Lee, M., Webb, S. E., Moreau, M. and Miller, A. L. (2003). Calcium transients triggered by planar signals induce the expression of ZIC3 gene during neural induction in Xenopus. *Dev Biol* **261**, 381-90.

Leclerc, C., Neant, I. and Moreau, M. (2011). Early neural development in vertebrates is also a matter of calcium. *Biochimie* **93**, 2102-11.

Leclerc, C., Webb, S. E., Daguzan, C., Moreau, M. and Miller, A. L. (2000). Imaging patterns of calcium transients during neural induction in Xenopus laevis embryos. *J Cell Sci* **113 Pt 19**, 3519-29.

Lee, J. K., Cho, J. H., Hwang, W. S., Lee, Y. D., Reu, D. S. and Suh-Kim, H. (2000a). Expression of neuroD/BETA2 in mitotic and postmitotic neuronal cells during the development of nervous system. *Dev Dyn* **217**, 361-7.

Lee, K. W., Moreau, M., Neant, I., Bibonne, A. and Leclerc, C. (2009). FGF-activated calcium channels control neural gene expression in Xenopus. *Biochim Biophys Acta* **1793**, 1033-40.

Lee, S. H., Lumelsky, N., Studer, L., Auerbach, J. M. and McKay, R. D. (2000b). Efficient generation of midbrain and hindbrain neurons from mouse embryonic stem cells. *Nat Biotechnol* **18**, 675-9.

Levine, A. J. and Brivanlou, A. H. (2006). GDF3, a BMP inhibitor, regulates cell fate in stem cells and early embryos. *Development* **133**, 209-16.

Li, X., Thomason, P. A., Withers, D. J. and Scott, J. (2010). Bio-informatics analysis of a gene co-expression module in adipose tissue containing the diet-responsive gene Nnat. *BMC Syst Biol* **4**, 175.

Li, Y. and Camacho, P. (2004). Ca2+-dependent redox modulation of SERCA 2b by ERp57. *J Cell Biol* **164**, 35-46.

Linker, C. and Stern, C. D. (2004). Neural induction requires BMP inhibition only as a late step, and involves signals other than FGF and Wnt antagonists. *Development* **131**, 5671-81.

Lisman, J. (1994). The CaM kinase II hypothesis for the storage of synaptic memory. *Trends in neurosciences* **17**, 406-12.

Liu, S., Liang, Y., Huang, H., Wang, L., Li, Y., Li, J., Li, X. and Wang, H. (2005). ERK-dependent signaling pathway and transcriptional factor Ets-1 regulate matrix metalloproteinase-9 production in transforming growth factor-beta1 stimulated glomerular podocytes. *Cell Physiol Biochem* **16**, 207-16.

Loh, Y. H., Wu, Q., Chew, J. L., Vega, V. B., Zhang, W., Chen, X., Bourque, G., George, J., Leong, B., Liu, J. et al. (2006). The Oct4 and Nanog

transcription network regulates pluripotency in mouse embryonic stem cells. *Nat Genet* **38**, 431-40.

Lonardo, E., Parish, C. L., Ponticelli, S., Marasco, D., Ribeiro, D., Ruvo, M., De Falco, S., Arenas, E. and Minchiotti, G. (2010). A small synthetic cripto blocking Peptide improves neural induction, dopaminergic differentiation, and functional integration of mouse embryonic stem cells in a rat model of Parkinson's disease. *Stem Cells* **28**, 1326-37.

Lopez, J. J., Jardin, I., Bobe, R., Pariente, J. A., Enouf, J., Salido, G. M. and Rosado, J. A. (2008). STIM1 regulates acidic Ca2+ store refilling by interaction with SERCA3 in human platelets. *Biochem Pharmacol* **75**, 2157-64.

Lotharius, J. and Brundin, P. (2002). Pathogenesis of Parkinson's disease: dopamine, vesicles and alpha-synuclein. *Nat Rev Neurosci* **3**, 932-42.

Lyons, A. B. and Parish, C. R. (1994). Determination of lymphocyte division by flow cytometry. *J Immunol Methods* **171**, 131-7.

Lytton, J., Westlin, M. and Hanley, M. R. (1991). Thapsigargin inhibits the sarcoplasmic or endoplasmic reticulum Ca-ATPase family of calcium pumps. *J Biol Chem* **266**, 17067-71.

MacLennan, D. H. and Kranias, E. G. (2003). Phospholamban: a crucial regulator of cardiac contractility. *Nat Rev Mol Cell Biol* **4**, 566-77.

MacPhee, D. J. (2010). Methodological considerations for improving Western blot analysis. *J Pharmacol Toxicol Methods* **61**, 171-7.

Mahmood, R., Bresnick, J., Hornbruch, A., Mahony, C., Morton, N., Colquhoun, K., Martin, P., Lumsden, A., Dickson, C. and Mason, I. (1995). A role for FGF-8 in the initiation and maintenance of vertebrate limb bud outgrowth. *Curr Biol* **5**, 797-806.

Mansour, S. L., Goddard, J. M. and Capecchi, M. R. (1993). Mice homozygous for a targeted disruption of the proto-oncogene int-2 have developmental defects in the tail and inner ear. *Development* **117**, 13-28.

Marazzi, G., Wang, Y. and Sassoon, D. (1997). Msx2 is a transcriptional regulator in the BMP4-mediated programmed cell death pathway. *Dev Biol* **186**, 127-38.

Marchal, L., Luxardi, G., Thome, V. and Kodjabachian, L. (2009). BMP inhibition initiates neural induction via FGF signaling and Zic genes. *Proc Natl Acad Sci U S A* **106**, 17437-42.

Martin, G. R. (1998). The roles of FGFs in the early development of vertebrate limbs. *Genes Dev* **12**, 1571-86.

Maruoka, Y., Ohbayashi, N., Hoshikawa, M., Itoh, N., Hogan, B. L. and Furuta, Y. (1998). Comparison of the expression of three highly related genes, Fgf8, Fgf17 and Fgf18, in the mouse embryo. *Mech Dev* **74**, 175-7.

Massague, J. and Chen, Y. G. (2000). Controlling TGF-beta signaling. *Genes Dev* **14**, 627-44.

Masui, S., Nakatake, Y., Toyooka, Y., Shimosato, D., Yagi, R., Takahashi, K., Okochi, H., Okuda, A., Matoba, R., Sharov, A. A. et al. (2007). Pluripotency governed by Sox2 via regulation of Oct3/4 expression in mouse embryonic stem cells. *Nat Cell Biol* **9**, 625-35.

Mattson, M. P. (2000). Apoptosis in neurodegenerative disorders. *Nat Rev Mol Cell Biol* **1**, 120-9.

Matzuk, M. M., Lu, N., Vogel, H., Sellheyer, K., Roop, D. R. and Bradley, A. (1995). Multiple defects and perinatal death in mice deficient in follistatin. *Nature* **374**, 360-3.

McManus, E. J., Sakamoto, K., Armit, L. J., Ronaldson, L., Shpiro, N., Marquez, R. and Alessi, D. R. (2005). Role that phosphorylation of GSK3 plays in insulin and Wnt signalling defined by knockin analysis. *EMBO J* **24**, 1571-83.

Meisenhelder, J., Suh, P. G., Rhee, S. G. and Hunter, T. (1989). Phospholipase C-gamma is a substrate for the PDGF and EGF receptor protein-tyrosine kinases in vivo and in vitro. *Cell* **57**, 1109-22.

Messam, C. A., Hou, J. and Major, E. O. (2000). Coexpression of nestin in neural and glial cells in the developing human CNS defined by a human-specific anti-nestin antibody. *Exp Neurol* **161**, 585-96.

Milanini-Mongiat, J., Pouyssegur, J. and Pages, G. (2002). Identification of two Sp1 phosphorylation sites for p42/p44 mitogen-activated protein kinases: their implication in vascular endothelial growth factor gene transcription. *J Biol Chem* **277**, 20631-9.

Minchiotti, G. (2005). Nodal-dependant Cripto signaling in ES cells: from stem cells to tumor biology. *Oncogene* **24**, 5668-75.

Missiaen, L., Taylor, C. W. and Berridge, M. J. (1991). Spontaneous calcium release from inositol trisphosphate-sensitive calcium stores. *Nature* **352**, 241-4.

Mitsui, K., Tokuzawa, Y., Itoh, H., Segawa, K., Murakami, M., Takahashi, K., Maruyama, M., Maeda, M. and Yamanaka, S. (2003). The homeoprotein Nanog is required for maintenance of pluripotency in mouse epiblast and ES cells. *Cell* **113**, 631-42.

Miyazono, K., Maeda, S. and Imamura, T. (2005). BMP receptor signaling: transcriptional targets, regulation of signals, and signaling cross-talk. *Cytokine Growth Factor Rev* **16**, 251-63.

Molenaar, M., van de Wetering, M., Oosterwegel, M., Peterson-Maduro, J., Godsave, S., Korinek, V., Roose, J., Destree, O. and Clevers, H. (1996). XTcf-3 transcription factor mediates beta-catenin-induced axis formation in Xenopus embryos. *Cell* **86**, 391-9.

Mukhopadhyay, M., Shtrom, S., Rodriguez-Esteban, C., Chen, L., Tsukui, T., Gomer, L., Dorward, D. W., Glinka, A., Grinberg, A., Huang, S. P. et al. (2001). Dickkopf1 is required for embryonic head induction and limb morphogenesis in the mouse. *Dev Cell* **1**, 423-34.

Munoz-Sanjuan, I. and Brivanlou, A. H. (2002). Neural induction, the default model and embryonic stem cells. *Nat Rev Neurosci* **3**, 271-80.

Munoz-Sanjuan, I., Smallwood, P. M. and Nathans, J. (2000). Isoform diversity among fibroblast growth factor homologous factors is generated by alternative promoter usage and differential splicing. *J Biol Chem* **275**, 2589-97.

Murayama, A., Matsuzaki, Y., Kawaguchi, A., Shimazaki, T. and Okano, H. (2002). Flow cytometric analysis of neural stem cells in the developing and adult mouse brain. *J Neurosci Res* **69**, 837-47.

Murry, C. E. and Keller, G. (2008). Differentiation of embryonic stem cells to clinically relevant populations: lessons from embryonic development. *Cell* **132**, 661-80.

Naito, A. T., Shiojima, I., Akazawa, H., Hidaka, K., Morisaki, T., Kikuchi, A. and Komuro, I. (2006). Developmental stage-specific biphasic roles of Wnt/beta-catenin signaling in cardiomyogenesis and hematopoiesis. *Proc Natl Acad Sci U S A* **103**, 19812-7.

Nakao, A., Afrakhte, M., Moren, A., Nakayama, T., Christian, J. L., Heuchel, R., Itoh, S., Kawabata, M., Heldin, N. E., Heldin, C. H. et al. (1997). Identification of Smad7, a TGFbeta-inducible antagonist of TGF-beta signalling. *Nature* **389**, 631-5.

Nakata, K., Nagai, T., Aruga, J. and Mikoshiba, K. (1997). Xenopus Zic3, a primary regulator both in neural and neural crest development. *Proc Natl Acad Sci U S A* **94**, 11980-5.

Nakata, K., Nagai, T., Aruga, J. and Mikoshiba, K. (1998). Xenopus Zic family and its role in neural and neural crest development. *Mech Dev* **75**, 43-51.

Nave, B. T., Ouwens, M., Withers, D. J., Alessi, D. R. and Shepherd, P. R. (1999). Mammalian target of rapamycin is a direct target for protein kinase B: identification of a convergence point for opposing effects of insulin and amino-acid deficiency on protein translation. *Biochem J* **344 Pt 2**, 427-31.

Nichols, J., Zevnik, B., Anastassiadis, K., Niwa, H., Klewe-Nebenius, D., Chambers, I., Scholer, H. and Smith, A. (1998). Formation of pluripotent stem cells in the mammalian embryo depends on the POU transcription factor Oct4. *Cell* **95**, 379-91.

Niehrs, C., Keller, R., Cho, K. W. and De Robertis, E. M. (1993). The homeobox gene goosecoid controls cell migration in Xenopus embryos. *Cell* **72**, 491-503.

Niehrs, C., Steinbeisser, H. and De Robertis, E. M. (1994). Mesodermal patterning by a gradient of the vertebrate homeobox gene goosecoid. *Science* **263**, 817-20.

Niswander, L. and Martin, G. R. (1992). Fgf-4 expression during gastrulation, myogenesis, limb and tooth development in the mouse. *Development* **114**, 755-68.

Nitta, K. R., Tanegashima, K., Takahashi, S. and Asashima, M. (2004). XSIP1 is essential for early neural gene expression and neural differentiation by suppression of BMP signaling. *Dev Biol* **275**, 258-67.

Ohtsuka, T., Shimojo, H., Matsunaga, M., Watanabe, N., Kometani, K., Minato, N. and Kageyama, R. (2011). Gene expression profiling of neural stem cells and identification of regulators of neural differentiation during cortical development. *Stem Cells* **29**, 1817-28.

Ornitz, D. M. and Itoh, N. (2001). Fibroblast growth factors. *Genome Biol* **2**, REVIEWS3005.

Osada, S. I. and Wright, C. V. (1999). Xenopus nodal-related signaling is essential for mesendodermal patterning during early embryogenesis. *Development* **126**, 3229-40.

Osterlund, C., Wramsby, H. and Pousette, A. (1996). Temporal expression of platelet-derived growth factor (PDGF)-A and its receptor in human preimplantation embryos. *Mol Hum Reprod* **2**, 507-12.

Oyang, E. L., Davidson, B. C., Lee, W. and Poon, M. M. (2011). Functional characterization of the dendritically localized mRNA neuronatin in hippocampal neurons. *PLoS One* **6**, e24879.

Pages, G. (2007). Sp3-mediated VEGF regulation is dependent on phosphorylation by extra-cellular signals regulated kinases (Erk). *Journal of cellular physiology* **213**, 454-63.

Paik, J. H., Ding, Z., Narurkar, R., Ramkissoon, S., Muller, F., Kamoun, W. S., Chae, S. S., Zheng, H., Ying, H., Mahoney, J. et al. (2009). FoxOs cooperatively regulate diverse pathways governing neural stem cell homeostasis. *Cell Stem Cell* **5**, 540-53.

Palmieri, S. L., Peter, W., Hess, H. and Scholer, H. R. (1994). Oct-4 transcription factor is differentially expressed in the mouse embryo during establishment of the first two extraembryonic cell lineages involved in implantation. *Dev Biol* **166**, 259-67.

Pandolfi, P. P., Roth, M. E., Karis, A., Leonard, M. W., Dzierzak, E., Grosveld, F. G., Engel, J. D. and Lindenbaum, M. H. (1995). Targeted disruption of the GATA3 gene causes severe abnormalities in the nervous system and in fetal liver haematopoiesis. *Nat Genet* **11**, 40-4.

Papanayotou, C., Mey, A., Birot, A. M., Saka, Y., Boast, S., Smith, J. C., Samarut, J. and Stern, C. D. (2008). A mechanism regulating the onset of Sox2 expression in the embryonic neural plate. *PLoS Biol* **6**, e2.

Paratore, C., Brugnoli, G., Lee, H. Y., Suter, U. and Sommer, L. (2002). The role of the Ets domain transcription factor Erm in modulating differentiation of neural crest stem cells. *Dev Biol* **250**, 168-80.

Parisi, S., D'Andrea, D., Lago, C. T., Adamson, E. D., Persico, M. G. and Minchiotti, G. (2003). Nodal-dependent Cripto signaling promotes cardiomyogenesis and redirects the neural fate of embryonic stem cells. *J Cell Biol* **163**, 303-14.

Patani, R., Compston, A., Puddifoot, C. A., Wyllie, D. J., Hardingham, G. E., Allen, N. D. and Chandran, S. (2009). Activin/Nodal inhibition alone accelerates highly efficient neural conversion from human embryonic stem cells and imposes a caudal positional identity. *PLoS One* **4**, e7327.

Pawlak, M. R., Scherer, C. A., Chen, J., Roshon, M. J. and Ruley, H. E. (2000). Arginine N-methyltransferase 1 is required for early postimplantation mouse development, but cells deficient in the enzyme are viable. *Molecular and cellular biology* **20**, 4859-69.

Peck, A. B. and Bach, F. H. (1973). A miniaturized mouse mixed leukocyte culture in serum-free and mouse serum supplemented media. *J Immunol Methods* **3**, 147-63.

Pegoraro, C., Pollet, N. and Monsoro-Burq, A. H. (2011). Tissue-specific expression of Sarcoplasmic/Endoplasmic Reticulum Calcium ATPases (ATP2A/SERCA) 1, 2, 3 during Xenopus laevis development. *Gene Expr Patterns* **11**, 122-8.

Pellegrini, L. (2001). Role of heparan sulfate in fibroblast growth factor signalling: a structural view. *Curr Opin Struct Biol* **11**, 629-34.

Penkov, L. I., Platonov, E. S. and New, D. A. (2001). Effects of fibroblast growth factor 2 and insulin-like growth factor II on the development of parthenogenetic mouse embryos in vitro. *In Vitro Cell Dev Biol Anim* **37**, 440-4.

Pera, E. M., Ikeda, A., Eivers, E. and De Robertis, E. M. (2003). Integration of IGF, FGF, and anti-BMP signals via Smad1 phosphorylation in neural induction. *Genes Dev* **17**, 3023-8.

Periasamy, M. and Kalyanasundaram, A. (2007). SERCA pump isoforms: their role in calcium transport and disease. *Muscle Nerve* **35**, 430-42.

Periasamy, M., Reed, T. D., Liu, L. H., Ji, Y., Loukianov, E., Paul, R. J., Nieman, M. L., Riddle, T., Duffy, J. J., Doetschman, T. et al. (1999). Impaired cardiac performance in heterozygous mice with a null mutation in the sarco(endo)plasmic reticulum Ca2+-ATPase isoform 2 (SERCA2) gene. *J Biol Chem* **274**, 2556-62.

Pesce, M. and Scholer, H. R. (2001). Oct-4: gatekeeper in the beginnings of mammalian development. *Stem Cells* **19**, 271-8.

Peters, K. G., Marie, J., Wilson, E., Ives, H. E., Escobedo, J., Del Rosario, M., Mirda, D. and Williams, L. T. (1992). Point mutation of an FGF receptor abolishes phosphatidylinositol turnover and Ca2+ flux but not mitogenesis. *Nature* **358**, 678-81.

Pevny, L. and Placzek, M. (2005). SOX genes and neural progenitor identity. *Curr Opin Neurobiol* **15**, 7-13.

Phippard, D. J., Weber-Hall, S. J., Sharpe, P. T., Naylor, M. S., Jayatalake, H., Maas, R., Woo, I., Roberts-Clark, D., Francis-West, P. H., Liu, Y. H. et al. (1996). Regulation of Msx-1, Msx-2, Bmp-2 and Bmp-4 during foetal and postnatal mammary gland development. *Development* **122**, 2729-37.

Piccolo, S., Sasai, Y., Lu, B. and De Robertis, E. M. (1996). Dorsoventral patterning in Xenopus: inhibition of ventral signals by direct binding of chordin to BMP-4. *Cell* **86**, 589-98.

Postigo, A. A. (2003). Opposing functions of ZEB proteins in the regulation of the TGFbeta/BMP signaling pathway. *EMBO J* **22**, 2443-52.

Poulain, M., Furthauer, M., Thisse, B., Thisse, C. and Lepage, T. (2006). Zebrafish endoderm formation is regulated by combinatorial Nodal, FGF and BMP signalling. *Development* **133**, 2189-200.

Poulin, G., Turgeon, B. and Drouin, J. (1997). NeuroD1/beta2 contributes to cell-specific transcription of the proopiomelanocortin gene. *Molecular and cellular biology* **17**, 6673-82.

Prasad, V., Okunade, G. W., Miller, M. L. and Shull, G. E. (2004). Phenotypes of SERCA and PMCA knockout mice. *Biochem Biophys Res Commun* **322**, 1192-203.

Raff, M. C., Miller, R. H. and Noble, M. (1983). A glial progenitor cell that develops in vitro into an astrocyte or an oligodendrocyte depending on culture medium. *Nature* **303**, 390-6.

Rappolee, D. A., Basilico, C., Patel, Y. and Werb, Z. (1994). Expression and function of FGF-4 in peri-implantation development in mouse embryos. *Development* **120**, 2259-69.

Rathjen, J., Lake, J. A., Bettess, M. D., Washington, J. M., Chapman, G. and Rathjen, P. D. (1999). Formation of a primitive ectoderm like cell population, EPL cells, from ES cells in response to biologically derived factors. *J Cell Sci* **112 (Pt 5)**, 601-12.

Ratzka, A., Baron, O. and Grothe, C. (2011). FGF-2 deficiency does not influence FGF ligand and receptor expression during development of the nigrostriatal system. *PLoS One* **6**, e23564.

Revill, K., Dudley, K. J., Clayton, R. N., McNicol, A. M. and Farrell, W. E. (2009). Loss of neuronatin expression is associated with promoter hypermethylation in pituitary adenoma. *Endocr Relat Cancer* **16**, 537-48.

Rex, M., Orme, A., Uwanogho, D., Tointon, K., Wigmore, P. M., Sharpe, P. T. and Scotting, P. J. (1997). Dynamic expression of chicken Sox2 and Sox3 genes in ectoderm induced to form neural tissue. *Dev Dyn* **209**, 323-32.

Reynolds, B. A. and Rietze, R. L. (2005). Neural stem cells and neurospheres--re-evaluating the relationship. *Nat Methods* **2**, 333-6.

Riddle, R. C., Taylor, A. F., Genetos, D. C. and Donahue, H. J. (2006). MAP kinase and calcium signaling mediate fluid flow-induced human mesenchymal stem cell proliferation. *Am J Physiol Cell Physiol* **290**, C776-84.

Rodriguez-Gallardo, L., Climent, V., Garcia-Martinez, V., Schoenwolf, G. C. and Alvarez, I. S. (1997). Targeted over-expression of FGF in chick embryos induces formation of ectopic neural cells. *Int J Dev Biol* **41**, 715-23.

Rodriguez-Mora, O. G., LaHair, M. M., McCubrey, J. A. and Franklin, R. A. (2005). Calcium/calmodulin-dependent kinase I and calcium/calmodulin-dependent kinase kinase participate in the control of cell cycle progression in MCF-7 human breast cancer cells. *Cancer Res* **65**, 5408-16.

Rogers, C. D., Archer, T. C., Cunningham, D. D., Grammer, T. C. and Casey, E. M. (2008). Sox3 expression is maintained by FGF signaling and restricted to the neural plate by Vent proteins in the Xenopus embryo. *Dev Biol* **313**, 307-19.

Rogers, C. D., Harafuji, N., Archer, T., Cunningham, D. D. and Casey, E. S. (2009). Xenopus Sox3 activates sox2 and geminin and indirectly represses Xvent2 expression to induce neural progenitor formation at the expense of non-neural ectodermal derivatives. *Mech Dev* **126**, 42-55.

Rosner, M. H., Vigano, M. A., Ozato, K., Timmons, P. M., Poirier, F., Rigby, P. W. and Staudt, L. M. (1990). A POU-domain transcription factor in early stem cells and germ cells of the mammalian embryo. *Nature* **345**, 686-92.

Rowitch, D. H. and McMahon, A. P. (1995). Pax-2 expression in the murine neural plate precedes and encompasses the expression domains of Wnt-1 and En-1. *Mech Dev* **52**, 3-8.

Saffer, J. D., Jackson, S. P. and Annarella, M. B. (1991). Developmental expression of Sp1 in the mouse. *Molecular and cellular biology* **11**, 2189-99.

Salomonis, N., Schlieve, C. R., Pereira, L., Wahlquist, C., Colas, A., Zambon, A. C., Vranizan, K., Spindler, M. J., Pico, A. R., Cline, M. S. et al. (2010). Alternative splicing regulates mouse embryonic stem cell pluripotency and differentiation. *Proc Natl Acad Sci U S A* **107**, 10514-9.

Sapkota, G., Alarcon, C., Spagnoli, F. M., Brivanlou, A. H. and Massague, J. (2007). Balancing BMP signaling through integrated inputs into the Smad1 linker. *Mol Cell* **25**, 441-54.

Sasai, Y., Lu, B., Piccolo, S. and De Robertis, E. M. (1996). Endoderm induction by the organizer-secreted factors chordin and noggin in Xenopus animal caps. *EMBO J* **15**, 4547-55.

Sasai, Y., Lu, B., Steinbeisser, H. and De Robertis, E. M. (1995). Regulation of neural induction by the Chd and Bmp-4 antagonistic patterning signals in Xenopus. *Nature* **376**, 333-6.

Sasai, Y., Lu, B., Steinbeisser, H., Geissert, D., Gont, L. K. and De Robertis, E. M. (1994). Xenopus chordin: a novel dorsalizing factor activated by organizer-specific homeobox genes. *Cell* **79**, 779-90.

Schlessinger, J. (2004). Common and distinct elements in cellular signaling via EGF and FGF receptors. *Science* **306**, 1506-7.

Schlessinger, J., Plotnikov, A. N., Ibrahimi, O. A., Eliseenkova, A. V., Yeh, B. K., Yayon, A., Linhardt, R. J. and Mohammadi, M. (2000). Crystal structure of a ternary FGF-FGFR-heparin complex reveals a dual role for heparin in FGFR binding and dimerization. *Mol Cell* **6**, 743-50.

Schneider, V. A. and Mercola, M. (2001). Wnt antagonism initiates cardiogenesis in Xenopus laevis. *Genes Dev* **15**, 304-15.

Schuldiner, M., Yanuka, O., Itskovitz-Eldor, J., Melton, D. A. and Benvenisty, N. (2000). Effects of eight growth factors on the differentiation of cells derived from human embryonic stem cells. *Proc Natl Acad Sci U S A* **97**, 11307-12.

Schulte-Merker, S. and Smith, J. C. (1995). Mesoderm formation in response to Brachyury requires FGF signalling. *Curr Biol* **5**, 62-7.

Scott, P. H. and Lawrence, J. C., Jr. (1997). Insulin activates a PD 098059-sensitive kinase that is involved in the regulation of p70S6K and PHAS-I. *FEBS Lett* **409**, 171-6.

Selander, L. and Edlund, H. (2002). Nestin is expressed in mesenchymal and not epithelial cells of the developing mouse pancreas. *Mech Dev* **113**, 189-92.

Selleck, M. A. and Stern, C. D. (1991). Fate mapping and cell lineage analysis of Hensen's node in the chick embryo. *Development* **112**, 615-26.

Sharma, G. and Vijayaraghavan, S. (2001). Nicotinic cholinergic signaling in hippocampal astrocytes involves calcium-induced calcium release from intracellular stores. *Proc Natl Acad Sci U S A* **98**, 4148-53.

Sharma, J., Rao, S. N., Shankar, S. K., Satishchandra, P. and Jana, N. R. (2011). Lafora disease ubiquitin ligase malin promotes proteasomal degradation of neuronatin and regulates glycogen synthesis. *Neurobiol Dis* **44**, 133-41.

Sheng, G., dos Reis, M. and Stern, C. D. (2003). Churchill, a zinc finger transcriptional activator, regulates the transition between gastrulation and neurulation. *Cell* **115**, 603-13.

Shi, Y., Katsev, S., Cai, C. and Evans, S. (2000). BMP signaling is required for heart formation in vertebrates. *Developmental biology* **224**, 226-37.

Shi, Y. and Massague, J. (2003). Mechanisms of TGF-beta signaling from cell membrane to the nucleus. *Cell* **113**, 685-700.

Shimada, T., Hasegawa, H., Yamazaki, Y., Muto, T., Hino, R., Takeuchi, Y., Fujita, T., Nakahara, K., Fukumoto, S. and Yamashita, T. (2004). FGF-23 is a potent regulator of vitamin D metabolism and phosphate homeostasis. *J Bone Miner Res* **19**, 429-35.

Siu, I. M., Bai, R., Gallia, G. L., Edwards, J. B., Tyler, B. M., Eberhart, C. G. and Riggins, G. J. (2008). Coexpression of neuronatin splice forms promotes medulloblastoma growth. *Neuro Oncol* **10**, 716-24.

Slusarski, D. C. and Pelegri, F. (2007). Calcium signaling in vertebrate embryonic patterning and morphogenesis. *Dev Biol* **307**, 1-13.

Smallwood, P. M., Munoz-Sanjuan, I., Tong, P., Macke, J. P., Hendry, S. H., Gilbert, D. J., Copeland, N. G., Jenkins, N. A. and Nathans, J. (1996). Fibroblast growth factor (FGF) homologous factors: new members of the FGF family implicated in nervous system development. *Proc Natl Acad Sci U S A* **93**, 9850-7.

Smith, J. C., Price, B. M., Green, J. B., Weigel, D. and Herrmann, B. G. (1991). Expression of a Xenopus homolog of Brachyury (T) is an immediate-early response to mesoderm induction. *Cell* **67**, 79-87.

Smith, W. C. and Harland, R. M. (1992). Expression cloning of noggin, a new dorsalizing factor localized to the Spemann organizer in Xenopus embryos. *Cell* **70**, 829-40.

Snetkov, V. A., Smirnov, S. V., Kua, J., Aaronson, P. I., Ward, J. P. and Knock, G. A. (2010). Superoxide differentially controls pulmonary and systemic vascular tone through multiple signalling pathways. *Cardiovasc Res* **89**, 214-24.

Sobue, K., Muramoto, Y., Fujita, M. and Kakiuchi, S. (1981). Calmodulin-binding protein of erythrocyte cytoskeleton. *Biochem Biophys Res Commun* **100**, 1063-70.

Sousa-Nunes, R., Rana, A. A., Kettleborough, R., Brickman, J. M., Clements, M., Forrest, A., Grimmond, S., Avner, P., Smith, J. C., Dunwoodie, S. L. et al. (2003). Characterizing embryonic gene expression patterns in the mouse using nonredundant sequence-based selection. *Genome Res* **13**, 2609-20.

Spann, P., Ginsburg, M., Rangini, Z., Fainsod, A., Eyal-Giladi, H. and Gruenbaum, Y. (1994). The spatial and temporal dynamics of Sax1 (CHox3) homeobox gene expression in the chick's spinal cord. *Development* **120**, 1817-28.

Spemann, H. and Mangold, H. (2001). Induction of embryonic primordia by implantation of organizers from a different species. 1923. *Int J Dev Biol* **45**, 13-38.

Stavridis, M. P., Lunn, J. S., Collins, B. J. and Storey, K. G. (2007). A discrete period of FGF-induced Erk1/2 signalling is required for vertebrate neural specification. *Development* **134**, 2889-94.

Stern, C. D. (2005). Neural induction: old problem, new findings, yet more questions. *Development* **132**, 2007-21.

Stern, C. D. (2006). Neural induction: 10 years on since the 'default model'. *Curr Opin Cell Biol* **18**, 692-7.

Stern, M. D., Capogrossi, M. C. and Lakatta, E. G. (1988). Spontaneous calcium release from the sarcoplasmic reticulum in myocardial cells: mechanisms and consequences. *Cell Calcium* **9**, 247-56.

Stitt, T. N., Drujan, D., Clarke, B. A., Panaro, F., Timofeyva, Y., Kline, W. O., Gonzalez, M., Yancopoulos, G. D. and Glass, D. J. (2004). The IGF-1/PI3K/Akt pathway prevents expression of muscle atrophy-induced ubiquitin ligases by inhibiting FOXO transcription factors. *Mol Cell* **14**, 395-403.

Storey, K. G., Crossley, J. M., De Robertis, E. M., Norris, W. E. and Stern, C. D. (1992). Neural induction and regionalisation in the chick embryo. *Development* **114**, 729-41.

Storey, K. G., Goriely, A., Sargent, C. M., Brown, J. M., Burns, H. D., Abud, H. M. and Heath, J. K. (1998). Early posterior neural tissue is induced by FGF in the chick embryo. *Development* **125**, 473-84.

Streit, A., Berliner, A. J., Papanayotou, C., Sirulnik, A. and Stern, C. D. (2000). Initiation of neural induction by FGF signalling before gastrulation. *Nature* **406**, 74-8.

Streit, A., Lee, K. J., Woo, I., Roberts, C., Jessell, T. M. and Stern, C. D. (1998). Chordin regulates primitive streak development and the stability of induced neural cells, but is not sufficient for neural induction in the chick embryo. *Development* **125**, 507-19.

Streit, A. and Stern, C. D. (1999a). Establishment and maintenance of the border of the neural plate in the chick: involvement of FGF and BMP activity. *Mech Dev* **82**, 51-66.

Streit, A. and Stern, C. D. (1999b). Mesoderm patterning and somite formation during node regression: differential effects of chordin and noggin. *Mech Dev* **85**, 85-96.

Suh, Y. H., Kim, W. H., Moon, C., Hong, Y. H., Eun, S. Y., Lim, J. H., Choi, J. S., Song, J. and Jung, M. H. (2005). Ectopic expression of Neuronatin potentiates adipogenesis through enhanced phosphorylation of cAMP-response element-binding protein in 3T3-L1 cells. *Biochem Biophys Res Commun* **337**, 481-9.

Sun, X., Meyers, E. N., Lewandoski, M. and Martin, G. R. (1999). Targeted disruption of Fgf8 causes failure of cell migration in the gastrulating mouse embryo. *Genes Dev* **13**, 1834-46.

Suter, D. M. and Krause, K. H. (2008). Neural commitment of embryonic stem cells: molecules, pathways and potential for cell therapy. *J Pathol* **215**, 355-68.

Suzuki, A., Raya, A., Kawakami, Y., Morita, M., Matsui, T., Nakashima, K., Gage, F. H., Rodriguez-Esteban, C. and Izpisua Belmonte, J. C. (2006). Nanog binds to Smad1 and blocks bone morphogenetic protein-induced differentiation of embryonic stem cells. *Proc Natl Acad Sci U S A* **103**, 10294-9.

Suzuki, A., Ueno, N. and Hemmati-Brivanlou, A. (1997). Xenopus msx1 mediates epidermal induction and neural inhibition by BMP4. *Development* **124**, 3037-44.

Tam, P. P. and Loebel, D. A. (2007). Gene function in mouse embryogenesis: get set for gastrulation. *Nat Rev Genet* **8**, 368-81.

Temple, S. (2001). The development of neural stem cells. *Nature* **414**, 112-7.

Thisse, B. and Thisse, C. (2005). Functions and regulations of fibroblast growth factor signaling during embryonic development. *Dev Biol* **287**, 390-402.

Tremblay, K. D., Hoodless, P. A., Bikoff, E. K. and Robertson, E. J. (2000). Formation of the definitive endoderm in mouse is a Smad2-dependent process. *Development* **127**, 3079-90.

Tropepe, V., Hitoshi, S., Sirard, C., Mak, T. W., Rossant, J. and van der Kooy, D. (2001). Direct neural fate specification from embryonic stem cells: a primitive mammalian neural stem cell stage acquired through a default mechanism. *Neuron* **30**, 65-78.

Tropepe, V., Li, S., Dickinson, A., Gamse, J. T. and Sive, H. L. (2006). Identification of a BMP inhibitor-responsive promoter module required for expression of the early neural gene zic1. *Dev Biol* **289**, 517-29.

Tsang, M. and Dawid, I. B. (2004). Promotion and attenuation of FGF signaling through the Ras-MAPK pathway. *Sci STKE* **2004**, pe17.

Tsien, R. Y., Pozzan, T. and Rink, T. J. (1982). Calcium homeostasis in intact lymphocytes: cytoplasmic free calcium monitored with a new, intracellularly trapped fluorescent indicator. *J Cell Biol* **94**, 325-34.

Tucker, A. S., Al Khamis, A. and Sharpe, P. T. (1998). Interactions between Bmp-4 and Msx-1 act to restrict gene expression to odontogenic mesenchyme. *Dev Dyn* **212**, 533-9.

Turner, N. and Grose, R. (2010). Fibroblast growth factor signalling: from development to cancer. *Nat Rev Cancer* **10**, 116-29.

Uchihara, T., Okubo, C., Tanaka, R., Minami, Y., Inadome, Y., Iijima, T., Morishita, Y., Fujita, J. and Noguchi, M. (2007). Neuronatin expression and its clinicopathological significance in pulmonary non-small cell carcinoma. *J Thorac Oncol* **2**, 796-801.

Uchikawa, M., Ishida, Y., Takemoto, T., Kamachi, Y. and Kondoh, H. (2003). Functional analysis of chicken Sox2 enhancers highlights an array of diverse regulatory elements that are conserved in mammals. *Dev Cell* **4**, 509-19.

Uchikawa, M., Takemoto, T., Kamachi, Y. and Kondoh, H. (2004). Efficient identification of regulatory sequences in the chicken genome by a powerful combination of embryo electroporation and genome comparison. *Mech Dev* **121**, 1145-58.

Ueda, Y., Hirai, S., Osada, S., Suzuki, A., Mizuno, K. and Ohno, S. (1996). Protein kinase C activates the MEK-ERK pathway in a manner independent of Ras and dependent on Raf. *J Biol Chem* **271**, 23512-9.

Vaccarino, F. M., Schwartz, M. L., Raballo, R., Nilsen, J., Rhee, J., Zhou, M., Doetschman, T., Coffin, J. D., Wyland, J. J. and Hung, Y. T. (1999). Changes in cerebral cortex size are governed by fibroblast growth factor during embryogenesis. *Nat Neurosci* **2**, 246-53.

Vallier, L., Touboul, T., Chng, Z., Brimpari, M., Hannan, N., Millan, E., Smithers, L. E., Trotter, M., Rugg-Gunn, P., Weber, A. et al. (2009). Early cell fate decisions of human embryonic stem cells and mouse epiblast stem cells are controlled by the same signalling pathways. *PLoS One* **4**, e6082.

van Der Luit, A. H., Olivari, C., Haley, A., Knight, M. R. and Trewavas, A. J. (1999). Distinct calcium signaling pathways regulate calmodulin gene expression in tobacco. *Plant Physiol* **121**, 705-14.

Verani, R., Cappuccio, I., Spinsanti, P., Gradini, R., Caruso, A., Magnotti, M. C., Motolese, M., Nicoletti, F. and Melchiorri, D. (2007). Expression of the Wnt inhibitor Dickkopf-1 is required for the induction of neural markers in mouse embryonic stem cells differentiating in response to retinoic acid. *J Neurochem* **100**, 242-50.

Verschueren, K., Remacle, J. E., Collart, C., Kraft, H., Baker, B. S., Tylzanowski, P., Nelles, L., Wuytens, G., Su, M. T., Bodmer, R. et al. (1999). SIP1, a novel zinc finger/homeodomain repressor, interacts with Smad proteins and binds to 5'-CACCT sequences in candidate target genes. *J Biol Chem* **274**, 20489-98.

Vincent, S. D., Dunn, N. R., Hayashi, S., Norris, D. P. and Robertson, E. J. (2003). Cell fate decisions within the mouse organizer are governed by graded Nodal signals. *Genes Dev* **17**, 1646-62.

Vrang, N., Meyre, D., Froguel, P., Jelsing, J., Tang-Christensen, M., Vatin, V., Mikkelsen, J. D., Thirstrup, K., Larsen, L. K., Cullberg, K. B. et al. (2010). The imprinted gene neuronatin is regulated by metabolic status and associated with obesity. *Obesity (Silver Spring)* **18**, 1289-96.

Wada, K., Nakajima, A., Katayama, K., Kudo, C., Shibuya, A., Kubota, N., Terauchi, Y., Tachibana, M., Miyoshi, H., Kamisaki, Y. et al. (2006). Peroxisome proliferator-activated receptor gamma-mediated regulation of neural stem cell proliferation and differentiation. *J Biol Chem* **281**, 12673-81.

Wang, E. A., Rosen, V., D'Alessandro, J. S., Bauduy, M., Cordes, P., Harada, T., Israel, D. I., Hewick, R. M., Kerns, K. M., LaPan, P. et al. (1990). Recombinant human bone morphogenetic protein induces bone formation. *Proc Natl Acad Sci U S A* **87**, 2220-4.

Wang, H., Huang, Z. Q., Xia, L., Feng, Q., Erdjument-Bromage, H., Strahl, B. D., Briggs, S. D., Allis, C. D., Wong, J., Tempst, P. et al. (2001). Methylation of histone H4 at arginine 3 facilitating transcriptional activation by nuclear hormone receptor. *Science* **293**, 853-7.

Wang, Q., Matsumoto, Y., Shindo, T., Miyake, K., Shindo, A., Kawanishi, M., Kawai, N., Tamiya, T. and Nagao, S. (2006). Neural stem cells transplantation in cortex in a mouse model of Alzheimer's disease. *J Med Invest* **53**, 61-9.

Wang, S. H., Sun, Z. L., Guo, Y. J., Yuan, Y. and Li, L. (2009). PPARgamma-mediated advanced glycation end products regulation of neural stem cells. *Mol Cell Endocrinol* **307**, 176-84.

Wawersik, S., Evola, C. and Whitman, M. (2005). Conditional BMP inhibition in Xenopus reveals stage-specific roles for BMPs in neural and neural crest induction. *Dev Biol* **277**, 425-42.

Wei, F., Qiu, C. S., Liauw, J., Robinson, D. A., Ho, N., Chatila, T. and Zhuo, M. (2002). Calcium calmodulin-dependent protein kinase IV is required for fear memory. *Nat Neurosci* **5**, 573-9.

Weissman, T. A., Riquelme, P. A., Ivic, L., Flint, A. C. and Kriegstein, A. R. (2004). Calcium waves propagate through radial glial cells and modulate proliferation in the developing neocortex. *Neuron* **43**, 647-61.

Weng, Q., Chen, Y., Wang, H., Xu, X., Yang, B., He, Q., Shou, W., Higashi, Y., van den Berghe, V., Seuntjens, E. et al. (2012). Dual-mode modulation of Smad signaling by Smad-interacting protein Sip1 is required for myelination in the central nervous system. *Neuron* **73**, 713-28.

Wessely, O., Agius, E., Oelgeschlager, M., Pera, E. M. and De Robertis, E. M. (2001). Neural induction in the absence of mesoderm: beta-catenin-dependent expression of secreted BMP antagonists at the blastula stage in Xenopus. *Dev Biol* **234**, 161-73.

Wiebe, M. S., Wilder, P. J., Kelly, D. and Rizzino, A. (2000). Isolation, characterization, and differential expression of the murine Sox-2 promoter. *Gene* **246**, 383-93.

Wijnholds, J., Chowdhury, K., Wehr, R. and Gruss, P. (1995). Segment-specific expression of the neuronatin gene during early hindbrain development. *Dev Biol* **171**, 73-84.

Wilkinson, D. G., Peters, G., Dickson, C. and McMahon, A. P. (1988). Expression of the FGF-related proto-oncogene int-2 during gastrulation and neurulation in the mouse. *EMBO J* **7**, 691-5.

Wilson, P. A. and Hemmati-Brivanlou, A. (1995). Induction of epidermis and inhibition of neural fate by Bmp-4. *Nature* **376**, 331-3.

Wilson, P. A., Lagna, G., Suzuki, A. and Hemmati-Brivanlou, A. (1997). Concentration-dependent patterning of the Xenopus ectoderm by BMP4 and its signal transducer Smad1. *Development* **124**, 3177-84.

Wilson, S. I. and Edlund, T. (2001). Neural induction: toward a unifying mechanism. *Nat Neurosci* **4 Suppl**, 1161-8.

Wilson, S. I., Graziano, E., Harland, R., Jessell, T. M. and Edlund, T. (2000). An early requirement for FGF signalling in the acquisition of neural cell fate in the chick embryo. *Curr Biol* **10**, 421-9.

Wilson, S. I., Rydstrom, A., Trimborn, T., Willert, K., Nusse, R., Jessell, T. M. and Edlund, T. (2001). The status of Wnt signalling regulates neural and epidermal fates in the chick embryo. *Nature* **411**, 325-30.

Wilson, V., Manson, L., Skarnes, W. C. and Beddington, R. S. (1995). The T gene is necessary for normal mesodermal morphogenetic cell movements during gastrulation. *Development* **121**, 877-86.

Wood, H. B. and Episkopou, V. (1999). Comparative expression of the mouse Sox1, Sox2 and Sox3 genes from pre-gastrulation to early somite stages. *Mech Dev* **86**, 197-201.

Wylie, C. C., Snape, A., Heasman, J. and Smith, J. C. (1987). Vegetal pole cells and commitment to form endoderm in Xenopus laevis. *Dev Biol* **119**, 496-502.

Xia, W., Mullin, R. J., Keith, B. R., Liu, L. H., Ma, H., Rusnak, D. W., Owens, G., Alligood, K. J. and Spector, N. L. (2002). Anti-tumor activity of GW572016: a dual tyrosine kinase inhibitor blocks EGF activation of EGFR/erbB2 and downstream Erk1/2 and AKT pathways. *Oncogene* **21**, 6255-63.

Xia, Z. and Storm, D. R. (2005). The role of calmodulin as a signal integrator for synaptic plasticity. *Nature reviews Neuroscience* **6**, 267-76.

Xu, D. S., Yang, C., Proescholdt, M., Brundl, E., Brawanski, A., Fang, X., Lee, C. S., Weil, R. J., Zhuang, Z. and Lonser, R. R. (2012). Neuronatin in a subset of glioblastoma multiforme tumor progenitor cells is associated with increased cell proliferation and shorter patient survival. *PLoS One* **7**, e37811.

Xu, J., Liu, Z. and Ornitz, D. M. (2000). Temporal and spatial gradients of Fgf8 and Fgf17 regulate proliferation and differentiation of midline cerebellar structures. *Development* **127**, 1833-43.

Yamoah, E. N., Lumpkin, E. A., Dumont, R. A., Smith, P. J., Hudspeth, A. J. and Gillespie, P. G. (1998). Plasma membrane Ca2+-ATPase extrudes Ca2+ from hair cell stereocilia. *J Neurosci* **18**, 610-24.

Yan, Y. T., Liu, J. J., Luo, Y., E, C., Haltiwanger, R. S., Abate-Shen, C. and Shen, M. M. (2002). Dual roles of Cripto as a ligand and coreceptor in the nodal signaling pathway. *Molecular and cellular biology* **22**, 4439-49.

Yanagida, E., Shoji, S., Hirayama, Y., Yoshikawa, F., Otsu, K., Uematsu, H., Hiraoka, M., Furuichi, T. and Kawano, S. (2004). Functional expression of Ca2+ signaling pathways in mouse embryonic stem cells. *Cell Calcium* **36**, 135-46.

Yang, L., Zhang, H., Hu, G., Wang, H., Abate-Shen, C. and Shen, M. M. (1998). An early phase of embryonic Dlx5 expression defines the rostral boundary of the neural plate. *J Neurosci* **18**, 8322-30.

Yao, Y., Li, W., Wu, J., Germann, U. A., Su, M. S., Kuida, K. and Boucher, D. M. (2003). Extracellular signal-regulated kinase 2 is necessary for mesoderm differentiation. *Proc Natl Acad Sci U S A* **100**, 12759-64.

Yeh, E., Cunningham, M., Arnold, H., Chasse, D., Monteith, T., Ivaldi, G., Hahn, W. C., Stukenberg, P. T., Shenolikar, S., Uchida, T. et al. (2004). A signalling pathway controlling c-Myc degradation that impacts oncogenic transformation of human cells. *Nat Cell Biol* **6**, 308-18.

Yi, S. E., Daluiski, A., Pederson, R., Rosen, V. and Lyons, K. M. (2000). The type I BMP receptor BMPRIB is required for chondrogenesis in the mouse limb. *Development (Cambridge, England)* **127**, 621-30.

Ying, Q. L., Stavridis, M., Griffiths, D., Li, M. and Smith, A. (2003). Conversion of embryonic stem cells into neuroectodermal precursors in adherent monoculture. *Nat Biotechnol* **21**, 183-6.

Ying, S. W., Futter, M., Rosenblum, K., Webber, M. J., Hunt, S. P., Bliss, T. V. and Bramham, C. R. (2002). Brain-derived neurotrophic factor induces long-term potentiation in intact adult hippocampus: requirement for ERK activation coupled to CREB and upregulation of Arc synthesis. *J Neurosci* **22**, 1532-40.

Yoo, Y. D., Huang, C. T., Zhang, X., Lavaute, T. M. and Zhang, S. C. (2011). Fibroblast Growth Factor Regulates Human Neuroectoderm Specification Through ERK1/2-PARP-1 Pathway. *Stem Cells* **29**, 1975-82.

Yoshikawa, Y., Fujimori, T., McMahon, A. P. and Takada, S. (1997). Evidence that absence of Wnt-3a signaling promotes neuralization instead of paraxial mesoderm development in the mouse. *Dev Biol* **183**, 234-42.

Yu, H. M., Wen, J., Wang, R., Shen, W. H., Duan, S. and Yang, H. T. (2008a). Critical role of type 2 ryanodine receptor in mediating activity-dependent neurogenesis from embryonic stem cells. *Cell Calcium* **43**, 417-31.

Yu, J., Vodyanik, M. A., Smuga-Otto, K., Antosiewicz-Bourget, J., Frane, J. L., Tian, S., Nie, J., Jonsdottir, G. A., Ruotti, V., Stewart, R. et al. (2007). Induced pluripotent stem cell lines derived from human somatic cells. *Science* **318**, 1917-20.

Yu, X., Zou, J., Ye, Z., Hammond, H., Chen, G., Tokunaga, A., Mali, P., Li, Y. M., Civin, C., Gaiano, N. et al. (2008b). Notch signaling activation in human embryonic stem cells is required for embryonic, but not trophoblastic, lineage commitment. *Cell Stem Cell* **2**, 461-71.

Yuan, S. and Schoenwolf, G. C. (1998). De novo induction of the organizer and formation of the primitive streak in an experimental model of notochord reconstitution in avian embryos. *Development* **125**, 201-13.

Yuasa, S., Itabashi, Y., Koshimizu, U., Tanaka, T., Sugimura, K., Kinoshita, M., Hattori, F., Fukami, S., Shimazaki, T., Ogawa, S. et al. (2005).

Transient inhibition of BMP signaling by Noggin induces cardiomyocyte differentiation of mouse embryonic stem cells. *Nat Biotechnol* **23**, 607-11.

Zhang, K., Li, L., Huang, C., Shen, C., Tan, F., Xia, C., Liu, P., Rossant, J. and Jing, N. (2010). Distinct functions of BMP4 during different stages of mouse ES cell neural commitment. *Development* **137**, 2095-105.

Zhang, X., Ibrahimi, O. A., Olsen, S. K., Umemori, H., Mohammadi, M. and Ornitz, D. M. (2006). Receptor specificity of the fibroblast growth factor family. The complete mammalian FGF family. *J Biol Chem* **281**, 15694-700.

Zhao, S., Nichols, J., Smith, A. G. and Li, M. (2004). SoxB transcription factors specify neuroectodermal lineage choice in ES cells. *Mol Cell Neurosci* **27**, 332-42.

Zheng, W., Nowakowski, R. S. and Vaccarino, F. M. (2004). Fibroblast growth factor 2 is required for maintaining the neural stem cell pool in the mouse brain subventricular zone. *Dev Neurosci* **26**, 181-96.

Zhong, L. and Inesi, G. (1998). Role of the S3 stalk segment in the thapsigargin concentration dependence of sarco-endoplasmic reticulum Ca2+ ATPase inhibition. *J Biol Chem* **273**, 12994-8.

Zimmerman, L., Parr, B., Lendahl, U., Cunningham, M., McKay, R., Gavin, B., Mann, J., Vassileva, G. and McMahon, A. (1994). Independent regulatory elements in the nestin gene direct transgene expression to neural stem cells or muscle precursors. *Neuron* **12**, 11-24.

Zimmerman, L. B., De Jesus-Escobar, J. M. and Harland, R. M. (1996). The Spemann organizer signal noggin binds and inactivates bone morphogenetic protein 4. *Cell* **86**, 599-606.